Development of a Unique Whole-Brain Model for Upper Extremity Neuroprosthetic Control

Dominic Nathan
Marquette University

DEVELOPMENT OF A UNIQUE WHOLE-BRAIN MODEL FOR UPPER EXTREMITY NEUROPROSTHETIC CONTROL

By:

Dominic Emmanuel Nathan, BSEE, BSCoE, MSBME

A Dissertation submitted to the Faculty of the Graduate School,
Marquette University,
In Partial Fulfillment of the Requirements for the Degree of
Doctor of Philosophy

Milwaukee, Wisconsin

December, 2010

ABSTRACT
DEVELOPMENT OF A UNIQUE WHOLE-BRAIN MODEL FOR UPPER EXTREMITY NEUROPROSTHETIC CONTROL

Dominic Emmanuel Nathan, BSEE, BSCoE, MSBME

Marquette University, 2010

Neuroprostheses are at the forefront of upper extremity function restoration. However, contemporary controllers of these neuroprostheses do not adequately address the natural brain strategies related to planning, execution and mediation of upper extremity movements. These lead to restrictions in providing complete and lasting restoration of function. This dissertation develops a novel whole-brain model of neuronal activation with the goal of providing a robust platform for an improved upper extremity neuroprosthetic controller. Experiments (N=36 total) used goal-oriented upper extremity movements with real-world objects in an MRI scanner while measuring brain activation during functional magnetic resonance imaging (fMRI). The resulting data was used to understand neuromotor strategies using brain anatomical and temporal activation patterns. The study's fMRI paradigm is unique and the use of goal-oriented movements and real-world objects are crucial to providing accurate information about motor task strategy and cortical representation of reaching and grasping. Results are used to develop a novel whole-brain model using a machine learning algorithm. When tested on human subject data, it was determined that the model was able to accurately distinguish functional motor tasks with no prior knowledge. The proof of concept model created in this work should lead to improved prostheses for the treatment of chronic upper extremity physical dysfunction.

ACKNOWLEDGEMENTS

I remember very vividly the words of Dr. William Wiener, then Dean of the Graduate school who assured us new graduate students on a warm fall afternoon that graduate education at Marquette is a life transforming experience. Life is a journey in which we continue to learn and grow. As I reflect upon my experience, my doctoral dissertation has been a significant part of this journey, and in looking back I realize how far I have traveled and how much I have learned. The successful completion of this doctoral dissertation would not have been possible if it were not for God's grace and also the many individuals who had played a significant part in making this project a success.

True and sincere, heartfelt gratitude cannot be completely expressed perfectly with merely a few sentences. However, I would like to extend, from the bottom of my heart sincere gratitude to my dissertation directors Dr. Dean C. Jeutter and Dr. Robert W. Prost, members of my dissertation committee, Dr. Stephen J. Guastello, Dr. Norman C. Reynolds, Dr. Kristina M. Ropella and Dr. John L. Ulmer who have been with me since day one of this wonderful journey, for always believing in me, for the unlimited patience, priceless advice and guidance, and who each had played a significant role in helping me, for without them this doctoral dissertation would not have been possible.

I am very thankful for my family, especially my mother, Christine, sister Jessica and father Selva, for the support, encouragement and prayers that they had provided for me along this journey.

In addition, I am sincerely grateful to the many individuals who have been instrumental towards helping me. The list is a long one but I would like to thank those who have played a significant part in assisting me:

Matthew Verber, MS	Jon Wieser	Ronald Brown,PhD
Richard Povinelli, PhD	Sandra K. Hunter, PhD	Marlyn Colegrove
Daniel Nahan	Karl Freund	Ted DeYoe, PhD
Daniel Auger, BA	Renee Burkett	Richard Kuhnen
Kevin Gilligan, BA	Diego Palacius	Catherine Marszalkowski
Timothy Badger	Carl Wainscott, MS	Mary Wesley
Said Audi, PhD	Gerald Harris, PhD	Lars Olsen, PhD
Brian Schmidt, PhD	Gerard Schumer, BS	Michael Schumer
Thomas Silman, MS	Karen Raflik, BA	Craig Pierce, MBA

I would also like to acknowledge the Department of Biomedical Engineering at Marquette University and the Department of Radiology at the Medical College of Wisconsin for the support in making this project possible. I would like to acknowledge the BioElectronics Research and Design Lab for skills and knowledge gained through the years and also for the support during this journey.

Special thanks to the physicians and therapists at the OT and PT clinics of the Zablocki VA Medical Center for the many 'lunch' meetings, the staff at CO and SCS for the many wise words on life, bright smiles, cheerful laughter and unending support that they have provided me over the years.

TABLE OF CONTENTS

LIST OF FIGURES

LIST OF TABLES

LIST OF ABBREVIATIONS

1. 3-D – Three Dimensional
2. ADL – Activities of Daily Living
3. ADLER – Activities of Daily Living Exercise Robot
4. ANN – Artificial Neural Network
5. EEG – Electro Encephalograms
6. EMG – Electromyogram
7. FES – Functional Electrical Stimulation
8. fMRI – Functional Magnetic Resonance Imaging
9. HWARD – Hand and Wrist Robot
10. LDA – Linear Disciminant Analysis
11. MA – Moving Average
12. MIT MANUS – Massachusetts Institute of Technology Mind and Hand
13. MRI – Magnetic Resonance Imaging
14. PET – Positron Emission Tomography
15. PMC – Primary Motor Cortex
16. RUPERT - Robotic Upper Extremity Repetitive Therapy
17. SMA – Supplementary Motor Area
18. US – United States of America
19. WHO – World Health Organization

CHAPTER 1

Dissertation Overview

1.1: INTRODUCTION.

The ability to perform reaching and grasping is an essential skill in our everyday lives. Individuals, who suffer from pathologies such as spinal cord injuries, stroke and amputations experience compromised upper extremity functioning that leads to limitations in activities of daily living, employment and social interaction. This often leaves an individual severely dependent on health care providers and reduces their overall quality of life. Neuroprostheses are at the fore-front of prosthetics research because of their potential to provide increased range of motion, better actuation and precision of control using natural human movements. A neuroprosthesis is a device which uses bio-generated signals to control a limb replacement device. These bio-generated signals originate from muscles, the brain or peripheral nerves. A key advantage of using natural bio-generated signals for controlling the neuroprosthetic is the potential to reduce compensatory behaviors. This is important because compensatory behaviors provide some limited short term function, but in the long term do not provide permanent recovery and could cause other physiological complications.

Neuroprosthetic design and development requires a multi faceted approach that consists of aesthetics, the actual prosthetic limb, a power supply, interface modules, a controller system and processing algorithms. Research into the design of efficient, light weight, esthetically pleasing neuroprostheses has been extensive [67,68,69,249]. Some of the key challenges lie in the development of appropriate control methods that would adequately reflect the actual user's intended movements for achieving functional tasks. The literature suggests the concept of internal models that dictate strategy pertaining to upper extremity neuromotor control during the execution of voluntary movements

[198,199]. However the exact neural correlates of the neuromotor strategies that are represented in the brain and their relationships with the concept of internal models are not clearly understood at this moment. Many neuroprosthetic controllers that rely on models to interpret natural neuromotor strategy are not able to adequately capture this information due to limitations in their recording modalities. Limitations in current sensing systems include the inability to sample all of the brain regions involved in generating intention to move. These limitations lead to upper extremity neuroprosthetic systems requiring the user to learn new strategies, movements or adaptation to produce sufficient control signals. Such requirements are not practical in afflicted patient populations and reduce the long term efficacy of the neuroprosthetic device. Furthermore, modifications of behavior or the oversimplification of control signals lead to natural occurring neuromotor strategy being ignored. This requires increased investment by the user in training and normal usage. The increased effort is often thwarted by the effects of various pathologies.

The goal of this study is to develop a whole-brain model for upper extremity neuroprosthetic control using data acquired with functional magnetic resonance imaging (fMRI) from the entire brain. This model is novel as it accounts for anatomical regions of the brain involved with reach-to-grasp planning, initiation and performance and the corresponding temporal activation patterns. Further, by sampling the entire brain, the model is not biased by the choice of sampled brain regions. The combination of whole brain anatomical regions and temporal patterns allows for the implementation of naturally occurring neuro motor strategies employed by the brain to realize reaching and grasping. The use of such information has significant potential to enable increased control,

movement resolution and range of motion; these are features that are not complete attainable in contemporary neuroprosthetic controllers [249].

In addition, information that pertains to neural correlates of movement and neuromotor strategy can be better understood because this whole-brain model is able to produce specific three dimensional cortical localization of upper extremity task specific activation. These key features are currently not available in upper extremity neuroprosthetic devices that use EMG or EEG signals for control. The ability to measure natural neuro activation should enable users of this neuroprosthetic model to apply previously employed skills and strategies. This should lead to more natural task performance that promote faster recovery of upper extremity function and reduce compensatory behaviors.

1.2: SPECIFIC AIMS.

The *first specific aim* of this dissertation was to identify regions of the brain that correspond to goal-oriented upper extremity motor tasks in neurologically intact healthy individuals using fMRI. During the experiment, subjects were required to perform actual motor tasks of reaching and grasping. This was a novel approach because many current studies that examine neural correlates of upper extremity motor control using fMRI or other imaging modalities do not use functional tasks with real world objects. The experimental paradigm that used functional upper extremity movements was designed to provide information in brain regions which were active when the subjects performs a functional task such as reach and grasp. Results from mapping of these regions have

shown varying locations and patterns of activation within the brain [188,189,273]. Motor imagery tasks were used as surrogates to understand how planning of upper extremity reaching and grasping occurs and to provide insight regarding brain strategy.

The goal of the *second specific aim* of this dissertation was to identify the temporal activation patterns in the whole brain during goal-oriented reaching and grasping in neurologically intact healthy individuals using fMRI. The use of neuromotor strategies to realize functional reaching and grasping involves several regions of the brain that experience combinations of series and parallel communications. Like all motor tasks, there exist feedback loops to fine tune the movement as well as sensory feedback loops as well. At present, many investigators are studying specific anatomical regions such as the motor cortex, SMA, parietal region, thalamus and cerebellum, but have not examined temporal information processing of the whole brain specific to functional reaching and grasping. If one were to concentrate on one or two specific brain regions, the result would provide only a partial view of the actual underlying neural mechanisms of reaching and grasping, which would lead to a loss of information about the entire process.

The *third specific aim* of the dissertation as to determine the feasibility of using information from specific aims one and two to develop a whole-brain model that can be used to predict functional goal-oriented task performance based on intention. The neuronal activation patterns which represent intention are based on a model of imagined reaching and grasping. This model is unique as it represents upper extremity function that uses naturally occurring strategies in the brain. Such a model will have the potential to be applied as a neuroprosthetic controller that could provide users with a robust platform for controlling and using upper extremity neuroprosthetic devices.

The *fourth specific aim* of the dissertation project was to validate the whole-brain model by using it to predict hand use in a group of neurologically intact human subjects. The prediction was based upon retrospectively analyzing fMRI data in the validation subject group by detecting the modeled pattern corresponding to the intention to reach and grasp.

1.3: DISSERTATION ORGANIZATION.

The organization of this dissertation is presented as a flow chart in figure 1.1.

FIGURE 1.1: Dissertation Overview.

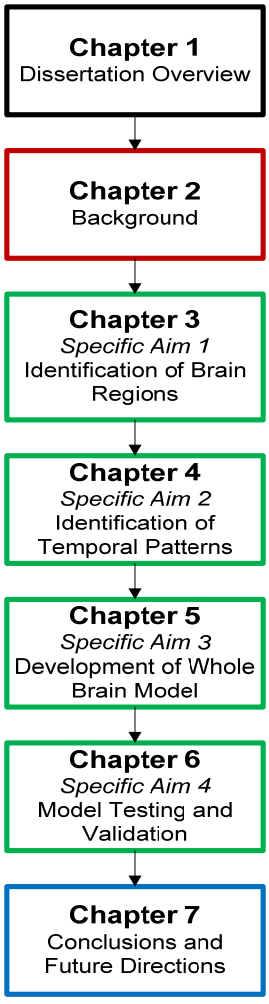

CHAPTER 2

Background

2.1: UPPER EXTREMITY PHYSICAL DYSFUNCTION AND ITS SIGNIFICANCE.

The ability to perform meaningful reaching and grasping is essential in our lives. Chronic upper extremity physical dysfunctions that are induced by physical or neurological pathologies prevent proper upper extremity function. This leads to disruptions in activities of daily living (ADL), social interaction and employment. The consequences include compromised independence, dignity and quality of life. Physiological injury that induces chronic upper extremity physical dysfunction and also hinders reaching and grasping can be caused by micro or macro mechanisms. Micro injuries are manifested at the cellular level and affect groups of neurons, cells such as muscle, cartilage and bone, connecting tissue or nervous system pathways. Neurological insults such as stroke, cerebral palsy, dystonia or arthritic types of diseases often induce micro injuries. In addition, micro injuries may originate from *in-vivo* cell signaling or abnormal gene expressions during fetal development that lead to congenital limb defects. The affects of macro injuries are much more substantial and at times can be the byproduct of chronic micro injury. Often a significant part of a specific limb is impaired, resulting in the partial or complete loss of function or the limb itself. Major causes of macro injury are traumatic accidents, amputations, spinal cord injury, paralysis etc. Several pathologies that induce chronic upper extremity physical dysfunction and their related statistics are presented in table 2.1.

TABLE 2.1: Chronic Upper Extremity Pathologies That Affect Proper Reaching and Grasping.

Pathology	**Number of affected individuals**	**Financial burden**
Spinal Cord Injury	255,000 (2008)	Treatment & living cost $~1 - 3m per individual annually. Total $255-$765 million per year
Stroke	6.4 million(2010)	Treatment costs $73.7 billion (2010)
Limb Loss (upper and lower)	1.7 million (2008)	Direct and indirect costs $~27.3billion (2005)
Dystonia	300,000 (2005)	Treatment costs 13.5 billion (2005)
Cerebral Palsy	800,000 (2006)	Average life time cost per person $900 million (2003)
Rheumatic and Musculoskeletal Conditions	46 million (2006)	Direct and indirect costs $128 billion (2003)

Trauma related incidents are the main cause of limb loss. Such incidences are prevalent in war affected regions, or in regions that are politically unstable. A larger number of limb losses occur due to direct encounters with violence [1,2]. Civilians in post war countries are prone to encountering left over ordinance in the form of mines that pose a very high risk of limb loss, especially in children [3,4]. Regions that are susceptible to catastrophic natural disasters, such as hurricanes, earth quakes and tsunamis, pose a high risk for the occurrence of limb loss and trauma related injuries [1,5]. The number of amputees in the United States (US) is estimated to be at 1.6 million people. A 1996 estimate identified 168,000 individuals with upper extremity limb loss and this number was predicted to double by 2030 [6-8]. The occurrence of upper extremity limb loss is less frequent when compared to lower extremity limb loss; however the disability, level of assistance, and associated financial cost for upper extremity limb loss is significantly higher [6,8,9].

Apart from complete loss of a limb or digits, accidents are also a major contributor to the loss of limb function, resulting from spinal cord injury and paralysis.

The World Health Organization (WHO) estimates that in developed countries, traffic accidents account for 15 – 20% of serious limb trauma while another 20% are the result of employment related injury from machinery or tool usage [10]. Individuals between the ages of 5-34 years and those above 75 years have been identified to be the most vulnerable to these types of injuries [10]. The National Spinal Cord Injury Statistics Center reports that there are 255,000 people living in the US with spinal cord injury, and the estimated annual financial burden for treatment and associated living cost is approximately $1 - $3 million dollars per person depending on the age of onset [11].

Non-traumatic injuries such as stroke affects blood circulation and the supply of oxygen and nutrients in the brain. This leads to disruptions in neuronal signaling that affects information processing and communication within cortical pathways. The damage caused by stroke is not limited to one function but rather may have a wide spread effect on memory, planning, emotion, fine motor control, and coordination. Stroke can severely impede upper extremity motor function and the ability to perform meaningful reaching and grasping. Furthermore, stroke is the leading cause of long term disability in the US and is the third major cause of death [12]. It is estimated that 6.4 million people in the US are affected by stroke, with an estimated financial burden of $73.7 billion dollars [12]. Unfortunately stroke is a growing epidemic and the World Health Organization projects that by the year 2030 stroke will account for 75% of deaths related to chronic diseases [13].

Dystonia is a neurological pathology that hinders upper extremity function by influencing the manner in which muscles contract or relax, resulting in involuntary movements and muscle spasms that often leave the limbs in severely contorted abnormal

postures. The causes of dystonia are often associated with heredity and genetics or acquired through trauma, poisoning or adverse reaction to medication. It is estimated that there are 300,000 dystonia patients in the US of which 100,000 are children [15,16]. Other pathologies that induce chronic upper extremity physical dysfunction and could benefit from neuroprosthetics are cerebral palsy, muscular dystrophy, rheumatic and musculoskeletal conditions. Cerebral palsy is a neurological condition associated with damage to the cortex during pregnancy and post-natally up to the age of three [46]. The effects of cerebral palsy are motor deficits, muscle spasms, tremors and contractions that lead to abnormal gait, posture and cognition [46]. Muscular dystrophy is a muscle wasting disease that causes progressive weakness in the muscle and eventually muscle cell death [17]. This disease is predominantly found in the pediatric population with a relatively smaller number of adults are affected [18]. Finally, rheumatic and musculoskeletal conditions cause pain and severe deformities of the joints that reduce the functional use of the upper extremities [10,14].

Unfortunately, most of these pathologies do not have clinical interventions that can provide long term functional restoration. There are a plethora of rehabilitative devices, methods and approaches; however therapeutic outcomes remain very highly variable where complete recovery and functional independence is neither guaranteed, nor consistent for all individuals. It is projected that the number of individuals who suffer from pathologies that affect upper extremity function will increase annually due to factors such as an increase in the global population, changes in lifestyle and diet [10,13]. This increase must be met with appropriate therapeutic interventions that can reduce upper extremity disability, restore function and increase quality of life.

2.2: CURRENT UPPER EXTREMITY TREATMENT OPTIONS.

There are several treatment options aimed at restoring function in the upper extremities. These methods encompass tissue engineering, physical therapy, and the use of technology assistive devices such as robots and neuroprosthetics. The following sections present each of these upper extremity treatment methods, their current status and limitations.

2.2.1: Tissue Engineering Procedures.

Tissue engineering approaches seek to restore upper extremity function using techniques of regeneration and replacement of damaged regions using methods that are biological in nature [92]. On a micro scale, tissue engineering consists of neuronal repair, regrowth and relinking of prior dendritic and synaptic connections [47,92]. This process is achieved by using methods such as cell therapy that could facilitate neuronal regeneration, dendrite resprouting and new axon formation [19-22,47]. Animal models and some limited human clinical trials have shown promising results through the restoration of function and suppression of pathology induced neurological impairments [23-27]. Macro level tissue engineering interventions consist of organogenesis, allotransplantation and xenotransplantation. Organogenesis is the process of growing replacement organs from stem cells [28-31]. Allotransplantation is the process of using a replacement organ from within the same species. There has been some limited use of allotransplantation for treating upper extremity physical dysfunction where the toes were used as replacements for fingers in reconstruction experiments [32]. Xenotransplantation involves using donor organs or cells from different species such as mice, pigs and

primates [33-41]. Tissue engineering methods are still largely in the theoretical and experimental phases. Some major challenges for tissue engineering are the compatibility of the transplant with the recipient and the risk of infectious agents being transmitted from donor to recipient [34,42-45]. Furthermore, cell therapy, organogenesis and transplantation do not guarantee proper functional and physiological adaptation leading to an increased potential for organ rejection or infection. This is specific to the development of appropriate vasculature, chemical expressions or functional form of the replacement organ [48,49]. If these challenges are adequately addressed in the years to come, then the tissue engineering approach could be a strong contender for providing most viable options through regenerative medicine for long term restoration of upper extremity function. Until then, tissue engineering approaches have little applicability for the restoration of function and especially for functional upper extremity reaching and grasping.

2.2.2: Physical Therapy.

Treatment of upper extremity physical dysfunction uses a multi-faceted approach, often beginning with physical therapy then leading to occupational therapy and sometimes to recreational therapy [51,52]. The goal of such treatment is to facilitate the retraining of motor skills, provide long term upper extremity functional recovery and promote independence. Physical therapy treatment has been used extensively to treat victims of stroke, spinal cord injury and amputations. The focus of initial treatment is the restoration of basic hand and arm function such as reaching, grasping, increased

coordination, control and range of motion. This is often achieved through a series of stretches, precision and resistive strength training, timed movements, and goal oriented tasks [51,52]. Once the patients have achieved sufficient independent limb control and coordination they are referred to occupational therapists. This next phase focuses on retraining the ability to perform functional movements in the activities of daily living such as feeding, grooming, hygiene, mobility, locomotion and employment related tasks such as writing and equipment use [51,52].

Current options for individuals who suffer from limb loss are prosthetic devices that are active (externally powered) or passive (self actuated). Active prostheses are often powered using pullies, gears or motor systems that obtain energy from a rechargeable battery source. The simplest powered upper extremity devices have a series of switches that can be controlled either with the unimpaired limb or with other body parts such as the shoulder, chin or neck. The switches dictate individual movements such as reaching out, hand rotation, grasping and releasing. There are also systems that use sip and puff techniques to provide mobility and control of external manipulators.

Passive devices are sometimes powered using wires and pulleys, and actuation is achieved by using the unimpaired hand. For both passive and active prosthesis, different functional tools can be attached to the tip of the prosthetic device to achieve a specific function as shown in figure 2.1. Functional tools are able to help the user with a variety of tasks such as the use of hooks for activities of daily living, manipulation of objects or specific attachments used for recreation such as a baseball glove attachment and a bowling ring attachment. Other attachments such as the voluntary opening hand provide aesthetics combined with some very basic function. Individuals who are fitted with active

or passive prosthetic devices are trained on how to use them to reach, grasp and manipulate objects.

FIGURE 2.1: Upper Extremity Prosthetic Attachments
(Images are copyrighted to Hosmer Dorrance Corporation. Used with permission).

Frustration is a limitation of current use of upper extremity prosthetic devices when these devices take too long to achieve many tasks and provide limited use due to fatigue, as some of these devices are heavy and bulky [53]. The negative impact of this leads to the user not wanting to wear or use the prosthetic device. In addition, the time and effort needed to learn how to use the prosthesis, combined with the appearance of the device, influences the acceptance and willingness of an individual to continue its use. Feelings of embarrassment and awkwardness combined with the social stigma attached to the disability are especially prevalent in public settings or when in the company of others

[54,55]. This has a negative psychological effect on the user and may lead to long term abandonment of the assistive prosthetic.

The manner in which these devices are used does not correspond to normal neuromotor strategy, which in turn does not promote complete recovery of function. The frustration that arises from the impairment encourages the development of compensatory behaviors. Compensatory behaviors are a form of coping mechanism and in the short term, are able to provide some limited function. However, in the long term the use of compensatory behaviors do not promote neuromotor recovery and the restoration of upper extremity function, and can lead to other complications [56,57].

Robot aided therapeutic interventions have shown some promising results in providing therapy for stroke and spinal cord injured subjects. Systems such as the MIT Manus, Hand and Wrist Robot (HWARD), Robotic Upper Extremity Repetitive Therapy (RUPERT) and ADL Exercise Robot (ADLER) have been able to provide some recovery by serving both as therapeutic and assistive devices [58-62]. These robotic devices are able to assist the user by moving their upper extremities to perform various tasks. The advantage of robotic therapy systems is the ability to provide quantifiable assistance and training in a consistent manner [63]. Although promising, however, a majority of these devices do not provide consistent gains post therapy and functional recovery is often transient [63]. In addition, although all patients receive the same therapy or methods, there is substantial variability in the individual outcomes [64-66]. Lastly, a majority of these robotic therapy devices are large, heavy and have poor portability that reduces the possibility of post-clinical use such as in the home environment.

2.3: UPPER EXTREMITY NEUROPROSTHESES.

2.3.1: Current Status of Upper Extremity Neuroprostheses.

Neuroprosthetic research for clinical applications that is aimed at treating upper extremity physical dysfunction has gained momentum in the past decade. Unlike traditional prosthetic devices that are mainly aesthetic or have limited use and control, contemporary neuroprostheses are capable of providing function that can be applied to task performance such as the restoration of reaching and grasping [67-69]. The core component of a neuroprosthesis is the control mechanism that is driven by certain physiological signals that originate from a human user, and is obtained through *in-vivo* methods [67-69]. The intent of neuroprosthetic interfaces such as EEG, direct neuron recording and EMG allows the user to interact with the prosthetic device in a more natural manner as they would an actual limb. This eliminates the need for alternative activation methods such as use of the unimpaired hand, compensatory or modified behaviors. In addition, the burden of having to learn new strategies or methods of motor control is much reduced, thereby decreasing the amount of time needed for training and familiarization. Such a device provides the user with a platform that has potential for quick adaptation and performance of functional tasks [70-73]. The ability to combine aesthetics with utility is an important aspect of restoring dignity for the user because, a device that can blend visually and function like an actual hand would be well received and easily assimilated [70-73]. Users would be more apt to regard the neuroprosthetic as something more than just an assistive device and this should increase the motivation to use the device.

Early work in search of suitable physiological signals that can be used to control upper extremity neuroprosthetic devices was conducted using animal models. Research that used direct neuron recording in the primary motor cortex of monkeys that performed various upper extremity motor tasks, with different orientations, delays and perturbations were geared toward understanding motor control and its cortical correlates [74-79]. The data suggested that there is a clear effect of delay, task orientation and planning that influenced neuronal discharges within an ensemble of neurons [74-79]. Furthermore, it was observed that interactions having specific task constraints and stimuli were able to generate distinct patterns of cortical activation [74-79]. This led to the exploration of methods to extract these signals directly from the cortex to control mechatronic devices, paving the way for the beginning of upper extremity neuroprosthetic development.

Animal models for experimentation with upper extremity neuroprosthetic integration and control have been extensively conducted on rats and monkeys. In a successful rat experiment, a rat was fitted with direct neuron recording electrodes placed in the primary motor cortex and the thalamus [80]. The signals extracted from these regions were sent to a neuroprosthetic arm that the rat was able to control and manipulate in a manner similar to its own paw. With sufficient training the rat was able to realize the task goal using the neuroprosthetic arm. Similar experiments were conducted using signals acquired through direct neuron recordings in cortical regions such as the supplementary motor area (SMA) and primary motor cortex (PMC) in monkeys. The results demonstrated the ability of animals to learn and successfully adapt to controlling upper limb neuroprosthetic devices to perform specific motor tasks [81-84].

The feasibility of training and controlling neuronal signals acquired by direct

neuron recording has been shown in human subjects. These subjects were paralyzed from different pathologies such as a brain stem stroke, spinal cord injury and even the 'locked-in' phase of amyotrophic lateral sclerosis [85-89]. Subjects were able to learn how to control the intensity and duration of the neuronal evoked potentials in a consistent manner using electrodes implanted in the regions such as the primary motor cortex. This control scheme was then extrapolated to control computer cursor movements and further extended to other controls such as lighting and a neuroprosthetic arm [90]. Many early studies have extensively used the method of direct neuron recording to observe activation in specific regions of the brain in animal models and human subjects. This is because other non-invasive recording methods such as Positron Emission Tomography (PET), Functional Magnetic Resonance Imaging (fMRI), and Electroencephalograms (EEG) were not available. When compared to imaging modalities such as fMRI, PET and EEG, direct neuron recording can provide a much higher signal-to-noise ratio, however the tradeoff is the highly invasive nature of implanted electrodes.

With the development of newer recording technologies for clinical research, non-invasive modalities such as EEGs have been used extensively in research pertaining to neuroprosthetic control and the human-machine interface. EEG systems provide a method of measuring the relative activity of neurons in cortical regions of the brain through electrodes that are placed on the surface of the scalp. A key advantage of EEG is the ability to provide high temporal resolution recordings of neuronal activity in a minimally invasive manner [91,92]. The high sampling rates of EEG systems permit them to be able to detect specific events in the brain that relate to task planning and execution, and features of these activations such as delay, duration of activation and

activation intensity. EEG systems are able to provide some anatomical localization of function and this is dependent upon the number of recording electrodes that are used. Typically a minimum of two electrodes are used in EEG systems and this can vary up to 256 or more electrodes. Increasing the number of electrodes increases the spatial resolution of the acquired signal. However, the EEG signal is scattered by its passage through the skull which ultimately limits the spatial resolution of the technique. This ability to detect specific signal characteristics makes EEG systems appealing for application in neuroprosthetic controllers. Often, with significant training, subjects are able to control simple tasks such as moving computer cursors [93,94]. Using acquired EEG signals, custom developed algorithms have enabled users with sufficient training to control mechatronic devices like robotic arms, functional electrical stimulators (FES) and even miniature mobile robots [95,96]. Some systems are able to provide tactile sensory feedback to users that enhance feedback and increase accuracy [97]. The use of custom developed software for EEG neuroprosthetic control provides the flexibility to incorporate custom training paradigms such as 3D depth perception and the use of virtual environments [98]. In addition, the use of custom software allows the implementation of ongoing improvements to the underlying signal processing algorithms such as enhanced detection and source localization, improvement of filtering out signal artifact and reducing the amount of training needed [99,100].

Electromyography (EMG) data acquisition methods consist of recording electrical potentials from muscle or nerve activity [91,92]. These are often achieved with high sampling rates for EMG data acquisition that can use surface or implanted electrodes. Surface EMG electrodes are placed at locations that can provide a consistent and stable

EMG signal such as the residual limb, unimpaired hand or other body parts such as the neck and shoulder. Implanted electrodes offer a long term portable solution with a higher signal-to-noise ratio when compared to surface electrodes as they can be embedded directly within the nerves [104]. In addition, the number of electrodes often range from a minimum of two upwards. An increase in the number of electrodes offers higher resolution of signal acquisition, thereby enabling more precise control, especially for multiple degrees of freedom. This method of upper extremity neuroprosthetic control has provided promising outcomes for the treatment of upper extremity physical dysfunction that is induced by different pathologies. In situations in which there is very little residual EMG signal that can be adequately detected with individuals who suffer from pathologies such as stroke or spinal cord injury or from individuals who experience partial or complete paralysis. Such instances require EMG signals to be extracted from the unimpaired limb or muscle groups that are activated following movement of other body parts (shoulder or wrist). These EMG signals are then used to control functional electrical stimulation (FES) devices that target specific muscle groups in the upper limb in order to create functional upper extremity motion [101-103]. With sufficient training, subjects are able to perform meaningful reaching and grasping using these EMG and FES neuroprosthetic devices.

Implanted EMG neuroprosthetic electrodes have been used to restore upper extremity function in amputees. The placement locations of these electrodes depend upon the level of amputation. The prosthetic attachment site and electrodes are often implanted in the forearm of individuals with below the elbow amputations [104]. Where one or both arms are completely lost in severe cases, there are limited EMG sources available to

provide the control needed for multiple degrees of freedom. The technique of targeted hyper re-innervation nerve transfer surgery is a novel approach that transfers residual nerves and transplants them in muscle areas near the affected region [105]. Neuro plasticity of the peripheral nerves and motor units occur at the transplanted site during recovery, resulting in the generation of stable voluntary EMG signals that can be harnessed to control upper neuroprosthetic devices for reaching and grasping [106].

The following table 2.3 lists the various recording modalities that have been used to record signals relating to neuromotor strategy as used by the brain during the performance of upper extremity functional tasks.

TABLE 2.3: Comparison of Recording Modalities.

	Electro myogram (EMG)	**Electro enchephelogram (EEG)**	**Magneto enchephelogram (MEG)**	**Direct Neuron Recording**
Recording Location	Body Surface or Limb Implanted	Surface	Surface	Implanted In brain
3D localization	No	Some	Yes	By choice of implant location
Information from deep brain regions	Not Available	Slight	Slight	Good
Multiple Brain Regions	Not Available	Good	Good	Poor
Brain Anatomical Localization	Not Available	Fair	Fair	Good
Long Term Use	Good	No	No	Good
Portability	Fair	Poor	No	Good

2.3.2: Limitations of Current Neuroprostheses and Challenges.

Although neuroprosthetic devices are at the forefront for providing restitution of functional reaching and grasping they are not without their limitations. A major challenge for neuroprosthetic devices is the inadequate generalization for most individuals [90,107-108]. To date there are very few impaired individuals who have successfully been integrated with neuroprosthetic devices and who are able to use them functionally in a home environment, post treatment [72,73].

The mechanisms employed by the brain during the selection and implementation of strategies that are specific to upper extremity task initiation, planning, learning and object manipulation is a subject of much research. There are many models and theories in the field of neuromotor control that have sought to explain how the underlying anatomical regions of the brain are involved and differences induced by the different pathologies affect normal upper extremity functioning [109-114]. However, many of these models are very theoretical, have overtly simplified experimental conditions or do not adequately correlate neuromotor strategies between the limbs and activation in the whole brain with functional tasks [109-114].

Signal reduction has been observed during an initial period after electrode placement or after some period of use in systems that use direct neuron recording [90]. It is hypothesized that this is caused by plasticity and regional reorganization, movement of the electrodes or neuronal apoptosis of cells at the implantation site [115-117]. Other studies suggest that scar tissue formation around the electrode and neuron interface or the presence of foreign particles that build up over time in this region cause a reduction in conductivity and signal-to-noise ratio [115-117]. EMG neuroprosthetic systems that use

implanted electrodes are also susceptible to these difficulties. Often, repositioning of the old implanted electrodes or replacement with new electrodes is needed but the process is very invasive for implanted electrodes and there are other health risks such as infection, in addition to post surgical recovery time and cost involved.

A majority of the recording techniques suffer from significant signal artifact that originate from physiological or environmental sources. Surface EEG and EMG neuroprosthetic systems are susceptible to interference caused by movement of the skin at or near the electrodes, breathing, cardiac rhythm, eye blink and even sweating. In addition, subject motion and radio frequency interference from the environment contribute to increasing noise artifact in the EEG and EMG signals. The physiological signals often range in amplitude from micro to milli Volts and require amplification on the order of 1000 to 100000 [91].These high gains increase the risk of diminished signal fidelity and cause poor signal to noise ratio or the amplification of noise that contributes to signal corruption. This necessitates the need for sophisticated algorithms for reconstruction or transformation of the information from the system in order to properly drive the neuroprosthetic controller. Unfortunately, the footprint for the associated technology needed to realize such algorithms is often bulky and heavy. Furthermore such equipment does not always guarantee robustness of neuroprosthetic use and functional mobility.

Surface recording techniques such as EEG and MEG lack the ability to provide accurate subcortical source localization and depth information from deep brain structures such as from the thalamus that contributes to reaching and grasping. This is currently an area of much research into algorithms that can provide these surface recording modalities

with information from deep brain structures of the brain or through the combination with other modalities such as PET and MRI [118-120]. However without the ability to accurately correlate the underlying anatomical structures of the brain with activation patterns from EEG data, information loss pertaining to strategy, intention and task execution occurs. This causes an incomplete representation of information flow within the brain for upper extremity task realization. Furthermore the use of EMG does not provide any information related to the representation of neuromotor strategy in the brain. EMG based neuroprosthetic systems rely on residual muscle activity from the unimpaired hand or other spared muscles. This does not allow the desired flexibility of use of EMG neuroprostheses for individuals who have severe motor dysfunction, high spasticity, are paralyzed or have amputations. In addition, the recruitment of alternative muscle groups and the use of unconventional movements encourage the use of compensatory behaviors that do not promote functional recovery.

Each recording modality requires significant effort in concentration along with considerable training to achieve sufficient control and utilization of a neuroprosthetic device. The user has to learn how to increase, decrease or sustain signal intensity to obtain signals that are usable for control. Certain pathologies that hinder upper extremity function often induce additional dysfunction that affects cognition or fine motor control skills. The result is a steep learning curve that increases frustration, physical and mental fatigue and susceptibility to mood swings; factors that could jeopardize learning and accurate control of the neuroprosthetic device.

Lastly, an important characteristic that is lacking in current neuroprosthetic systems is the inadequate representation of sensory motor integration and a high

emphasis on visual adaptation. During voluntary upper extremity function, pertinent information is conveyed from proprioceptive and tactile sensory receptors that combine with the visual system to guide and produce meaningful and accurate movements [74,75,113,114]. Proprioceptive receptors that help determine hand position and orientation coupled with tactile feedback are important for manipulating objects. Many upper extremity neuroprosthetic devices do not account for these two sensory receptors, but rather rely more heavily on the visual system to adapt. This does not promote recovery or the utilization of natural neuromotor strategies, rather encourages unwanted compensatory behaviors.

2.4: UPPER EXTREMITY NEUROPROSTHESES.

2.4.1: Feature extraction, data classification and modeling of brain activity in contemporary upper extremity neuroprostheses control.

Natural human movement is a complex process that requires the control of multiple degrees of freedom as expressed by the limbs [121]. To use physiological signals of the brain to control upper extremity neuroprosthetic devices, appropriate algorithms need to be developed to perform feature extraction, data classification and ultimately modeling of functional activation and information flow from the brain. Such algorithms and brain models are crucial for the understanding of how neuromotor strategies are retrieved and applied to upper extremity function. There are numerous tools that can be used to create models for the extraction and classification of patterns that are specific to brain function and neuromotor strategies. Some of these tools are regression

analysis, components analysis, nonlinear dynamics, multivariate analysis, fuzzy logic, machine learning and parametric statistical methods.

The use of Principal Component Analysis (PCA) focuses on identifying common correlations among data elements of a specific data set by increasing the variability [107]. In doing so, data elements of high correlation are removed, and the relationship of low correlated elements are assessed [107]. The removal of highly correlated data elements and the analysis of the remaining data elements is an important part of the PCA algorithm that enables dimensionality reduction of the raw data set [107]. A key assumption of PCA is that there is a common source of data activation, or common signals within a given data set present. The use of PCA in functional imaging studies that use fMRI, PET, MEG and EEG have shown the successful identification of stimulus specific activation areas in the brain during the performance of upper extremity motor tasks such as finger tapping and grasping [123-125]. Although primarily used as an exploratory technique, PCA can also be combined with other methods such as regression analysis, fuzzy logic, and Bayesian analysis to yield information such as connectivity analysis and modeling among brain regions for memory and motor task performance [126-127]. The implementation of PCA techniques for the analysis of hand use and posture in human and primate studies has shown the feasibility of incorporating PCA techniques in to neuroprostheses controllers. [128,129].

An alternative analysis algorithm is Independent Component Analysis (ICA), which can be thought of as the inverse of PCA. ICA is based on the concept of blind source separation that suggests the notion of a data set being a composite of several separable independent sources [130]. The goal of ICA is to identify the independent

factors from which the data set is composed by maximization of independence among elements of the data set. This method of data extraction has been used extensively in functional imaging studies that used fMRI and EEGs to detect active regions corresponding to upper extremity motor tasks [131-134]. The use of ICA for determining hand use through the analysis of EEG signals has shown the feasibility of using this method in neuroprosthetic control. The ICA concept has shown promising results in determining hand use. Furthermore, models created using ICA methods have been used to determine functional connectivity among regions of the brain such as motor and sensory cortex during the performance of voluntary motor tasks [135-137]. The ICA approach is appealing due to its properties of nonparametric association and minimal initial assumptions for data distributions and structure [130].

Cluster analysis methods used with functional imaging data are to identify stimulus induced activations that are considered to be significant within a data set. This analysis considers the amplitude and location of an activation with respect to the underlying anatomy. The data is often sorted by distance to yield specific areas or 'clusters' of activation [138]. There are many different flavors of clustering methods such as Hierarchical, *K*-means, dynamic clustering and spectral clustering that vary based on the criteria for determining the distance of data elements [139-142]. These different clustering methods have been successfully used in the analysis of EEG and fMRI imaging data to reveal regions activated during the planning and performance of functional upper extremity motor tasks [143-145]. Separate studies that used animal models to examine data acquired using implanted electrodes in the brain, direct neuron recordings, and spinal cord stimulation induced EMGs, have successfully identified

steady and distinct upper extremity related control signals and patterns using cluster analysis tools [146-148]. These results have been tested for use in upper extremity neuroprosthetic control application and have shown successful results in providing control of actuation [146-148].

Often, physiological signals are inherently chaotic and of high dimensionality. Such features of physiological signals make nonlinear dynamic principles an appealing tool for analysis and modeling. Nonlinear dynamics tools such as attractors, fractals and self organization have been used for structural equation modeling of brain activity [149-151]. The application of such tools have been reported in the literature in studies using imaging modalities such as super conduction quantum interference device recording (MEG), EEGs and fMRI [149-151]. For each of these studies, nonlinear dynamics have been used to model the specific response of local magnetic fields, electrical evoked potentials or the change in the hemodynamic response using specific features such as phase plots that show transitions from one state of cognitive processing to another. This method has also been used to model simulated hand trajectory data and direct neuron recording of activity in the hippocampus during performance tasks by rodents, in order to produce quantifiable results that could be used in neuroprosthetic controllers [152]. Other statistical methods such as the spatial statistical methods of graph theory, motifs and network connectivity have been used to develop models that describe information flow between regions of the brain [153-156]. Initially used in animal studies with felines and primates, graph theory has been used to analyze functional connectivity pertaining to anatomical regions of the brain that are involved with motor and sensory information processing [157,158]. These are features that have implications for neuroprosthetic

control. The graph theory method has also provided connectivity analysis and information flow data between cortical structures in human studies that used EEG, MEG and fMRI recording modalities [159-161].

Linear Discriminant Analysis (LDA) is the process in which two or more linear combinations of independent variables within a data set can be separated using predefined *a priori* information [138]. The LDA method is closely related to regression, ANOVA and components analysis however there are some differences among these methods. LDA requires that the dependent variable be a categorical quantity which is nominal or non-metric and that the independent variable is metric. This is different from regression analysis that requires the dependent variable to be metric and differs from ANOVA analysis which has the opposite assumptions of LDA for the dependent and independent variables, respectively [138]. When comparing LDA with PCA, LDA is concerned with the differences between data sets. A distinction between LDA and ICA is the requirement to predefine data set information *a priori* for LDA analysis [138]. LDA has been used to determine regions of specific stimulus induced activations in the brain during functional imaging experiments that use EEGs and fMRI [162,163]. In successful clinically implemented upper extremity EMG neuroprosthetic device on subjects who were treated with nerve hyper-reinnervation surgery and fitted with implanted electrodes, the main algorithm of their neuroprosthetic controller used LDA [164,165]. This LDA control algorithm was able to distinguish hand movements from implanted electrode EMG recordings which were then used to control the use of the neuroprostheses to perform various tasks [164,165].

The relationship between one or more independent variables that have a common dependent variable can be analyzed using regression analysis [138,166]. This process predicts the behavior of the dependent variable through the development of linear or non linear regression model that can be used for forecasting and estimation of future output states [138,166]. This is beneficial when attempting to describe a system or a response such as the hemodynamic Blood-Oxygenation-Level Dependent (BOLD) response in fMRI or stimulus induced changes in voltage potentials measured using EEG or direct neuron recording methods [167-170]. In neuroprosthetic applications, linear regression analyses of animal and human data from direct neuron and nerve recording data in which the net output of a population of neurons was summed, and subsequent regression analysis yielded information pertaining to voluntary movement intention [171,172,272]. The ability to extract and accurate classify these voluntary physiological signals have shown promise for the application to upper extremity neuroprosthetic controllers.

2.4.2: Limitation of current feature extraction, data classification and modeling approaches in contemporary upper extremity neuroprostheses control.

Current models of the brain, feature extraction and data classification are able to provide some representation of cortical activity, information flow and pattern identification; however most of these models are not ideal candidates for upper extremity neuroprosthetic control. This is attributable to several factors. The first is that pattern identification methods that require mathematical operations such as smoothing, rotations, filtering, etc. are challenging to use in real time data acquisition and analysis. This is

because significant effort needs to be invested to assure that the underlying assumptions of these mathematical tools are not violated. Violations of the underlying assumptions of the statistical tools could result in skewed results that lead to misrepresentation of the data and potential false discoveries. Furthermore, most feature extraction methods require key information of the data set such as the variance, mean and standard deviation to be specified prior. These parameters are crucial in the correction operations that remove drift and filter noise. However most of these parameters pertaining to the dataset population can only be estimated off-line after task performance and this is not practical for feed forward neuroprosthetic applications.

The development of brain models and the use of feature extraction and data classification tools often seem to be paradoxical in terms of the level of complexity involved. On one hand, the use of simple tools such as LDA and linear regression analysis for the analysis of brain activity have shown promising results in limited applications of real time neuroprosthetic control [149,150,156,157]. However the use of linear regression and LDA in direct neuron recording or EMG neuroprosthetic devices performs similar to a threshold detector that reduces to a binary ON/OFF switch. This over simplification combined with the limited number of recording locations do not reflect or promote understanding of the naturally occurring neuromotor control strategies used by the brain during reaching and grasping. In addition, the need for *a priori* specification of information related to the data being analyzed does not promote flexibility in application or tolerance of real-world noise effects.

On the other hand, when models fail to account for the data set or if extraction and classification tools are not able to perform well, there is a high tendency to create

models or to use extraction and classification tools of increasing complexity. However, the increase in complexity does not guarantee accurate results, rather it reduces the ability to apply and use such models or pattern identification tools in practical applications due to the resulting higher computing cost [63,173]. The concern for computing cost is also prevalent with many of the pattern identification and extraction procedures such as nonlinear dynamics, ICA and PCA that require iterative processing. This is a further concern because most pattern identification methods cannot provide causal modeling of a system as it evolves in time, and to do so would require tremendous computer processing power. While offline data processing would allow addressing the issue of computing resources, this does not provide for a viable real-time application for upper extremity neuroprosthetic applications.

A third limitation of most current brain models is the focus on a limited number of brain regions that are often located on the surface of the cortex. Deep brain structures such as the thalamus or the cerebellum are often excluded from these models This is largely due to the recording techniques used, such as EEG or MEG, that are only able to capture data from the surface of the brain. The use of PET and fMRI in functional studies has been concentrated on specific regions of the brain such as the motor, sensory and parietal cortex. The assumption that all relevant information arises from a limited number of brain areas and the over simplification by recording techniques does not adequately capture motor strategy, and information flow across anatomical regions of the brain. This limitation is also seen in analysis performed using feature extraction and data classification tools that often simplify data sets through dimension reduction resulting in 2-D data sets and the loss of spatial localization. Data acquisition methods such as direct

neuron recording can only collect data from a few selected regions of the brain. Using this recording modality, activation is determined based on threshold detection. Studies have shown that morphological changes at the electrode insertion site occur when implanted electrodes are employed, and there is a decrease in signal over time [90]. Such a signal reduction over time would severely affect threshold detection algorithms such as LDA, regression and also other statistical methods such as spatial statistics, connection networks and nonlinear dynamics, thereby rendering them ineffective.

A final limitation of contemporary brain models and pattern analysis techniques lies in the data used for the development of such models. Often, most of these models use data collected from subjects who are performing non functional tasks such as finger tapping, virtual reality interaction or cognitive processes that require visual imagery. Such experiments produce data that resembles functional mapping but do not provide information that relates to the strategies that are specific to the performance of functional tasks. Developing models using data that does not adequately represent the natural neuromotor strategies of functional tasks would lead to imperfect representations of naturally occurring neuromotor strategies in the brain. Overall, this would cause inaccuracies in the control of neuroprosthetic devices leading to more effort in training or the encouragement of developing unwanted compensatory behaviors.

2.5: THE DEVELOPMENT OF AN UPPER EXTREMITY BRAIN MODEL FOR NEUROPROSTHETIC CONTROL.

The focus of this dissertation is to develop a brain model that will serve as the proof-of-concept for an upper extremity feed-forward neuroprosthetic controller. An ideal

upper extremity neuroprosthetic controller model should be able to predict movement of the upper extremities using naturally occurring information from planning or movement intention. This is important in order to provide a target neuroprosthetic device with real-time control options and to mimic as closely as possible the functionality of an actual limb. Secondly, an ideal model for upper extremity neuroprosthesis control should adequately account for natural neuromotor strategies as represented in the brain; this is a distributed process involving several brain regions [74,75]. A central purpose in the development of this brain model is to adequately capture the naturally occurring neuromotor strategies that relate to movement intention. This is achieved by understanding and incorporating the concomitant neuro-anatomical regions and associated brain signals that are involved with functional upper extremity tasks. This model is not limited to a single region of the brain but rather uses information from all regions that contribute toward functional upper extremity movements.

Such features in a whole brain model for upper extremity neuroprosthetic control are paramount to providing the user with a platform that can promote the use of natural brain strategies relating to upper extremity function. It is hoped the emphasis on natural brain strategies in the model will allow faster learning and device acceptance, better control and more consistent long term recovery, while minimizing the risk of developing compensatory behaviors and frustration with neuroprosthetic device use. In addition, it is hoped that the emphasis on incorporating natural brain strategies with brain anatomy enhances the potential of a robust brain model that can accommodate various patient populations. Individuals who suffer from different pathologies such as limb loss, spinal cord injury and perhaps even stroke and cerebral palsy will benefit from this upper

extremity brain model because its development is not tied to a specific pathology or anatomical location of the brain [50]. A common characteristic of chronic upper extremity pathologies are the presence of spared cortical regions. These regions have a high probability of containing information related to reaching and grasping and corresponding neuromotor strategy encoding that can be used for upper extremity neuroprosthetic control.

Furthermore, the development of a whole brain model has the potential to serve as an assistive device and also as a measurement tool. There is no reliable method of quantifying activation in the cortex or the lack thereof during functional upper extremity task performance to date. As the central design of the model is rooted in naturally occurring signals from specific neuro-anatomical regions, changes in the signal pattern or intensity can be analyzed to determine characteristics of learning, of adaptation, or to quantify the effects of brain injury.

The proposed upper extremity brain model will be designed using fMRI data acquired from neurologically intact subjects. This method of data acquisition was chosen for three main reasons, the first is that fMRI provides three dimensional images of cortical activation and anatomical information in a non-invasive manner. Second, when compared to other imaging modalities, such as Positron Emission Tomography (PET), fMRI does not require the injection of radioisotopes and can be performed quickly. Lastly, research using fMRI has shown distinct stimulus activation in regions related to upper extremity motor performance, task planning and sensory feedback [174,175]. Further research has shown that subjects can be trained to produce fMRI activations that

can be controlled for different tasks to yield extractable control signals that can be used in potential neuroprosthetic control applications [176,177].

In practical applications it would be unrealistic to have patients moving about with fMRI scanners attached to their heads to control a neuroprosthetic device. At this moment in time, the practical application of the described whole brain model is limited due to restrictions in having portable whole brain sensors that are capable of measuring blood flow or perhaps direct detection of signals from many regions in the brain. However this whole brain model was developed as a proof-of-concept for upper extremity neuroprosthetic control. It is important to highlight the use of information from the entire brain, to use functional tasks that use real world objects in order to adequately capture natural neuromotor strategy as represented in the brain. The second goal of this model is to show the feasibility of modeling natural neuromotor strategies and to illustrate the advantages of this method such as reduced training, calibration and modification of behaviors for practical application as an upper extremity neuroprosthetic controller.

2.6: FUNCTIONAL MAGNETIC RESONANCE IMAGING (fMRI).

Motor, sensory and cognitive processing occurs in the brain by virtue of the interaction of several brain regions [74,75]. Information is relayed by neurons using chemical signaling mechanisms and electrical potentials. This is an active process and requires energy in the form of adenosine triphosphate (ATP) [74,75]. ATP is an oxidative process that requires oxygen and glucose. An adequate and steady supply of glucose and

oxygen are needed. This is achieved through the vascular system in which glucose and oxygen are transported to active neuronal sites by blood. During elevated levels of neuronal activity, there is a corresponding increase in the metabolic rate which is supplied by the vasodilatation of feeding vessels of the local capillary beds within the activated region of the brain. Vasodilatation causes an increase in cerebral blood flow and blood volume. Oxygen bound in the hemoglobin molecule causes the iron centers in the hemoglobin to be shielded from the local environment, rendering the molecule diagmagnetic [174,175]. When the oxygen molecule is released from the hemoglobin, the conformational change in the protein exposes the iron centers more fully, causing the molecule to become paramagnetic. At the time of activation, the bulk magnetic character of the blood turns from slightly paramagnetic to diamagnetic [174,175]. The shift from paramagnetic to diamagnetic in the blood lengthens T2* relaxation time of protons in the nearby parenchyma causing a small (1-3%) increase in the signal when sampled with a T2* sensitive sequence such as echoplanar imaging [174]. This process is termed the Blood-Oxygenation-Level Dependent (BOLD) contrast that can be measured using MRI [174,175].

The BOLD effect was first described by Ogawa from Bell Labs [178]. In experiments using rats, changes in blood oxygenation of the rats brains were induced at specific intervals by altering the metabolic demand or blood flow within the brain. During these induced changes to blood oxygenation, the rats were imaged with a gradient echo MRI. Changes in the blood oxygenation were observed to revealed structural differences and visibility of blood vessels within the rats brains. Furthermore, the early human experiments that examined the feasibility of using the BOLD principle as the

underlying contrast mechanism were performed simultaneously by Bandetinni from the Medical College of Wisconsin on a human subject who performed a motor task consisting of finger tapping in a 1.5T MRI scanner [179]. Changes in regional signal intensity in the primary motor cortex were observed that corresponded to the finger tapping task being performed. Simultaneously work by Kwong used visual and motor stimulation that confirmed these findings and furthermore showed the presence of distinct activation regions in the visual cortex and primary motor cortex for the visual and motor stimulations respectively [180].

The BOLD hemodynamic response is not a direct measurement of neuronal activity, but rather it is a surrogate of neuronal activity. The literature suggests that the amplitude and peak response duration are influenced by the intensity and duration of a corresponding stimulus. The exact shape (ie: amplitude and duration) of the BOLD hemodynamic response is still under extensive research [174,175]. The onset of the BOLD activity is approximately 1 – 2 seconds after onset of the stimulus. Some studies have reported the presence of an initial ‘dip’ at the start of the response and this is believed to be attributable to the initial increase in deoxygenated hemoglobin that reduces the local regional signal [180]. However the mechanisms of this initial dip is not agreed upon because it cannot be consistently replicated across fMRI experiments [174]. The maximum peak of the BOLD response is achieved between 5 – 7 seconds after the onset of neuronal activity and would result in a plateau of approximately 2 – 3 seconds. This plateau would increase in duration if neuronal activity was prolonged. At the conclusion of neuronal activity, the BOLD response experiences a period of ‘undershoot’ where the

BOLD response drops below the baseline for a recovery period of approximately 3 – 5 seconds before returning to the baseline value (figure 2.2) [174,175].

FIGURE 2.2: Ideal BOLD Response [174].

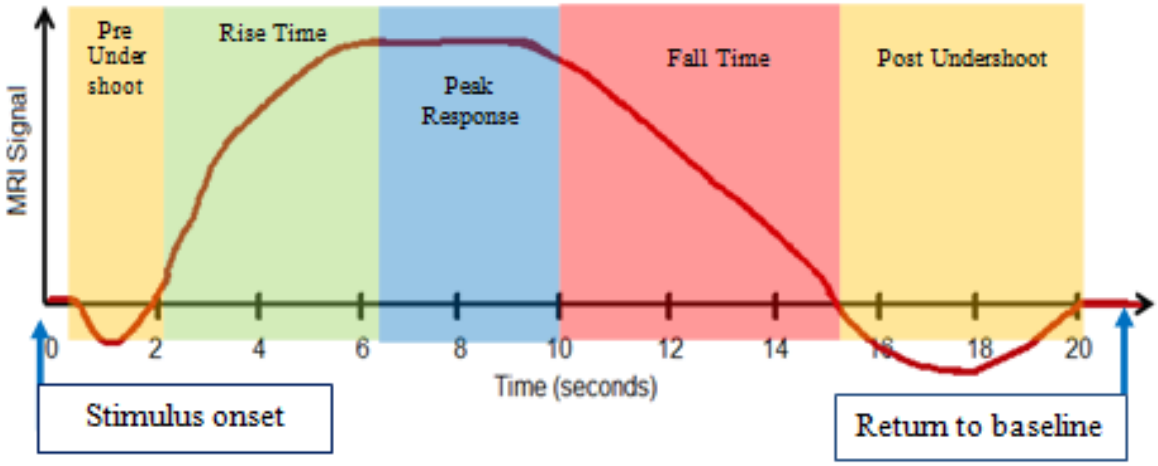

It is the temporal characteristics of the BOLD signal that have enabled the development of experimental paradigms such as block and event related design paradigms that allow the study of brain function.

2.7: CHAPTER CONCLUSION.

The understanding of the pathologies that induce chronic upper extremity physical dysfunction and effective associated treatment options is a crucial step in developing appropriate new therapeutic tools. A review of present upper extremity neuroprosthetic devices highlights the current state of the art for these devices and reveals the areas that need improvement for neuroprosthetic control. The identification of potential benefits of upper extremity neuroprosthetic systems has set a new frontier in the realm of therapeutic

and intervention options needed to treat chronic upper extremity physical dysfunction. The main objective of this study is to develop a whole brain model that adequately captures natural upper extremity neuromotor strategies. This model is to serves as a proof-of-concept for future neuroprosthetic controller development. In the long term, such a model is important because it suggests the basis for technology aided natural neuromotor control based therapy. It is hoped that by employing natural brain models and strategy, lasting functional restoration can be obtained.

CHAPTER 3

Cortical Region Identification Relating to Upper Extremity Function

3.1: ABSTRACT.

This chapter explores cortical regions and their corresponding activation patterns that relate to goal-oriented upper extremity movements. This information is crucial to understanding the relevant anatomical regions of the brain that contribute to strategy, mediation and execution of functional prehension. A robust upper extremity neuroprosthetic controller needs to appropriately account for the neural correlates of upper extremity function. The design of this experiment is novel because many fMRI studies only focus on rhythmic movements such as finger tapping and do not incorporate real world objects. Subjects (N=18) performed three actual motor tasks and corresponding motor imagery tasks in a block paradigm. The use of motor imagery tasks was to serve as surrogates to determine factors that relate to planning, initiation and sensory integration. The results suggest the presence of distinct, common and overlapping regions for each of the different motor and motor imagery tasks. These findings suggest the sharing of some basic common strategy for upper extremity function and the presence of task specific strategy. Furthermore the results from the reaching and grasping motor task and reaching only motor task indicate that there are distinct differences of activation patterns within specific regions of the brain. These results are important because they show that the extrapolation of strategy from finger tapping tasks cannot completely account for strategies used during goal-oriented reaching and grasping.

3.2: BACKGROUND.

3.2.1: Upper Extremity Neuroprosthetics and Neuromotor Control.

The first step to develop a robust upper extremity neuroprosthetic controller is to understand the neural correlates of upper extremity movement as represented in the cortex. Early results from electrophysiological studies involving direct stimulation of the cortex have determined that the brain is somatotopically organized [74,75]. Each anatomical region of the body and its sensory, motor, and functional representation is mapped to specific regions of the cortex and cerebellum. Within the primary motor and sensory cortices, this specific mapping is known as the motor homunculus and sensory homunculus respectively as shown in figure 3.3 [74,75]. This specific organization of the brain requires the interaction of several cortical regions to realize strategy and control of upper extremity movements. Information processing in the brain relating to functions such as planning, execution, sensory feedback, learning and movement correction are distributed across several regions that work in series and parallel [74,112,181,182]. Information is transmitted directly from cells in one region of the cortex to another adjacent region by means of projecting axons, or through indirect pathways consisting of axons that link several cortical regions [181,182]. Further, the neuronal cell bodies act to sum both facilitory and inhibitory inputs. The axon then carries the action potential to the dendrites through synapses where most information transmission is mediated by the excretion and detection of chemical transmitters. Supporting this neurochemical transmission as well as the recycling of neurochemical messengers requires the supply of glucose and oxygen [75,181,182].

FIGURE 3.1: Main Anatomical Regions of the Outer Cortex. Image rendered using AFNI and SUMA.

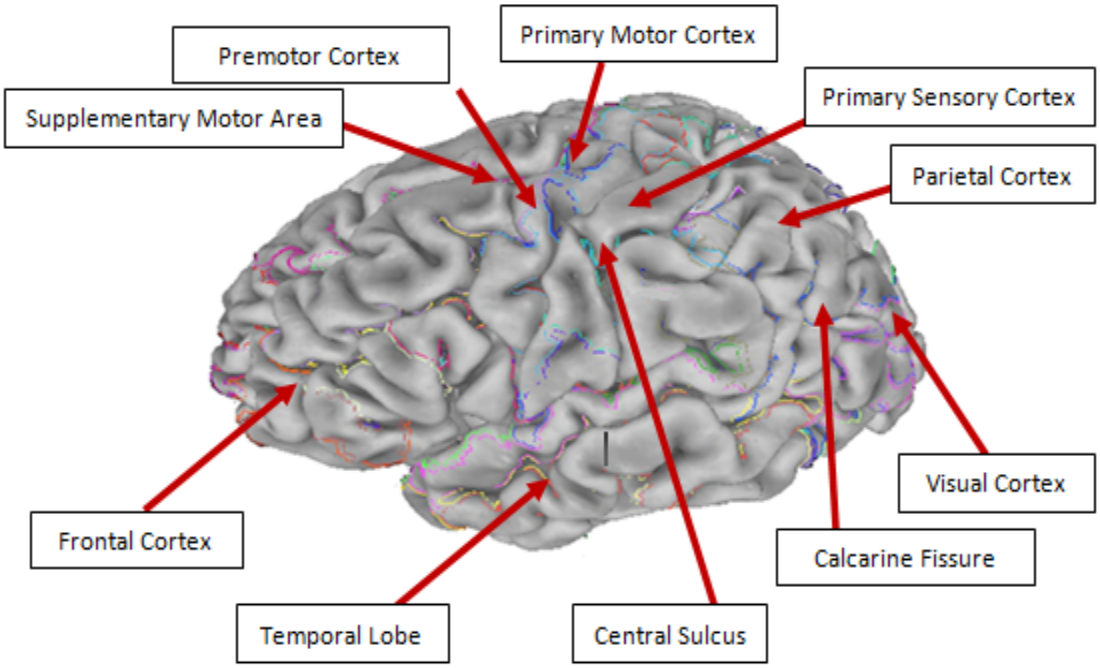

FIGURE 3.2: Main anatomical regions on the inside of the Cortex. Image rendered using AFNI and SUMA.

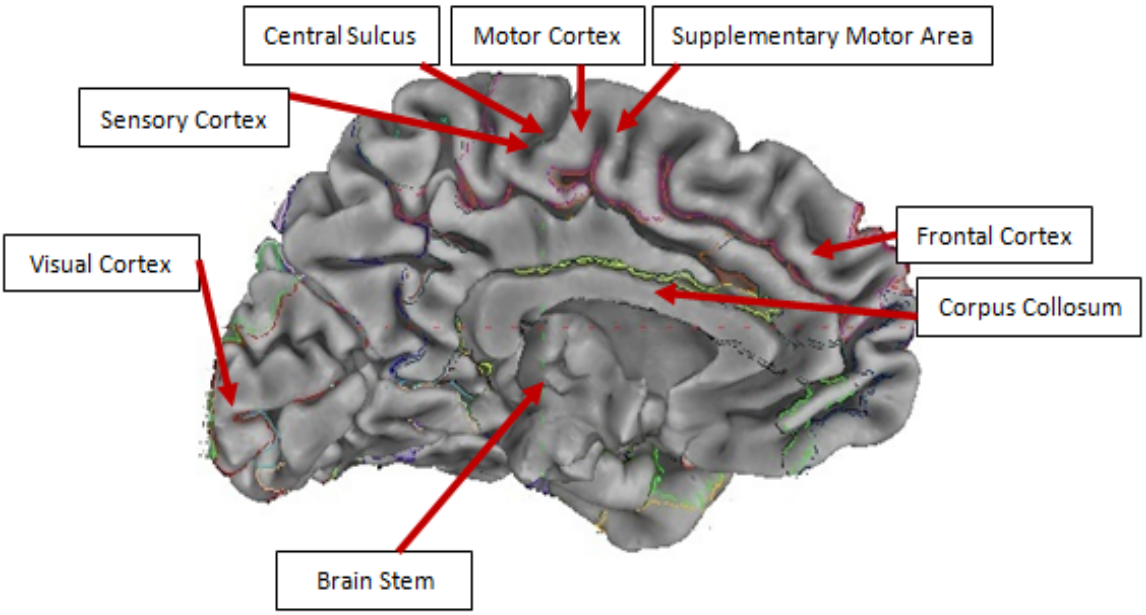

FIGURE 3.3: Homunculus of Primary Motor and Primary Sensory Cortex.

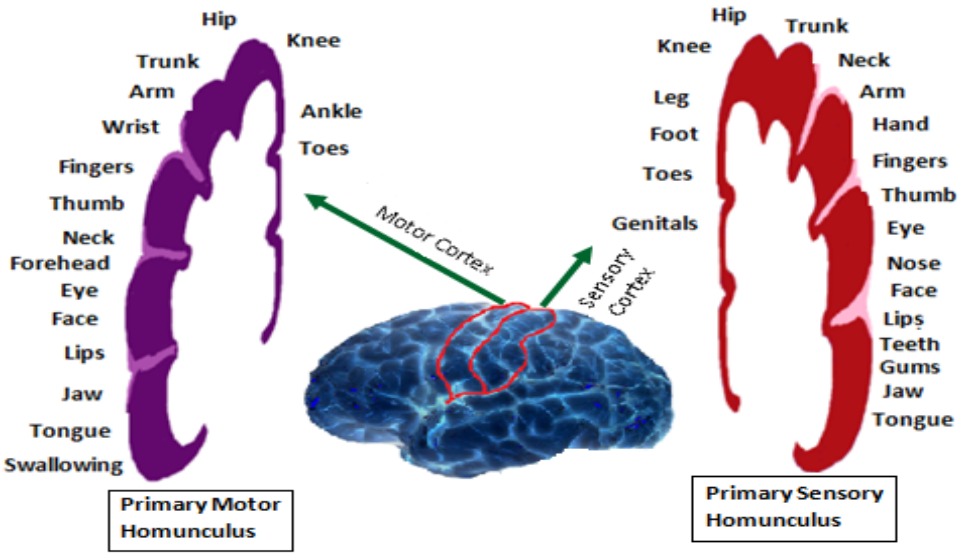

The primary motor cortex is located on the anterior bank of the central sulcus. This region receives its input from the thalamus, basal ganglia, supplementary motor area (SMA) and premotor area [183]. Information to and from the primary motor cortex originates from the premotor cortex, SMA, thalamus, motor nuclei of the brainstem, cerebellum and spinal cord through multiple pathways [183]. The motor cortex is responsible for initiating movement and is instrumental in the regulation of fine precision movements [74,112,183]. Upper extremity movement is controlled by the motor cortex of the cortical hemisphere that is contralateral to the limb [183]. The primary sensory cortex is located posterior to the central sulcus. It is in this region that all sensory information, especially key sensory feedback such as proprioceptive and haptic information is processed [75,112,183]. Information feedback to the primary sensory region comes from the contralateral side of the body in a manner similar to the primary motor cortex [183]. The premotor cortex and SMA are located on the anterior portion of the precentral gyrus

[183]. These regions are thought to be involved with the planning and organization of movement and actions that are rhythmic or sequential in nature [112,183]. The parietal lobe is posterior to the sensory cortex [183]. The specific role of this region is not clearly understood. In primate experiments, the posterior parietal region has been associated with forming upper extremity movement strategies in an area called the posterior parietal reach region [184,185]. However, in human subjects, it is thought that the posterior parietal region is involved with sensory motor integration and for organizing motor strategies [74,75,112,187]. This is achieved through interaction with the premotor cortex, primary motor cortex and SMA prior to movement [74,75,112,183].

Deep structures of the brain are also involved with functional reaching and grasping. One such region, the thalamus has been labeled the 'relay station of the brain' because it is responsible for receiving and integrating neural signals from the brain stem and spinal cord with the cerebral cortex as well as providing inhibitory feedback to the motor cortex [74,75,112,181-183]. The cerebellum is responsible for the execution of smooth and accurate movements, often relating to hand-eye coordination, as well as timed movements [74,75,112,183]. This is achieved by movement error detection and correction and it is hypothesized that the cerebellum contains multiple homunculi within itself that allow the comparison and error correction to occur accurately [183].

Early work that identified cortical region function was largely based on direct stimulation of the cortex or through clinical studies that examined the effects of injury to specific parts of the brain. Often the resulting motor and cognitive deficits were observed and post mortem analyses of the brain would be performed to determine anatomical changes from structural abnormality caused from disease or injuries [186]. With the

development of imaging modalities such as Computer aided Tomography (CT), Positron Emission Tomography (PET) and fMRI, the anatomy and function of the brain could be correlated in a noninvasive manner [186].

However, the specific manner in which each of these regions interact with one another, and the extent of distinct and overlapping function is not completely understood within the context of a particular task. Results from imaging studies that have examined upper extremity tasks such as planning of movements and execution of simple motor tasks have shown variations in activation patterns and regions [188,189,273]. It is hypothesized that discrepancies are the result of limitations that are specific to the recording modality and the design of the experiment paradigm. A majority of the imaging and direct neuron studies that have addressed cortical activation in sensory and motor stimuli have been limited in obtaining data from specific regions of the cortex. Surface recording modalities such as EEG can only collect information from the surface of the skull and the use of direct neuron recording or fMRI have focused on specific cortical regions such as the primary motor cortex, parietal cortex, regions of the cerebellum or SMA [188,189]. Many studies do not account for the entire brain and the other cortical regions that are activated during task performance. In view of the fact that information processing and strategy relating to the performance of voluntary upper extremity movement involves multiple cortical regions, it would seem that focusing on a single region and ignoring the others creates an incomplete view of neural correlates of movement, and suggests that information loss has occurred.

A second major limitation of many current imaging studies is the use of rhythmic movements of the digits and wrist, with little emphasis on the complete reaching and

grasping process. In addition, very few studies incorporate the use of real-world objects in their experiment paradigms. Rhythmic tasks such as finger tapping perform well for the identification of specific cortical motor and sensory areas, and are similar to homunculus mapping [190]. Although there is some overlap in strategy and the anatomical representation of rhythmic and non-functional movement within the cortex, there is a lot of task specific strategy that is specific for goal-oriented upper extremity movements. Motion analysis studies have determined the presence of differences in strategy as expressed by kinematic properties of the limbs during rhythmic and goal-oriented upper extremity movements [191-193,275]. Furthermore, the importance of specific goal-oriented movements with real world objects have been shown to produce better recovery in physical therapy studies, as compared to rote movements of the upper extremities [194-197]. Therefore, extrapolation of strategies from rhythmic movements of only the hand, digits or wrist do not necessarily produce accurate representation of strategy used during functional goal oriented movements that involve reaching and grasping real-world objects such as would be used during normal daily interaction with the environment. Such simplification of movements previously used in experiment paradigms limits the understanding of cortical region activation involved in planning, control, error correction and mediation.

A third major limitation of upper extremity imaging studies is the incomplete understanding of the neural correlates pertaining to neuromotor control strategies used by the brain to realize voluntary upper extremity movements. More specifically, the linkage of upper extremity movements, their kinematic and kinetic properties correlated with actual cortical activations is very limited. The concept of an internal model is proposed in

the literature as a method that is used within the brain to dictate strategy selection and produce accurate and meaningful upper extremity movements [198-204]. The notion of an internal model can be viewed from a physiological perspective and from an engineering applications perspective. From a physiological perspective, an internal model describes how information regarding movement initiation, planning, execution and error correction is conveyed to the various functional regions of the brain. The important aspect from a physiological perspective is an understanding of how these regions of the brain interact with each other, the extent of activation, intensity and duration of excitement or inhibition for each distinct brain region.

The specific manner in which an internal model is represented or used from an engineering applications perspective depends on how the internal model performs information representation, retrieval and processing tasks. There are several theories pertaining to upper extremity neuromotor control and the complete representation, use and behavior of the internal model is the subject of significant debate [205-211,276,277]. One approach is to consider the internal model as analogous to a video recorder that plays back specific movements. The movements are learned through practice and then stored in long term memory for retrieval in the future. However, this type of representation would require a single ‘movie’ for each movement intended to be performed and requiring significant effort to learn the movements resulting in increased lag times for motor responses. Overall, on its own, this is not a practical solution. An alternative explanation is that the internal model is a robust and adaptive system that can accommodate different situations without the need for extensive learning. To achieve this, there would have to be short and long term memory units that are accessed through a combined set of weights or

rules. These controlling parameters would then dictate the use of specific movements and other more general motor schemes. Fine tuning of the control rule and weights is achieved over the course of cognitive and physical development and through the performance of various motor tasks in daily life. When relating this to cortical anatomy, activation in a specific region is not solely based on the firing of a single neuron, but rather a collective group of neurons firing in synchrony to produce a summed output in a specific region [74,75,181,182]. The combination of strategies from several brain regions, revealed by their activations, lead to the performance of meaningful and accurate upper extremity movements. It was initially believed that the internal model resides in a single region of the brain, however some studies have suggested the presence of multiple internal models that are present within several brain regions used simultaneously during functional task performance [212,213].

3.2.2: Motor Imagery.

As the saying goes, ‘a penny for your thoughts’, cognitive processing consists of a huge range of signals that activate many regions of the brain. The ability to parse out the specific aspects of cognition that relate to upper extremity motor control is a significant challenge. Motor imagery of actual movements has been determined to be a reliable representation for task planning and initiation of neuromotor control for upper extremity movement [214-216, 278]. Motor imagery is different from visual imagery or mental ideation. The latter is a more general form of eliciting thoughts that are general and may not directly relate to the present task or to neuromotor control [215]. Motor imagery

consists of specific thoughts that pertain to the kinesthetic sensation of moving and controlling the limbs in preparation for goal oriented movements [215]. The ability to actively visualize the limbs performing a motor task enhances sensory feedback during the subsequent performance of the task and is important for movement planning, initiation, correction and learning.

Functional imaging studies that have examined the cognitive contents of motor imagery have largely focused on finger tapping tasks or other indirect motor representation and stimuli [217-219].Various regions such as the parietal cortex, SMA, primary motor cortex, primary sensory cortex, frontal cortex and cerebellum show activation during functional motor imagery, however the results from imaging studies seem contradictory at times [217 – 219,279,280]. It is hypothesized that although a general motor strategy may be present for neuromotor control that results in brain regions experiencing common and overlapping activation, however there are specific strategies manifested as specific activations within the brain that pertain to goal-oriented functional upper extremity motor tasks [281,282]. These task specific activations many not have been adequately studied through experiments that employ rote tasks, for rote rhythmic movements do not accurately translate into goal-oriented movements [284]. In addition, the majority of the experimental paradigms used in most motor imagery studies have focused on auditory or visual cues without direct feedback of limb position or movement. The use of virtual reality interfaces in functional imaging studies may require modifications of behavior and the utilization of neuromotor strategies. Such changes do not necessarily reflect actual neuromotor strategies used by the upper extremities during functional task performance in the real world. Lastly, the use of real world objects is an

important part of motor imagery and has been determined to produce stronger activations as compared to performing tasks with only auditory or visual cues [220,221].

3.2.3: Study Goals.

The first objective of this study is to map activated region in the whole brain during functional reaching and grasping motor tasks with real world objects. This study compares the performance of three specific goal-oriented upper extremity motor tasks using real world objects and the corresponding activation patterns in anatomical regions of the brain. The hypothesis for specific aim one is whole brain activations by motor tasks that involve functional reaching and grasping of real world objects can be mapped using fMRI.

The second objective of this study is to map activated regions in the whole brain during motor imagery of functional reaching and grasping tasks. This is achieved through the use of motor imagery tasks of three distinct hand movements, which are reaching, grasping and a combination of reaching and grasping. The hypothesis for this second objective is whole brain activations during motor imagery that involve functional reaching and grasping tasks can be mapped using fMRI.

The third objective is to compare activation maps of real motor tasks with motor imagery fMRI results. This is important to understand and quantitatively examine the extent of distinct and overlapping activations in cortical regions that correspond to the specific motor and motor imagery tasks.

3.3: DATA PRESENTATION AND FLAT MAPS.

The optimal method of presenting functional data of the entire brain with adequate visibility and compactness while minimizing data distortions is a challenge. Traditional cardinal views of axial, coronal and sagittal orientations for fMRI data would result in a large number of figures that are needed to present activation in several regions. Other forms of data representation such as the smooth, ellipsoid and native 3D brain models are not without their tradeoffs and ultimately culminate in a large number of figures needed to display activation in outer and inner brain structures. The use of cortical flat maps is an effective means of viewing functional brain data that involves multiple cortical regions that are activated simultaneously [222]. The flat map is based on the Visible Man atlas in which virtual incisions are made at key locations and the cortex is 'unfolded' and flattened [222]. This allows for a compact representation of the hemispheres and the cerebellum separately.

FIGURE 3.4: Flat Map view of the Cortex, showing Right Hemisphere [222].

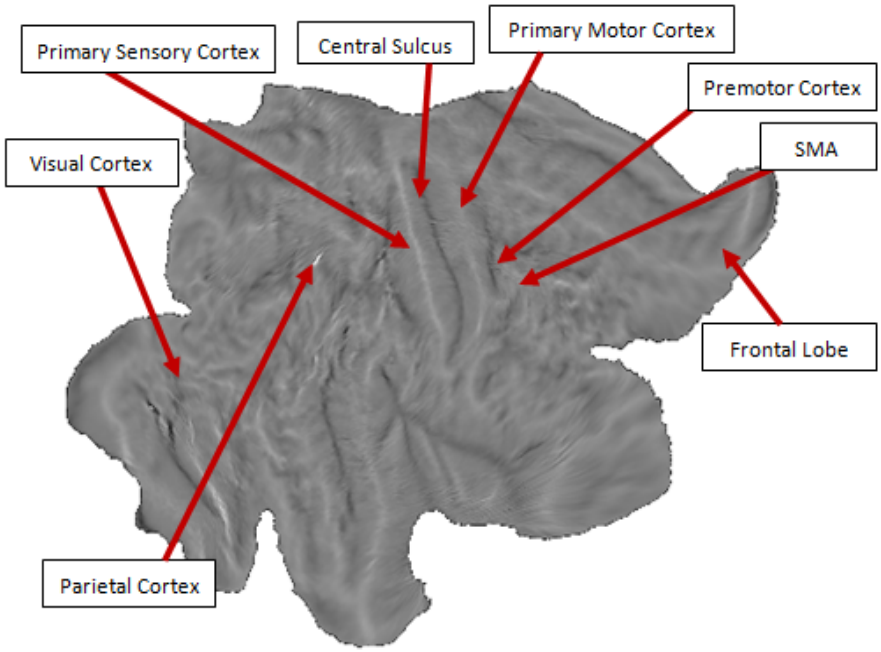

3.4: METHODS.

A total of 19 neurologically intact volunteers (M = 12 F = 6 mean age 22.5 years) were recruited for this study. Only one subject was dropped due to claustrophobia and the inability to participate in the study. Subjects were handedness were determined using the Edinburgh handedness survey (17R and 1L) [223]. The study was approved by the Institutional Review Boards of the Medical College of Wisconsin and Marquette University. Prior to the start of the experiment, subjects were screened using the Medical College of Wisconsin MRI safety screening questionnaire to ensure safety compliance with MRI scanning requirements.

3.4.1: fMRI Scanner Parameters And Pulse Sequences.

Data was acquired using a 1.5T General Electric (GE) Signa MRI scanner [General Electric Healthcare, Waukesha, WI, USA] that was located in the Department of Radiology of the Froedtert Hospital. Subjects were instructed to lie supine in the scanner. An 8-channel high resolution head coil was used during data acquisition. To reduce head movement, a set of head sponges were placed between the subject's head and the head coil. The subject was also provided with a pair of ear buds to attenuate the MRI scanner noise. A knee bolster was used to ensure subject comfort during experimentation. A high resolution anatomical data set was collected for functional data localization (SPGR pulse sequence, echo time (TE) of 2.984 ms., image repetition rate (TR) of 7.78 ms., flip angle of 10º, field of view (FOV) of 24 mm., slice thickness 1.3 mm., 256x192 matrix with 120 slices acquired in the Axial plane, individual voxel dimension of 0.09375x0.9375x1.3 mm.). This high resolution anatomical image was collected at the start of the experiment

prior to the functional data acquisition. A Gradient Echo - Echo Planar Imaging (GE-EPI) pulse sequence was used for acquisition of the functional data (TE of 40ms, a TR of 2s, a flip angle of 90º, a FOV of 24mm, data matrix of 64x64 with 29 slices and a slice thickness of 5mm, no gap and acquired in the sagittal plane, individual voxel dimension of 3.75mm × 3.75mm × 5mm). The functional data was acquired in the sagittal plane as this orientation allowed maximum coverage of the brain from the frontal lobe to the cerebellum without sacrificing relevant anatomical and spatial information.

3.4.2: Experimental Paradigm.

A block paradigm consisting of alternating 'RELAX' and 'TASK' states was designed. The total duration of the paradigm was 3 minutes long with each state lasting for 30 seconds and repeated 3 times each during the paradigm. For the 'RELAX' state the subjects laid still in the scanner and during each 'TASK' state the subjects performed 15 repetitions of the instructed movement task at a rate of 1 repetition every 2 seconds within the 30 second task block. Timing of the task performance was cued by the appearance of the task appropriate word every two seconds. This assured a constant task rate. Activation levels have been previously shown to vary with the repetition rate of the function [250]. The subject was guided using a custom developed visual cue that was back projected through an MR compatible LCD projector [Avotec, Inc., Stuart, FL, USA]. The visual display screen was attached on top of the head coil and adjusted for clarity of vision prior to the start of the experiment.

FIGURE 3.5: Experiment Block Paradigm.

A custom developed video cue was used to inform the subject of the state and the task to be performed. A total of 6 tasks were performed separately following the above 3 minute block paradigm. These tasks consisted of motor imagery tasks and actual motor tasks. During the motor imagery tasks, the subjects did not move their limbs but were asked to imagine performing the movement. In order to maximize motor imagery efforts, the actual motor tasks were presented first followed by the motor imagery counterpart in the preceding paradigm. The tasks performed are listed in table 3.1.

TABLE 3.1: Tasks and Descriptions

Task	**Description**
Real Reach and Grasp	1.Reach out and grasp target 2. Release target. 3. Return to start position
Imagined Reach and Grasp	Imagine performing reaching and grasping movement of target
Real Reach	1.Reach out and touch target without grasping 2.Return to start position
Imagined Reach	Imagine reaching out and touching target
Real Grasp	1.Grasp target in hand 2. Release target.
Imagined Grasp	Imagine grasping target in hand and releasing

Prior to the start of the paradigm, the subjects were instructed as to which task was to be performed. Upon completion of the paradigm, the subject was queried regarding their comfort and ability to perform the task. The target used in this experiment was an MRI compatible sponge ball mounted on an acrylic handle and secured to a Delrin™ base. The target was secured to the patient table using Velcro™ straps and was adjusted to be within easy reaching distance of the subject laying supine in the scanner. The experimental set up is shown in the following figure 3.6 and the sponge ball target is shown in figure 3.7.

FIGURE 3.6: Experiment set up showing human subject lying in scanner with mounted sponge ball target mounted at a reachable location. The knee bolster was used to provide back support and head sponger were placed between the subject's head and the head coil to reduce head movement. A viewing apparatus was attached to the top of the head coil to enable the subject to view the visual cue.

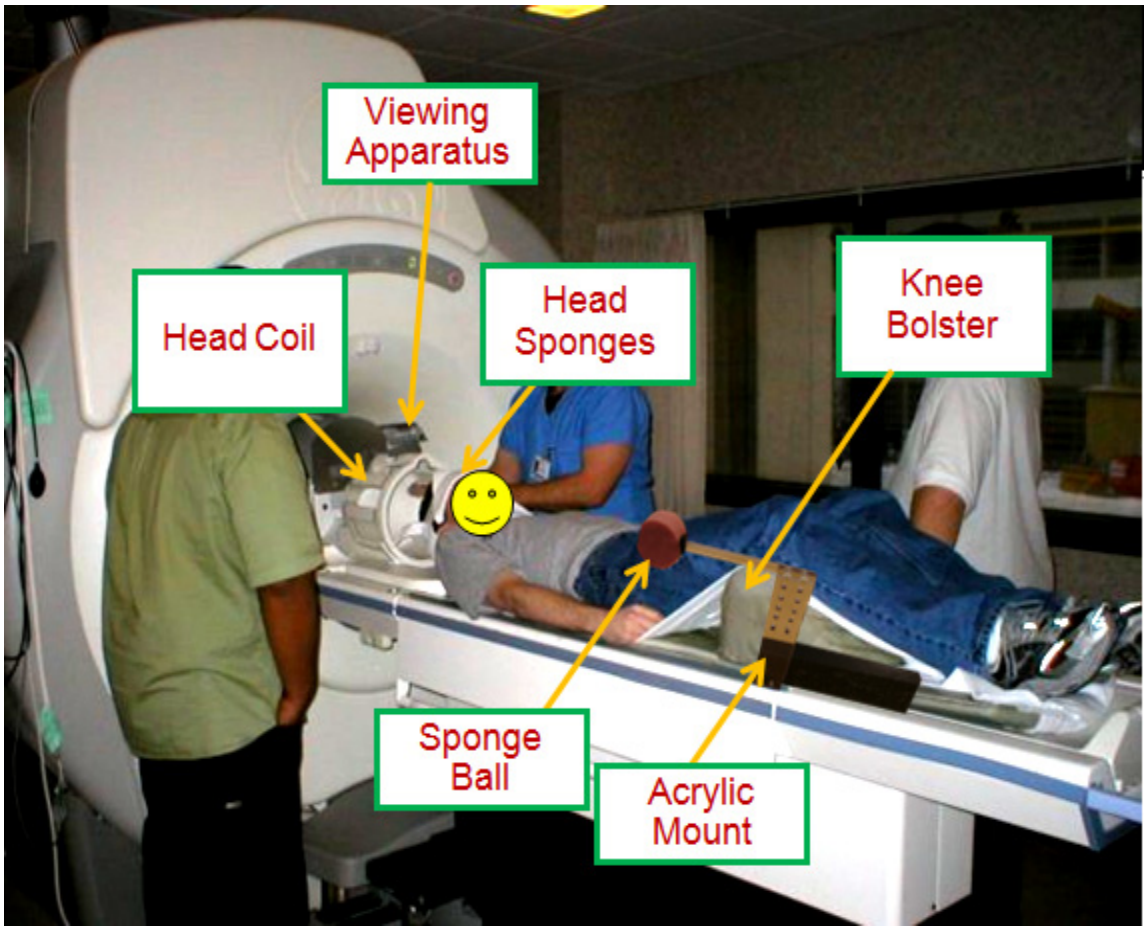

FIGURE 3.7: Sponge ball target mounted on adjustable Acrylic and Delrin base.

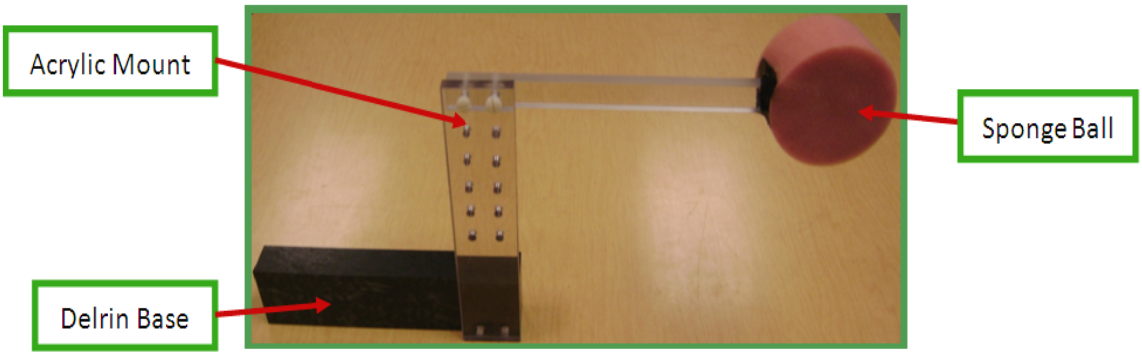

3.4.3: fMRI Data Analysis.

Reconstruction of the raw acquired *k*-space data was performed by the Signa MR System with the product reconstruction. The reconstructed images were transformed into anatomical and functional MRI datasets respectively, using the Analysis of Functional Neuro Images (AFNI) software package [224]. All processing was done using custom written AFNI scripts. The reconstruction program saved the data sets into a pair of files that were in HEAD and BRIK format. To correct for subject movement during the data acquisition, 3D volume registration was performed on the data sets by aligning each dataset to repetition #45 of the data set acquired during the first block paradigm, immediately after acquisition of the anatomical data set.

In order to determine regions of activation, a cross correlation analysis was done in a voxel-by-voxel manner between the raw data and a specified reference waveform. During this analysis, the first 3 data points were discarded to account for the equilibration of longitudinal magnetization. The reference waveform was obtained by convoluting the ideal series of events as shown by the blue plot in figure 3.3 with the gamma variate function resulting in the reference function shown in the red plot of figure 3.3 [224].

FIGURE 3.8: Ideal waveform (blue) and gamma variate convolved waveform (red).

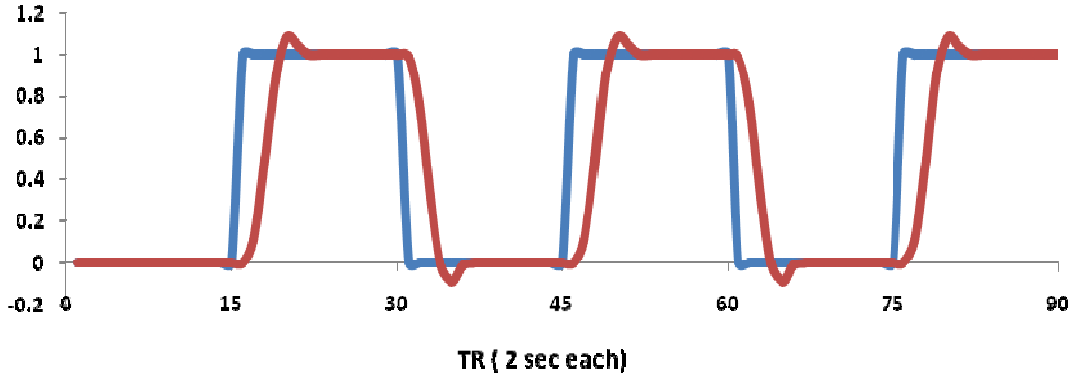

To determine regions of activation, the reconstructed fMRI time series data sets were cross correlated voxel by voxel with the expected fMRI response to the stimulus yielding the Pearson's Correlation value. Following this, all of the individual data sets were transformed into Tailarach space using the TTN27 brain template [224]. A 3D *t*-test was done on the group data on a voxel-by-voxel manner to determine regions of activation and to compare activations within and across the real and motor imagery tasks [224]. An anatomical mask as created using the TTN27 EZ ML brain template and region specific voxels that were deemed significant by the *t*-test within each region were saved to a file. The specific activation of a region was determined by computing the percent region activation by dividing the number of voxels with the total number of voxels within that specific region. Using custom written programs, these data files were exported from AFNI in MATLAB [Mathworks Inc., Natick, MA, USA] and the results tabulated in table 3.4.

The false discovery rate (FDR) method of thresholding was used to determine the level of activation [225]. The FDR method controls for the total number of voxels falsely declared active. This method of thresholding is more powerful for large data sets as

compared to familywise error rate (FWER) correction methods. This is because FWER methods such as Bonferonni correction seek to control for the probability of having even one false discovery over the entire data set [225]. When working with large numbers of data sets and multiple tests, the FWER correction method is too conservative. Even relevant information may be lost in regions that are known to be active. The FDR correction produces a q value that is specific to the level of activation within a dataset, thus having a fixed q value across data sets will not always result in similar p values. A conservative q value of 0.01 was chosen as the threshold for all the data sets [225].

3.4.4: Sample Size Calculation.

The signal data in 3 predefined regions of interest (ROIs) were examined for 5 subjects to determine appropriate sample size, power and statistical significance. These regions were the supplementary motor area (SMA) for the motor imagery tasks, the primary motor cortex (PMC) for the real motor tasks and a region that had no activation in both types of tasks. The SMA and PMC were chosen because these regions yield the most activation for the motor imagery and real motor task respectively. A custom written MATLAB program was used to analyze the signal extracted from these regions and to calculate the intra-subject variability and the, percent signal change, within ROI variability and inter subject variability [226].

3.4.5 : Quantitative Analysis of Motor Task and Motor Imagery Types.

A 2 factor repeated measures ANOVA analysis was performed using SPSS [IBM Corp., Somers, NY, USA] in order to quantitatively determine differences among the 3 motor tasks and 3 motor imagery tasks (reaching and grasping, reaching only and grasping only). To accurately perform a repeated measures ANOVA analysis, the underlying assumptions of the data set distribution that is specific for accurate ANOVA analysis needs to be preserved. The consequence of violating the distribution assumptions will yield ANOVA analysis results that are not trustworthy. The ANOVA analysis assumes that within a data set the observations within and between samples are independent, the distribution is normal and there is equal variance [138,227]. In addition, each of the groups within a data set needs to be of the same size without any missing data samples [138,227].

Mauchly's test of Sphericity as performed to validate the assumptions of the repeated measures factor ANOVA [228]. Sphericity is the extent of variances between levels of a repeated measures factor being equally distributed [138,228]. If the results from Mauchly's test of Sphericity indicate significant differences meaning that the sphericity assumption of the data set is violated, then an appropriate correction method to calculate the ANOVA is needed. A conservative correction method for calculating the repeated measures ANOVA is the Greenhouse – Geisser method which was used [229].

The second assumption for repeated measures ANOVA is that the distribution is normal and is the same across the data sets. Friendman's test was performed to determine if the distribution was the same among data sets. In addition, the Kolmogorov-Smirnov test was used to determine if the distribution was normal [138]. Typical patterns of non-

normal distribution are skewed or flat distributions. Common methods of correcting the distribution are to implement transformation of the data set such as square root, logarithmic, squared or cubed transforms [138]. In the present case, the data was log transformed and the goodness of fit for this new distribution was recorded. Results from the repeated measures ANOVA analysis can be found in section 3.5.2 for the real motor tasks and section 3.5.3 for the motor imagery tasks.

3.5: RESULTS.

3.5.1: Sample Size Analysis Results.

Table 3.2 presents the sample size analysis results for the real motor tasks and table 3.3 shows the results for the motor imagery tasks. The intra subject variability was the highest for the real reach task but was low for the imagined reach and real grasp tasks. The real reach and grasp had the higher percent signal change of 3.25%. When comparing the real motor tasks with the motor imagery tasks, the percent signal change was higher for the real motor tasks. The within ROI variability and inter subject variability were lower for the motor imagery tasks. Of these motor imagery tasks, the imagined reach had the lowest values.

TABLE 3.2: Sample Size analysis results for Real tasks.

Task Type	Intra subject variability(%)	Percent signal change (%)	Within ROI variability (%)	Inter subject variability (%)
Real Reach and Grasp	0.84	3.25	0.36	1.76
Real Reach	0.97	2.85	0.42	1.63
Real Grasp	0.78	2.13	0.33	1.42

TABLE 3.3: Sample Size analysis results for Motor Imagery Tasks.

Task Type	Intra subject variability(%)	Percent signal change (%)	Within ROI Variability (%)	Inter subject variability(%)
Imagined Reach and Grasp	0.80	0.66	0.36	0.73
Imagined Reach	0.78	0.58	0.35	0.68
Imagined Grasp	0.83	0.76	0.37	0.79

3.5.2 : Motor Task Activation Regions.

In this section, the distribution plots (figures 3.5a – 3.5d) show the percent region activation computed using the number of voxels that were considered to be significantly active ($q = 0.01$) per region as defined by the TTN27 EZ ML atlas (Table 3.4). These region activation percentages represent the activation that corresponds to voluntary motor tasks of reaching and grasping (RRG), reaching only (RR) and grasping only (RG).

TABLE 3.4: Number of Active Regions for Motor and Motor Imagery Tasks.

Tasks	Number of Active Regions
Real Reaching and Grasping	73
Real Reaching	53
Real Gasping	72

To determine if the variances are different, the Mauchy's test of Sphericity was performed at a significance level of $p<0.05$. The results indicate that the data was not

TABLE 3.5: Mauchly's Test of Sphericity.

Within Subjects Effect	Mauchly's W	Approx Chi-Square	df	Calculated *p-value*	Epsilon Greenhouse - Geisser
Factor 1	0.596	58.993	2	$p<0.0001$	0.712

spherical and Maulchy's test of Sphericity had been violated, therefore the conservative Greenhouse-Geisser correction (p<0.05) was used. The results from the Greenhouse-Geisser calculations are in table 3.6. These results indicate that there is a significant difference between the three motor tasks, F(1.425,163.820) = 9.224, p<0.0001.

TABLE 3.6: Repeated Measured ANOVA calculations comparing RRG, RR and RG using Greenhouse-Geisser Correction.

Source		**Type III Sum of Squares**	**df**	**Mean Square**	**F**	**Calculated *p*-value**
Factor1	Greenhouse-Geisser	565.827	1.425	397.205	9.224	p<0.0001
Error	Greenhouse-Geisser	7054.405	163.820	43.062		

The distribution of the data set as examined using the Friedman test indicated that the distribution among data sets were different. Furthermore, the Kolmogorov-Smirnov test to determine if the data sets were normal indicated that none of the three data sets had a normal distribution. It was observed that the data sets had an exponential distribution and using a log transformation, the goodness of fit for each data indicated to be close to 1 (R^2_{RRG} = 0.990, R^2_{RR} = 0.977 and R^2_{RG} =0.945) as shown in the following figures 3.9a through 3.9b. The results therefore validate the use of the repeated measures ANOVA for calculating the differences in means and standard deviations simultaneously because of the demonstrated consistency in the distribution among data sets.

FIGURE 3.9a: P-P Plots for Real Reach and Grasp Data Distribution.

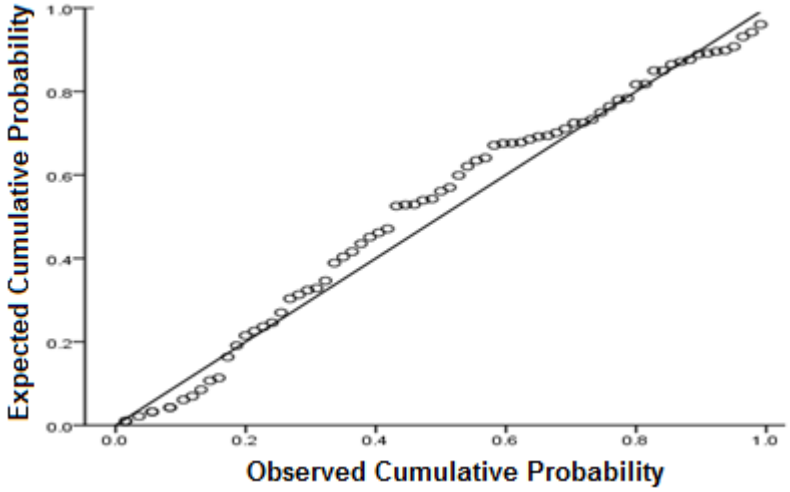

FIGURE 3.9b: P-P Plots for Real Reach Task Data Distribution.

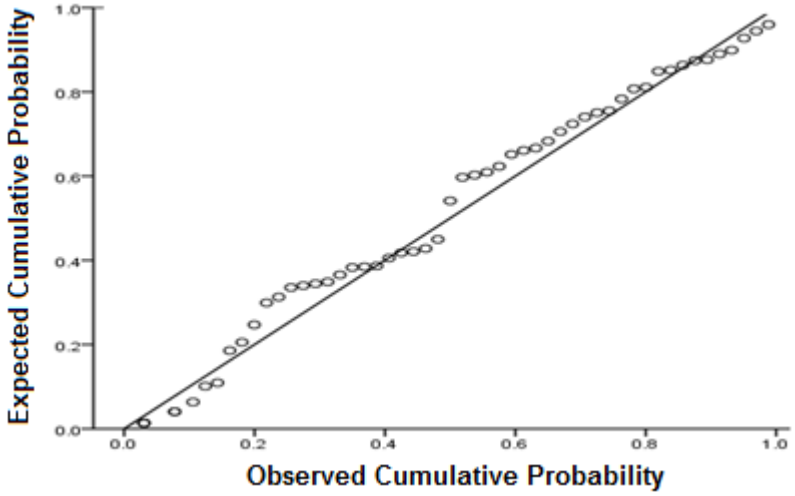

FIGURE 3.9c: P-P Plots for Real Grasp Data Distribution.

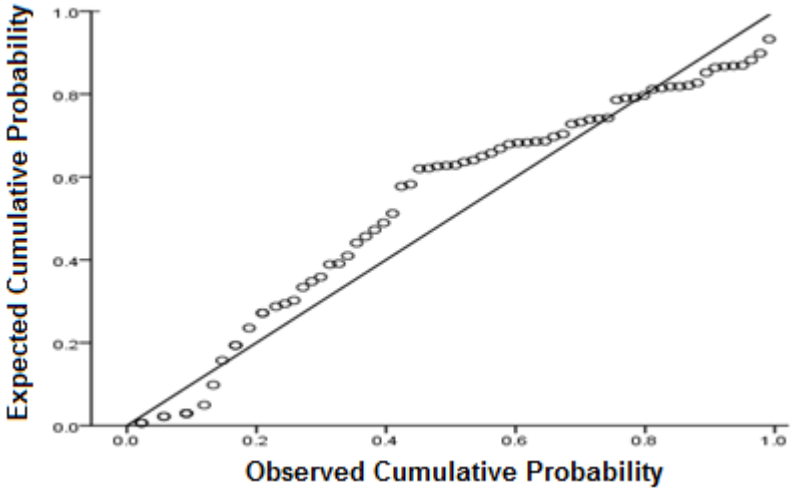

The data from figure 3.10 indicate that for the motor tasks using real world objects, there were activations within specific regions of the brain. Of these functional movements, the real reach and grasp motor task had the most number of active regions (N=73), followed by the real grasp (N=72) and the real reach (N=53). Of these regions the real reach and grasp task had the highest number of activations.

TABLE 3.7: Comparison of Common and Distinct Regions Among Motor Tasks.

Tasks	Real Reaching and Grasping	Real Reaching	Real Gasping
Real Reaching and Grasping	12	2	12
Real Reaching	2	2	X
Real Gasping	12	X	11

When comparing common regions of activation, it was observed that there were 47 common regions among all three motor tasks. In addition, there were distinct areas of the brain that were selectively activated for each specific motor task (RRG = 12, RR = 2, RG = 11). The overlap of activation among pairs of tasks showed that the real reach and grasp had 12 overlapping regions with the real grasp and 2 with the real reach. The real reach had 2 overlapping regions with the real grasp task.

FIGURE 3.10: Anatomical locations of Real motor tasks.

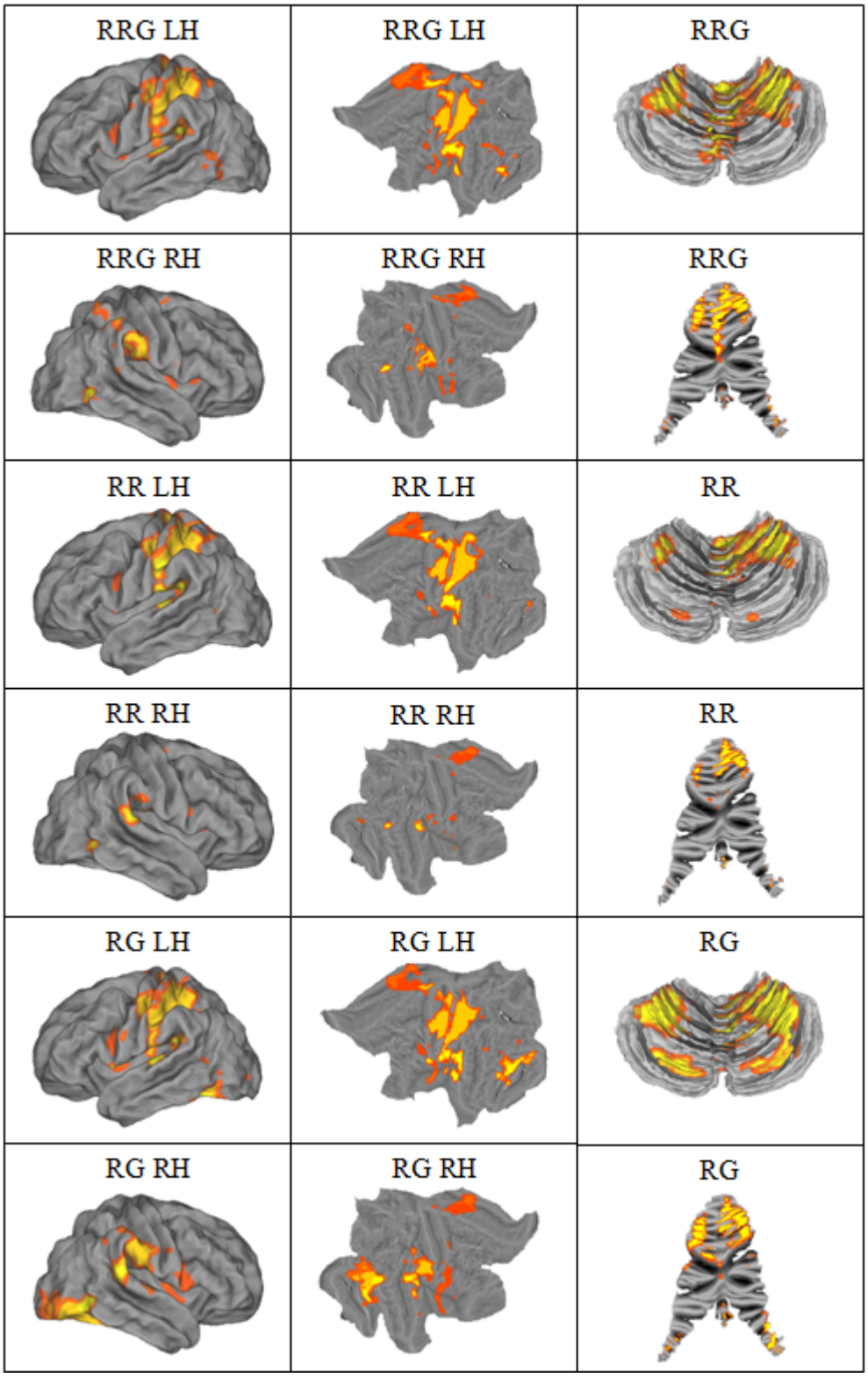

FIGURE 3.11a: Anatomical Regions (1 – 29) for Real Reach and Grasp, Real Reach and Real Grasp (Region Guide in Appendix A).

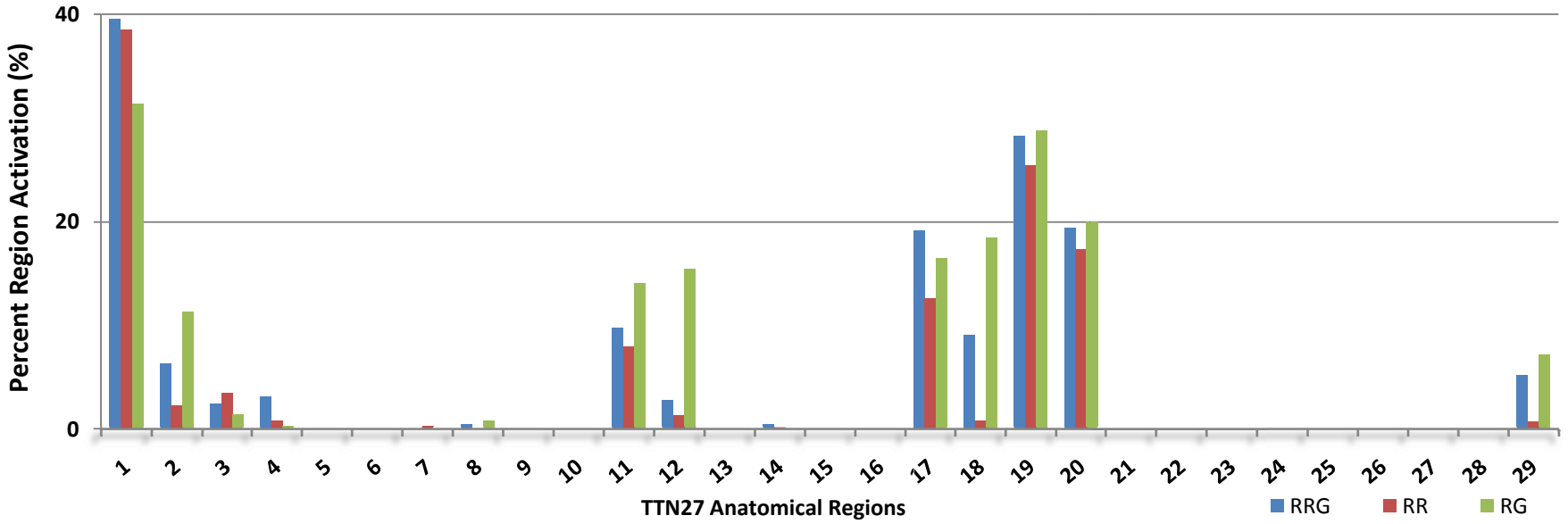

FIGURE 3.11b: Anatomical Regions (30 – 59) for Real Reach and Grasp, Real Reach and Real Grasp (Region Guide in Appendix A).

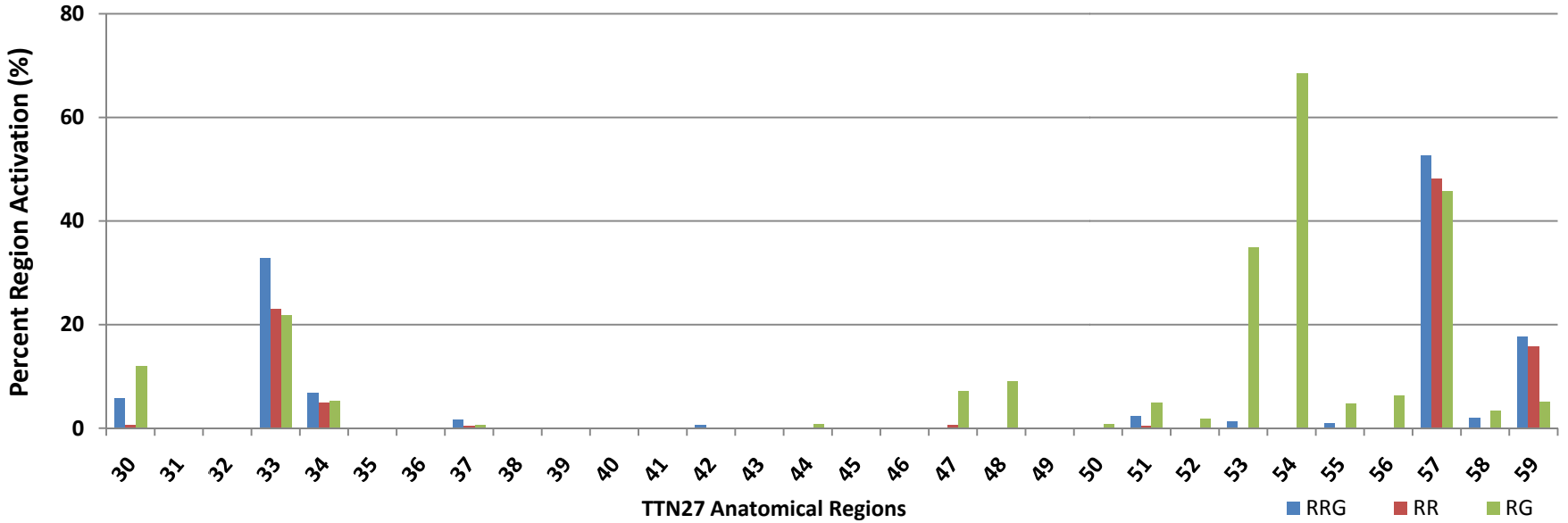

FIGURE. 3.11c: Anatomical Regions(60 – 89) for Real Reach and Grasp, Real Reach and Real Grasp (Region Guide in Appendix A).

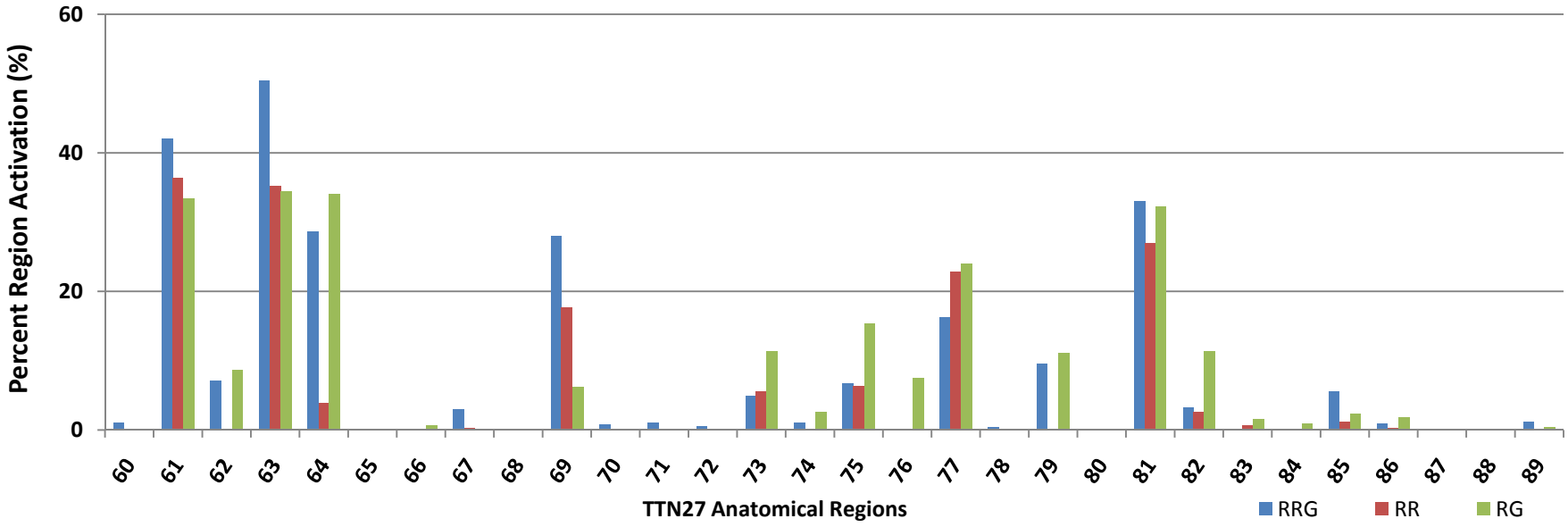

FIGURE 3.11d: Anatomical Regions (90 – 116) for Real Reach and Grasp, Real Reach and Real Grasp (Region Guide in Appendix A).

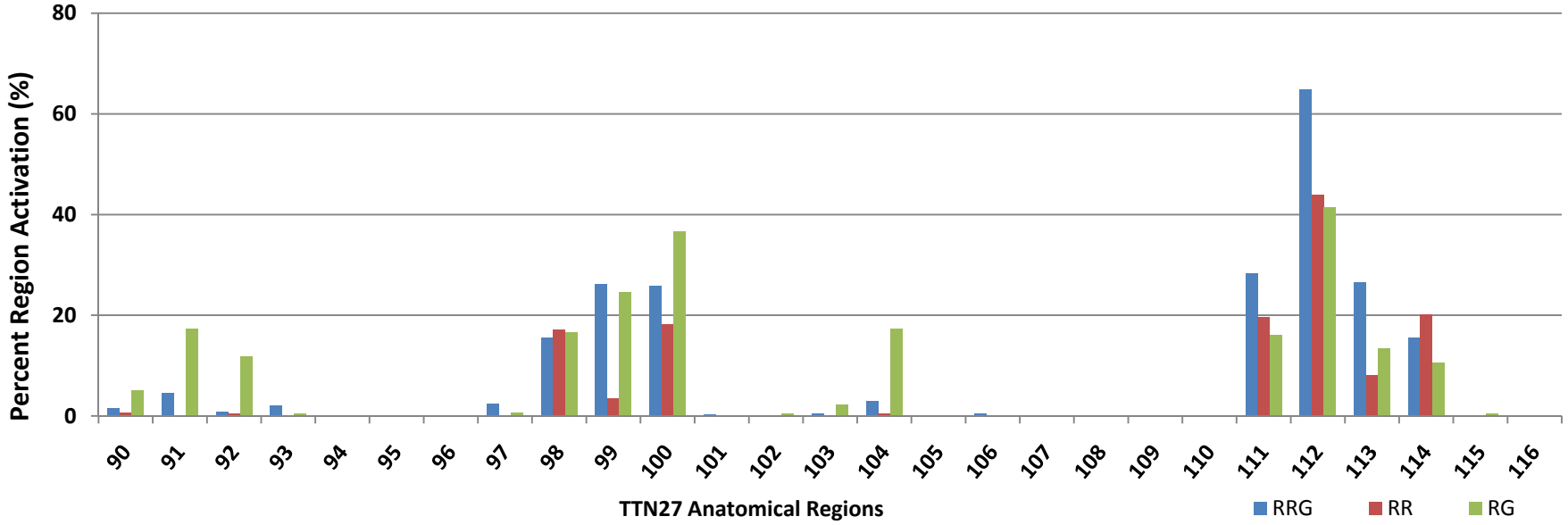

3.5.3 : Motor Imagery Task Activation Regions.

This section presents the distribution plots (figures 3.6a – 3.6d) of the percent region activation computed using the number of voxels that were considered to be significantly active ($q = 0.01$) per region as defined by the TTN27 EZ ML atlas (Table 3.4) for the motor imagery tasks. These motor imagery tasks were imagined reaching and grasping (IRG), imagined reaching only (IR) and imagined grasping only (IG). The total number of active regions for each of these motor imagery tasks is presented in the following table 3.6.

TABLE 3.8: Number of Active Regions for Motor and Motor Imagery Tasks.

Tasks	Number of Active Regions
Imagined Reaching and Grasping	81
Imagined Reaching	55
Imagined Grasping	51

The results from table 3.6 indicate that the imagined reaching and grasping task had the most number of active regions followed by the imagined reaching and lastly, the imagined grasp task. The repeated measures ANOVA was performed to quantitatively determine if each motor imagery task was different from the amount of activation voxels in reach region. The Mauchy's test of sphericity ($p<0.05$) results as presented in table 3.7 indicate that sphericity had been violated. To correct for the sphericity violation, the

TABLE 3.9: Mauchly's Test of Sphericity for Motor Imagery Tasks

Within Subjects Effect	Mauchly's W	Approx Chi-Square	df	Calculated *p*-value	Epsilon Greenhouse – Geisser
Factor 1	0.262	152.521	2	$p<0.0001$	0.576

Conservative Greenhouse-Geisser correction was used to calculate the repeated measures ANOVA. It was determined that each motor imagery task was significantly different, $F(1.151,132.366) = 21.332$, $p<0.0001$.

TABLE 3.10 : Repeated Measures ANOVA calculations comparing IRG, IR and IG

Source		Type III Sum of Squares	df	Mean Square	F	Calculated *p*-value
Factor1	Greenhouse-Geisser	813.466	1.151	706.741	21.332	$p<0.0001$
Error	Greenhouse-Geisser	4385.379	132.366	33.131		

The results from the Friedman test indicated that the distribution was significantly different for all of the motor imagery tasks and furthermore the Kolmogorov-Smirnov test ($p<0.05$) indicated that the distribution for each of the data sets were not normal and resembled an exponential distribution. A log transformation of each data set was performed to correct the distributions, and the goodness of fit was determined to be approximately 1 ($R^2_{IRG} = 0.972$, $R^2_{IR} = 0.976$ and $R^2_{IG} = 0.974$).

FIGURE 3.12a: P-P Plots for Distribution for Reach and Grasp Motor Imagery Task.

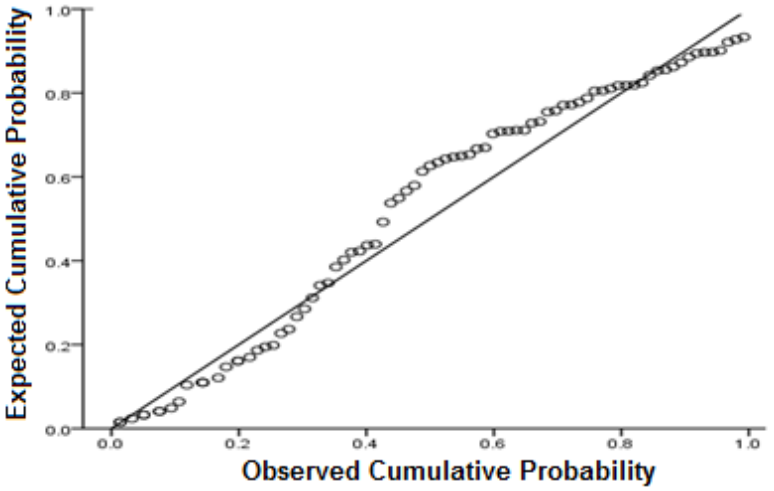

FIGURE 3.12b: P-P Plots for Distribution for Reach Motor Imagery Task.

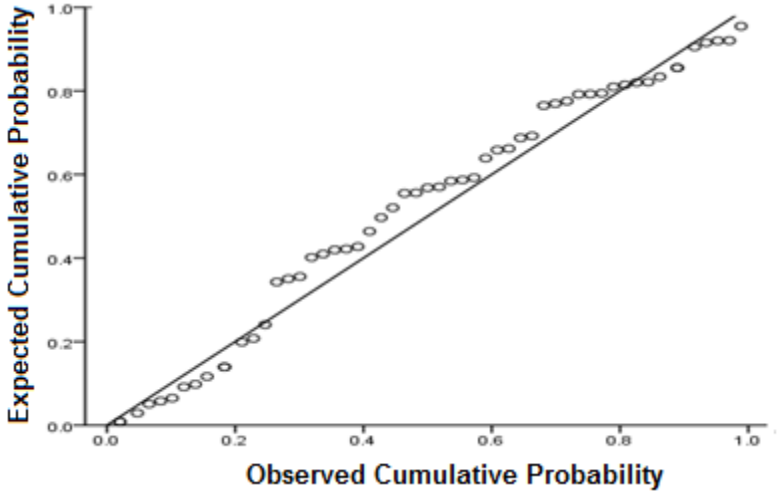

FIGURE 3.12b: P-P Plots for Distribution for Grasp Motor Imagery Task.

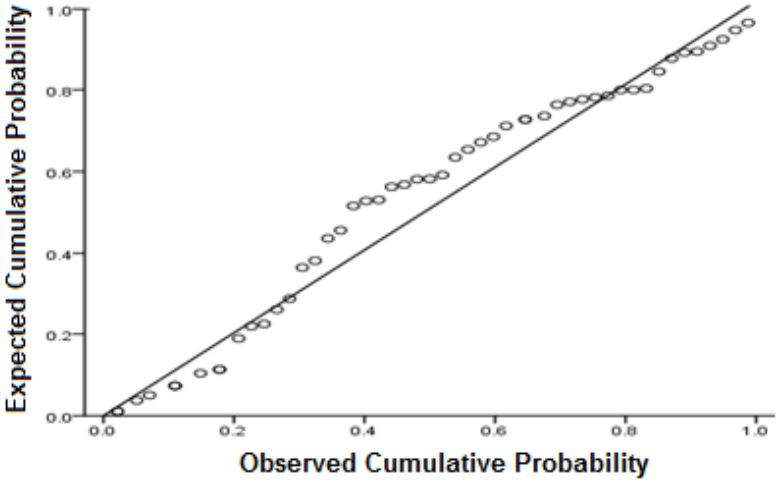

The comparison of the number of active regions for each of the motor imagery tasks, showed that the imagined reach and grasp had the highest number of active regions (N = 81), followed by the imagined reach (N=55) and the imagined grasp (N=51). When comparing distinct regions of task activation, the imagined reach and grasp had 27 regions of specific activation, the imagined grasp had 3 specific regions of activation. The imagined reach task did not have any task specific regions of activation. It was further determined that there were 9 regions that overlapped for the imagined reach and grasp and imagined reach tasks and 2 regions that overlapped between the imagined reach and grasp with the imagined grasp tasks. There were three regions that overlapped between the imagined reach and imagined grasp tasks. The results for common and distinct regions for motor imagery tasks are shown in the following table 3.9.

TABLE 3.11: Comparison of Common and Distinct Regions Among Motor Imagery Tasks.

Tasks	Imagined Reaching and Grasping	Imagined Reaching	Imagined Gasping
Imagined Reaching and Grasping	27	9	2
Imagined Reaching	9	2	X
Imagined Gasping	2	X	3

FIGURE 3.13: Anatomical locations of Motor Imagery Tasks.

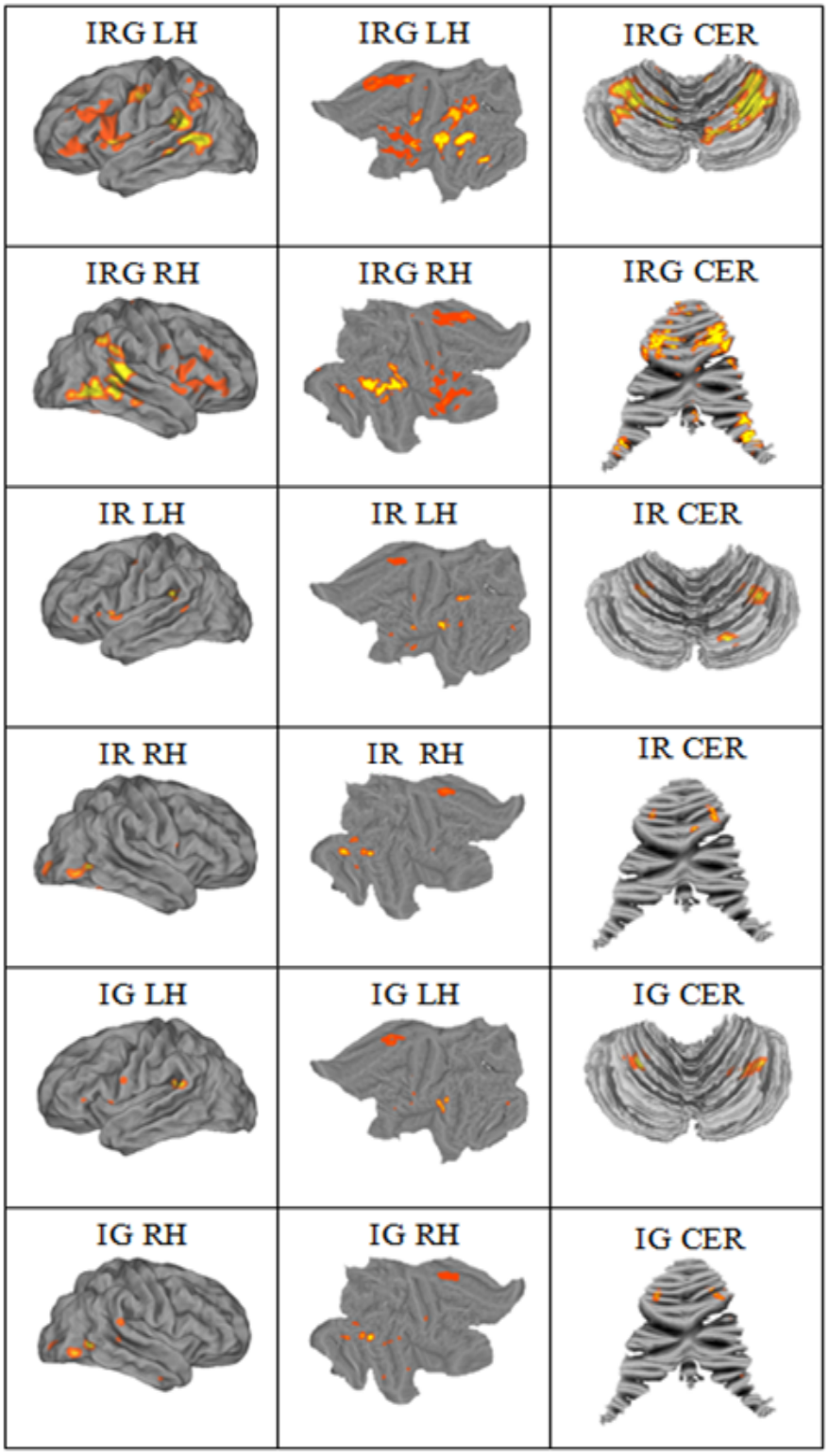

FIGURE 3.14a: Anatomical Regions (1 – 29) for Imagined Reach and Grasp, Imagined Reach and Imagined Grasp.

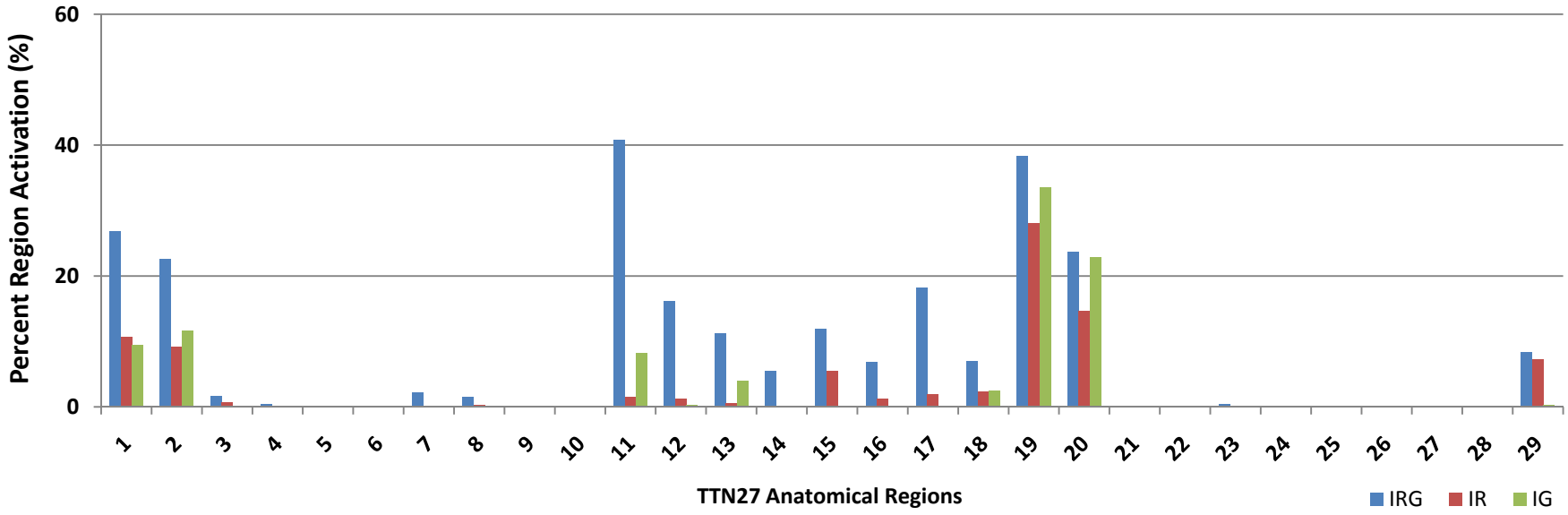

FIGURE 3.14b: Anatomical Regions (30 – 59) for Imagined Reach and Grasp, Imagined Reach and Imagined Grasp.

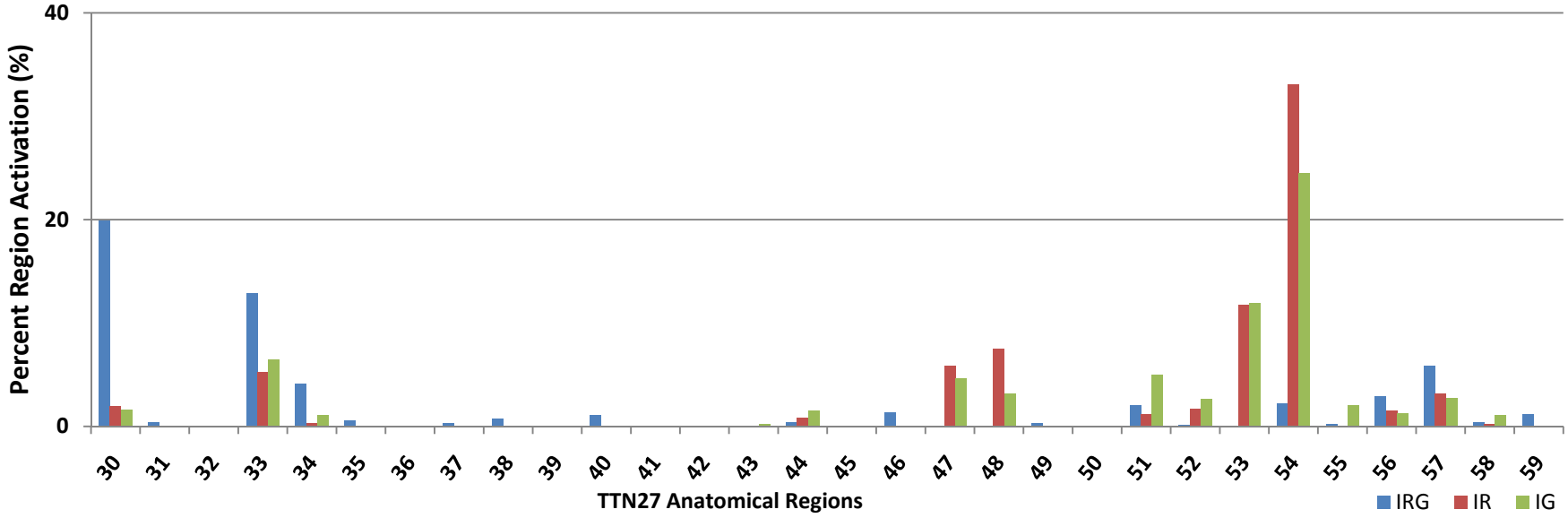

FIGURE 3.14c: Anatomical Regions (60 – 89) for Imagined Reach and Grasp, Imagined Reach and Imagined Grasp.

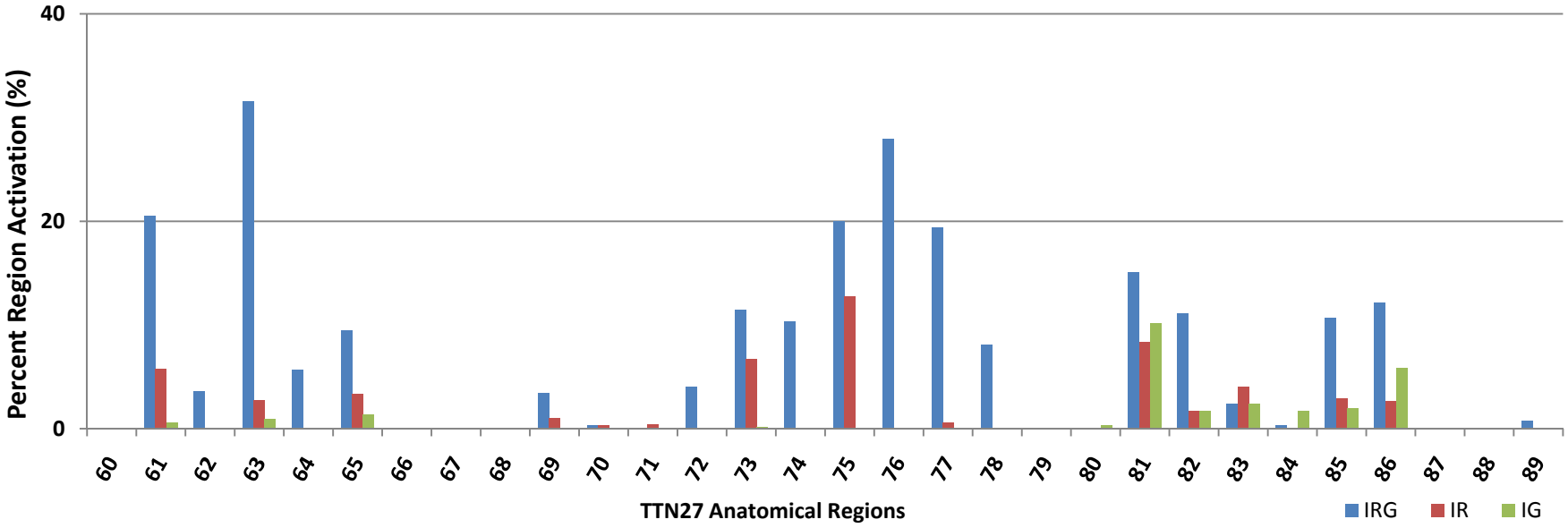

FIGURE 3.14d: Anatomical Regions (90 – 116) for Imagined Reach and Grasp, Imagined Reach and Imagined Grasp.

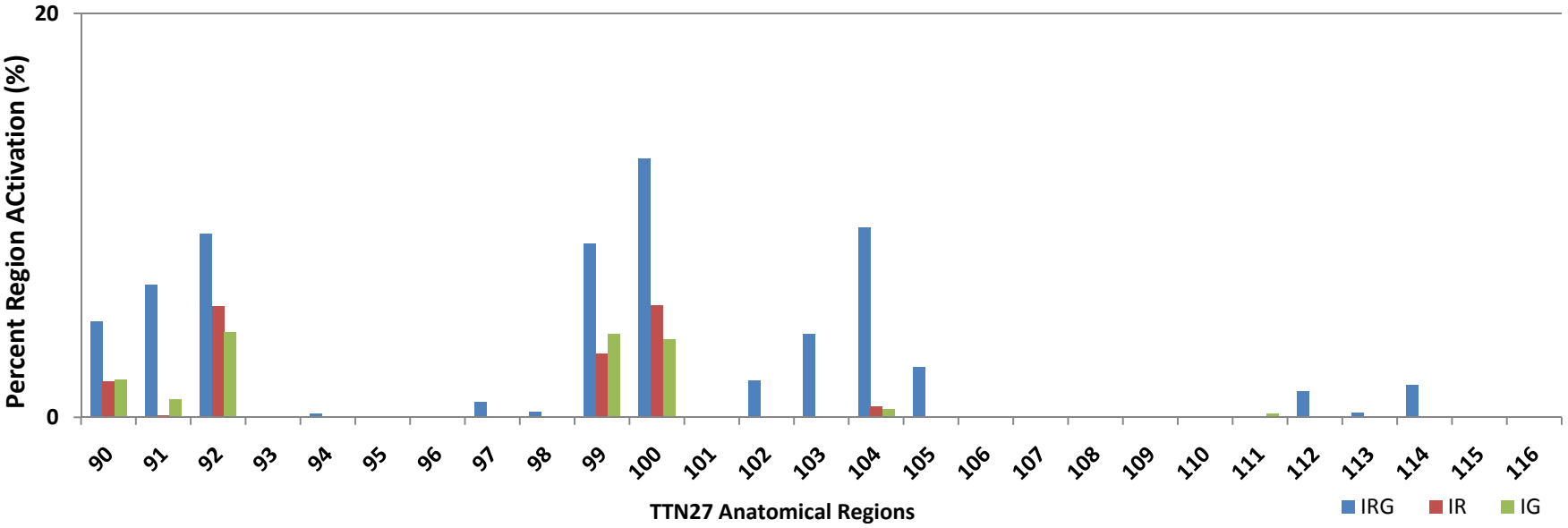

3.5.4: Motor Imagery Tasks Compared with Motor Tasks Regions.

Tables 3.4a through 3.4c present comparison of activation in regions of the brain from real motor and motor imagery tasks. These tables display activation in common regions across motor tasks and motor imagery tasks and distinct regions that are specific to each task.

TABLE 3.12a: Regions of activation between real motor tasks and motor imagery tasks.

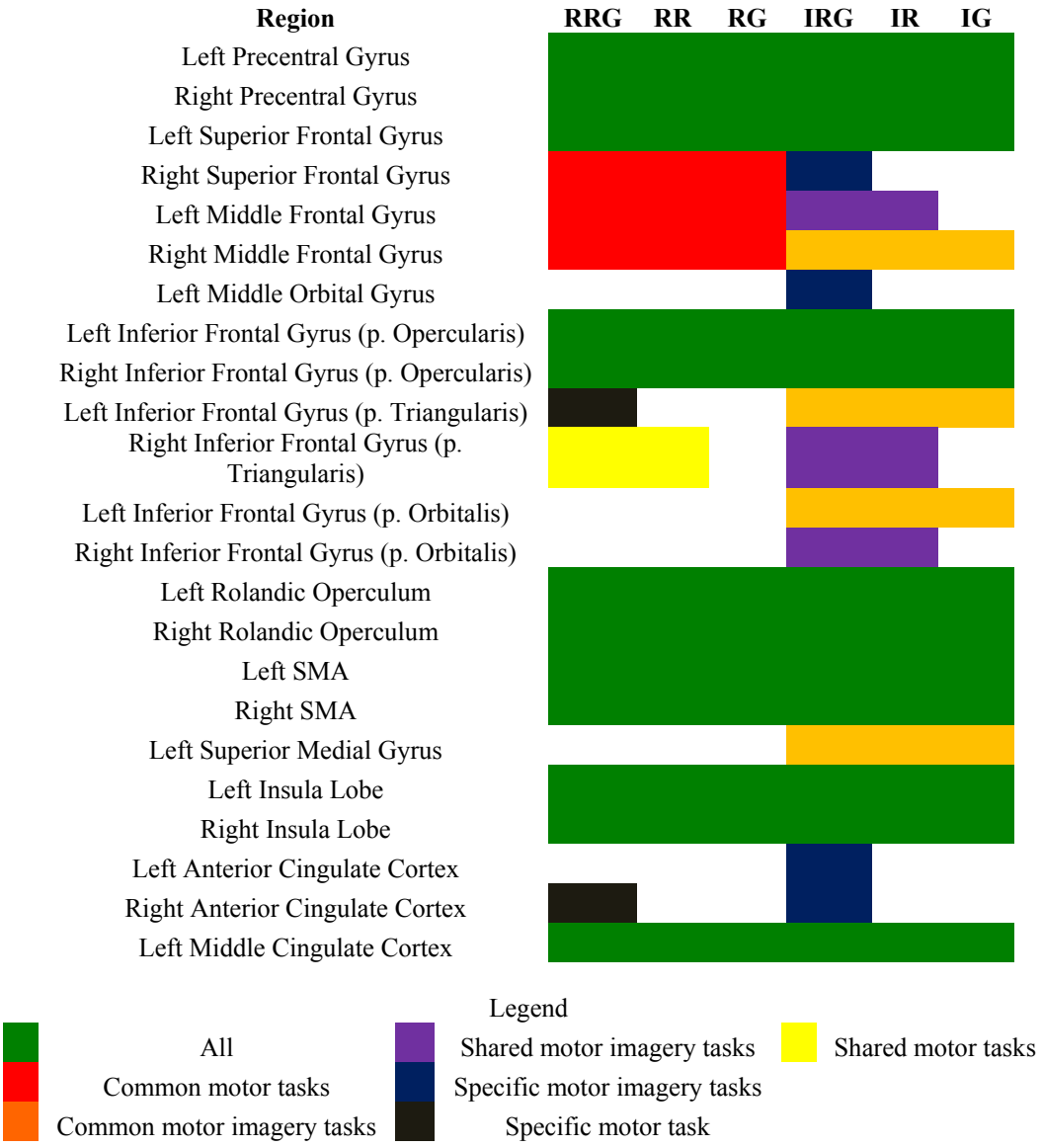

TABLE 3.12b: Regions of activation between real motor and motor imagery tasks.

Region	RRG	RR	RG	IRG	IR	IG
Right Middle Cingulate Cortex						
Left Posterior Cingulate Cortex						
Right Posterior Cingulate Cortex						
Left Hippocampus						
Right Hippocampus						
Left ParaHippocampal Gyrus						
Right ParaHippocampal Gyrus						
Right Amygdala						
Left Calcarine Gyrus						
Right Calcarine Gyrus						
Right Cuneus						
Left Lingula Gyrus						
Right Lingula Gyrus						
Left Superior Occipital Gyrus						
Right Superior Occipital Gyrus						
Left Middle Occipital Gyrus						
Right Middle Occipital Gyrus						
Left Inferior Occipital Gyrus						
Right Inferior Occipital Gyrus						
Left Fusiform Gyrus						
Right Fusiform Gyrus						
Left Postcentral Gyrus						
Right Postcentral Gyrus						
Left Superior Parietal Lobule						
Right Superior Parietal Lobule						
Left Inferior Parietal Lobule						
Right Inferior Parietal Lobule						
Left SupraMarginal Gyrus						
Right SupraMarginal Gyrus						
Left Angular Gyrus						
Right Angular Gyrus						
Left Precuneus						
Right Precuneus						
Left Paracentral Lobule						
Right Paracentral Lobule						
Left Caudate Nucleus						
Right Caudate Nucleus						

TABLE 3.12c: Regions of activation between real motor and motor imagery tasks.

Region	RRG	RR	RG	IRG	IR	IG
Left Putamen						
Right Putamen						
Left Pallidum						
Right Pallidum						
Left Thalamus						
Right Thalamus						
Left Heschls Gyrus						
Right Heschls Gyrus						
Left Superior Temporal Gyrus						
Right Superior Temporal Gyrus						
Left Temporal Pole						
Right Temporal Pole						
Left Middle Temporal Gyrus						
Right Middle Temporal Gyrus						
Left Inferior Temporal Gyrus						
Right Inferior Temporal Gyrus						
Left Cerebellum (Crus 1)						
Right Cerebellum (Crus 1)						
Left Cerebellum (Crus 2)						
Right Cerebellum (Crus 2)						
Right Cerebellum (III)						
Left Cerebellum (IV-V)						
Right Cerebellum (IV-V)						
Left Cerebellum (VI)						
Right Cerebellum (VI)						
Left Cerebellum (VII)						
Right Cerebellum (VII)						
Left Cerebellum (VIII)						
Right Cerebellum (VIII)						
Left Cerebellum (IX)						
Right Cerebellum (IX)						
Left Cerebellum (X)						
Cerebella Vermis (3)						
Cerebella Vermis (4/5)						
Cerebella Vermis (6)						
Cerebella Vermis (7)						
Cerebella Vermis (8)						
Cerebella Vermis (9)						
Cerebella Vermis (10)						

In order to determine differences between motor imagery tasks and real motor tasks from activation patterns and regions of the brain in a quantitative manner, the group data from real motor tasks were compared with their motor imagery task counter parts. The voxel differences were obtained from a 3D voxel wise *t*-test analysis performed using AFNI with a significance level of $p<0.05$ on the group (N=18) data sets for motor imagery and actual motor tasks. The results are illustrated in the following figures 3.14a through 3.14d. The distribution plots show the percent regional activation that differ for each pertinent anatomical region of the brain. Higher values indicate larger differences with respect to the number of percent region activation and smaller numbers indicate stronger similarity between actual motor and motor imagery tasks.

FIGURE 3.15a: Anatomical Region (1 – 29) Comparison Between Real and Imagined Tasks.

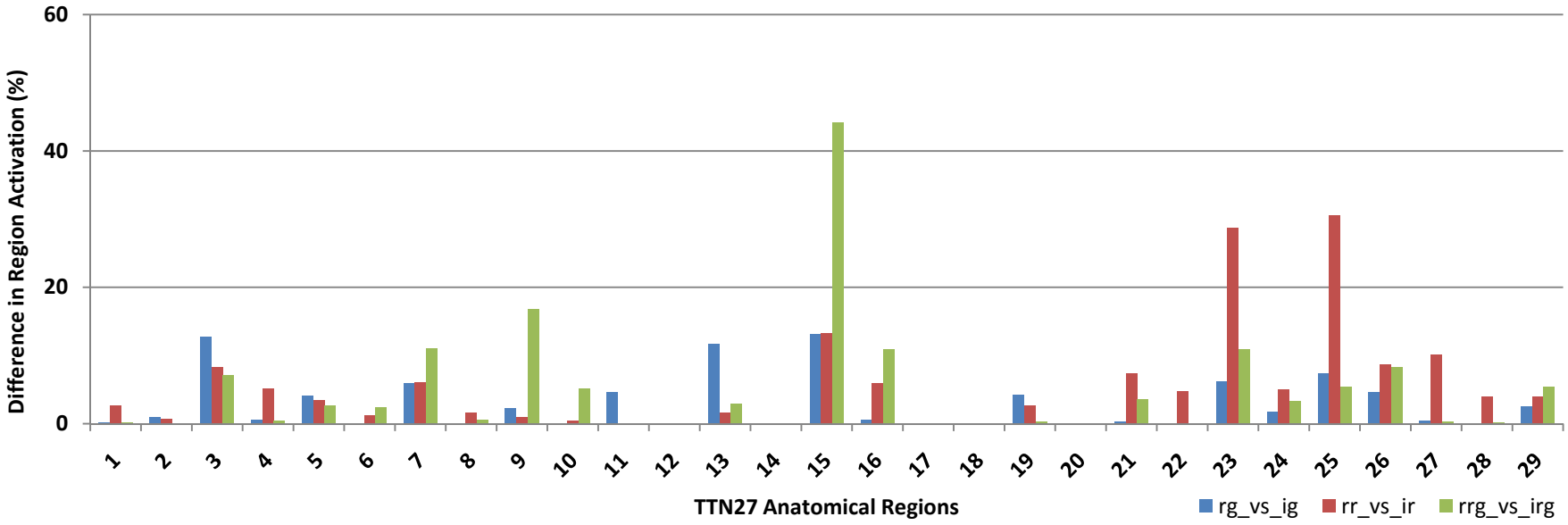

FIGURE 3.15b: Anatomical Region (30 – 59) Comparison Between Real and Imagined Tasks.

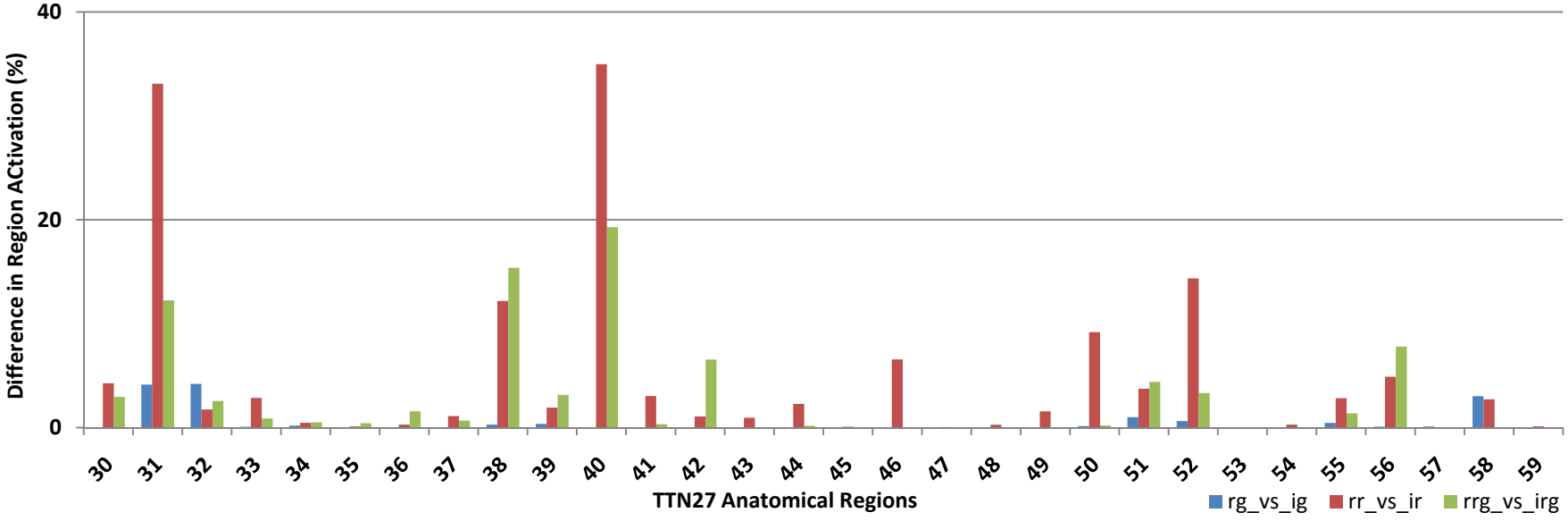

FIGURE 3.15c: Anatomical Region (60 – 89) Comparison Between Real and Imagined Tasks.

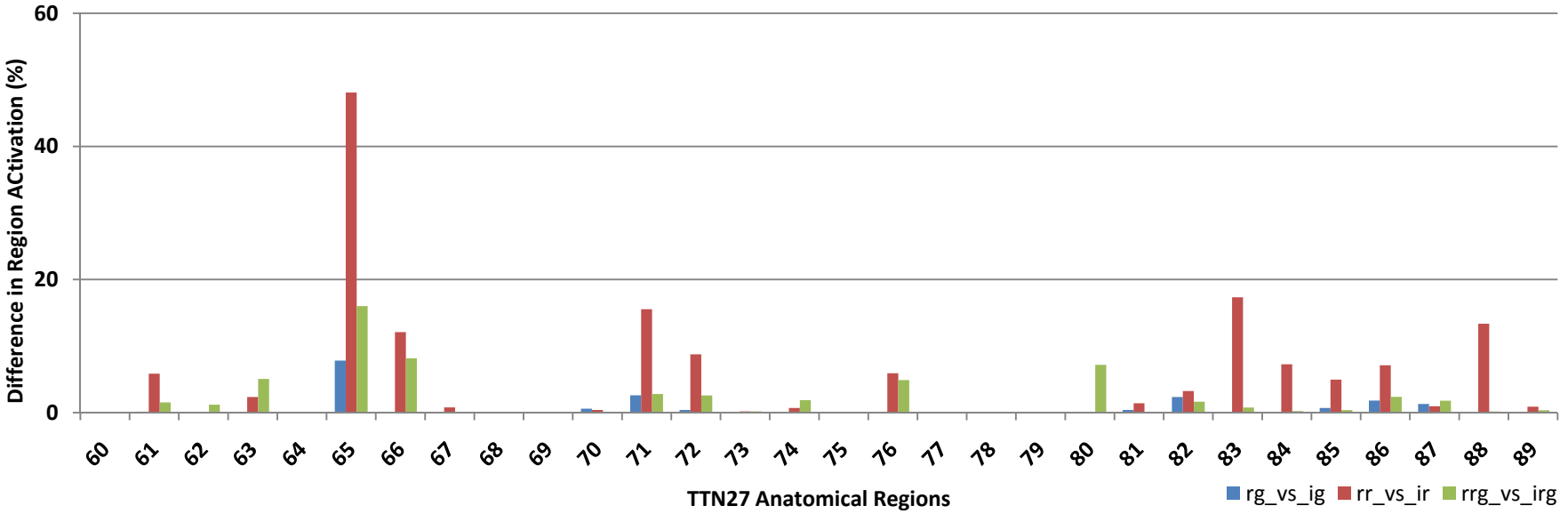

FIGURE 3.15d: Anatomical Region (90 – 116) Comparison Between Real and Imagined Tasks.

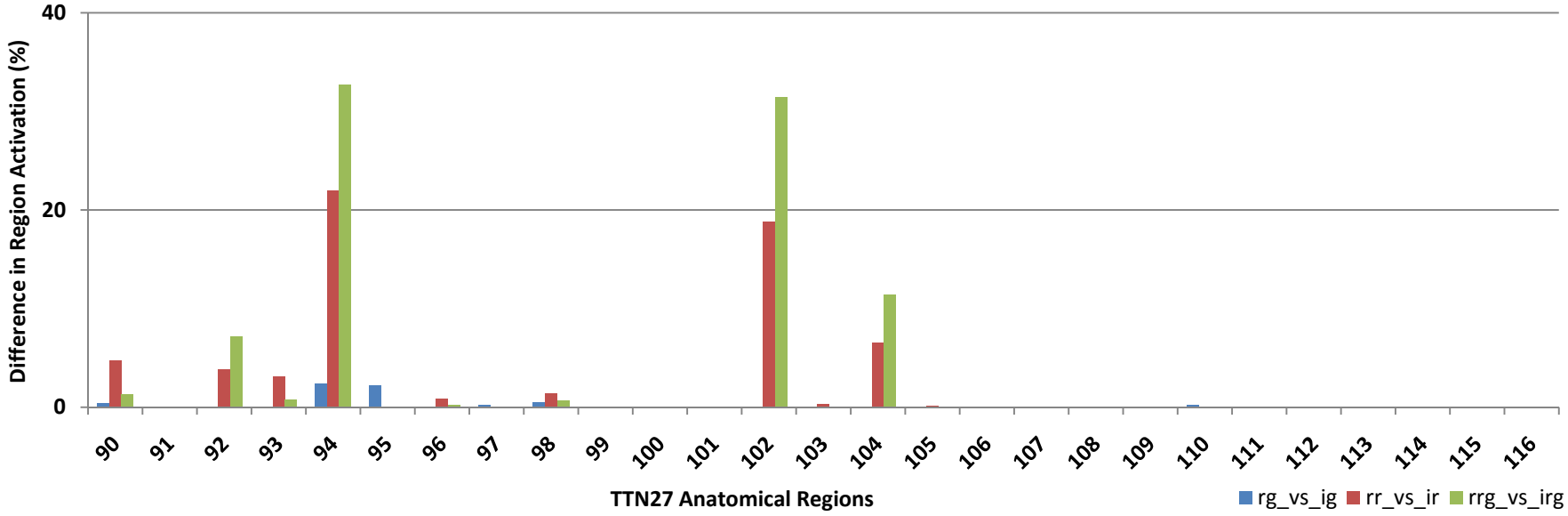

3.5.5: Difference in regional activation between Motor Tasks.

Differences among motor tasks were analyzed in order to quantitatively understand the effects of strategic planning that is represented in the activation patterns of brain regions. A 3D voxel wise *t*-test analysis performed using AFNI with a significance level of $p<0.05$ comparing the group (N=18) data sets for each motor task**.** Distributions of high percent region activations imply significant differences in motor strategy for that particular region of the brain. Region on the x-axis with no values imply no significant activation or differences among motor task strategies. The results from this analysis are displayed in the following figures 3.15a through 3.15d.

FIGURE 3.16a: Anatomical Region (1 – 29) Comparison Between Real Motor Tasks.

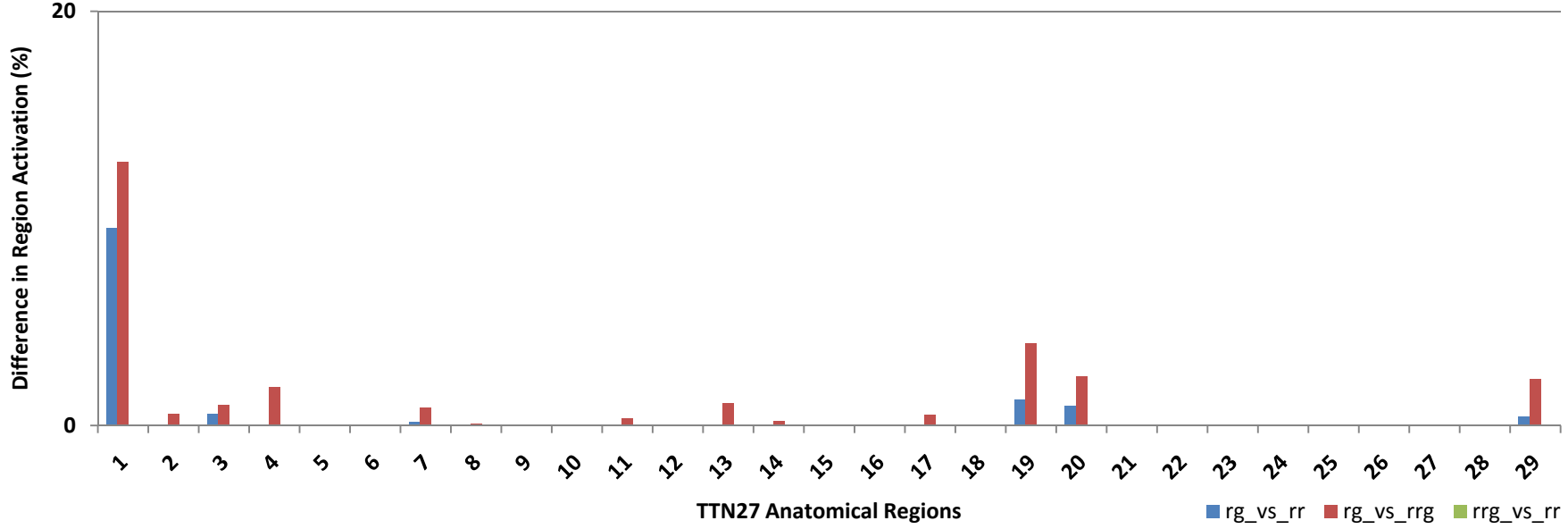

FIGURE 3.16b: Anatomical Region (30 – 59) Comparison Between Real Motor Tasks.

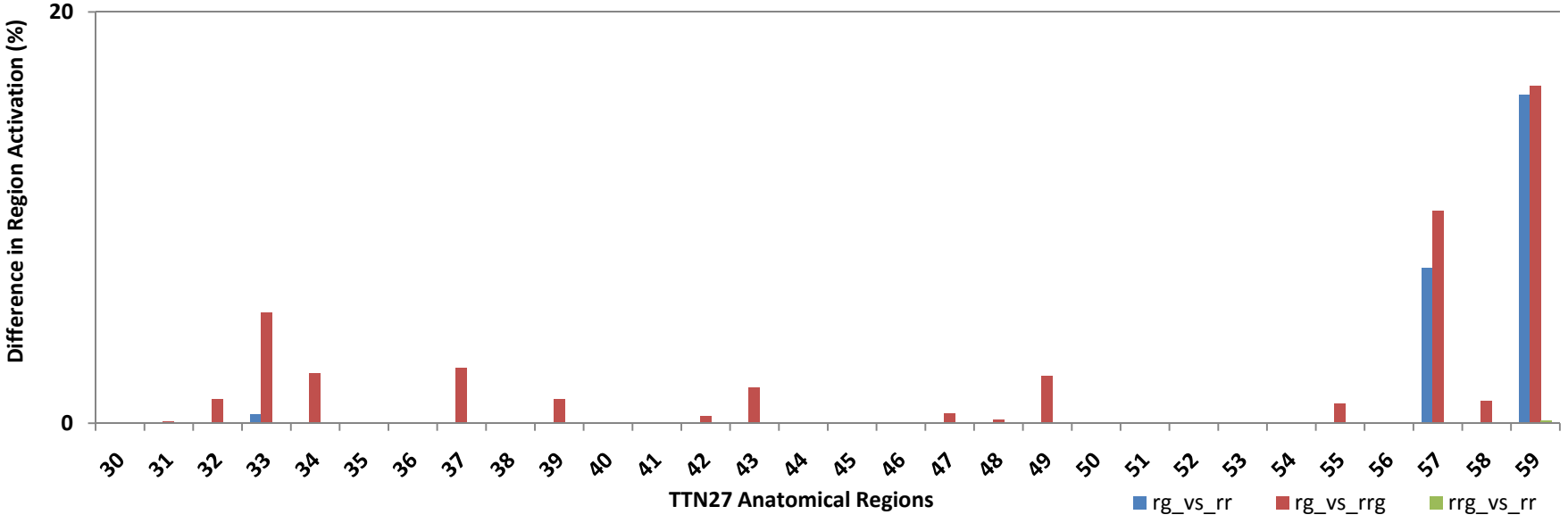

FIGURE 3.16c: Anatomical Region (60 – 89) Comparison Between Real Motor Tasks.

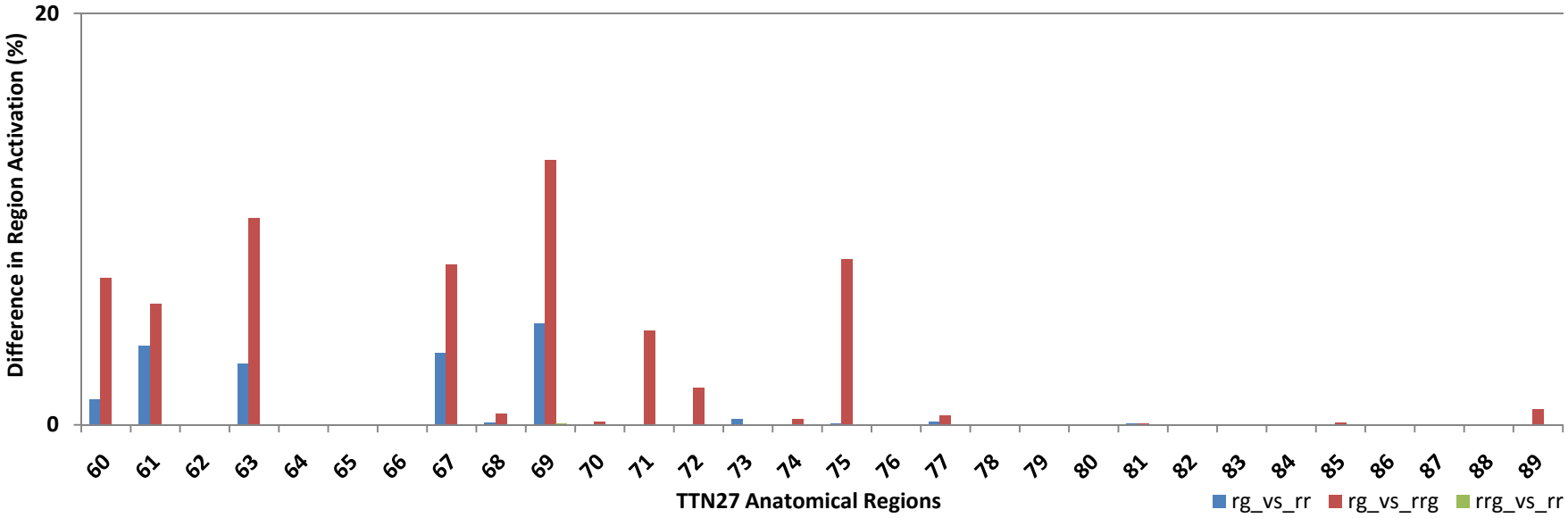

FIGURE 3.16d: Anatomical Region (90 – 116) Comparison Between Real Motor Tasks.

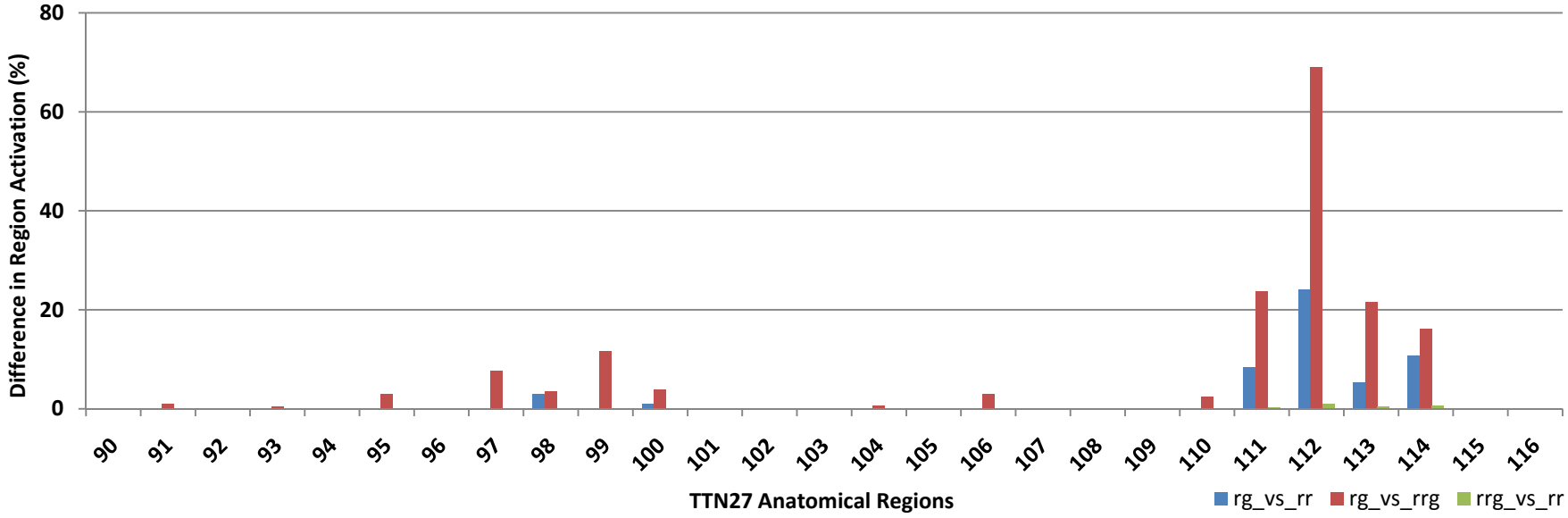

3.6: DISCUSSION.

3.6.1: Sample Size Analysis.

The data identified with the lowest percent signal change was used to determine an appropriate sample size with imagined reach movement defining the worst case scenario. The data set suggested that in order to adequately show significance at an alpha level of 0.002 (two tailed) and with a power of 90%, a minimum of 16 subjects were needed [226]. Therefore, the data analysis using 18 subjects met these criteria for the sample size.

3.6.2 : Motor and Motor Imagery Task Activation Regions.

The results from the actual motor tasks support the first hypothesis of the study, which is that that activation can be mapped in the whole brain for functional reaching and grasping using real world objects with fMRI. The data indicates the quantifiable presence of common and task specific activation patterns pertaining to upper extremity neuromotor control. The presence of several activated regions based on the motor task performance, supports the notion of cognitive processing and that supports the proposition that planning, initiation and control of upper extremity movement is a distributed process [74,75,113,114,182]. This is in agreement with what is known about motor, sensory and functional organization of the brain where each anatomical region of the brain has a specific role [74,75,113,114,182]. Cortical areas such as the primary motor cortex, sensory cortex, parietal lobule have significant activations located on the hemisphere contra-lateral to the limb of which the action was performed. In addition,

there were regions such as the SMA that were bilaterally activated. These activation results of existing common regions were expected and are confirmed in the literature [74,75,113,114,182].

The presence of distinct, task specific regions and varying activation patterns among motor tasks suggests the utilization of a dual control mechanism that is synergistic in nature [230]. The common regions represent a 'generic' motor plan that enables the performance of basic upper extremity movements. However, this 'generic' motor plan needs to be fine tuned by the brain for the specific task goals. Therefore the presence of distinct cortical regions and patterns that are unique to each performed motor task strongly suggest the presence of specific motor strategies. This is an important finding because a majority of the literature that reports on upper extremity motor control using fMRI has used non-goal oriented movements such as finger tapping. The use of the grasp only task was intended to mimic finger tapping paradigms. When comparing this movement to the reach only and reach and grasp motor task, it can be seen that although some anatomical regions of the brain overlap, differences in region specific activation magnitude and the presence of distinct anatomical regions are present. This suggests that there is a motor plan or strategy that is unique to the task being performed. Therefore, extrapolation of strategies from currently reported rhythmic paradigms, such as finger tapping and the use of non goal-oriented movements without real world objects, do not adequately represent actual the motor strategies used in functional reaching and grasping as would occur during activities of daily living.

When examining activation in the cerebellum, it was observed that the grasp only task had activation that was mostly concentrated on the lateral portions or the

hemispheric areas of the cerebellum. This finding was in agreement with the literature that had examined finger tapping tasks [231,232]. However, the real reach and grasp task had some hemispheric activation and a majority of the activation was focused on the medial portion or the vermis of the cerebellum. The literature proposes of the possibility of multiple independent homunculi that are present within the cerebellum. These homunculi are located in the left and right cerebella hemispheres and also the vermis [183]. Somatotopic organization of the cerebellum suggests that lateral portions of the cerebellum correspond to activity in more distal parts of the body [231,232]. The role of the cerebellum in coordinating precision and timing related movements would require continuous comparisons between movements of the different joints in the upper extremity to assure continued accuracy [233]. During a functional task such as reaching and grasping, this would require an increase in activations from medial regions corresponding to the arm combined with lateral portions pertaining to the hand. Conversely during grasp only activations, the visibility of increased lateral activation and very minimal medial activation support the somatotopic organization of the cerebellum [183,231]. These variations in activation patterns corresponding to functional motor task performance shows distinct differences in neuromotor strategy among functional goal oriented movements.

Motor imagery information provides an important tool that yields a means to understand the manner in which the brain is involved with planning a particular movement. The planning phase is a crucial element of the internal model and to the understanding of the neural correlates associated with voluntary task planning. Results from the motor imagery tasks show the presence of common and overlapping activation,

combined with distinct activity and patterns that are induced by task specific motor imagery. These results strongly support the second hypothesis of this study; which states that activation of the whole brain can be mapped for functional motor imagery reaching and grasping tasks using fMRI.

When comparing the motor imagery task results to actual motor task results, some overlapping regions of activation were observed; however the total number of regional activation was much lower for the motor imagery tasks, suggesting that actual motor tasks are able to produce stronger activations. These findings are consistent with the literature that has compared motor imagery with motor tasks [220,221]. The primary motor cortex had very little activation during motor imagery and supports the role of the primary motor cortex as being involved with initiating and mediating the actual execution of movements [74,114,183]. Areas that are known to be involved with motor planning such as the SMA, occipital gyrus, parietal lobule show significant activation for the motor imagery tasks [74,114,183]. Overall, activation was much higher for the motor imagery task of reaching and grasping as compared to reach only or grasp only. This increase in activation may have been because the reach and grasp task is more complex and requires more cognitive effort. The common regions that were active across all tasks suggest their role in task planning. Similar to the actual motor tasks, the presence of specific activation patterns and distinct cortical regions were present for the motor imagery tasks and the motor imagery of reaching and grasping had the most active regions. These differences in activation patterns and anatomical regions suggest the presence of strategies that are task dependent and specific.

Unlike the actual motor tasks performance data, the motor imagery tasks data followed a pattern in which the activation intensity in the regions of the brain decreased with decreasing task complexity. The results show that the reach and grasp motor imagery task was the most complex and the grasp only motor imagery task was the least cognitively demanding. Significant differences were observed in the cerebellum and regions of the cortex, namely the SMA, premotor cortex and parietal cortex, in which the amount of activation increased with increased task complexity. This finding is important because current literature that examines motor imagery movements has been inconclusive regarding the specific location and patterns of activations [219,234,235]. A reason for these discrepancies could be the result of the motor imagery tasks used in the literature were not based upon functional upper extremity movements. This discrepancy would suggest that motor imagery of stimuli not related to functional tasks do not necessarily translate to similar strategies used during functional motor tasks and therefore cannot be fully used to explain or represent goal oriented movements. Motor imagery tasks are challenging and much of the literature has not considered motor imagery in terms of specific functional upper extremity movements. The experimental paradigm used in the present study enforces strong motor imagery by pairing up these tasks immediately after the performance of the actual motor movements. Such an approach encourages the use of task specific planning that relates to upper extremity function. When comparing the motor imagery movements with the actual motor movements, there are common regions that overlap for each of the tasks.

Overall, the findings from both the motor imagery tasks and the actual motor tasks suggest that there is a combination of common strategies and task specific strategies

present. Furthermore, extrapolation of results from non functional tasks that do not incorporate real world objects for the purpose of understanding motor strategies may not yield an accurate picture of the upper extremity neuromotor control process.

3.7: CHAPTER CONCLUSION.

The results obtained for the motor imagery and actual motor tasks suggest that there are common brain activation patterns and regions for particular voluntary motor actions, the most important of which are the frontal gyrus, SMA, pre motor cortex, primary motor cortex, parietal region and cerebellum. In addition, there are also distinct activation patterns and regions for each of the tasks, most prominent being in the SMA, pre motor cortex, parietal cortex and cerebellum. Combination of these two observations suggests the possible existence of neuromotor control strategies that consist of 'generic' movements that can be fine tuned by the brain to achieve specific task goals. The results strongly support all of the hypotheses that were proposed in section 3.2.3. The paradigm of this study is unique because it uses functional task performance combined with real-world objects and these are features currently not used in the majority of functional imaging studies. Finally, the findings from this specific aim are important to the understanding of the roles that anatomical regions of the brain play and their involvement with upper extremity motor initiation, planning, execution and control. Such information is critical to the development of neuroprosthetic controllers and appropriate upper extremity therapeutic interventions.

These results show that, when comparing results from two tasks where the only difference was the actual performance of the task, several important observations can be

made. In the actual task, areas known to be involved in planning are activated just as these same areas are in the imaged task. Therefore we surmise that activity in these areas represent the intention to perform the task. The principal differences between the imagined and actual tasks are greatly reduced activity or the absence of activity, and variations of the activation patterns. Regions that exhibited such responses were the cerebellum, SMA, angular gyrus, premotor cortex, superior medial gyrus, anterior cingulated cortex and the parahippocampal gyrus. This suggests that these regions are active in imagined movements or the so called ‘strategy’ regions. Additional regions active in imagined tasks but not in the real tasks may either be involved in blocking the translation of intention to action, or may be due to visualization of the task. Determining which is correct will require additional study.

CHAPTER 4

Brain Region Temporal Information During Functional Upper Extremity Reaching and Grasping

4.1: ABSTRACT.

The neuromotor control that enables one to perform meaningful upper extremity movements of reaching and grasping is a distributed process that is dependent upon the contribution of strategy from several cortical regions of the brain. The mechanisms of information flow, activation sequence and patterns, and the interaction between anatomical regions of the cortex that are specific to upper extremity motor tasks are not clearly understood at this moment. The objective of this chapter is to identify strategies used by the brain to accomplish a functional upper extremity task. The design of this experiment and analysis methods of active brain regions that pertain to task performance is novel. The use of time resolved fMRI is able to capture activation in the entire brain and provide 3-D anatomical localization of function. The utilization of motor imagery tasks provides insight to the planning and strategy selection process of upper extremity motor tasks. The results (N=18) revealed a number of activation regions for each of the specific task states of planning and execution. This information is highly valuable in the development of upper extremity neuroprosthetic controllers.

4.2: INTRODUCTION.

When performing upper extremity motor tasks, information processing in the brain that pertains to control and motor strategy is a distributed process and is dependent upon activity in several cortical regions. The brain is organized with specific functions for regions such as the SMA and premotor cortex that are involved with task planning, the primary motor cortex being responsible for task execution and the cerebellum for the mediation movement coordination [74,75,114, 182,183]. The literature suggests the

presence of an internal model that provides appropriate strategy to produce accurate and meaningful movement [198-204]. However, the specifics of when and how each of these brain regions activate to realize appropriate neuromotor strategy to produce accurate and meaningful reaching and grasping is a subject of much contention [205-211]. Information processing in the brain occurs in series and parallel with sometimes overlapping activation in regions of the brain for various motor tasks.

Studies have examined functional connectivity in the brain using modalities such as EEG, fMRI, and direct neuron recording [135-137]. Functional connectivity is the process of describing how information flows from one region of the brain to another, including the temporal aspects of this information flow with respect to specific tasks and stimuli. EEG studies have shown the emergence of phenomena such as the Breitschaft potential that predict motor movement and this potential is hypothesized to be a part of the planning phase for movement [236,237]. However, limitations in the recording modality which provides information only from the cortical surface, or experimental paradigms that only focus on one specific cortical region, do not detect signals arising from the multiple brain regions that are involved with reaching and grasping. Furthermore, the majority of the imaging studies and direct neuron recording methods have only focused on finger tapping or motor imagery tasks that do not directly translate into voluntary upper extremity movements. In addition, there are a very limited number of studies that have incorporated the use of real world objects in their experiment paradigms. There are distinct and overlapping regions of activation in the brain that correspond to movements of the limbs, however there is a lot of task specific information that is lost from experiments that do not take into consideration actual reaching and

grasping of real-world objects. Finger tapping tasks work very well for motor localization and to determine regions of activation within the homunculus. However the extrapolation of strategies from rhythmic, limited movements does not necessarily produce accurate representation of functional goal oriented movements that involve real world objects [190-194]. In addition, finger tapping or passive movement studies only provide information or activation in the cortex that relates to specific region activation. There is limited activation in other planning, control, error correction and mediation regions. This clearly suggests that the strategy used is different and extrapolation of information that pertains to understanding strategy of upper extremity functional tasks are not entirely accurate.

The main objective of this chapter is to map temporal activation patterns of specific brain regions that are involved with functional reaching and grasping of real world objects. The hypothesis for this chapter is that upper extremity neuromotor strategy can be identified using distinct temporal brain activation patterns that relate to specific planning and execution task states.

4.3: METHODS.

A separate set of 25 neurologically intact subjects were recruited (M = 15 F = 10 mean age 21.5 years) in order to fulfill the objectives of the second specific aim in this dissertation. Only 18 (M= 10 F = 8 mean age 21.6) of the recruited 25 subjects were used. Five subjects were excluded because they failed to comply with the experimental protocol and the other two subjects were excluded from this analysis for being left hand

dominant. The Edinburgh handedness survey was used to measure the handedness of the subjects and it was determined that all the subjects (N=18) used for this dissertation chapter were right hand dominant [223]. The Institutional Review Boards (IRB) of both Marquette University and the Medical College of Wisconsin approved the research protocol. Subjects gave informed consent and were screened using the Medical College of Wisconsin MRI safety screening questionnaire prior to the start of the experiment to ensure safety compliance with MRI scanning requirements.

4.3.1: Scanner parameters and pulse sequences.

Data acquisition was performed using a 1.5T General Electric (GE) Signa [General Electric Health Care, Waukesha, WI, USA] MRI scanner located in the Department of Radiology of the Froedtert Hospital. Subjects were instructed to lie supine in the scanner. An 8 channel high resolution head coil was used for data acquisition and sponges were placed between the subject's head and the head coil to reduce movement. A knee bolster was used to ensure subject comfort during data acquisition and a pair of ear plugs were provided to attenuate scanner noise. A single high resolution anatomical data set was collected for functional data localization (SPGR pulse sequence, echo time (TE) of 2.984ms, image repetition rate (TR) of 7.78ms, flip angle of 10º, field of view (FOV) of 24mm, slice thickness 1.3mm, 256x192 matrix with 120 slices acquired in the Axial plane, individual voxel dimension of 0.09375mm×0.9375mm×1.3mm). This high resolution anatomical image was collected at the start of the experiment and prior to functional data. A Gradient Echo - Echo Planar Imaging (GE-EPI) pulse sequence was used for acquisition of the functional data (TE of 40ms, a TR of 2s, a flip angel of 90º, a

FOV of 24mm, data matrix of 64x64 with 29 slices and a slice thickness of 5mm, no gap and acquired in the sagittal plane, individual voxel dimension of 3.75x3.75x5). The functional data was acquired in the sagittal plane as this orientation allowed maximum coverage of the brain from the frontal lobe up to the cerebellum. The selection of this acquisition orientation was made to ensure that relevant anatomical and spatial information was preserved.

4.3.2: Experimental paradigm.

Two paradigms were used in this experiment. The first paradigm consisted of 2 block trials that required subjects to reach out, grasp a foam target, and return to the starting position. Each block trial was performed in a unilateral manner in its entirety, the first with the right hand and the latter with the left hand. The block trial paradigm consisted of 3 ‘task’ states and 3 ‘relax’ states in an alternating arrangement, beginning with ‘relax’ as shown in figure 4.1. During the relax states, the subject was told not to move and to remain calm. Next, during the ‘task’ states the subjects reached out and grasped the sponge target followed by returning their hand to the rest position. The entire movement lasted for 2 seconds and was repeated 15 times during each of the designated ‘task’ blocks. The subject was guided using a custom developed visual cue that was back projected through a MR compatible LCD projector [Avotec, Inc., Stuart, FL, USA] onto a custom viewing apparatus attached to the top of the head coil. The objective of these two block trials were to locate regions of brain function for all three tasks and the imagined version of each. These data sets later assisted with identifying functional anatomy of the data acquired in the second paradigm.

FIGURE 4.1: Experiment Paradigm for task set1

The second part of the experiment used a modified event related fMRI paradigm. Subjects were required to reach and grasp the foam target using either right or left hand as specified by the visual cue. The subject was primed with the hand to be used followed by a variable delay of either 2, 4 or 6 seconds prior to actual movement execution of the task, to reduce the effect of learning or task performance prior to the cue. This pre-priming of the task also served as a strong stimulus for motor imagery pertaining to specific task planning for the hand to be used. The entire process lasted for 30 seconds and was repeated a total of 6 times for each delay per hand; therefore the entire block of tasks was 18 minutes in duration. The delay duration and hand use were presented in random order. The entire second paradigm was performed twice.

FIGURE 4.2: Experiment Paradigm for task set 2

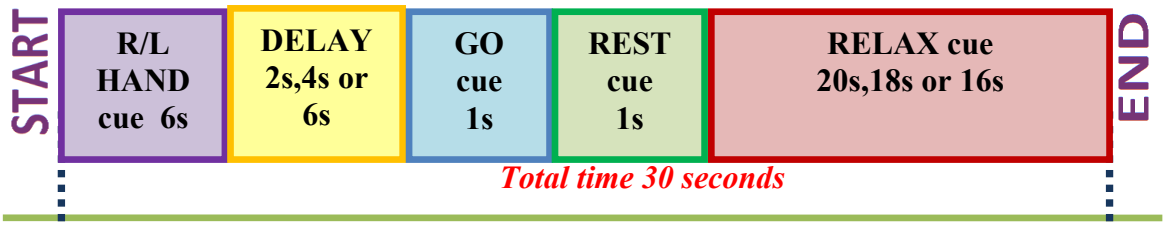

The foam target used in this experiment was a sponge ball attached to a custom made acrylic base that was secured to the table using Velcro straps (Fig.3.5). The target was adjusted to be within easy reach of the subject prior to the start of the experiment.

4.3.3: Analysis.

Reconstruction of the raw acquired *k*-space data was performed by the Signa MR System. The reconstructed images were processed into anatomical and functional MRI datasets respectively, using the Analysis of Functional Neuro Images (AFNI) software package [224]. All processing was done using custom written Bash Shell scripts. The reconstruction process saved the data sets into a pair of files that were in HEAD and BRIK format. Three dimensional volume registration was performed on the data sets by aligning each dataset to repetition #45 of the data set acquired during the first block paradigm, immediately after acquisition of the anatomical data set, in order to correct for subject movement during the data acquisition. BRIK #45 was chosen because this was the center data set acquired in a set of 90 data sets.

The first 3 data points of the data set were discarded during data analysis to account for the equilibration of longitudinal magnetization. The reference waveform was obtained by convoluting the ideal series of events (see the blue plot in figure 4.3) with the gamma variate function resulting in the reference function shown in the red plot of figure 4.3 [224].

FIGURE 4.3 Ideal waveform (blue) and gamma variate convolved waveform (red).

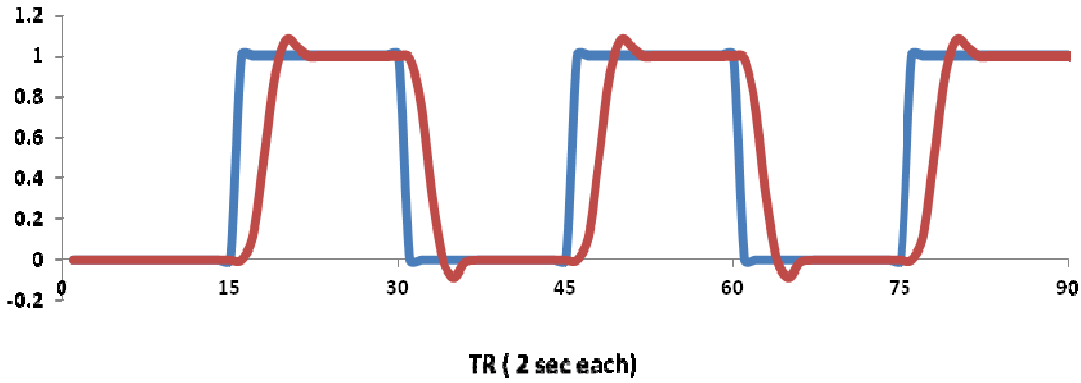

The reconstructed fMRI time series data sets were cross correlated voxel-by-voxel, with the expected fMRI response to the stimulus yielding the Pearson's correlation value, in order to determine regions of activation. The individual data sets were transformed into Tailarach space using the TTN27 template resulting in a group activation map. A 3D *t*-test ($p<0.05$) was done on the group data to identify common active regions in the group data. The False Discovery Rate (FDR) method was subsequently used to determine appropriate thresholds for the functional data sets with a conservative *q* value of 0.02 [152]. An anatomically labeled mask, based on the TTN27 EZ ML template, was created using the processed data sets [224]. This mask was resized to each subject's individual anatomy and the voxels that were deemed active for each experimental paradigm were extracted. These data sets were further processed in MATLAB to determine the delay effects and also to understand stimulus induced region activation.

The specific time series corresponding to specific hand and delay cues were extracted from the second paradigm's data set. These time series were for each voxel contained within a specific region of the brain as determined by the TTN 27 EZ ML

cortical atlas [224]. The start of each individual voxel's time series was normalized to zero. Next the average, standard deviation and standard error about the mean were calculated across all voxels to produce the net activation for that particular region.

An analysis was performed to determine the effect of the varying the inter task delay on the activation characteristics. THIs analysis was constrained to the execution phase of the right and left motor tasks. An ANOVA was performed to determine the effect of varying inter task durations on the area under the curve, duration of activation, slope and maximum amplitude of activation. The duration of activation was defined as the time between the start of the actual movement till the signal returned to baseline, after completion of the task. The maximum activation amplitude was the highest value during the duration of activation and the area under the curve was calculated for the duration of activation. The slope was calculated using a linear equation specified to be between the 10% and 90% values of the rising phase for the time series activation. This analysis was performed for the right motor tasks and left motor tasks separately.

4.4: RESULTS.

4.4.1 : Comparisons Between Left and Right Motor Tasks.

Figures 4.4a through 4.4d show the distributions of active voxels for 18 subjects that allow comparison of the motor tasks performed during the block paradigm using the right and left hands respectively. The data shows that there are 34 common activation regions during the right and left hand motor tasks. The observed increase in voxel activity corresponded to the hemisphere that was contra-lateral to that of hand use. Overall, the

motor tasks that used the right hand had a higher number of active voxels as compared to the motor tasks that used the left hand in the respective locations for that side of the body. Furthermore, the data showed the presence of 20 distinct regions that are specific to the right hand motor task and 6 regions that are specific to the left hand motor task.

FIGURE 4.4a: Comparison of Activation Regions (1 – 29) between Right and Left hand motor tasks.

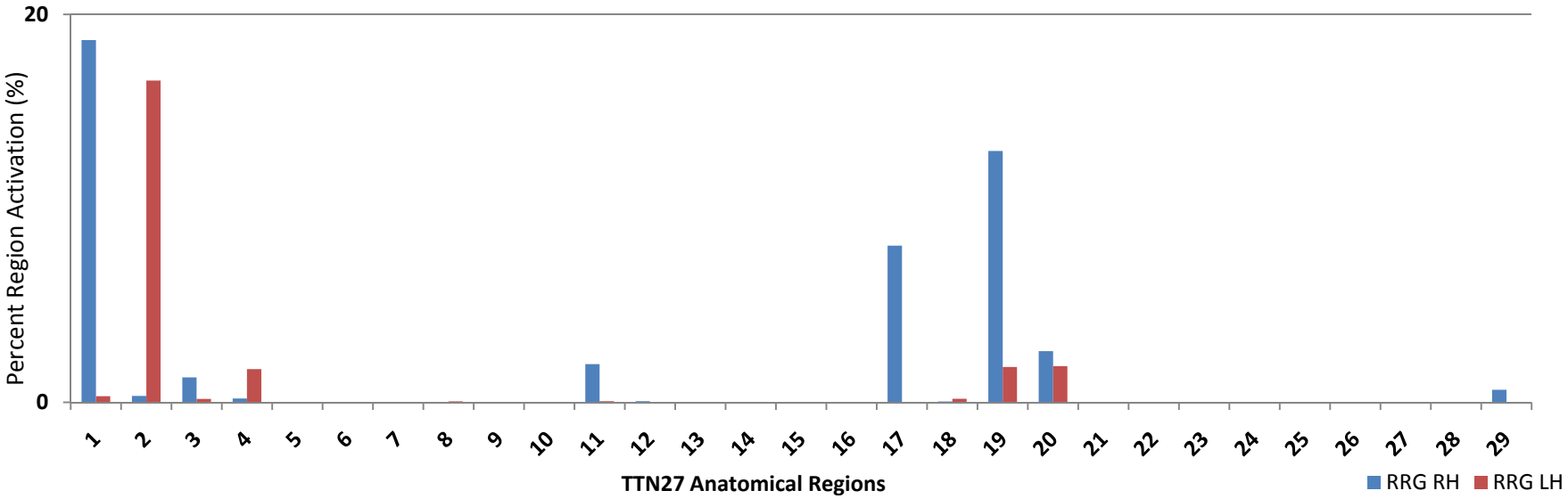

FIGURE 4.4b: Comparison of Activation Regions (30 – 59) between Right and Left hand motor tasks.

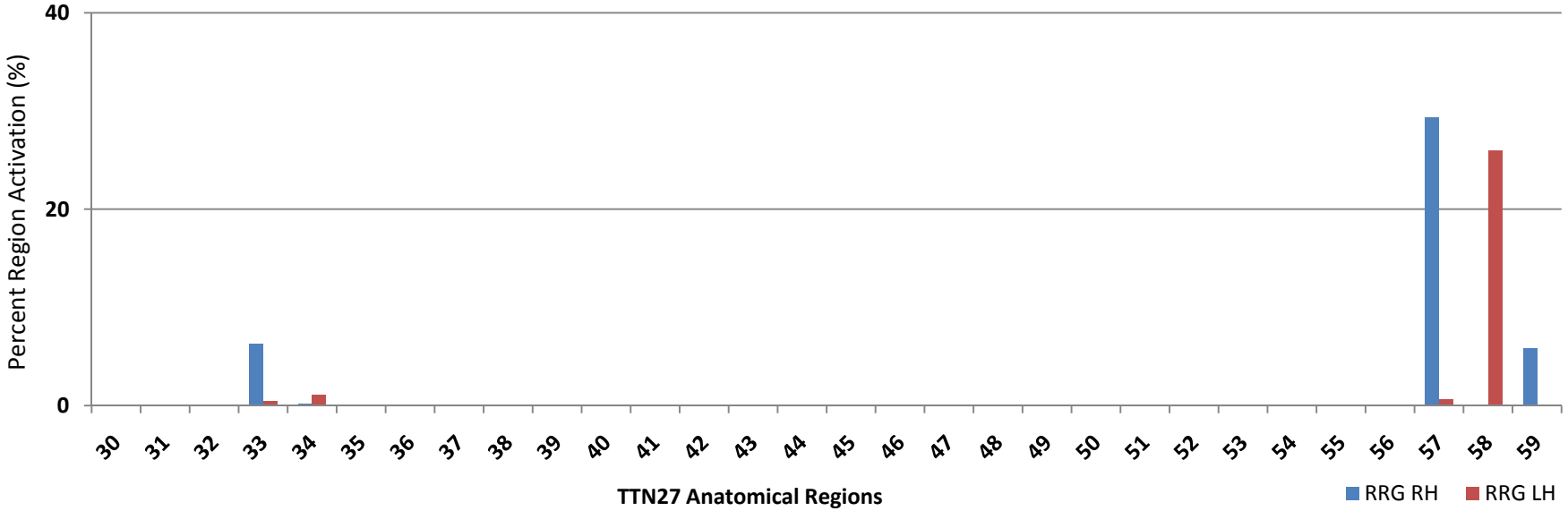

FIGURE 4.4c: Comparison of Activation Regions (60 – 89) between Right and Left hand motor tasks.

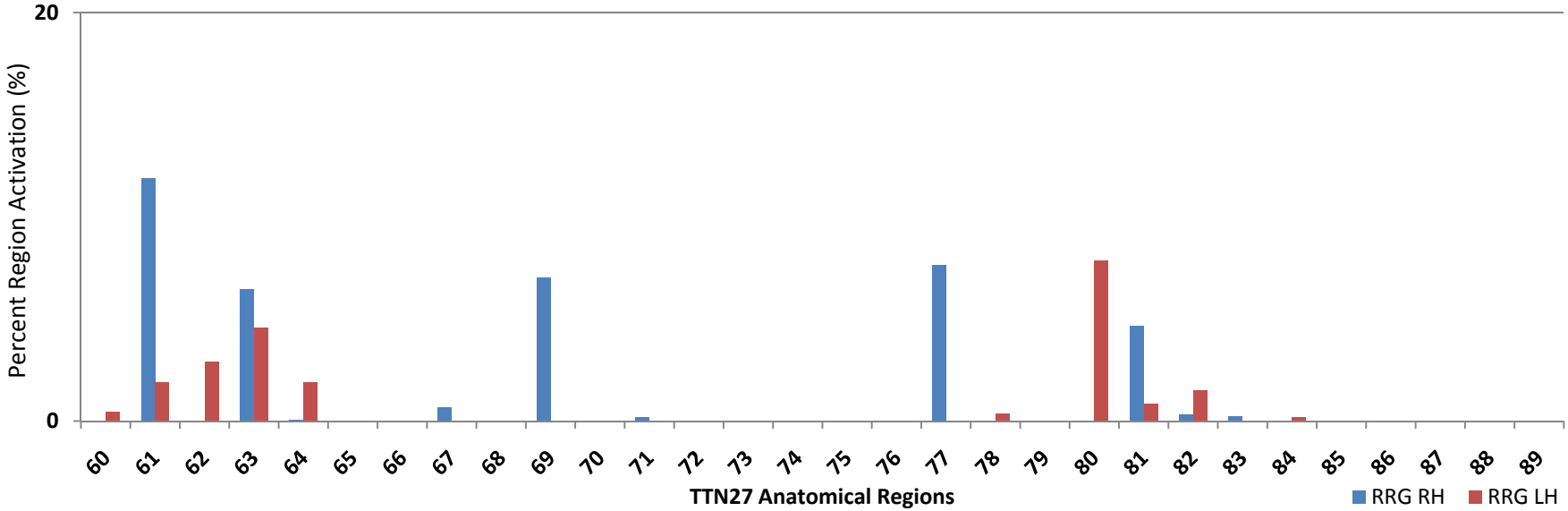

FIGURE 4.4d: Comparison of Activation Regions (90 - 112) between Right and Left hand motor tasks.

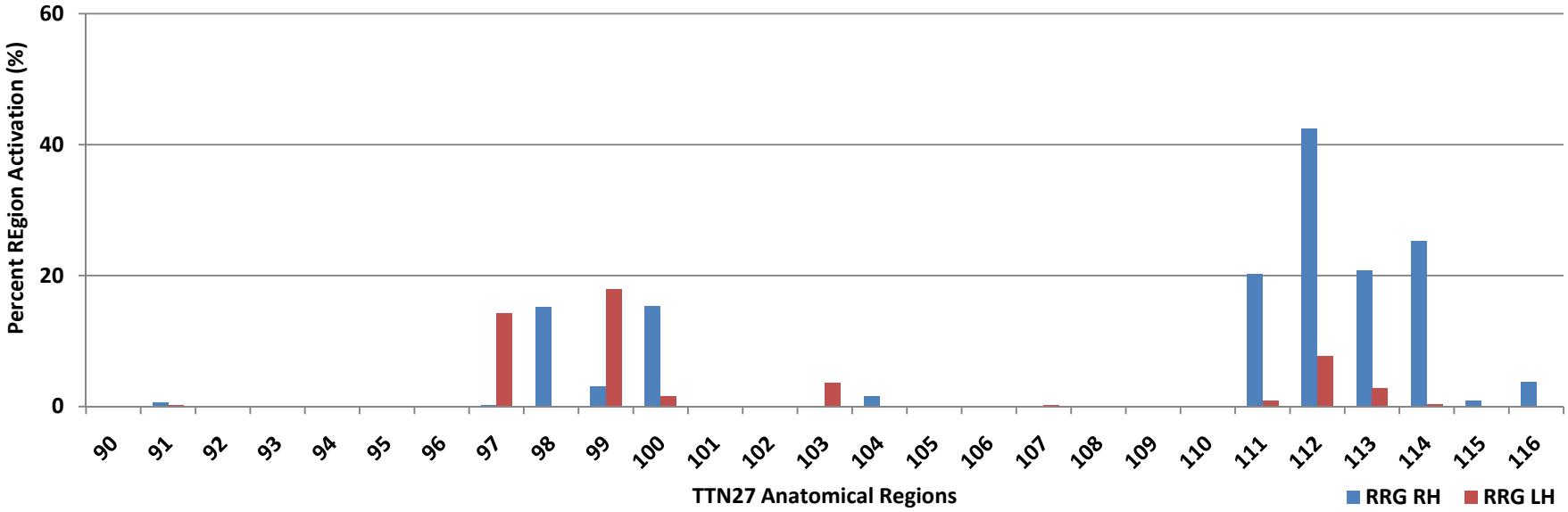

4.4.2 : Activation Regions for Right Motor Task.

The individual time courses from each activation region were extracted for each subject and averaged to determine activation profiles for each of the regions shown in the distribution plots of figures 4.4a through 4.4d for the right hand motor task,. The net activation for motor tasks that involve the right hand at inter stimulus delays of 2,4 and 6 seconds are displayed as color maps in figures 4.5a through 4.5c. Data from the activation regions are stacked on top of one another in the vertical axis and the time profiles is shown in the horizontal axis. Notice the onset of task planning in the first 4 time points, the induced delay and the execution. The positive and negative amplitudes of the time profiles are represented by magenta and cyan hues respectively. Figures 4.6a through 4.6q show the time series activation profiles for each individual region of the brain. Task performance of the right motor task with 2seconds (blue), 4 seconds (green) and 6seconds (red) delay are overlaid on top of one another.

TABLE 4.1: Activation Regions for Right Motor Tasks

	Regions		Regions		Regions
1	L Precentral Gyrus	19	R Lingula Gyrus	37	L Cerebellum (Crus 1)
2	R Precentral Gyrus	20	L Middle Occipital Gyrus	38	R Cerebellum (Crus 1)
3	L Superior Frontal Gyrus	21	L Inferior Occipital Gyrus	39	L Cerebellum (Crus 2)
4	R Superior Frontal Gyrus	22	L Fusiform Gyrus	40	L Cerebellum (IV-V)
5	L Middle Frontal Gyrus	23	L Postcentral Gyrus	41	R Cerebellum (IV-V)
6	R Middle Frontal Gyrus	24	R Postcentral Gyrus	42	L Cerebellum (VI)
7	L Inferior Frontal Gyrus	25	L Superior Parietal Lobule	43	R Cerebellum (VI)
8	R Inferior Frontal Gyrus	26	L Inferior Parietal Lobule	44	L Cerebellum (VIII)
9	L Rolandic Operculum	27	L SupraMarginal Gyrus	45	R Cerebellum (VIII)
10	R Rolandic Operculum	28	R SupraMarginal Gyrus	46	L Cerebellum (IX)
11	L SMA	29	L Precuneus	47	Cerebella Vermis (4/5)
12	R SMA	30	L Paracentral Lobule	48	Cerebella Vermis (6)
13	L Insula Lobe	31	L Caudate Nucleus	49	Cerebella Vermis (7)
14	R Insula Lobe	32	L Thalamus	50	Cerebella Vermis (8)
15	L Middle Cingulate Cortex	33	L Superior Temporal Gyrus	51	Cerebella Vermis (9)
16	R Middle Cingulate Cortex	34	R Superior Temporal Gyrus	52	Cerebella Vermis (10)
17	L Calcarine Gyrus	35	L Temporal Pole		L - Left
18	L Lingula Gyrus	36	R Temporal Pole		R - Right

FIGURE 4.5a: Reaching And Grasping with the Right Hand at 2s. Delay.

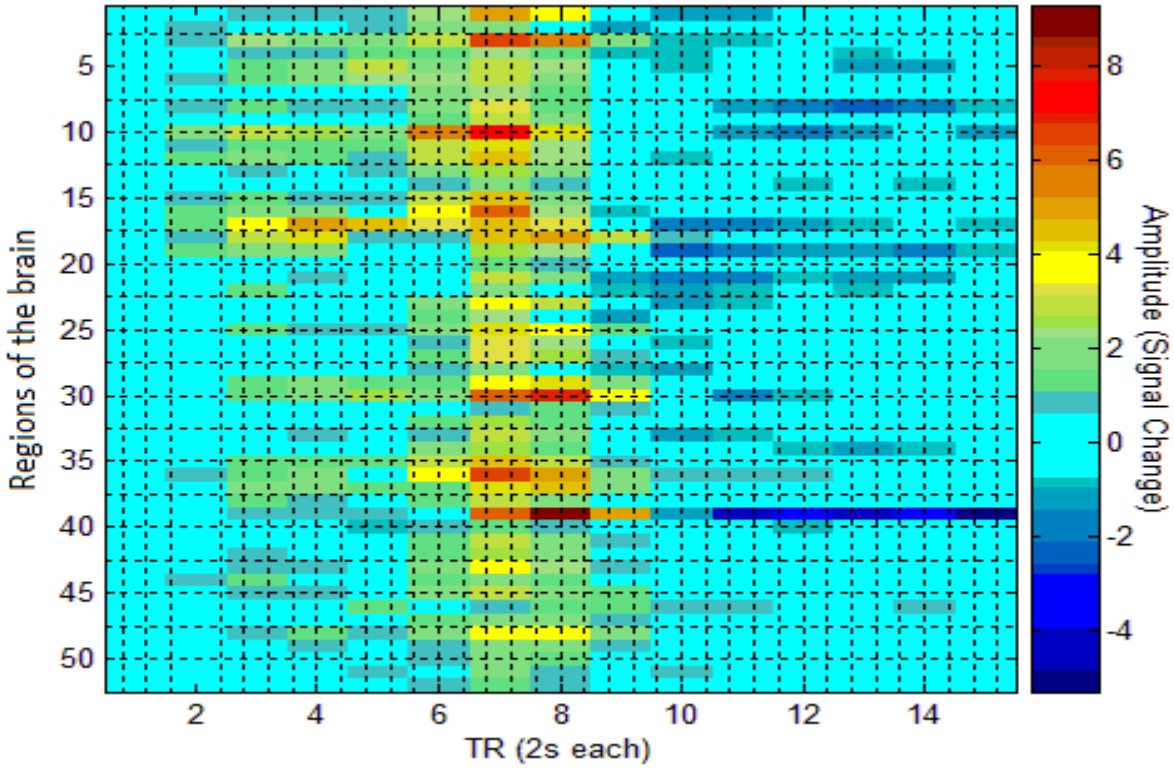

FIGURE 4.5b: Reaching and Grasping with the Right Hand at 4s. Delay.

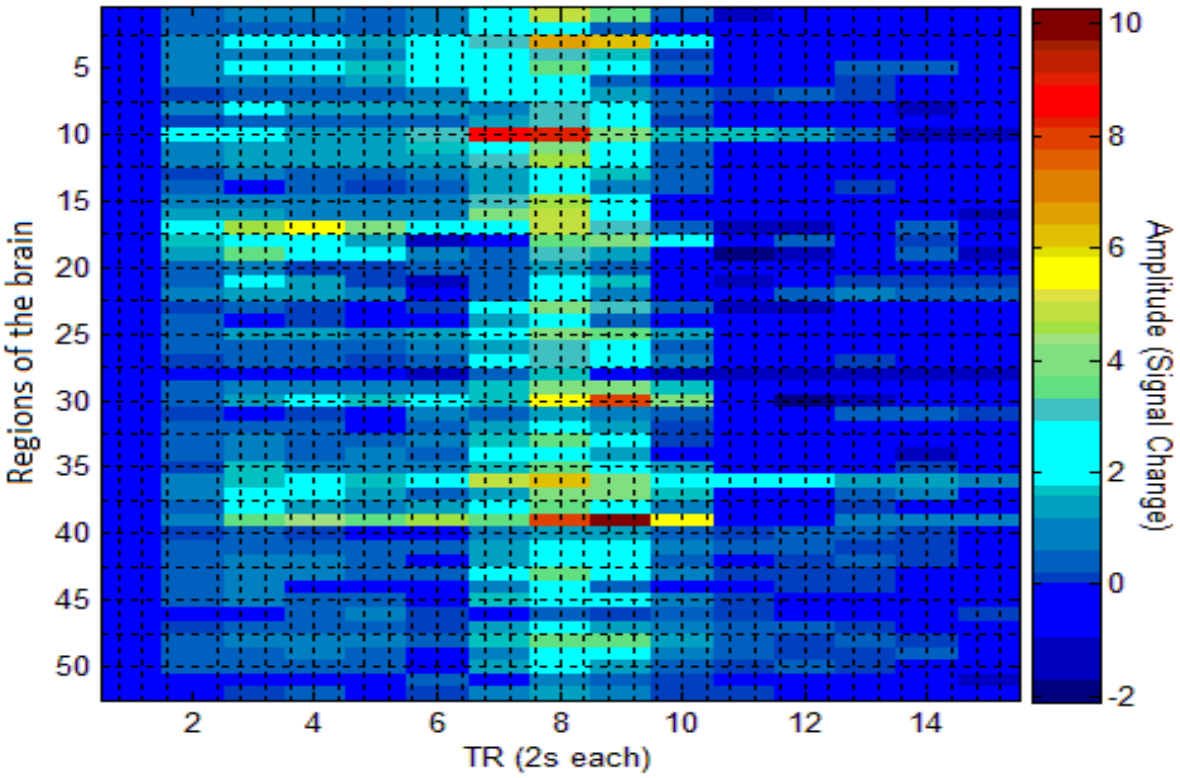

FIGURE 4.5c: Reaching and Grasping with the Right Hand at 6s. Delay.

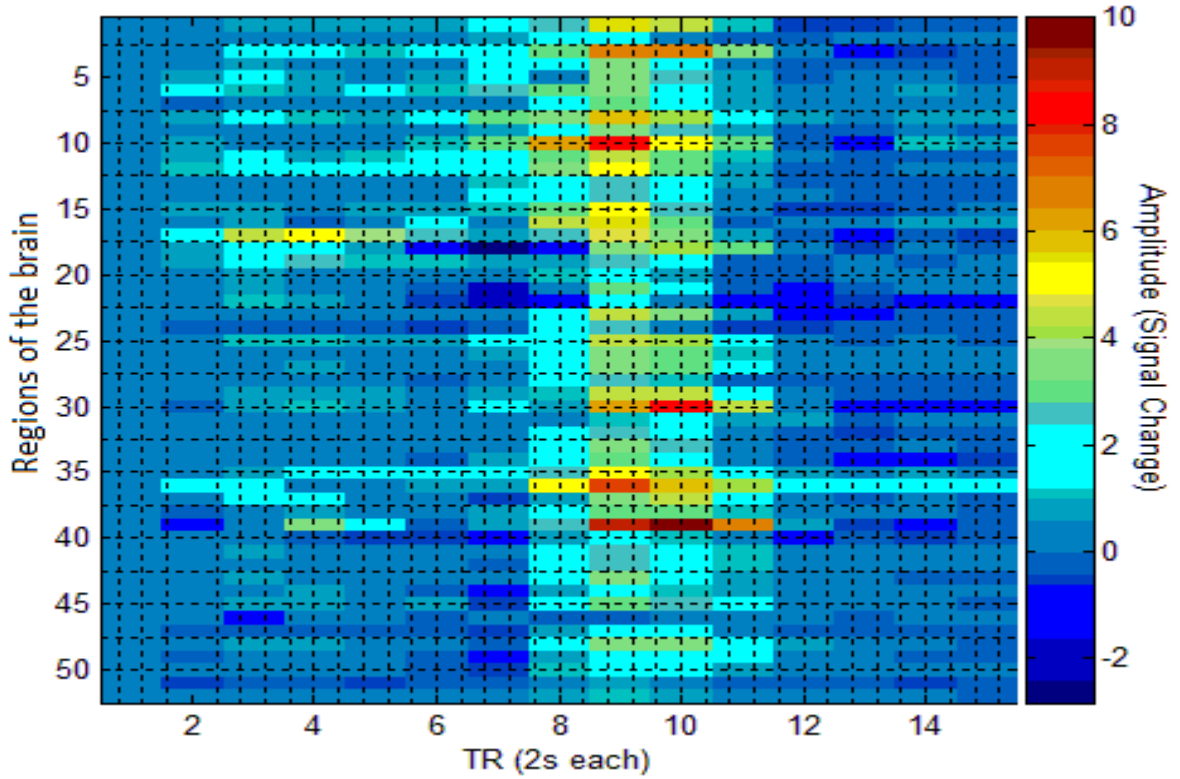

FIGURE 4.6a: Activation Profiles Corresponding to Motor Task Performed with the Right Hand (Data plotted with ±1 SEM, Regions 1-3).

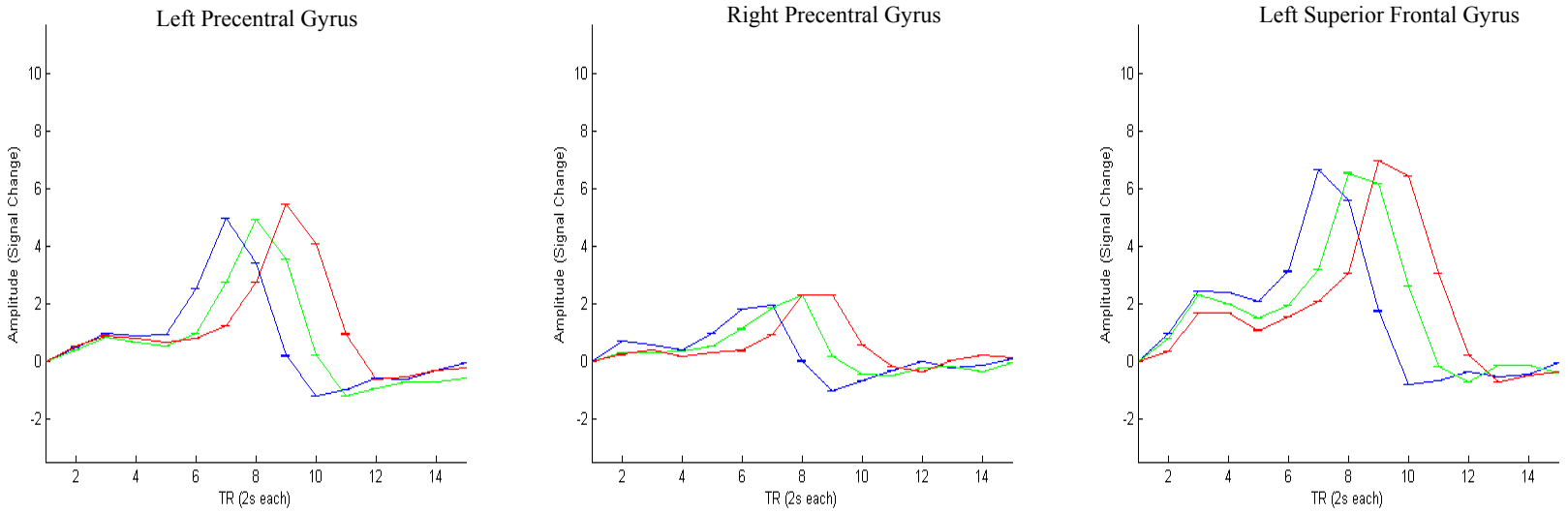

FIGURE 4.6b: Activation Profiles Corresponding to Motor Task Performed with the Right Hand (Data plotted with ±1 SEM, Regions 4-6).

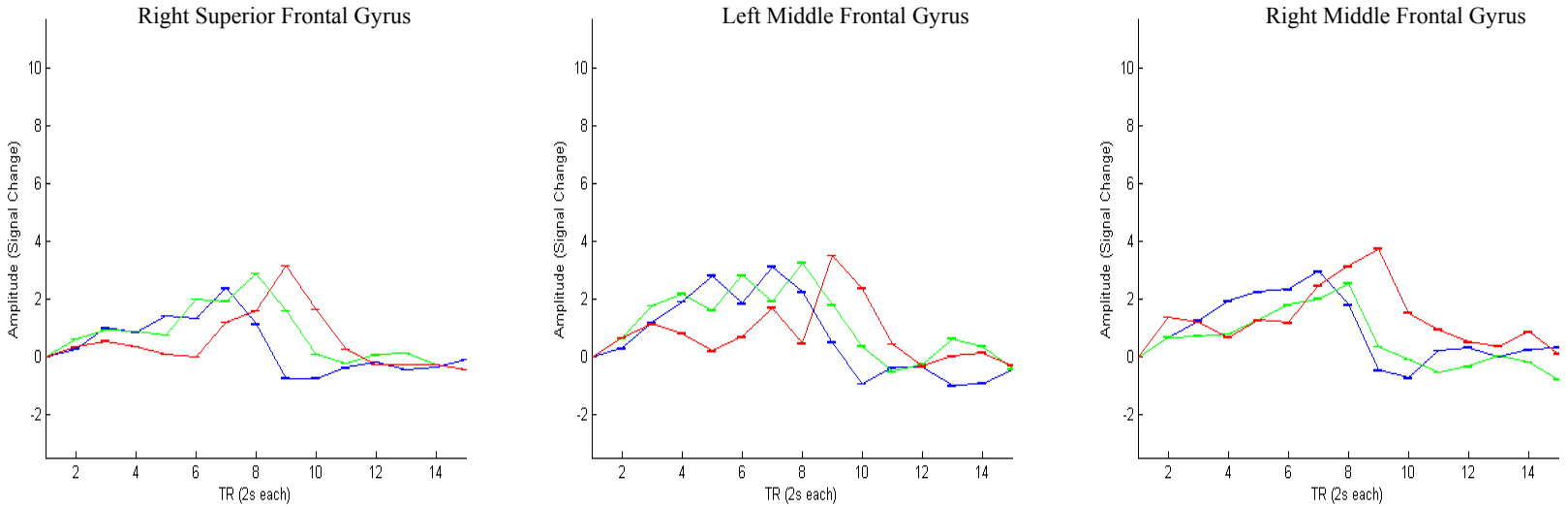

FIGURE 4.6c: Activation Profiles Corresponding to Motor Task Performed with the Right Hand (Data plotted with ±1 SEM, Regions 7-9).

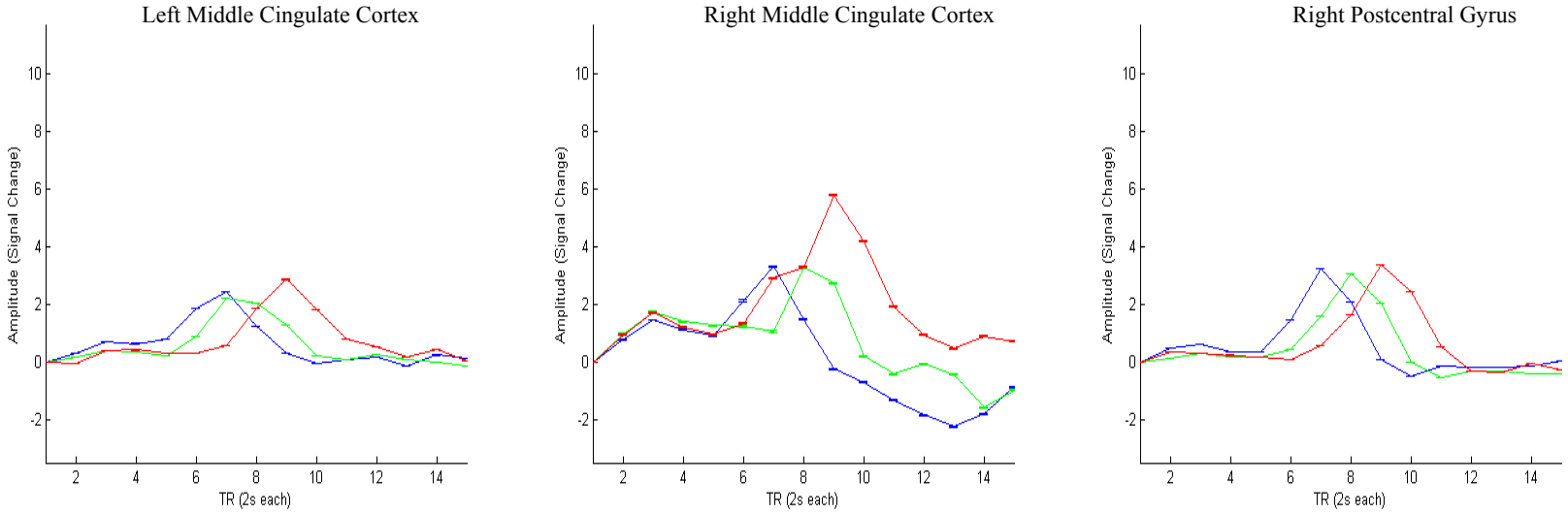

FIGURE 4.6d: Activation Profiles Corresponding to Motor Task Performed with the Right Hand (Data plotted with ±1 SEM, Regions 10-12).

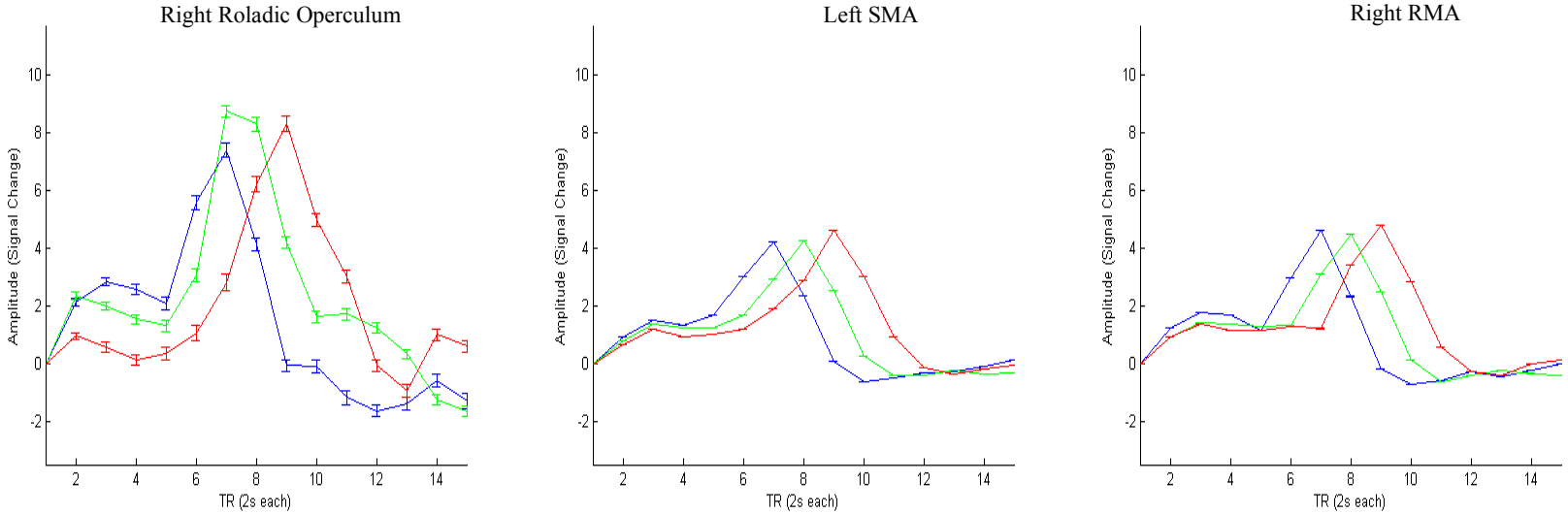

FIGURE 4.6e: Activation Profiles Corresponding to Motor Task Performed with the Right Hand (Data plotted with ±1 SEM, Regions 13-15).

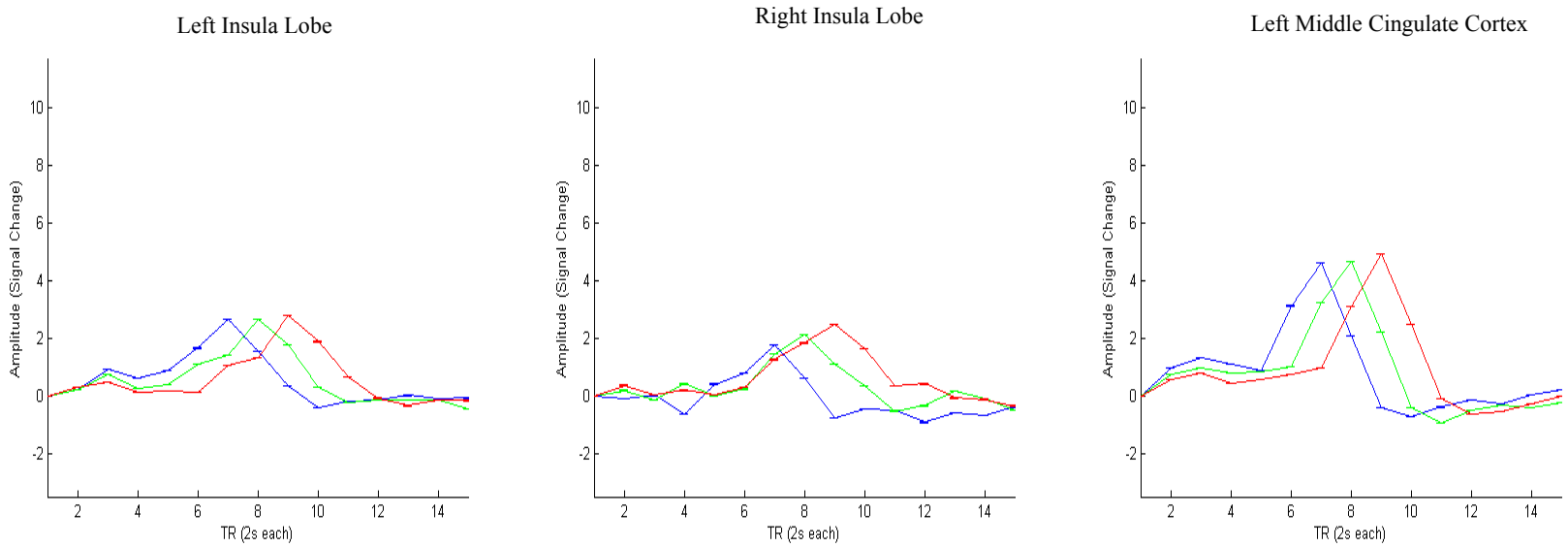

FIGURE 4.6f: Activation Profiles Corresponding to Motor Task Performed with the Right Hand (Data plotted with ±1 SEM, Regions 16-18).

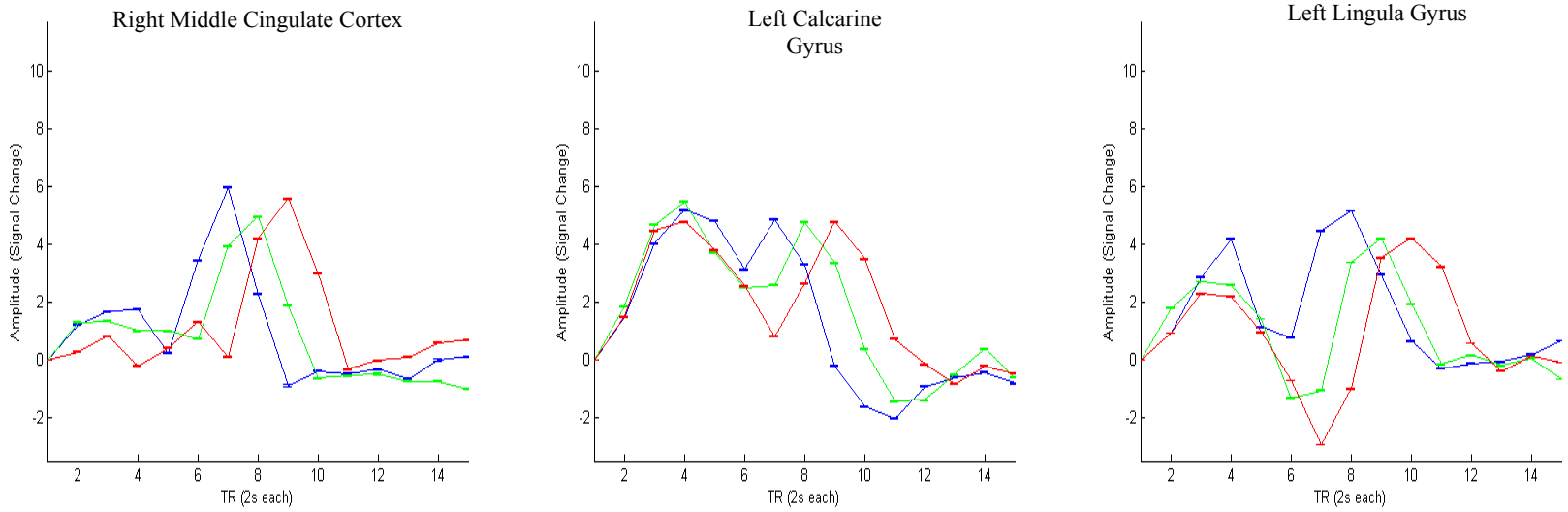

FIGURE 4.6g: Activation Profiles Corresponding to Motor Task Performed with the Right Hand (Data plotted with ±1 SEM, Regions 19-21).

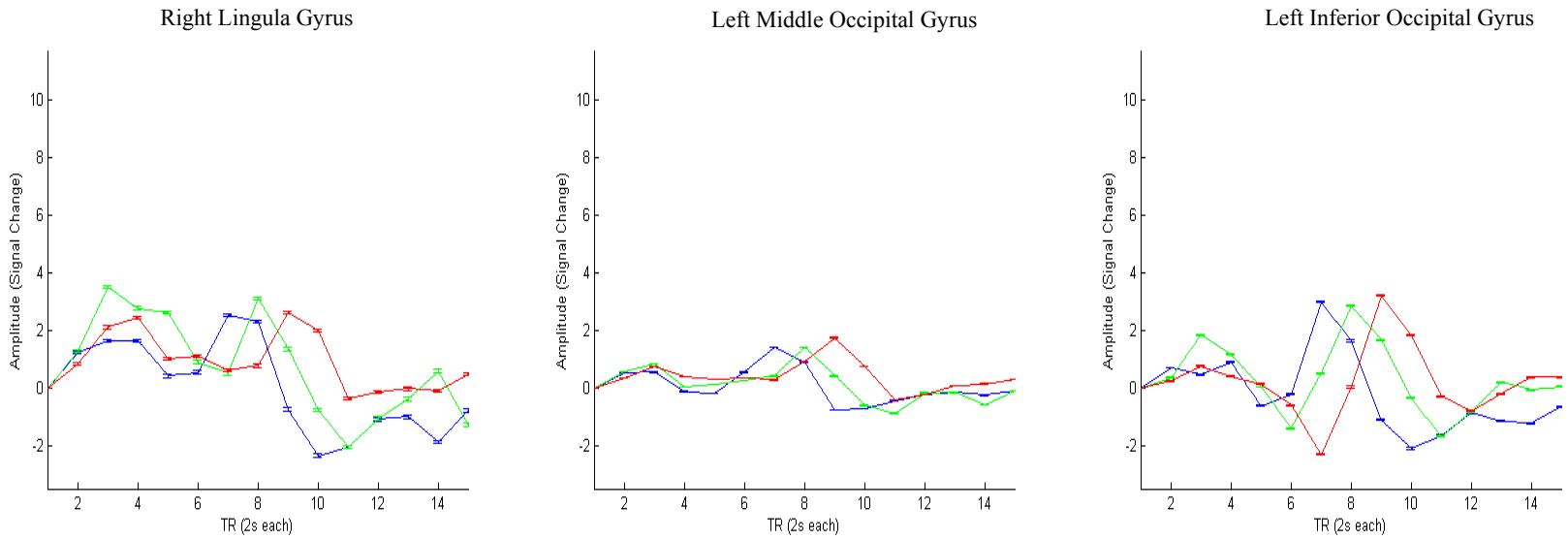

FIGURE 4.6h: Activation Profiles Corresponding to Motor Task Performed with the Right Hand (Data plotted with ±1 SEM, Regions 22-24).

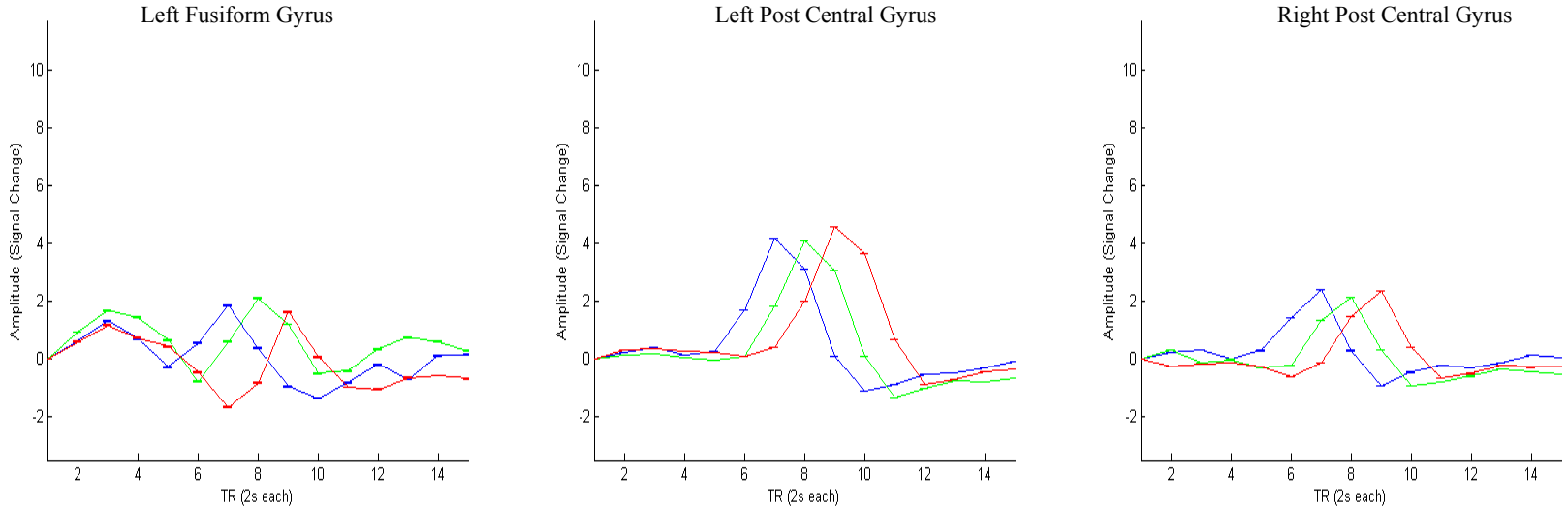

FIGURE 4.6i: Activation Profiles Corresponding to Motor Task Performed with the Right Hand (Data plotted with ±1 SEM, Regions 25-27).

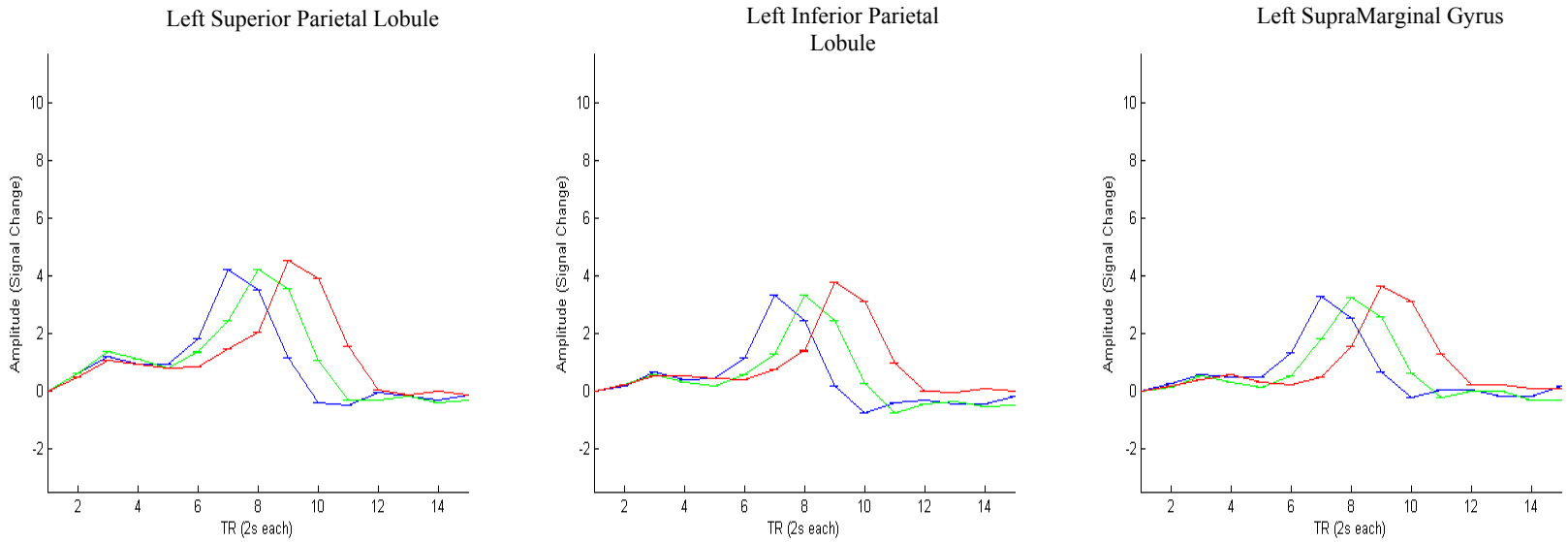

FIGURE 4.6j: Activation Profiles Corresponding to Motor Task Performed with the Right Hand (Data plotted with ±1 SEM, Regions 28-30).

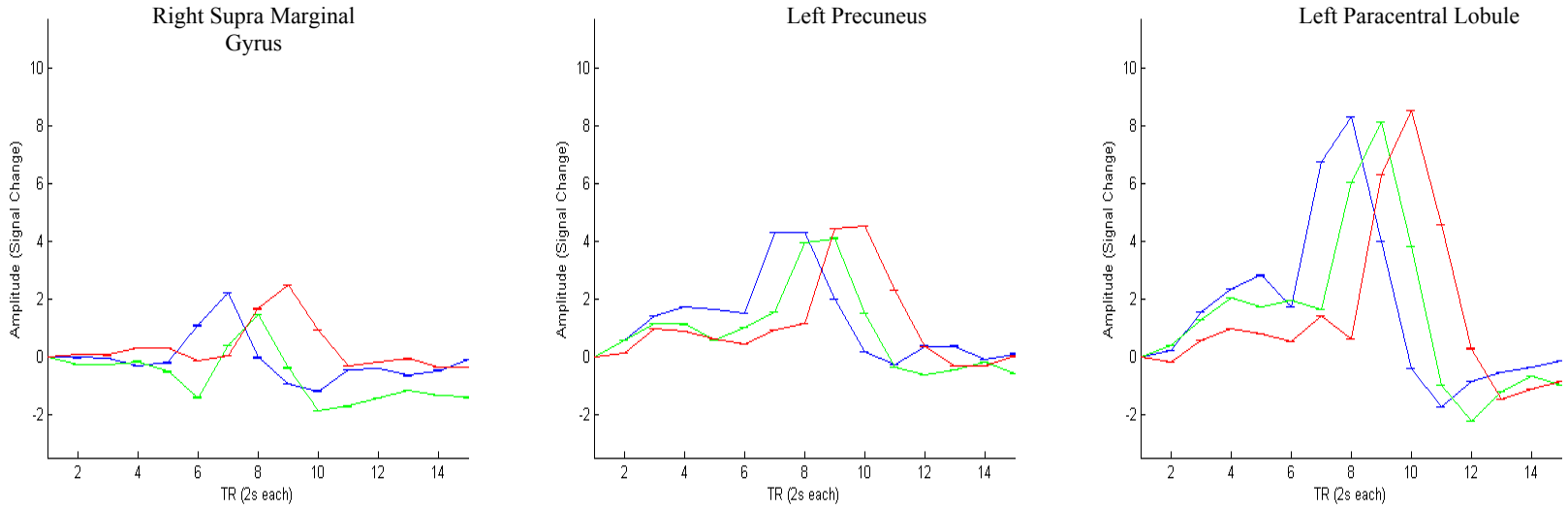

FIGURE 4.6k: Activation Profiles Corresponding to Motor Task Performed with the Right Hand (Data plotted with ±1 SEM, Regions 31-33).

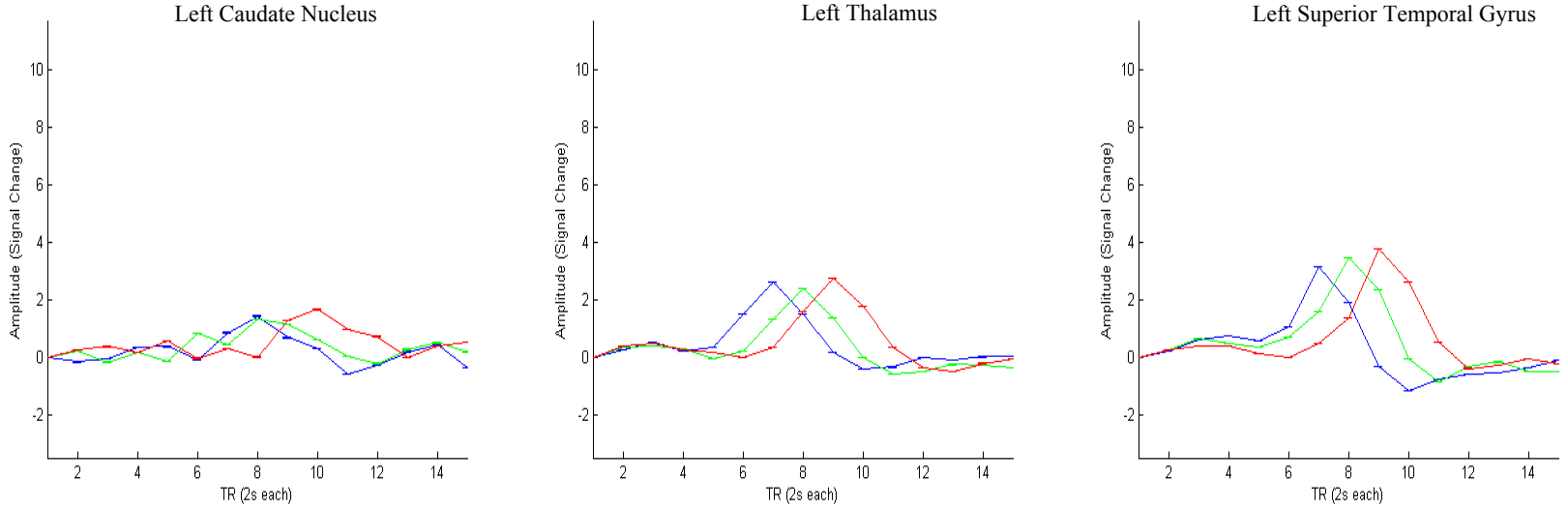

FIGURE 4.6l: Activation Profiles Corresponding to Motor Task Performed with the Right Hand (Data plotted with ±1 SEM, Regions 34-36).

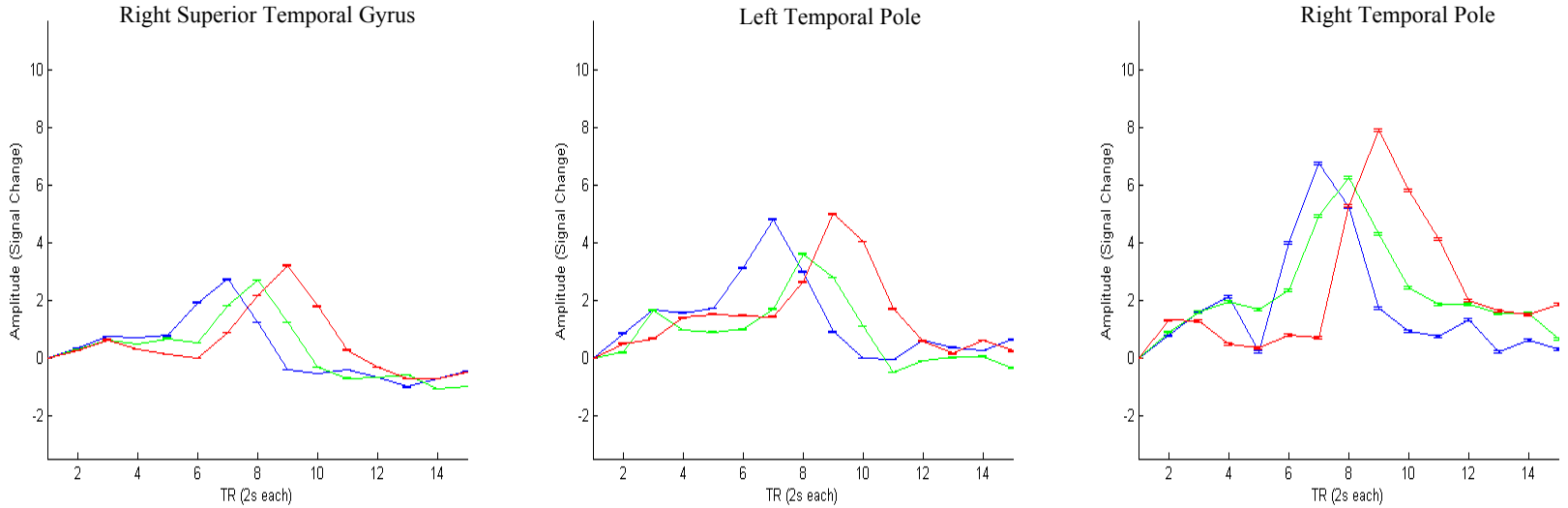

FIGURE 4.6m: Activation Profiles Corresponding to Motor Task Performed with the Right Hand (Data plotted with ±1 SEM, Regions 37-39).

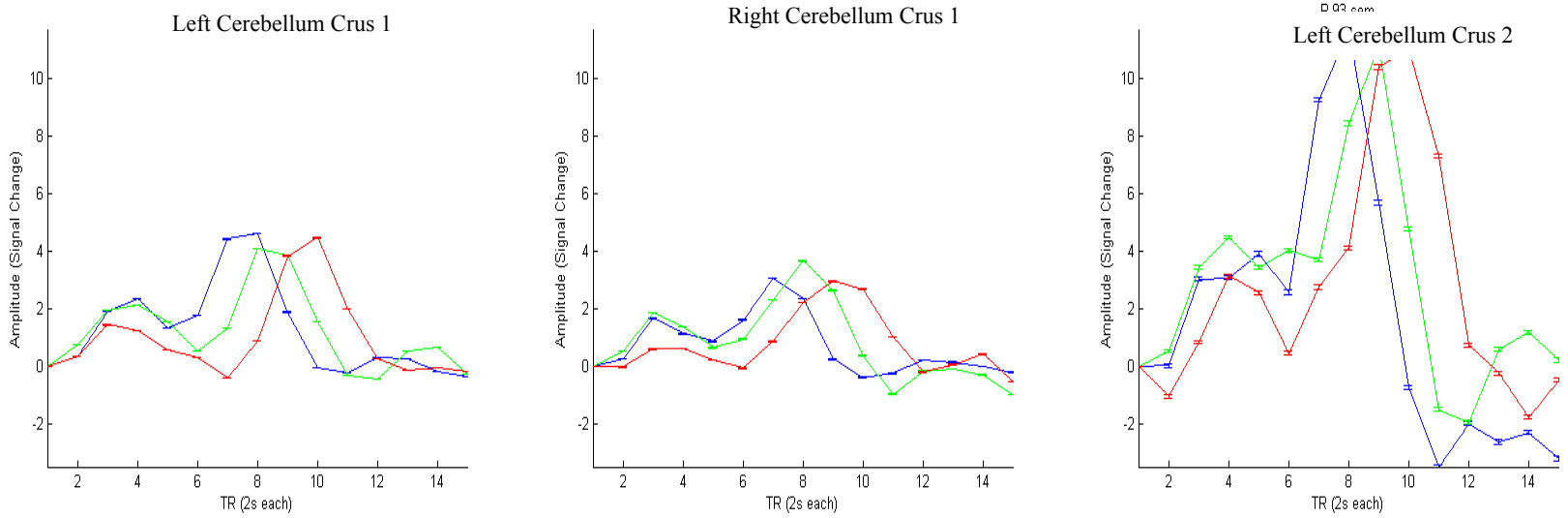

FIGURE 4.6n: Activation Profiles Corresponding to Motor Task Performed with the Right Hand (Data plotted with ±1 SEM, Regions 40-42).

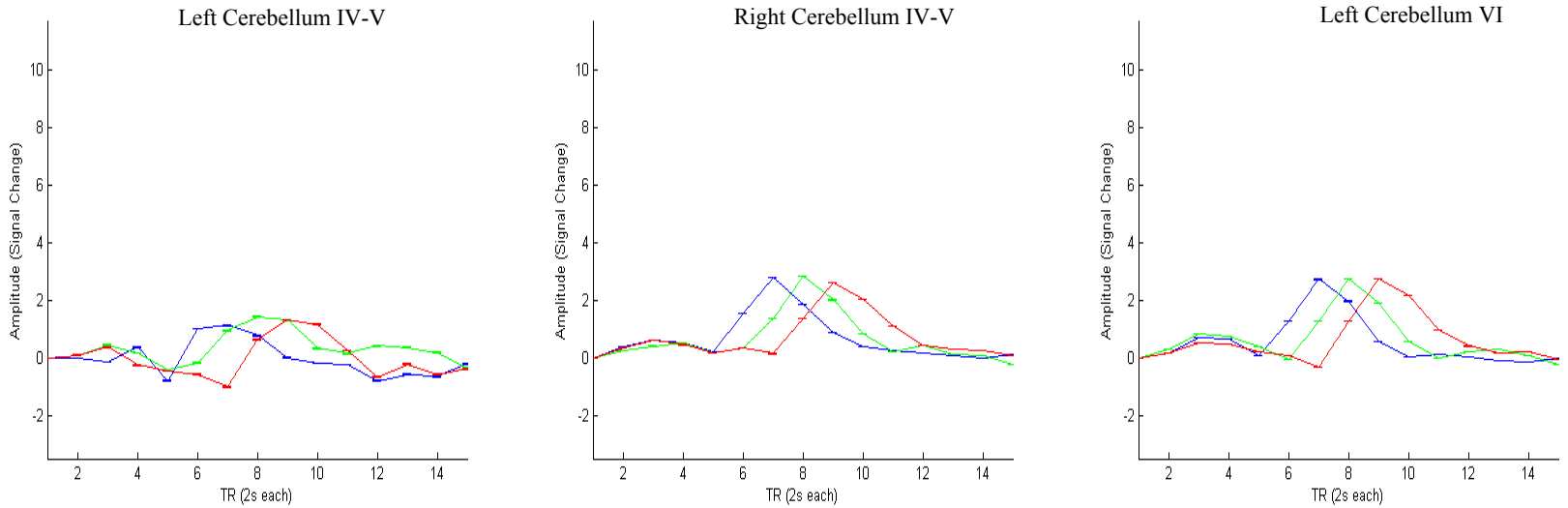

FIGURE 4.6o: Activation Profiles Corresponding to Motor Task Performed with the Right Hand (Data plotted with ±1 SEM, Regions 43-45).

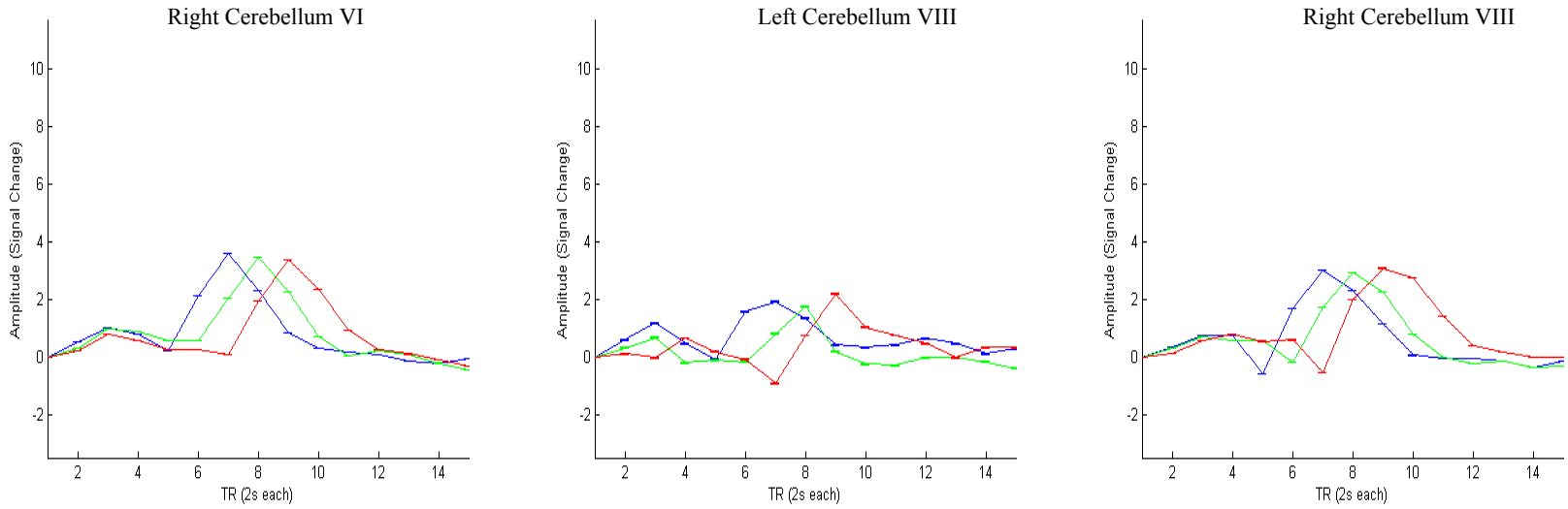

FIGURE 4.6p: Activation Profiles Corresponding to Motor Task Performed with the Right Hand (Data plotted with ±1 SEM, Regions 46-48).

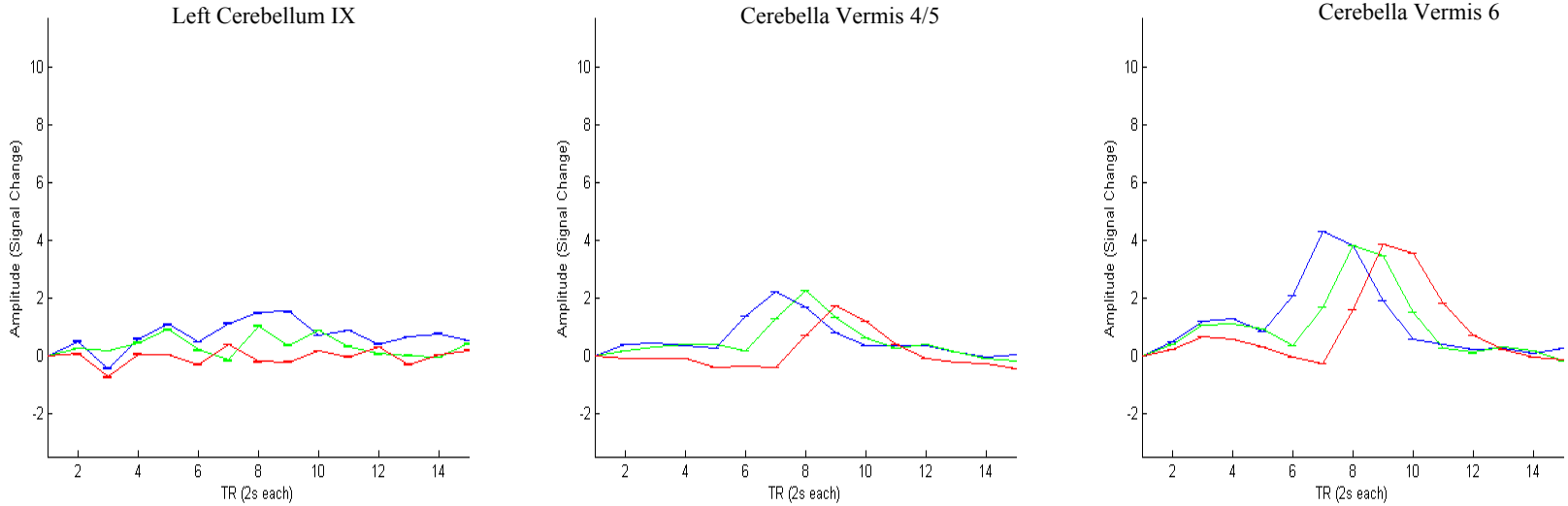

FIGURE 4.6q: Activation Profiles Corresponding to Motor Task Performed with the Right Hand (Data plotted with ±1 SEM, Regions 49-51).

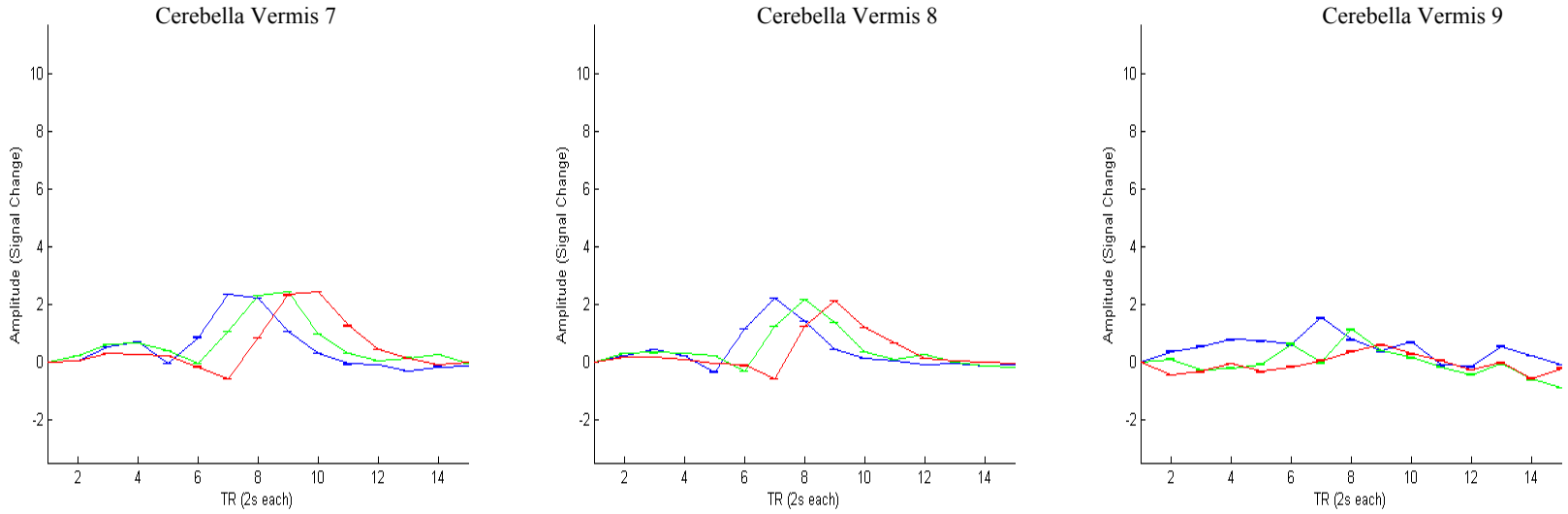

FIGURE 4.6r: Activation Profiles Corresponding to Motor Task Performed with the Right Hand (Data plotted with ±1 SEM , Region 52).

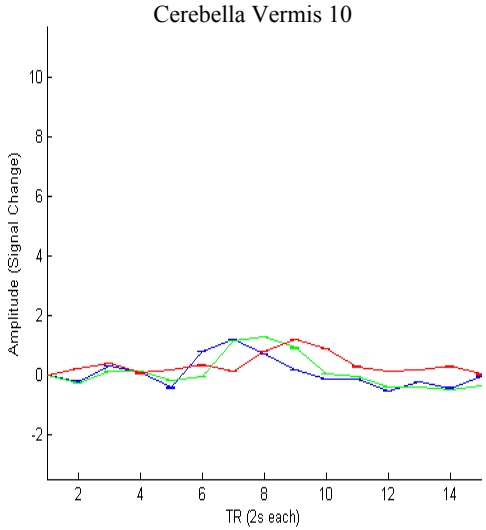

4.4.3 : Activation Regions for Left Motor Task.

The individual time courses from each activation region were extracted for each subject and averaged to determine activation profiles for each of the regions shown in the distribution plots for the left motor task of figures 4.4a through 4.4d. The net activation for motor tasks involving the right hand at inter stimulus delays of 2,4 and 6 second are displayed as color maps in figures 4.7a through 4.7c. Each activation region is stacked on top of another in the vertical and the corresponding time profiles are shown in the horizontal axis. Temporal activation pertaining to task planning, the induced delay and the execution can be seen. The positive and negative amplitudes for the time profiles are represented by magenta and cyan hues respectively. Figures 4.8a through 4.8q show the time series activation profiles for each individual brain region where left hand motor task with 2s. (blue), 4s. (green) and 6s. (red) of delay are overlaid on top of one another .

TABLE 4.2 Activation Regions for Left Motor Task.

	Region		Region		Region
1	L Precentral Gyrus	16	L Postcentral Gyrus	31	L Cerebellum (IV-V)
2	R Precentral Gyrus	17	R Postcentral Gyrus	32	L Cerebellum (VI)
3	L Superior Frontal Gyrus	18	L Superior Parietal Lobule	33	R Cerebellum (VI)
4	R Superior Frontal Gyrus	19	R Superior Parietal Lobule	34	L Cerebellum (VIII)
5	R Middle Frontal Gyrus	20	L Inferior Parietal Lobule	35	L Cerebellum (X)
6	L Inferior Frontal Gyrus	21	R Inferior Parietal Lobule	36	Cerebella Vermis (4/5)
7	R Rolandic Operculum	22	L SupraMarginal Gyrus	37	Cerebella Vermis (6)
8	L SMA	23	R SupraMarginal Gyrus	38	Cerebella Vermis (7)
9	R SMA	24	L Paracentral Lobule	39	Cerebella Vermis (8)
10	R Insula Lobe	25	R Thalamus		L – Left
11	L Middle Cingulate Cortex	26	R Heschls Gyrus		R – Right
12	R Middle Cingulate Cortex	27	L Superior Temporal Gyrus		
13	R Hippocampus	28	R Superior Temporal Gyrus		
14	L Calcarine Gyrus	29	R Temporal Pole		
15	L Fusiform Gyrus	30	L Cerebellum (Crus 1)		

Figure 4.7a: Reaching and Grasping with the Left hand at 2s. delay

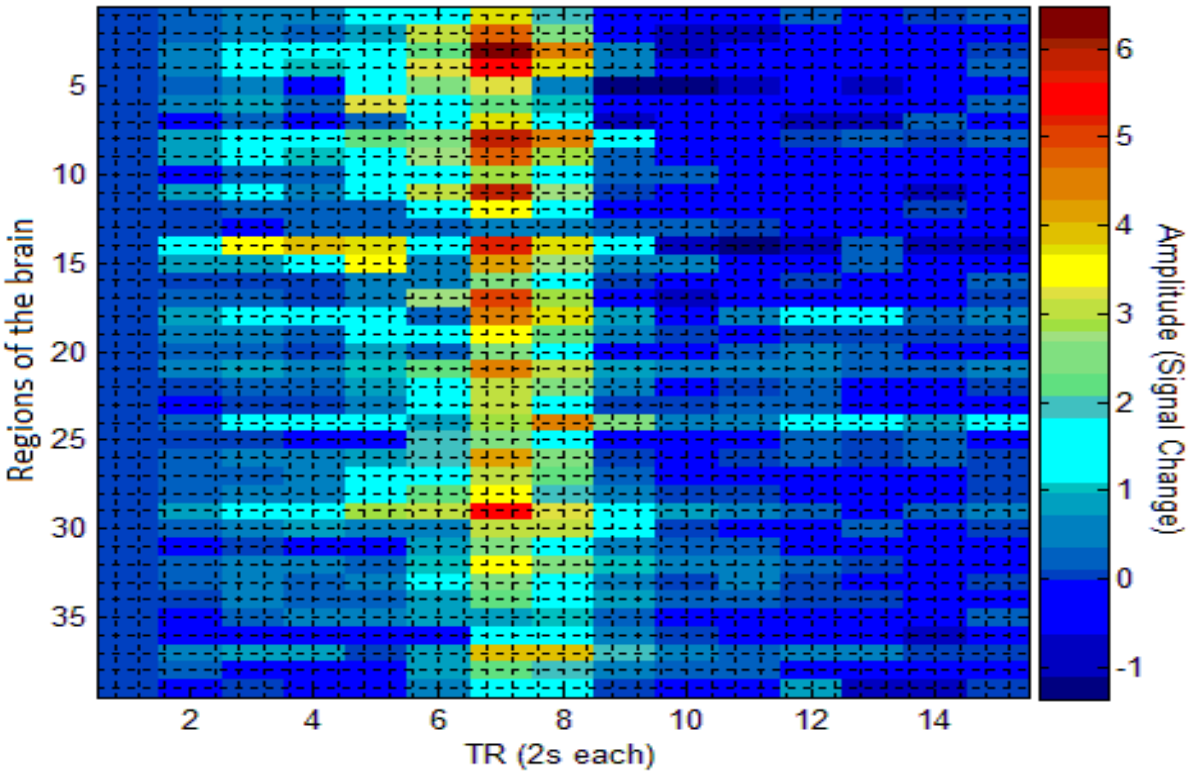

FIGURE 4.7b: Reaching and Grasping with the Left hand at 4s. delay

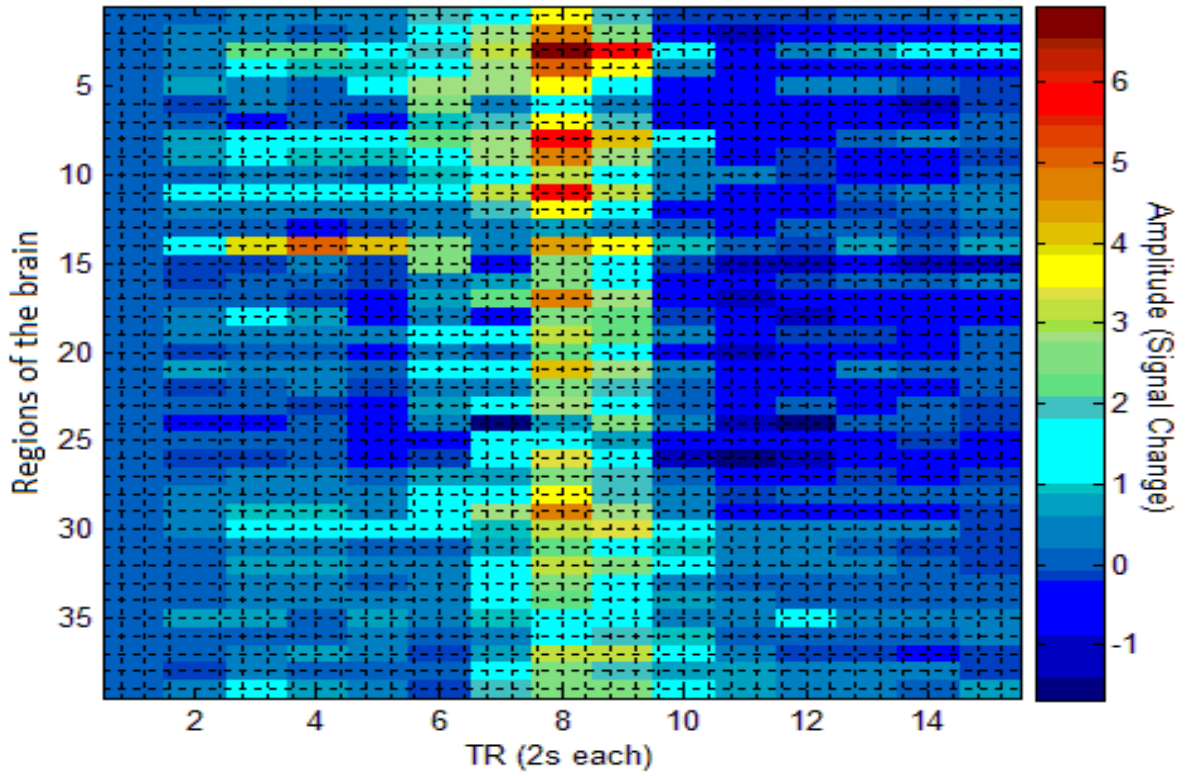

FIGURE 4.7c: Reaching and Grasping with the Left hand at 6s. delay

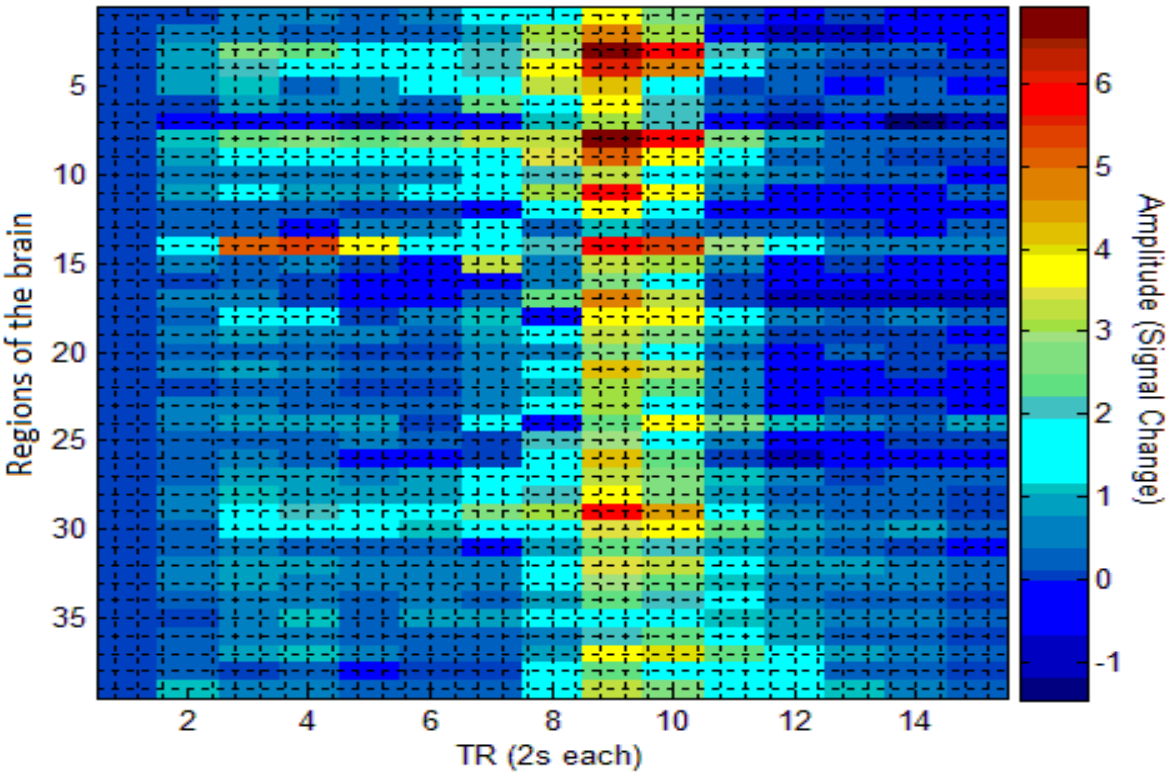

FIGURE 4.8a: Activation Profiles Corresponding to Motor Task Performed with the Left Hand (Data plotted with ±1 SEM, Regions 1-3).

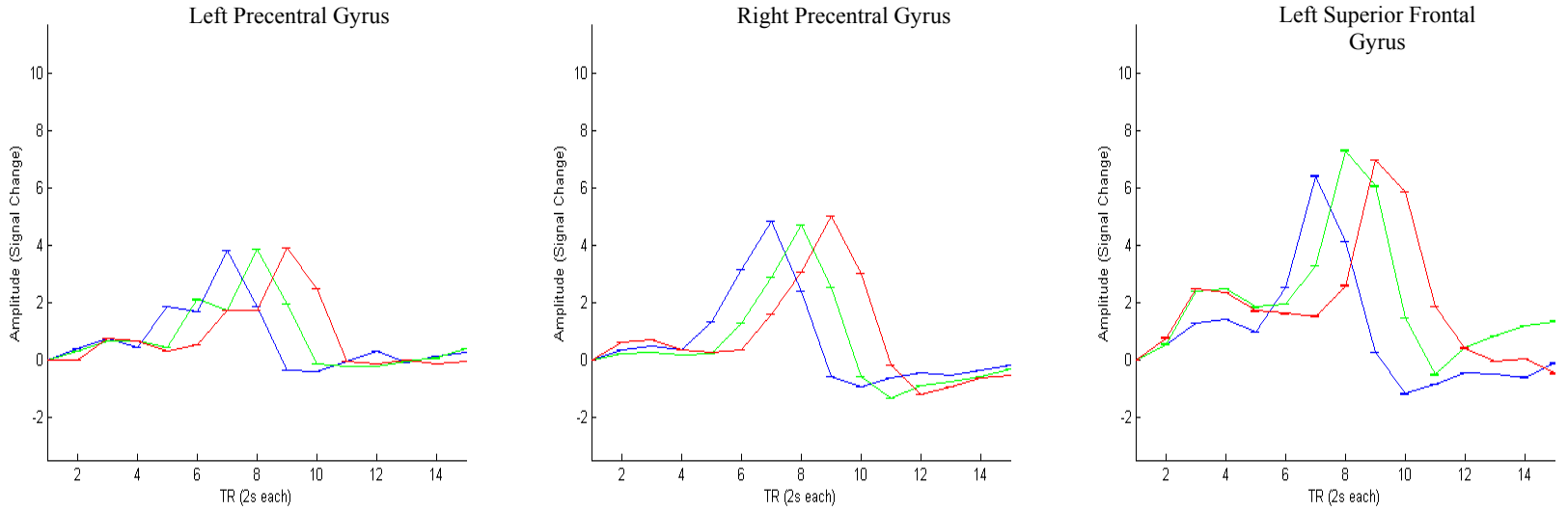

FIGURE 4.8b: Activation Profiles Corresponding to Motor Task Performed With The Left Hand (Data plotted with ±1 SEM, Regions 4-6).

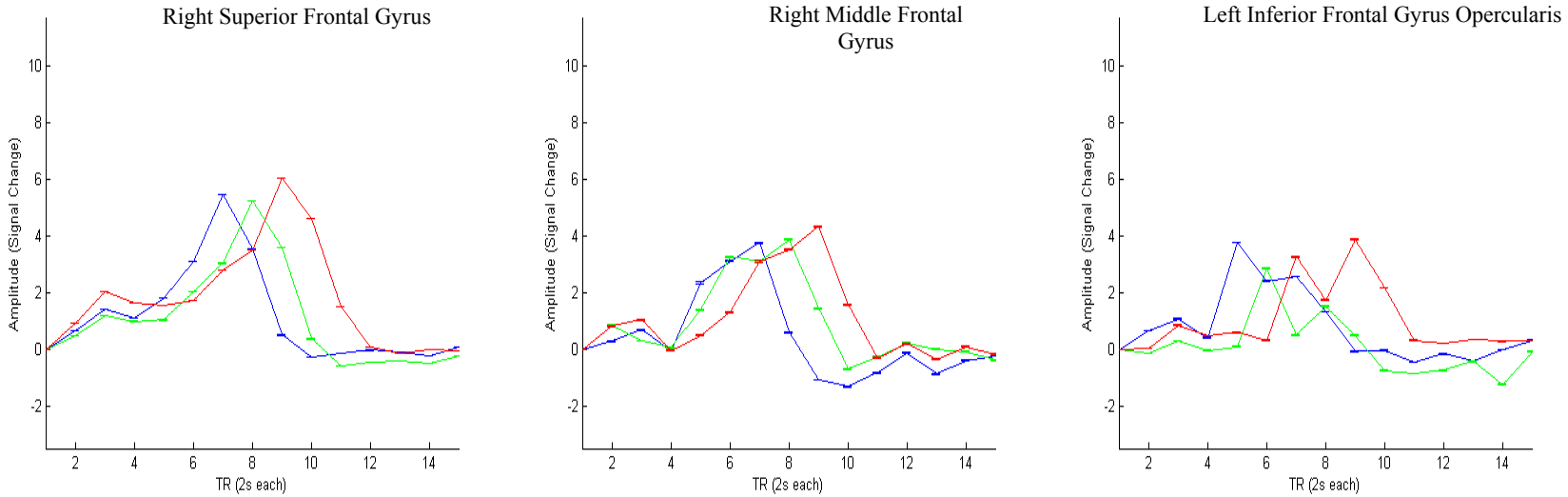

FIGURE 4.8c: Activation Profiles Corresponding to Motor Task Performed with the Left Hand (Data plotted with ±1 SEM, Regions 7-9).

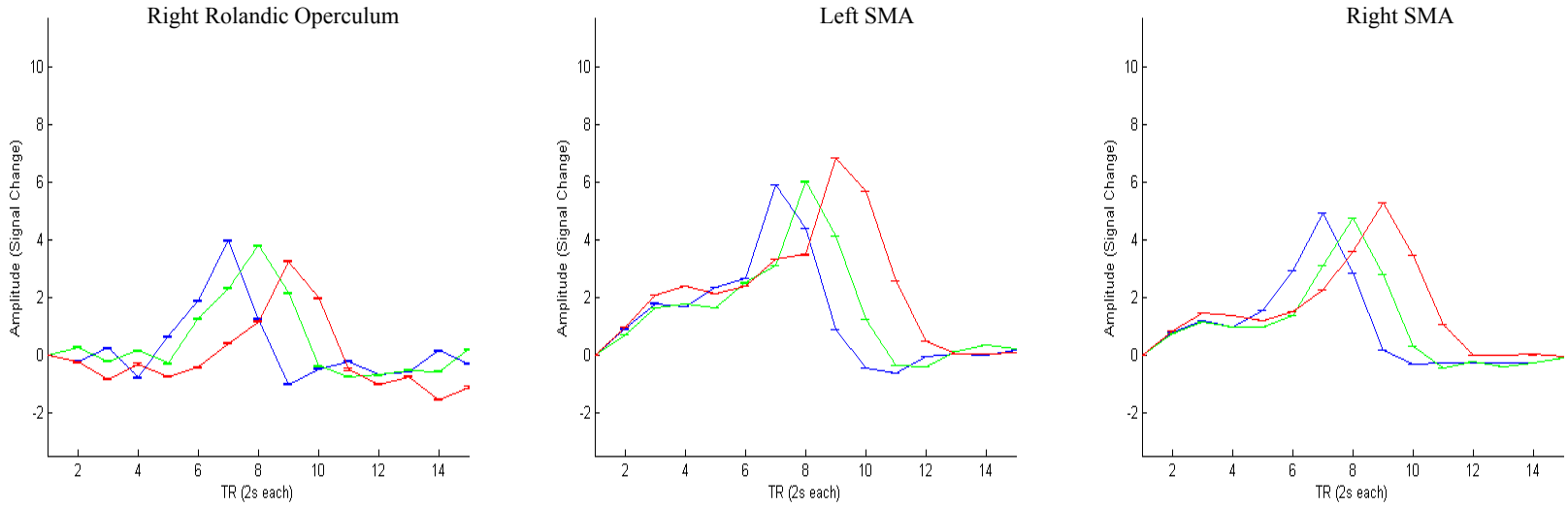

FIGURE 4.8d: Activation Profiles Corresponding to Motor Task Performed with the Left Hand (Data plotted with ±1 SEM, Regions 10-12).

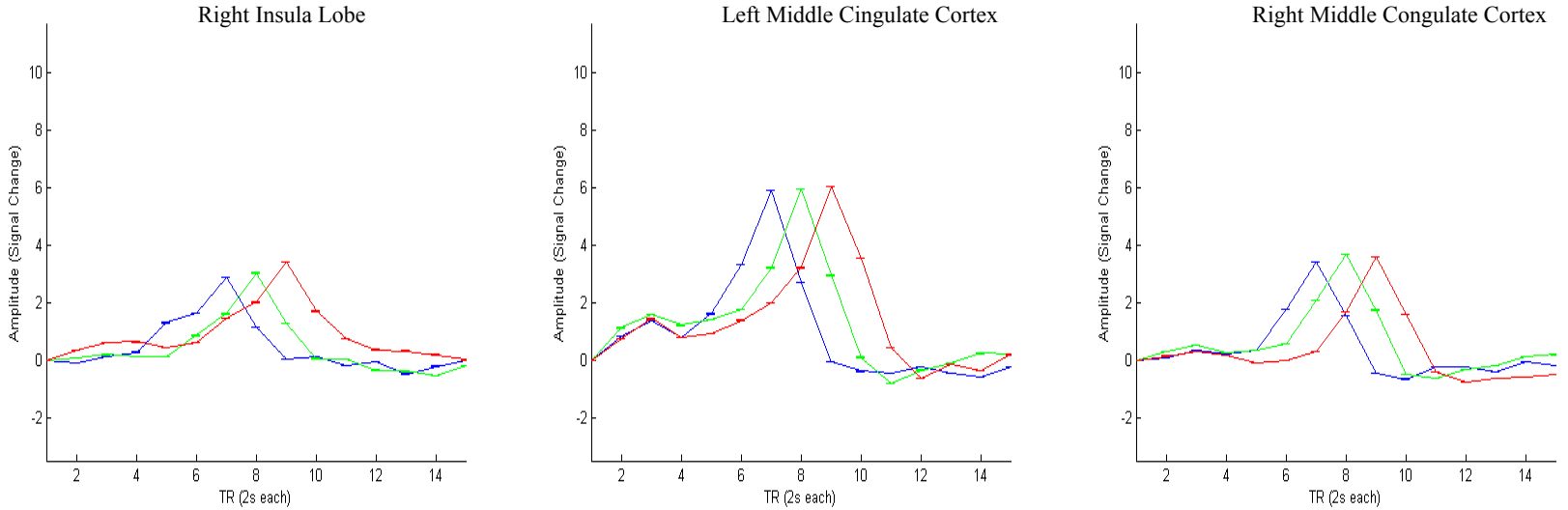

FIGURE 4.8e: Activation Profiles Corresponding to Motor Task Performed with the Left Hand (Data plotted with ±1 SEM, Regions 13-15).

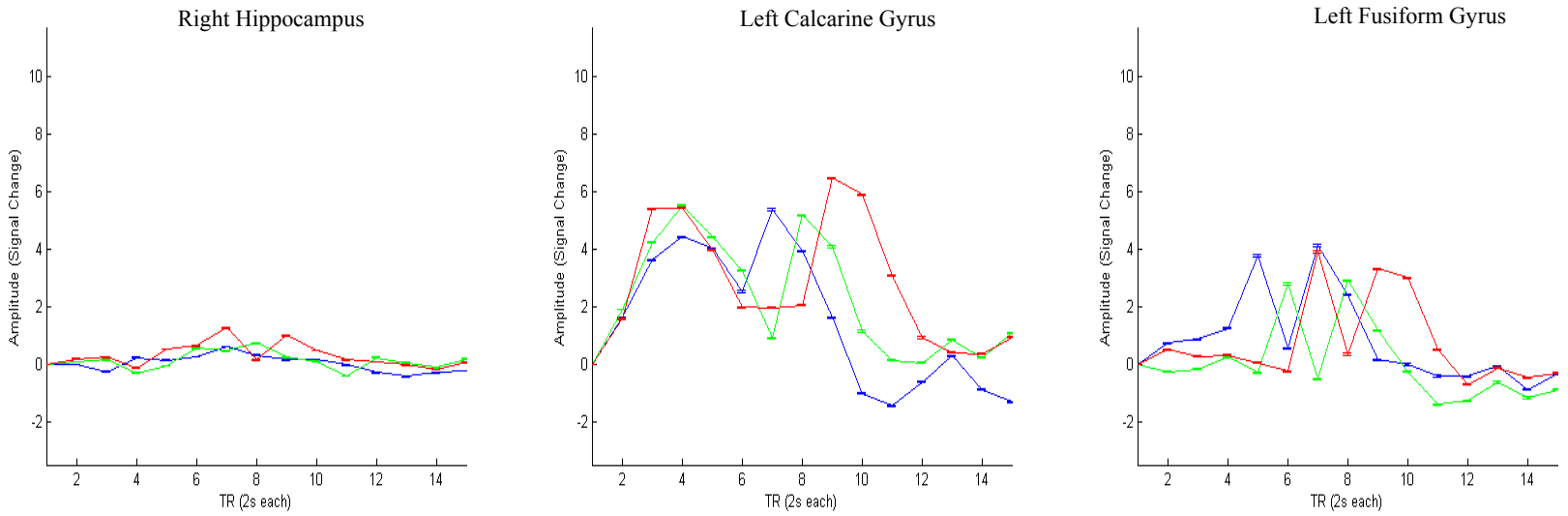

FIGURE 4.8f: Activation Profiles Corresponding to Motor Task Performed with the Left Hand (Data plotted with ±1 SEM, Regions 16-18).

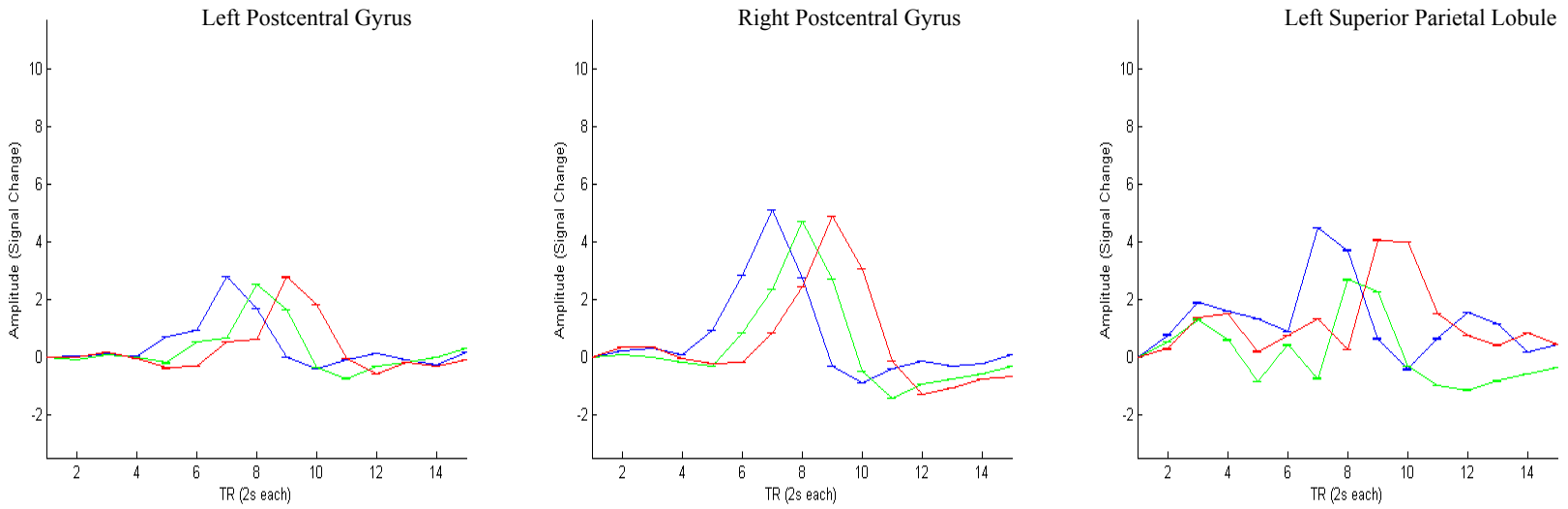

FIGURE 4.8g: Activation Profiles Corresponding to Motor Task Performed with the Left Hand (Data plotted with ±1 SEM, Regions 19-21).

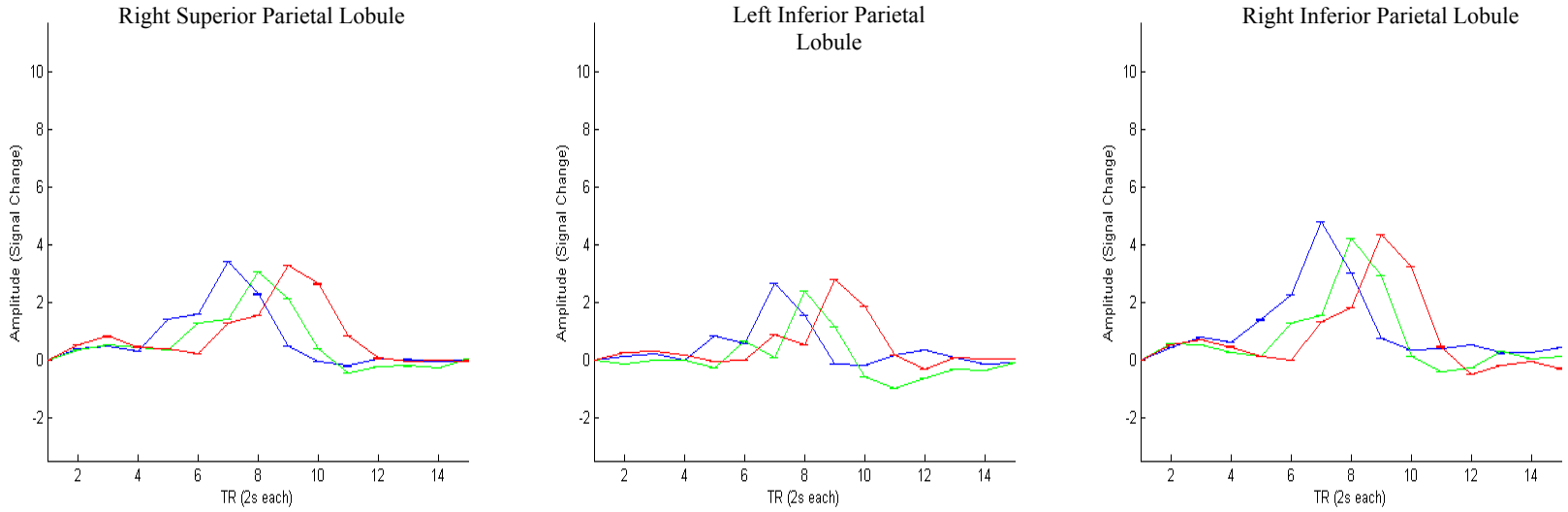

FIGURE 4.8h: Activation Profiles Corresponding to Motor Task Performed with the Left Hand (Data plotted with ±1 SEM, Regions 22-24).

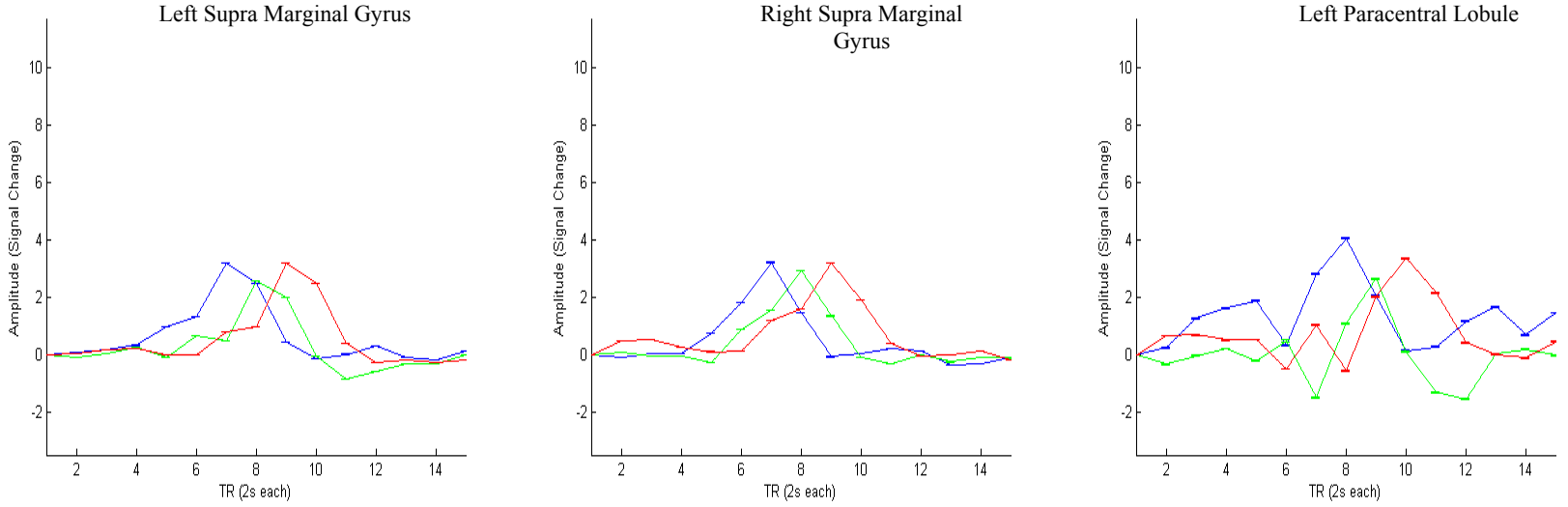

FIGURE 4.8i: Activation Profiles Corresponding to Motor Task Performed with the Left Hand (Data plotted with ±1 SEM, Regions 25-27).

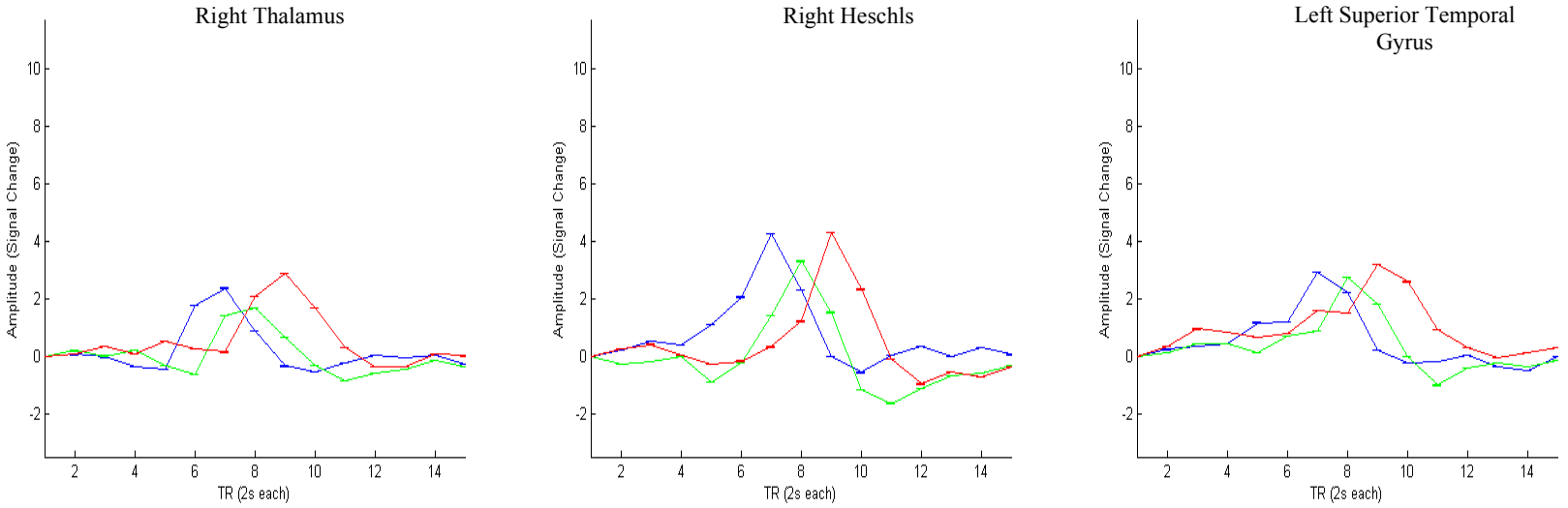

FIGURE 4.8j: Activation Profiles Corresponding to Motor Task Performed with the Left Hand (Data plotted with ±1 SEM, Regions 28-30).

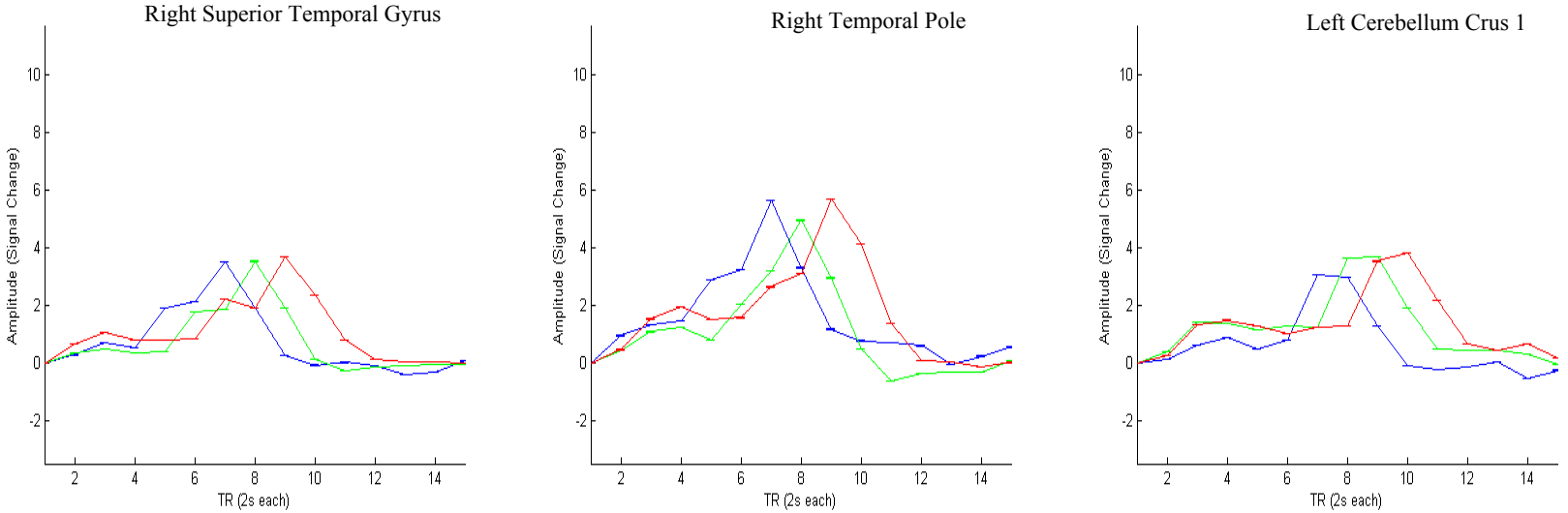

FIGURE 4.8k: Activation Profiles Corresponding to Motor Task Performed with the Left Hand (Data plotted with ±1 SEM, Regions 31-33).

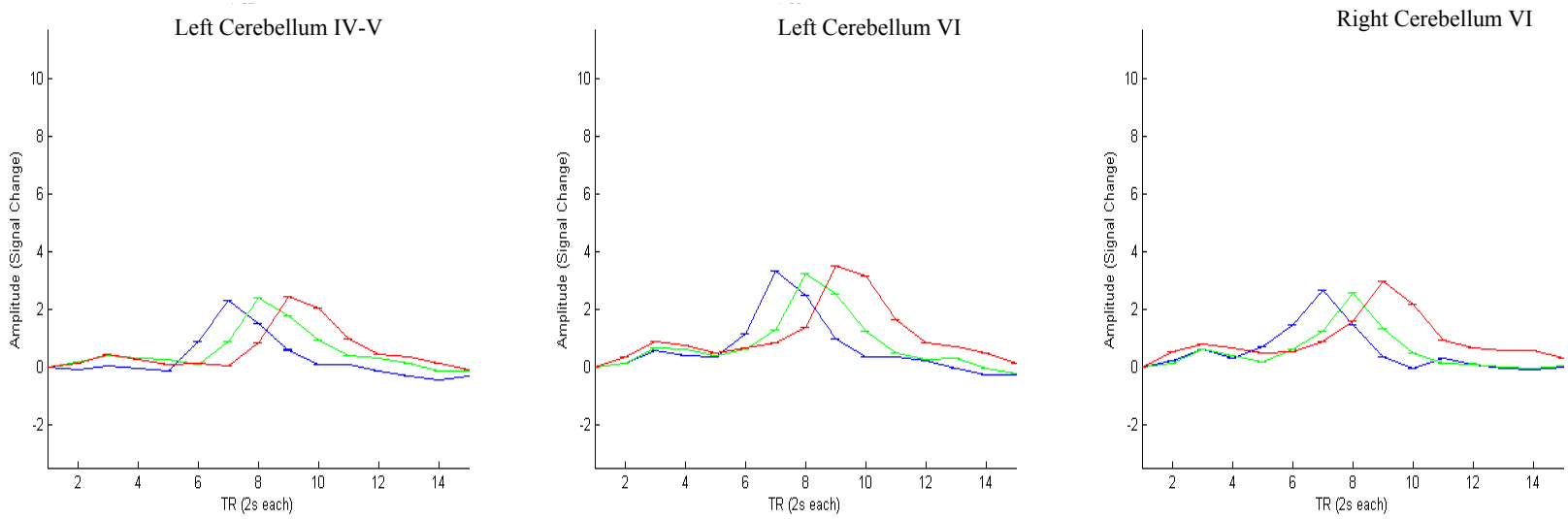

FIGURE 4.8l: Activation Profiles Corresponding to Motor Task Performed With The Left Hand (Data plotted with ±1 SEM, , Regions 34-36).

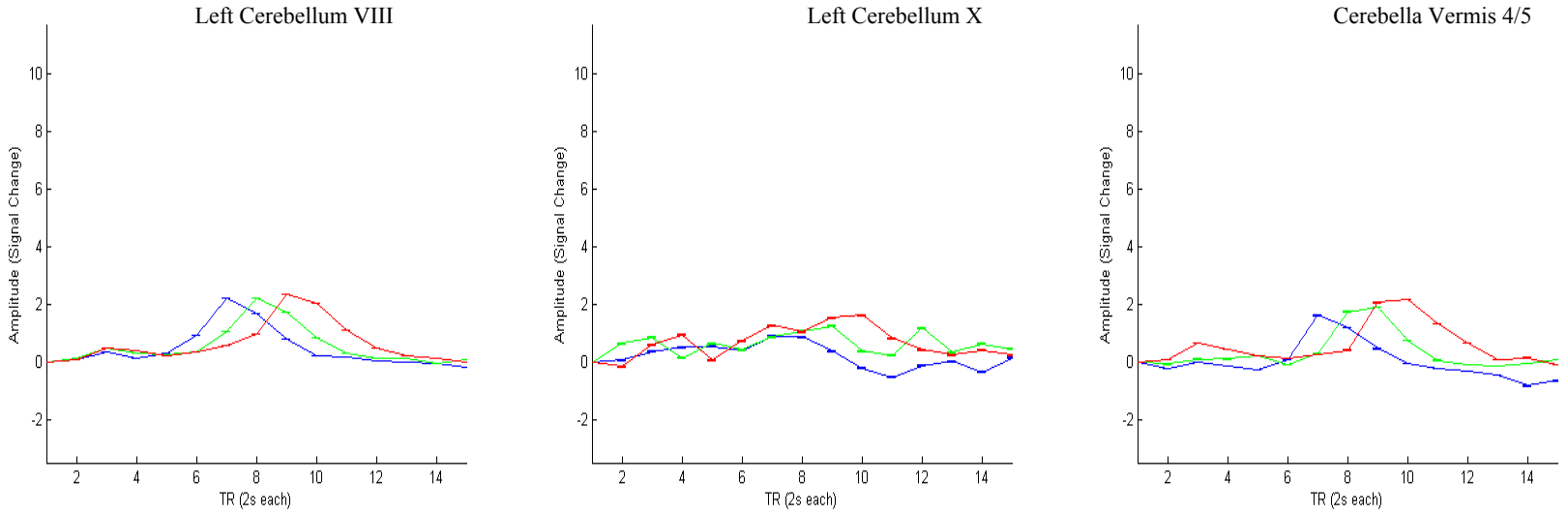

FIGURE 4.8m: Activation Profiles Corresponding to Motor Task Performed with the Left Hand (Data plotted with ±1 SEM, Regions 37-39).

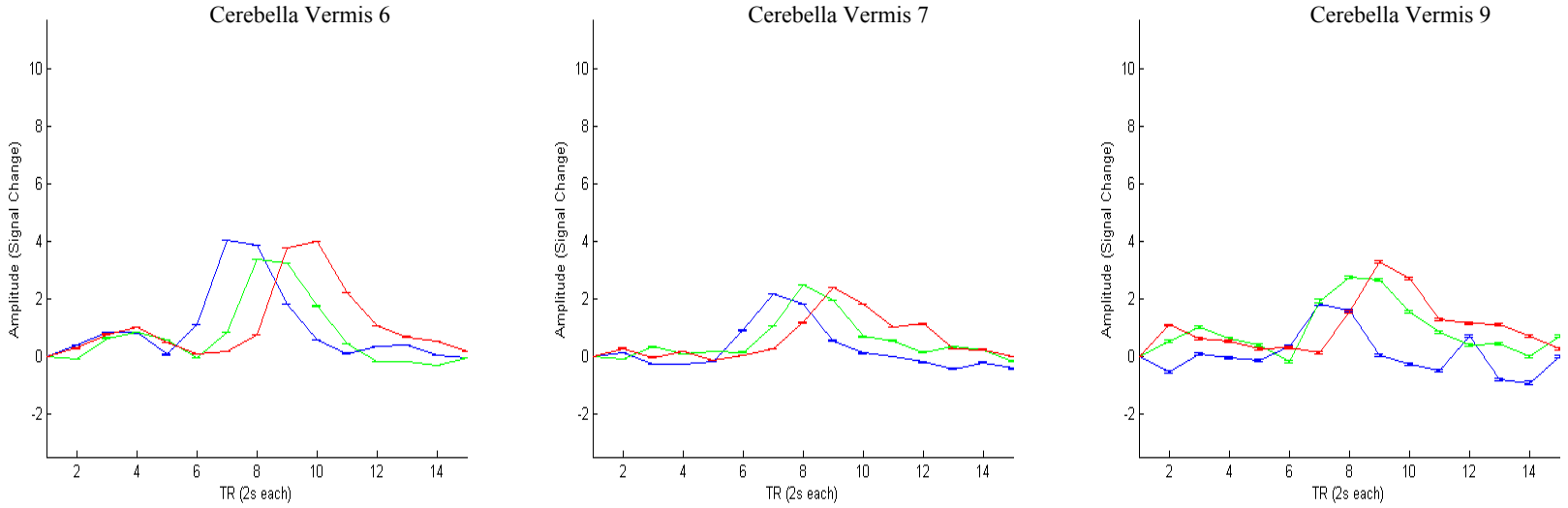

4.4.4 : Analysis of Varying Inter Task Delays on Movement Execution Time Series Features.

Mauchly's test of sphericity ($p<0.05$) was performed to determine that the assumptions of the ANOVA were not violated. Results for Mauchly's test of sphericity indicated that the ANOVA assumptions were preserved for each of the comparisons (slope, maximum amplitude, duration of activation and area under the curve). The following tables 4.3 through 4.10 show the results from the ANOVA calculations (p significant <0.05) for the execution part of the right and left motor tasks. These ANOVA results (tables 4.3 – 4.6) indicate that the delays had induced significant differences on the area under the curve $F(1,17) = 155.397$, $p<0.001$, duration of activation $F(1,17) = 3914.014$, $p<0.001$, maximum amplitude $F(1,17)=238.833$, $p<0.001$, and slope of activation $F(1,17) = 153.985$, $p<0.001$ for the right motor task.

TABLE 4.3 : Delay Effects on the Area Under the Curve for the Right Motor Task.

Source	Type III Sum of Squares	df	Mean Square	F	Calculated p value
Intercept	3.2×10^5	1	3.1×10^5	155.397	$p < 0.0001$
Error	34632.765	17	2037.221		

TABLE 4.4 : Delay Effects on the Duration of Activation During the Right Motor Task.

Source	Type III Sum of Squares	df	Mean Square	F	Calculated p value
Intercept	1.5×10^5	1	1.5×10^5	3914.014	$p < 0.0001$
Error	643.213	17	37.836		

TABLE 4.5 : Delay Effects on the Maximum Amplitude of Activation During the Right Motor Task.

Source	Type III Sum of Squares	df	Mean Square	F	Calculated *p* value
Intercept	3.3×10^4	1	3.3×10^4	238.833	$p < 0.0001$
Error	2355.938	17	138.585		

TABLE 4.6 : Delay Effects on the Slope of Activation During the Right Motor Task.

Source	Type III Sum of Squares	df	Mean Square	F	Calculated *p* value
Intercept	3945.263	1	3945.263	153.985	$p < 0.0001$
Error	435.559	17	25.621		

These ANOVA results (tables 4.7 – 4.10) indicate that the delays had induced significant differences on the area under the curve $F(1,17) = 274.262$, $p<0.001$, duration of activation $F(1,17) = 4440.927$, $p<0.001$, maximum amplitude $F(1,17) = 317.876$, $p<0.001$, and slope of activation $F(1,17) = 67.630$, $p<0.001$ for the right motor task.

TABLE 4.7 : Delay Effects on the Area Under the Curve for the Left Motor Task.

Source	Type III Sum of Squares	Df	Mean Square	F	Calculated *p* value
Intercept	2.3×10^5	1	2.3×10^5	274.262	$p < 0.0001$
Error	14574.698	17	857.335		

TABLE 4.8 : Delay Effects on the Duration of Activation During Left Motor Task.

Source	Type III Sum of Squares	df	Mean Square	F	Calculated *p* value
Intercept	1.1×10^5	1	1.1×10^5	4440.927	$p < 0.0001$
Error	414.808	17	24.400		

TABLE 4.9 : Delay Effects on the Maximum Amplitude of Activation During Left Motor Task.

Source	Type III Sum of Squares	df	Mean Square	F	Calculated *p* value
Intercept	2.9×10^4	1	2.9×10^4	317.876	$p < 0.0001$
Error	1582.268	17	93.075		

TABLE 4.10 : Delay Effects on the Slope of the Left Motor Task.

Source	Type III Sum of Squares	df	Mean Square	F	Calculated *p* value
Intercept	4002.018	1	4002.018	67.630	$p < 0.0001$
Error	1005.981	17	59.175		

4.5: DISCUSSION.

During information processing in the brain pertaining to a motor task, there is a sequence of events that includes sensory perception, strategy selection and the execution of movements. The information flow in these sequences of events occurs over several brain regions induced by neuronal activity in the form of chemical signaling and electrical evoked potentials [74,75,181-183]. The result of this neuronal activity leads to increased tissue oxygen consumption and a vascular response that is used as a surrogate to detect neuronal activity in the active brain regions [174,175]. The use of time-resolved FMRI to capture these vascular responses in the whole brain has been determined to be a reliable method of correlating activation with independently measurable task specific parameters such as stimulus [238-241]. This is seen from the results of the analysis of the delay effects on the activation patterns during the execution phase of the motor task.

These results confirm that time resolved fMRI is sensitive and is able to capture stimulus induced effects of the activation characteristics for motor task execution. Furthermore, the results from the study indicate that there are three distinct activation profiles present for the brain regions mapped during the motor task paradigm. These phases are the planning, induced delay and motor execution phase.

During the planning phase, there was an increase in activation of the specific brain regions that were involved with task planning. The regions that showed large positive activation during task planning were the Calcarine gyrus, temporal gyrus, temporal poles, cingulate cortex, SMA and regions of the cerebellum. Regions that were specifically involved with task execution such as the primary motor cortex and primary sensory cortex exhibited little or no activity or some negative activation during the planning phase. Regions that were positively activated during the planning phase were also activated during motor task execution with similar or higher positive activation amplitudes. Other regions that were involved in the execution phase of the tasks showed strong positive activation during the motor execution phase.

When planning for a motor task, the brain formulates appropriate task dependent neuromotor strategy that is reliant upon information from perceived sensory stimuli. In the experiments that were done for this study, visual cues dictated the movement to be performed. The results from figures 4.5 and 4.7 are indicative of information processing pertaining to the visual stimuli through the expression of the high positive activation in the left calcarine gyrus, an area associated with visual processing [182,183]. The perception of this visual cue also activates other regions that are involved with visual processing such as the lingula gyrus [182,183]. The early onset of positive activation is

also visible in the SMA, an area that is associated with task planning and neuromotor strategy selection especially for sequential movements. Activation in the SMA agrees with the literature for motor imagery tasks [214]. However, from the results in figures 4.5, temporal activation in the SMA suggests higher amplitudes of activation in the right SMA that occurred prior to the left SMA. These activation amplitudes in the SMA were sustained from the onset of the visual cue until the motor task performance. Similarly, in figures 4.7 during the performance of the left motor task, the left SMA experiences an early increase in amplitude of activation as compared to the right SMA. Studies that examined the role of specific parts of the SMA have found somatotopic organization within this region [242]. If the SMA is involved with planning the sequencing of movement, these differences in activation could account for comparisons of strategy pertaining to movement. However, the effect of these varying activation onset and duration between the left and right SMA and its relationship to neuromotor strategy is presently not clearly understood from the data, and warrants more experimentation.

The pre and post central gyrus are associated with the primary motor cortex and primary sensory cortex. The primary motor cortex is involved with task mediation and the execution of voluntary movements [74,112,114,183]. The primary sensory cortex is responsible for the processing of sensory information [74,112,114,183]. Activity in the pre and post central gyrus was observed during the motor execution phase of the task as would be expected. Activation of the pre and post central gyrus were much more prevalent in the contralateral side to which the motor activity was performed because of the need for neuromotor control of the limb and also sensory feedback pertaining to proprioceptive and tactile stimuli of the limb. These results are in agreement with the

literature for voluntary motor task performed with the upper extremities [74,112,114, 183]. Following the execution of the motor task, there is a clearly visible negative phase of activation. This negative activation correlates with the recovery period for the BOLD hemodynamic response as detailed in the literature [174,175,180].

The cerebellum has been traditionally associated with mediation of motor task performance especially those involving timed and precision movements [74,75,112,114,183]. The specific manner in which the cerebellum achieves this process is not presently understood and there are several theories that examine this process. The literature suggests the presence of multiple homunclei that reside in the cerebellum that allow multiple comparisons of movement and strategy to produce optimal and accurate movements [243,183]. The specific number of homunculi is not known and some studies believe that there are more than two that are present [244, 183]. Other studies have proposed the presence of fractured cerebella maps or the presence of multiple internal models in the cerebellum that contribute to sensory feedback and motor control [245,285]. Other studies have also suggested that the cerebellum is involved with other tasks such as voluntary movement planning, motor imagery, emotion and cognitive processing [214, 286,287].

If the cerebellum was indeed strictly involved with mediation of movements, then activation in this area would be limited to the execution of the motor task. Some imaging studies have examined this proposition and found no significant activation in the cerebellum during motor imagery tasks [288]. However if the cerebellum was involved with motor task planning, there would be activation in the cerebellum during the motor imagery and planning part of the task. Other imaging studies have reported activations in

the cerebellum during motor imagery and actual motor tasks [214,246,]. However, these activations have been reported to be in different locations with varying patterns of activation [214,246,]. A reason for this variability could be the result of the stimulus that was used. Finger tapping or rhythmic movements do not adequately represent functional neuromotor strategy. The results from figures 4.5 and 4.7 indicate that the task planning phase had induced the start of positive activation in the cerebellum that increased during the motor execution phase of the task. These results suggest that the involvement of the cerebellum in potentially contributing to task planning neuromotor strategy that relate to voluntary upper extremity movements [245,246].

Overall, the results from this study support the objective of the second specific aim of this dissertation and that was to map the temporal activation patterns of specific brain regions involved with functional reaching and grasping of real world objects. Furthermore, the distinction between activation in specific anatomical regions of the brain that correspond to task planning and the activation that correspond to the execution of the motor task confirm the hypothesis of the study and that was upper extremity neuromotor strategy can be identified using distinct temporal brain activation patterns that relate to specific planning and execution task states.

The complete analysis and modeling of large scale data sets through manual inspection is very cumbersome and inefficient and could lead to error and the loss of important information. Machine learning tools are ideal candidates for analysis and classification of large scale data sets of high dimensionally. In addition, machine learning tools are able to store information and retrieve them in practical applications.

These features are much sought after especially in practical applications of developing brain models for use as upper extremity neuroprosthetic controllers.

4.6: CHAPTER CONCLUSION.

The results for the time resolved fMRI study showed the presence of distinct information flow and sequencing of activation between brain regions. Distinct patterns were observed that pertain to task planning and execution that allow detection of both. The distinct and quantifiable activation strongly suggests suitability of using machine learning tools such as artificial intelligence and neural networks to model this process.

CHAPTER 5

Development of a Unique Whole-Brain Model for Upper Extremity Neuroprosthetic Control

5.1: ABSTRACT.

This chapter addresses on the development of a unique artificial intelligence model that can identify, extract and classify activations of specific anatomical regions of the brain, that are involved with functional upper extremity tasks. This model consists of 2 phases: a dimension reduction and pattern identification phase and a pattern classification and learning phase. Principles of machine learning, artificial intelligence and Artificial Neural Networks (ANNs), are used to classify brain activation patterns and identify the sequence of events that relate to the neuromotor strategies that are specific for upper extremity tasks. The model is designed using data from neurologically intact human subjects (N=13) who performed actual goal oriented movements of reaching and grasping using real world objects. This model is unique because it uses information from the entire brain and is able to capture strategy that pertains to functional task performance. Information from this model is important for the development of feed forward upper extremity neuroprosthetic controllers.

5.2: INTRODUCTION.

The effective use of upper extremity neuroprostheses to perform functional tasks is heavily dependent upon the control and interface of these devices [67,68,69,247,248, 292]. Naturally occurring neuromotor strategies within the brain that are related to upper extremity function provide an ideal source for physiological control. The use of these physiological signals is highly beneficial to the development of a neuroprosthetic controller that can accommodate varying pathologies and implement needed neuromotor strategies of natural human movements instead of requiring compensatory behaviors. To

adequately use natural human neuromotor strategies represented by brain activation, a neuroprosthetic controller would need to parse out the different aspects of voluntary upper extremity motor task performance. More specifically, in a neuroprosthetics controller, the phases of task planning, initiation, and execution need to be appropriately recognized.

The development of a neuroprosthetic controller that uses natural neuromotor strategy is a complex process because, during functional reaching and grasping, there are different strategies that can be used to produce multiple limb movements and postures to achieve the specific task goal - the manipulation of objects or interaction with the environment [121,249,250]. Several factors such as task goal, environment, tool usage, workspace and range of limb motion dictate the limits of movement and posture of the upper extremities [251-254,289-291]. These factors are instrumental to the decision making process of the brain when selecting a set of strategies to be applied.

The brain is able to optimize and select the best strategy that would produce limb movement in the most accurate manner, consistent with the task goals and yet minimize energy expenditure [112-114,121,204]. However, in each situation, there often are multiple strategies of limb movement and position that are available, and are manifested as neuromotor correlates within the brain [112-114,121,204]. These neuromotor correlates consist of activations within specific anatomical regions of the brain that experience explicit changes in amplitude, timing and intensity as the result of the motor task being performed. During functional upper extremity movement, the presence of common and overlapping activation patterns creates an ill-posed problem of neural signal

decoding [121,234,255,256]. This is because there is a many-to-one mapping of brain activation with respect to the motor output of the limbs [112-114,234,257].

FIGURE 5.1: Workspace and range of motion for the shoulder, elbow and wrist joints showing that functional movement of reaching and grasping consists of combinations of movements of these joints. The free range of motion of these joints and variety of neuromotor strategy available to brain provides the opportunity for multiple combinations of joint movements that could be used to produce accurate and meaningful reaching and grasping, thus forming an ill-posed problem.

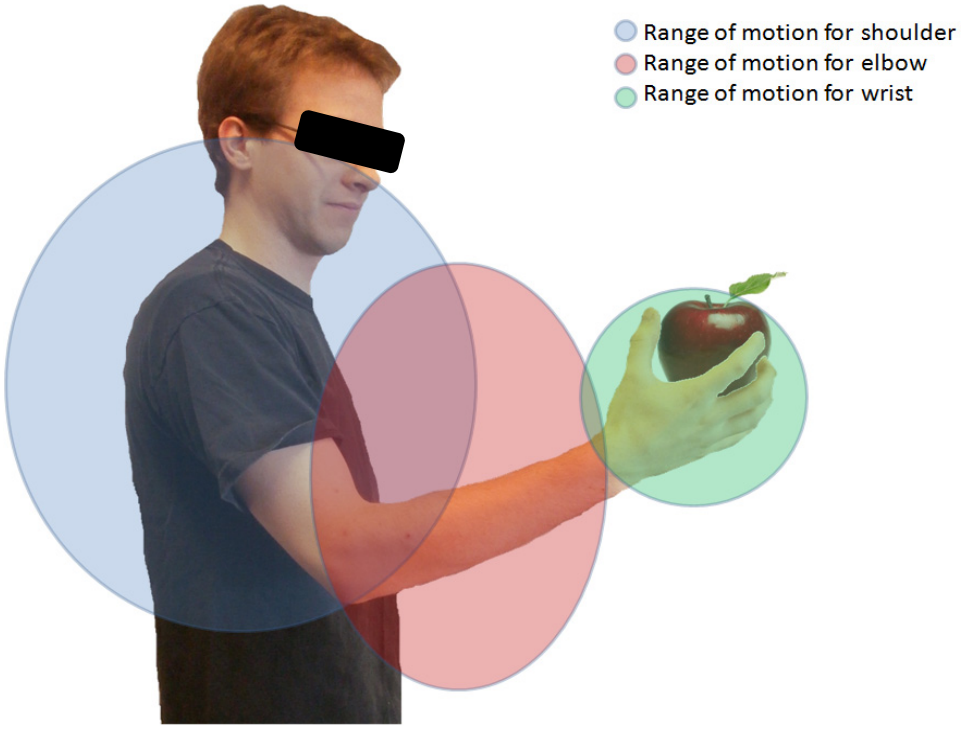

Activation in a specific region of the brain consists of multiple neurons that are firing. Specific activity is the net result of these groups of neurons within a specific region that produce excitatory or inhibitory activations [74,75,181,182]. Collectively, activation of these brain regions contributes to realizing upper extremity neuromotor strategies [181,182]. A precise one-to-one correlation of neuronal firing with respect to

motor output of the limbs is not clearly established at this moment. Furthermore, information communication and processing in voluntary upper extremity function involves multiple regions of the brain and occurs both in series and parallel [74,75]. Understanding the temporal characteristics of information flow among anatomical regions of the brain is complex due to the high dimensionality of data involved.

To use natural neuromotor information, an appropriate brain model needs to be created that can account for neuromotor strategies expressed by activations of the multiple functional regions in the brain. There are three major components that need to be considered in the development of a brain model for neuroprosthetic control. The *first* is a feature extraction process that identifies features (activity) from specific anatomical regions of the brain that are expected to be significant or contain information from a pool of otherwise noise or baseline data. The *second* component of the brain model is pattern classification that involves classifying important aspects of the extracted physiological signals or data sets. This is a key step needed to determine the presence of specific trends or temporal patterns that correlate with distinct events such as planning, initiation and execution of upper extremity function. The *third* component of the brain model is the learning portion. This is an important part that incorporates knowledge related to the patterns and events obtained from the extracted physiological signals. Learning enables the brain model to identify specific activation patterns that relate to neuromotor control strategies of the upper extremities, which result in natural human control of the limbs.

The first specific aim of this chapter is to design and develop a unique whole-brain model using machine-learning tools for application to upper extremity neuroprosthetic control. The second specific aim of this chapter is to verify that the

model developed is able to accurately represent the physiological data and that the training process did not saturate or bias the learning process of the model. The hypothesis for this chapter is that temporal patterns of the brain that correspond to functional reaching and grasping can be modeled accurately in a population of normal subjects.

5.3: PROPOSED MODEL.

Neuromotor strategy development does not lie in a single region of the brain, but rather several regions are involved during the performance of functional goal oriented movements of reaching and grasping. fMRI is able to provide information from the whole brain in a noninvasive manner without the need for contrast agents, or invasive procedures. However information entropy is a cause for concern because of the sampling frequency that is in the order of 0.5Hz - 2Hz. The brain's hemodynamic response varies in different regions due the characteristics of the vasculature. In an fMRI experiment, typical response times for first contact with a stimulus have a latency of 1-2s. and a time to peak of 4-6s. [174,180]. This is because the hemodynamic response is a slower process as compared to the electrical activity or neuronal discharge that occur on a micro to millisecond time scale [174,180]. However, the hemodynamic response has been determined to be a good correlate of brain activity and to partially overcome the temporal limitations, time resolved fMRI data acquisition can be used [238-241]. Time resolved fMRI consists of an event related experiment paradigm where stimuli are presented at specified intervals, and the corresponding activation in the brain measured [238-241].

The implementation of the time resolved paradigm allows for the estimation of specific stimulus activation in anatomical regions of the brain.

The following is the process flow chart of the custom developed whole brain model (figure 5.2).

FIGURE 5.2 : Model flow chart.

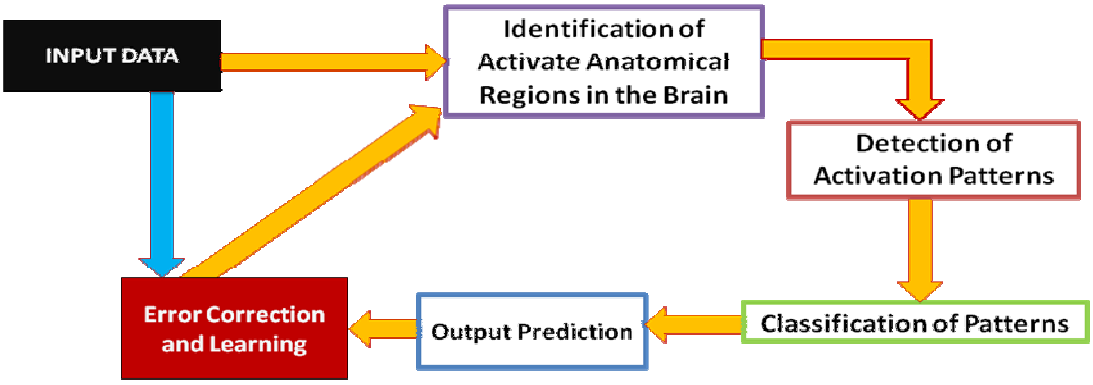

The described whole brain model consists of 4 major components which are anatomical region identification, activation pattern detection, classification of patterns, and learning. The *first* part of the model identifies anatomical regions of the brain that are active using the TTN27 brain atlas [224]. The determination of whether or not an area of the brain has significant activation that is related to functional upper extremity tasks was discussed in chapters 3 and 4. The *second* part of the model addresses the detection of activation patterns and the separation of signal from noise or baseline data. This *second* component extracts the time series data from each voxel within the specified significant regions of the brain. A moving average (MA) windowing function was performed using a specified width, point-by-point averaging of all the voxel values in that region, as

specified by the width of the MA windowing function. This produced a specific time series activation profile for each of the specific regions involved with functional task performance. The data contained within the window was normalized with respect to the value of the first point within the window. This was done to reduce the physiological effects of noise, post processing assumptions, and to enhance detection as a feed forward neuroprosthetic. The following equation (1a) shows the MA process with normalization within a specific width of the sliding window.

$$Raw\ Net\ Activation_{Region\ R,time\ t} = \frac{\sum_{m=1}^{M}(V_m - V_1)}{M} \quad (1)$$

In equation 1, *M* represents the total number of voxels (V_m) per region, *R* is the total number of brain regions that were determined to be active and *t* is the time for each point within the sliding window. This equation is independently used for each region, per time point.

The *third* component of the model is pattern classification. There are several methods of pattern classification. The field of machine learning provides tools that are able to address the required characteristics for a brain model that is intended for upper extremity feed forward neuroprosthetic control and its application. More specifically, the machine learning principles of ANNs provide tools that enable training and quantitative learning of pattern classification in datasets of high dimensionality. This can be achieved without having to manually provide *a priori* knowledge of the activation profiles, temporal dynamics and regional information flow to the ANN model. This is important when comparing other pattern classification tools in the repertoire of machine-learning as such as fuzzy logic or Bayesian belief networks. These tools are capable of performing

pattern classification on physiological data sets however are dependent on all of the prior mentioned parameters to be explicitly defined *a priori*. These *a priori* parameter definitions are needed to form rules or tolerances that can then be provided to the model for data classification [258-261]. Such *a priori* definition of parameters poses several challenges in practical applications of data classification for large or high dimensional data sets. This is because processing of such information in real-time as a neuroprosthetic controller would incur tremendous computing costs and high susceptibility to artifact from noise interference and variations within physiological signal. The creation of fuzzy rules or Bayesian weights requires designation of this response function, characteristics of changes in multiple regions and clearly defined spatial and temporal limits of activation for each brain region during functional task performance. This process is much too complex without dimension reduction and could potentially lead to increased information entropy, information misrepresentation and loss of accuracy. Furthermore, the use of pre-specified detection values for a whole brain model is not an optimal solution and could lead to decreased accuracy. This is due to the inflexibility of hard coded rules to adapt and accommodate physiological changes or variables that are task or time dependent. ANNs are able to perform pattern classification and to incorporate some degree of flexibility that is important when accommodating individual differences and changes in activation intensity during task performance [262,263]. The ability of ANNs to process, store and retrieve information for later use makes this machine learning tool an ideal contender for pattern classification and recognition in a brain model that is to be applied for upper extremity neuroprosthetic applications.

The *fourth* component is learning which involves the implementation of the ANN with back propagation [262,263]. The use of back propagation enables the model to learn new patterns in a supervised manner during the training of the model. During supervised training, the model's predicted output is compared with the actual classification data to produce an error signal. Learning is achieved through successive changes in the weights at each of the ANN layers using the calculated error signal during the back propagation phase.

5.4 : METHODS.

5.4.1 : Physiological Data Acquisition and Preparation.

The data used in the development of the model was obtained from the time resolved fMRI experiment detailed in Chapter 4. This data consists of whole brain fMRI data acquired during the performance of functional goal-oriented upper extremity motor tasks of reaching and grasping. The task consists of an initial priming cue that dictates which hand is to be used. Subsequently, an inter-task interval of 2s,4s, or 6s, was presented in random order. During this time the screen went blank and was followed by a "go" cue at the end of an inter task delay. The importance of using this inter task delay was to randomize the sequence of task performance and reduce the effect of stimulus anticipation which could lead to a shift from intentional movements to rote rhythmic movements. This randomization of task delays also helped to preserve subject concentration and maintain the heightened level of task motor imagery. A total of 12 trials were performed for each hand and delay to yield a total of 72 task events.

The time series data from each individual subject (N=13 M = 5 F = 8 mean age 21.2 years) was extracted from AFNI and imported into MATLAB. This process was achieved using custom written Bash scripts for AFNI data extraction and m-file scripting for MATLAB data analysis. To extract data for use in the development of the model, the TTN 27 EZ ML Atlas was transformed to fit each individual subject's anatomy [224]. However during this transformation process, due to the variability among the predefined regions of TTN 27 EZ ML Atlas and the actual anatomy of the individual subject, some regions did not show activation for a few subjects. Brain regions in which there were no activations for a single subject were discarded to ensure consistency of results and reliability of the model. Data from a total of 5 regions (Right Rolandic Operculum, Right Middle Cingulate Cortex, Right Lunal Gyrus, Right Temporal Pole, Left Cerebellum (IV-V)) were discarded for the right motor task, and data from 3 regions (Right middle frontal gyrus, Right Rolandic Operculum and Cerebellar Vermis (8)) were discarded for the left motor task. Therefore the total number of regions for the right hand motor task and left hand motor task was 46 and 36 respectively (82 regions total).

The time series data for the anatomical regions of the brain that were active for the right motor tasks were stacked on top of the regions that were active for the left motor task, to create activation patterns (figure 5.3). Subsequently, data for all subjects were appended in sequence to create time series of brain anatomical regions based on the TTN27 EZ ML Atlas [224]. This data set was the training data set used for the development of the model. For each subject, there were a total of 72 events as presented in the following table 5.1.

FIGURE 5.3: Activation Block for Time Series Data.

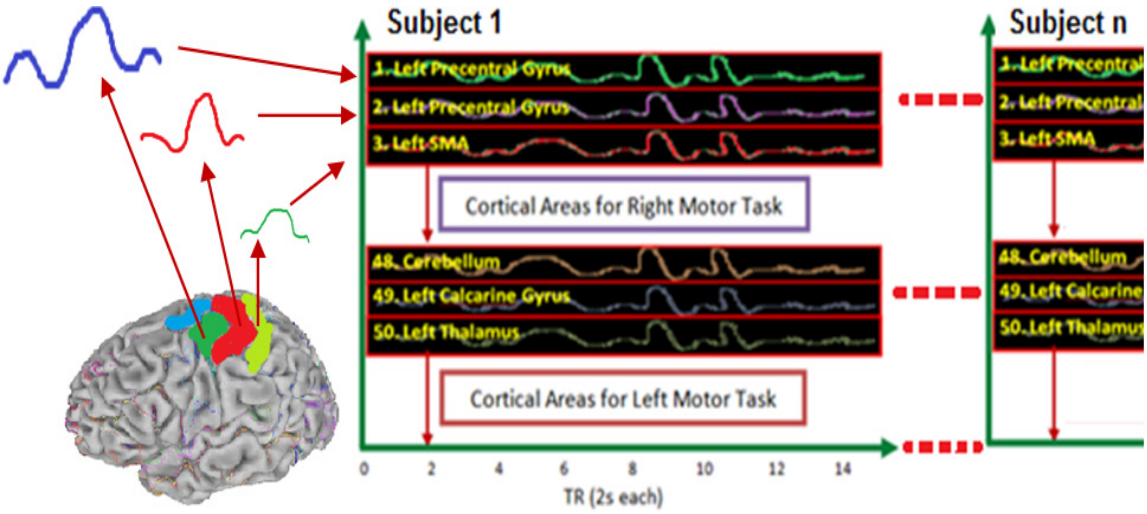

TABLE 5.1 : Task Performance.

Task Type	**Delay (s)**	**Repetitions**
Right Reach and Grasp	2	12
	4	12
	6	12
Left Reach and Grasp	2	12
	4	12
	6	12
	Total	72 events

5.4.2: Model Development and Architecture.

The ANN model consists of an input layer, output layer and a total of 8 hidden layers. The activation function of a specific ANN layer would determine the net output of the layer. A design constraint of ANNs is that the output function must be nonlinear and differentiable [262,263]. For this model, the hyperbolic tangent function was used and the

output characteristics of this function are show in the following figure 5.4. This function was selected as it was a common activation function used in the ANN literature [262,263].

FIGURE 5.4: The learning curve generated using the Hyperbolic Tangent Function. This learning curve is used as the activation function for the ANN model.

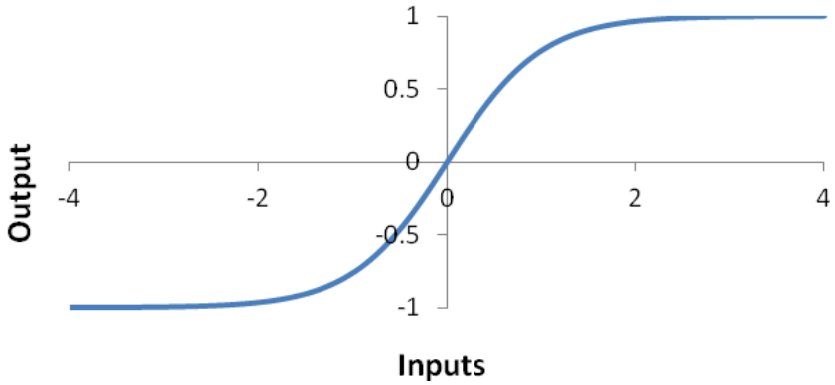

Information enters the ANN model through an input array during forward propagation. This array is defined by the data points from the data matrix, based on the MA windowing function of finite width. The windowing function that is incorporated is important because it allows for tuning of features that the model will concentrate on detecting and training. These features correspond with distinct task events such as planning and the execution of motor task movements. Tuning of the windowing function can be achieved by adjusting the lag time or the width of the window. A large lag time will include both the execution and planning phases, and tuning the lag time down could encourage the model to selectively identify features solely pertinent to task planning. This is a desired feature especially for the application of the model in neuroprosthetic controllers due to the ability to predict movement from motor intension.

The input data consists of time data from regions specified by the window in the form of an $82 \times W_{width}$ matrix. The moving window was specified to be 4 time points (4TRs = 8s.) wide. This window size was chosen because it was determined to be the time in which task planning had completely occurred for all the motor tasks performed, and excluded the task performance portion of the task.

The final layer of weights consisted of a *10x6* matrix. The first three output neurons of the final weight layer were for detecting right handed events and the latter three were for detecting left handed events. The net output from each group of the three 3 artificial neurons was sent through a hard limiter as expressed by HL1 for the right hand and HL2 for the left hand in the following figure 5.5.

FIGURE 5.5: Forward Propagation.

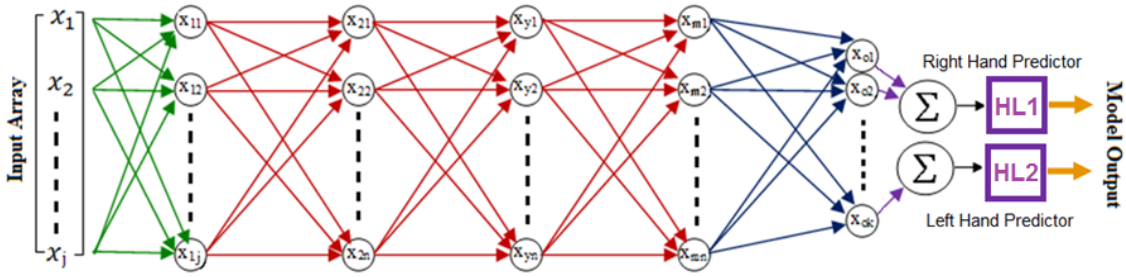

The hard limiters serve as threshold detectors and produce a logic output corresponding to the state (right hand, left hand, undefined) of the task being performed. The output states are listed in the following table 5.2.

TABLE 5.2 : Output States for the Model.

	Hard Limiter 1	**Hard Limiter 2**
Right Hand Task	1	0
Left Hand Task	0	1
Undefined	0	0
Undefined	1	1

The pattern classification and detection by the ANN model occurs during the f*orward propagation* phase. The weights in all the layers are initialized to random values at the start of the first processing iteration. The input data is reshaped from an *82×4* to a *1×328* matrix and sent to the input layer. The input layer consists of a (*82×*W_{width}, layer) matrix. A total of 10 layers were used therefore the input layer had a *328×10* structure. The use of 8 hidden layers was determined experimentally in which the number of hidden layers and their matrix sizes were varied. The first step of analysis at the input layer is based on the following equation (2). In each of the following equations, LWM refers to the *Layer Weight Matrix*.

$$Layer\ 1\ Output\ = \tanh\left(Data\ Matrix_{1\times 328} \times Input\ LWM_{328\times 10}\right) \quad (2)$$

Using equation (2) with matrix multiplication, the data is reduced dimensionally and the output to the first hidden layer consists of a *1×10* weight matrix. The next part of the forward propagation phase is to propagate this data to the subsequent hidden layers. Each hidden layer consists of *10×10* weight matrices and activation is computed using the following equation (3).

$$Hidden\ Layer\ Output\ _{present\ layer} = \tanh\left(Input\ Signal_{prior\ layer\ output\ _{1\times10}} \times LWM_{present\ layer\ 10\times10}\right) \quad (3)$$

The output from the final hidden layer is sent to the last ANN layer as shown in dark blue in figure 5.5. This last ANN layer conists of a *10×6* matrix. Activation is computed based on the following equation (4). For this output layer, the output from the first three artificial neurons corresponds to predictions of right hand use. The output from the subsequent three artificial neurons corresponds to predictions of left hand use.

$$Final\ Layer\ Output\ = \tanh\left(Input\ Signal_{prior\ layer\ output\ _{1\times10}} \times LWM_{present\ layer\ 10\times6}\right) \quad (4)$$

The net output from the last ANN layer is compared to the desired value of the input data as specified by the trainer and the error function is calculated using equation 5. Output from the last output layer is also sent to the hard limiters and processed to give logic outputs that correspond to prediction of the task being performed.

$$Error = Desired\ Response_{1\times6} - Out_{1x6} \quad (5)$$

The ANN model with back propagation undergoes supervised learning. The *supervisor* facilitates learning of pattern classification through the calculation of the output error from the last layer and using this, it changes the synaptic weights of each layer [262,263]. This process is known as the *back-propagation* phase beginning with the final ANN layer and ending with the input layer as shown in figure 5.6.

FIGURE 5.6: Back Propagation.

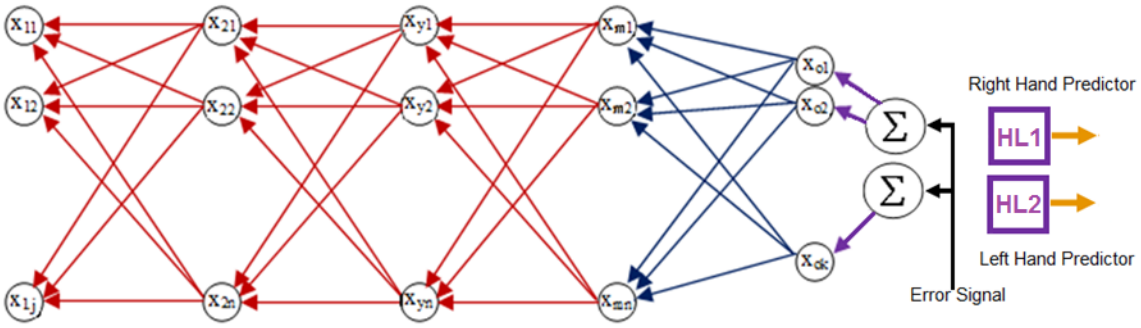

The error is back propagated through the network and adjustments are made at each of the weight layers based on the following equations (6) and (7). The local gradient in equation 6 is equal to the product of the corresponding error signal and the derivative of the associated activation function [262,263].

$$Weight\ Correction = lrng\ rate \times local\ gradient \times input\ signal \tag{6}$$

$$Weight_{Updated} = Weight_{Present} + Weight\ Correction \tag{7}$$

Changes to the weights consist of adjustments to the previous weight matrix and to the last layer. The ANN input layer's change is a weighted change of the input signal as shown in equation (8)

$$Weight\ Correction = lrng\ rate \times local\ gradient \times input\ data\ set \tag{8}$$

This ANN reaches convergence when the error at the output final layer is sufficiently small; this corresponds to a minimization of the squared error. The learning rate is an important parameter that controls the speed of learning and ultimately the convergence rate of the model. Small learning rates result in slower learning and convergence and require a large number of iterations. High learning rates could lead to instability due to oscillations at the output and the system does not reach equilibrium [262-264]. The model developed used a learning rate of 0.001 [262-264].

Training of the model consisted of feeding the time series data that contained data stacks for each subject, linked with other subjects in sequence (figure 5.3). The model was trained to recognize motor task performance and to identify handedness of the task being performed. Two major concerns for an ANN model are the tendency to over train and the occurrence of weight saturation [262,263]. Over training causes an ANN model to memorize a specific data set and could also cause neuronal death [262-264]. Neuronal death occurs when the ANN model perceives the presence of excessive artificial neurons in the hidden weight layers of the ANN and seeks to optimize the learning process by eliminating these irrelevant weights. Neuronal death within the weight layers can consist of a single neuron or groups of neurons within a weight matrix that have the value of zero. However, with over training, the perceived optimization by the model is inaccurate, resulting in the ability to provide flexible discrimination to be severely impeded. This causes the ANN model fail when used to analyze other data sets that are independent of the training data set. Weight saturation could lead to memorization of specific data sets or cause system instability. Both of these would cause the model to fail to find real events in subjects who were outside of the training set. To safeguard against data set memorization

and over training, analysis of the weights was performed to ensure that weight saturation did not occur and that the model was not unstable. Analysis of the weights in the hidden layers was performed to determine that there were no neuronal deaths, saturation in the layers or biasing of output predictions, a one factor repeated measures ANOVA was performed on the weights of layers 2 through 9. Mauchly's test of sphericity was performed to determine if the variances of the experimental conditions were equal; if equal, assumptions of the ANOVA are preserved.

5.4.3 Model Implementation.

The model was implemented using custom written MATLAB (version R2010a) code on an HP Compaq dc7900 convertible minitower [Hewlett-Packard Company, Palo Alto, CA, USA]. The computer had an Intel [Intel Corporation, Santa Clara, CA, USA] Core 2 Duo 3.16GHz processor with 4.0GB of Random Access Memory (RAM) and was running the 32-bit version of Windows 7 [Microsoft Corporation, Redmond, WA, USA] operating system. The raw data sets that were processed in AFNI were arranged in the format as specified in section 5.4.1 where the time series for the right hand was stacked on top of the left hand. The combined time series data set for all 13 subjects had a total of 14,040 time points and a single training pass through all of these points was considered successful completion of one epoch. The model was trained for a total of 500 epochs. The model's output and prediction error for each iteration was calculated and saved. Once training was complete, the net error of each epoch was plotted to reveal the level of convergence and stability of the model. The model took approximately 4 hours to converge.

5.5: RESULTS.

5.5.1: Right Hand Physiological Data.

Table 5.3 shows the physiological regions that were active during the performance of the right motor task used in the model development. The data indicate regions that were consistent across all subjects (5 dropped out of the study). Figures 5.7a through 5.7c show the active regions for the right motor task as determined from table 5.3 for the right motor task performed with 2s., 4s. and 6s. inter-stimulus delays. Each of the figures show the activation for task planning represented by the first 4 time points when the visual cue was presented to the subject. The effect of the delay follows the task planning phase. The activation corresponding to task execution can clearly be seen by a high, sustained, positive activation that lasts between 4 – 5 seconds. These characteristics are still preserved and the features in the figure resemble information from figures 4.5a, 4.5b and 4.5b even with the removal of 5 regions that had dropped out.

TABLE 5.3: Activation Regions for Right Motor Tasks.

	Regions R		**Regions R**		**Regions R**
1	L Precentral Gyrus	17	L Inferior Occipital Gyrus	33	R Cerebellum (Crus 1)
2	R Precentral Gyrus	18	L Fusiform Gyrus	34	L Cerebellum (Crus 2)
3	L Superior Frontal Gyrus	19	L Postcentral Gyrus	35	R Cerebellum (IV-V)
4	R Superior Frontal Gyrus	20	R Postcentral Gyrus	36	L Cerebellum (VI)
5	L Middle Frontal Gyrus	21	L Superior Parietal Lobule	37	R Cerebellum (VI)
6	R Middle Frontal Gyrus	22	L Inferior Parietal Lobule	38	L Cerebellum (VIII)
7	L Inferior Frontal Gyrus Opercularis	23	L SupraMarginal Gyrus	39	R Cerebellum (VIII)
8	R Inferior Frontal Gyrus Opercularis	24	R SupraMarginal Gyrus	40	L Cerebellum (IX)
9	L SMA	25	L Precuneus	41	Cerebellar Vermis (4/5)
10	R SMA	26	L Paracentral Lobule	42	Cerebellar Vermis (6)
11	L Insula Lobe	27	L Caudate Nucleus	43	Cerebellar Vermis (7)
12	R Insula Lobe	28	L Thalamus	44	Cerebellar Vermis (8)
13	L Middle Cingulate Cortex	29	L Superior Temporal Gyrus	45	Cerebellar Vermis (9)
14	L Calcarine Gyrus	30	R Superior Temporal Gyrus	46	Cerebellar Vermis (10)
15	L Lingula Gyrus	31	L Temporal Pole	R	Right
16	L Middle Occipital Gyrus	32	L Cerebellum (Crus 1)	L	Left

FIGURE 5.7a: Reaching and Grasping with the Right Hand at 2s. Delay.

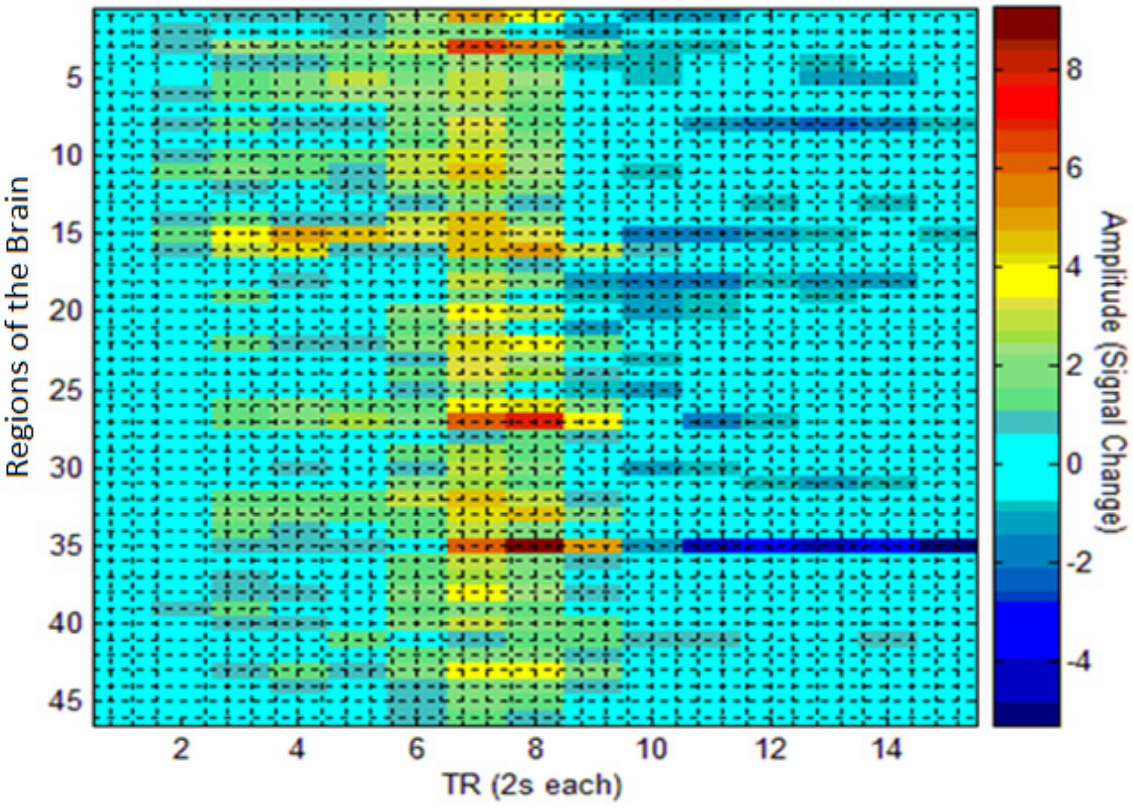

FIGURE 5.7b: Reaching and Grasping with the Right Hand at 4s. Delay.

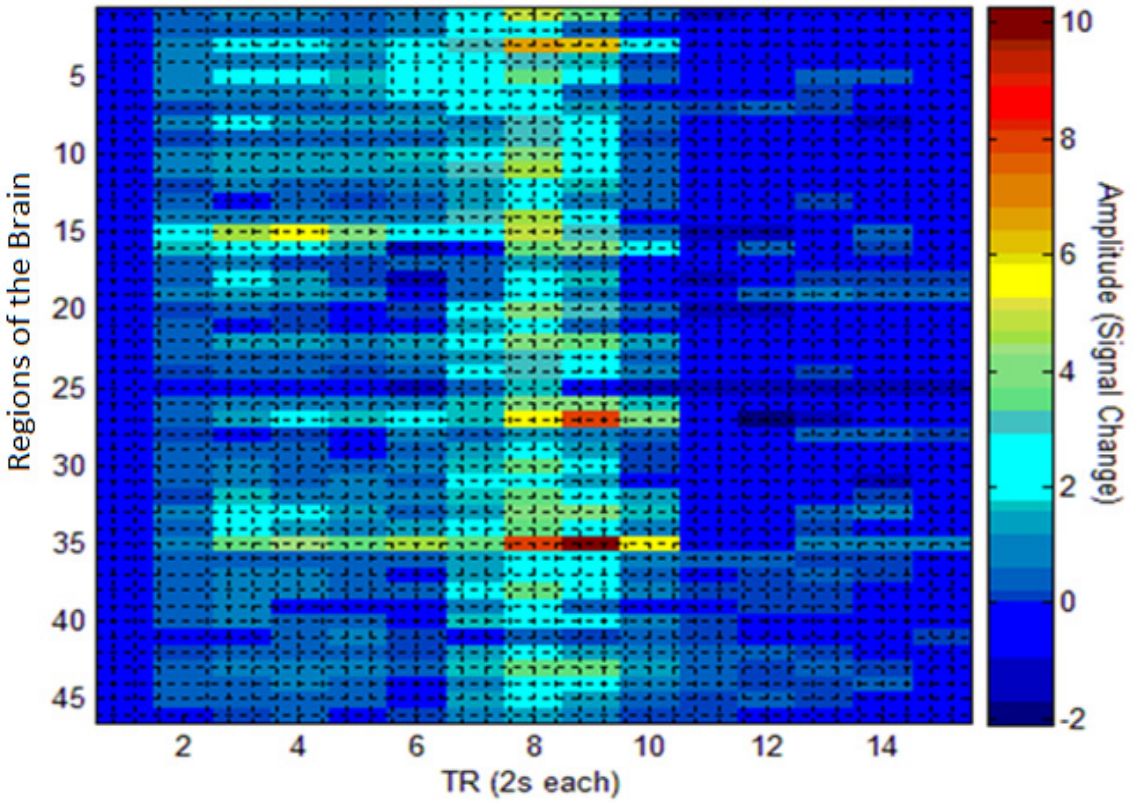

FIGURE 5.7c: Reaching and Grasping with the Right Hand at 6s. Delay.

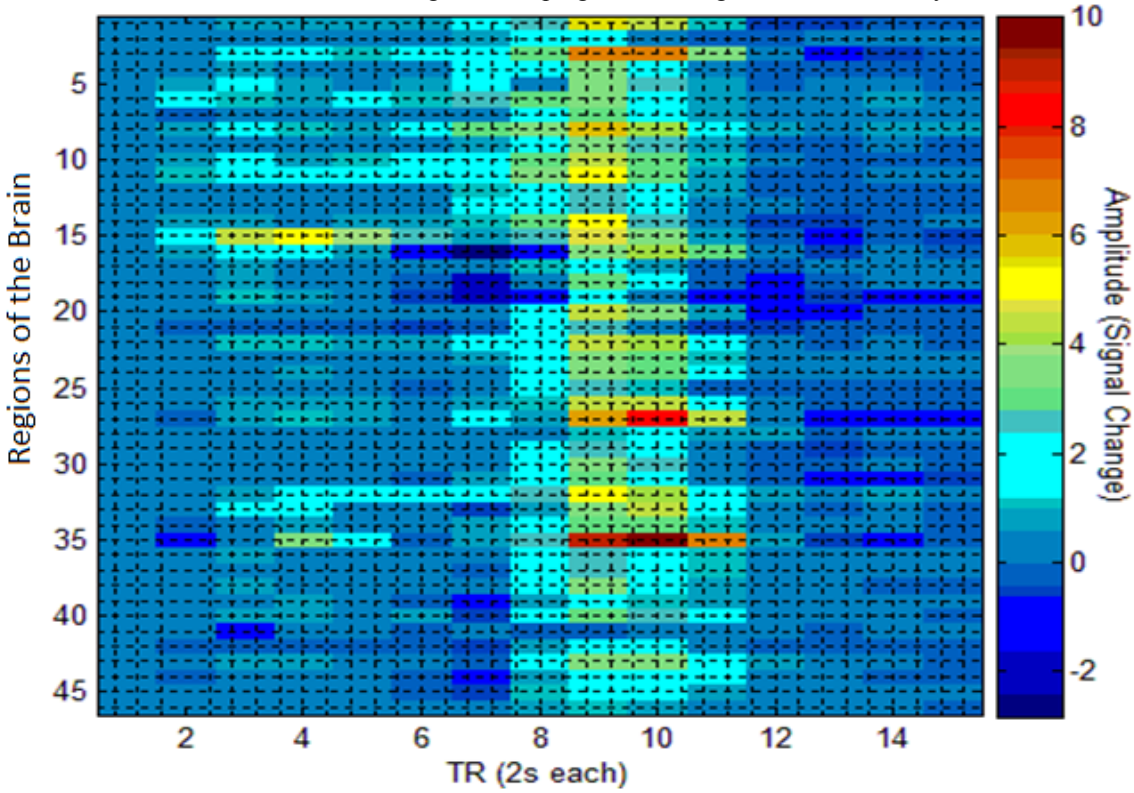

5.5.2: Left Hand Physiological Data.

Table 5.4 shows the active physiological regions that are associated with the performance of the left motor tasks and used in the development of the model. The data in table 5.4 represent regions that are consistent across all subjects without activation drop out. The data in figures 5.8a through 5.8c show the active regions for the left motor task as determined from table 5.4 for the left motor task performed with 2s., 4s. and 6s. inter-stimulus delays. The figures show the time where task planning occurs during the first 4 seconds of the task when subjects were presented with the visual cue. The effect of the task execution phase is represented by high, positive and sustained activation that can clearly be seen in figures 5.8. The effect of the inter-task delays on the task execution phase can be seen as an induced lag of two seconds that delays the activations of the task execution phase by shifting these activations the right (figures 5.8a through 5.8c). These important task features are still preserved and resemble information from figures 4.7a, 4.7b and 4.7c even after discarding 3 regions as the result of individual subject drop out.

TABLE 5.4 Activation Regions for Left Motor Task.

	Regions L		**Regions L**
1	L Precentral Gyrus	20	L SupraMarginal Gyrus
2	R Precentral Gyrus	21	R SupraMarginal Gyrus
3	L Superior Frontal Gyrus	22	L Paracentral Lobule
4	R Superior Frontal Gyrus	23	R Thalamus
5	L Inferior Frontal Gyrus (p. Opercularis)	24	R Heschls Gyrus
6	L SMA	25	L Superior Temporal Gyrus
7	R SMA	26	R Superior Temporal Gyrus
8	R Insula Lobe	27	R Temporal Pole
9	L Middle Cingulate Cortex	28	L Cerebellum (Crus 1)
10	R Middle Cingulate Cortex	29	L Cerebellum (IV-V)
11	R Hippocampus	30	L Cerebellum (VI)
12	L Calcarine Gyrus	31	R Cerebellum (VI)
13	L Fusiform Gyrus	32	L Cerebellum (VIII)
14	L Postcentral Gyrus	33	L Cerebellum (X)
15	R Postcentral Gyrus	34	Cerebellar Vermis (4/5)
16	L Superior Parietal Lobule	35	Cerebellar Vermis (6)
17	R Superior Parietal Lobule	36	Cerebellar Vermis (7)
18	L Inferior Parietal Lobule	R	Right
19	R Inferior Parietal Lobule	L	Left

FIGURE 5.8a: Reaching and Grasping with the Left Hand at 2s Delay.

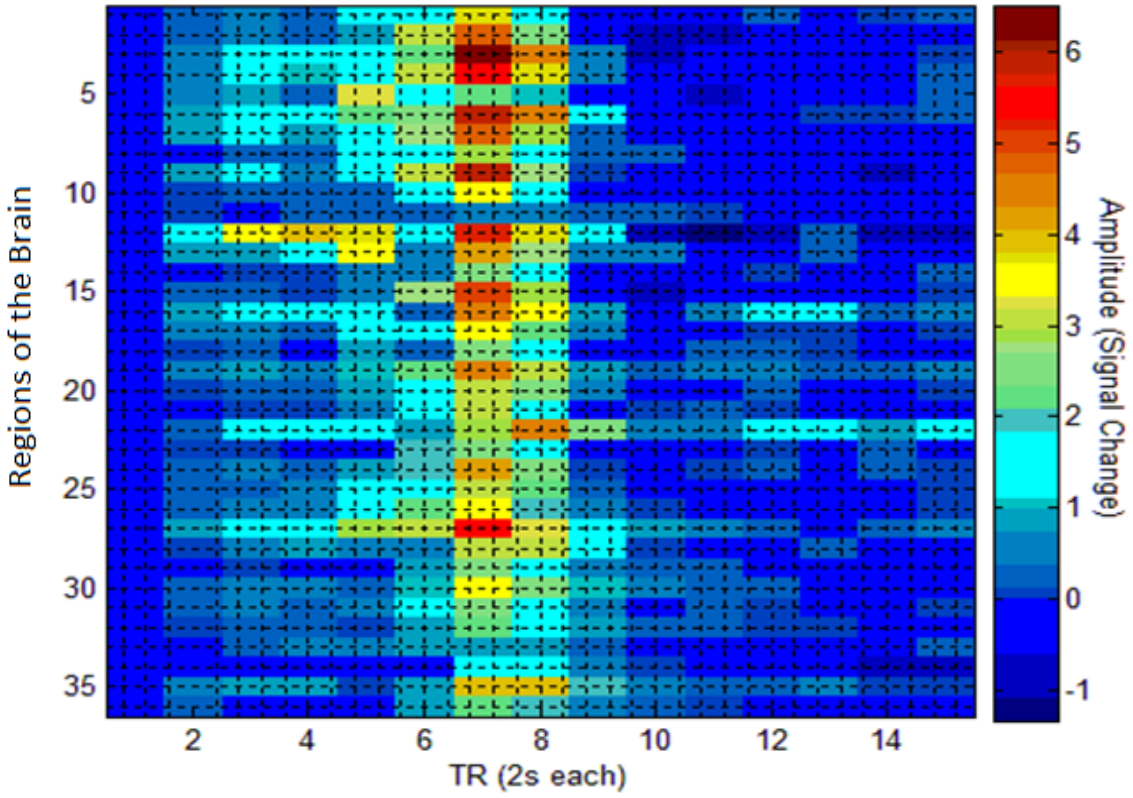

FIGURE 5.8b: Reaching and Grasping with the Left Hand at 4s Delay.

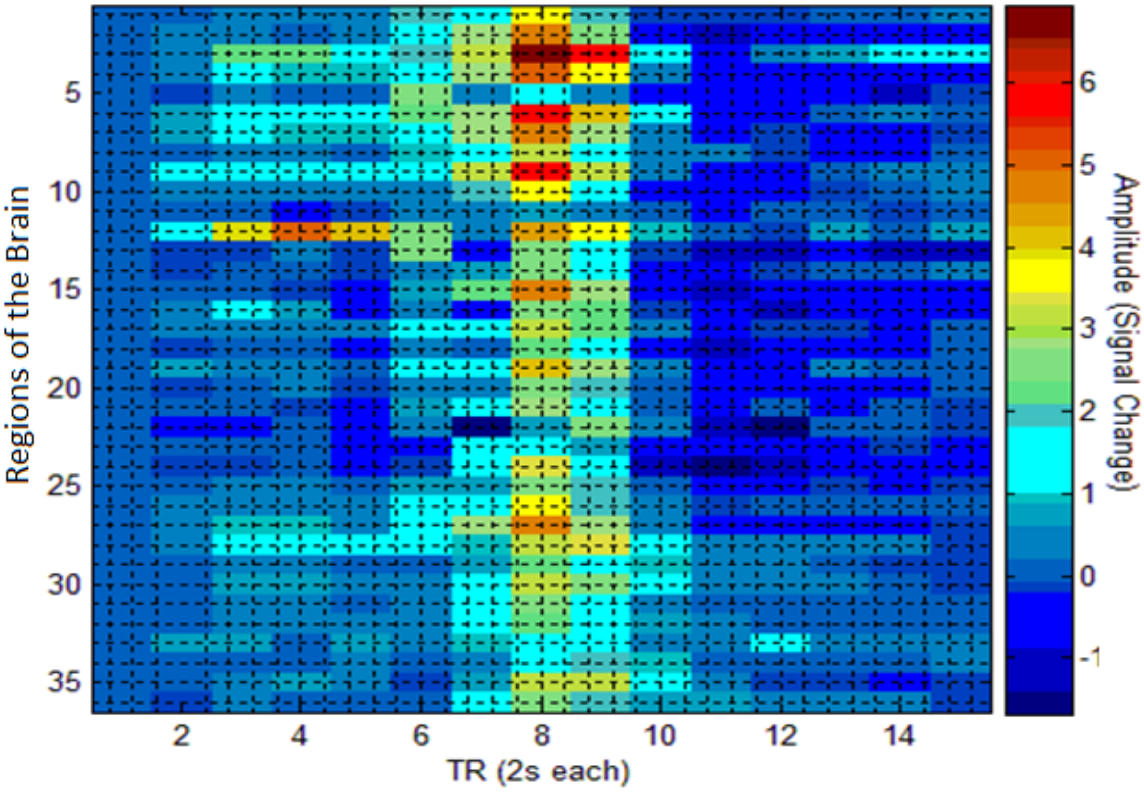

FIGURE 5.8c: Reaching and Grasping with the Left Hand at 6s Delay.

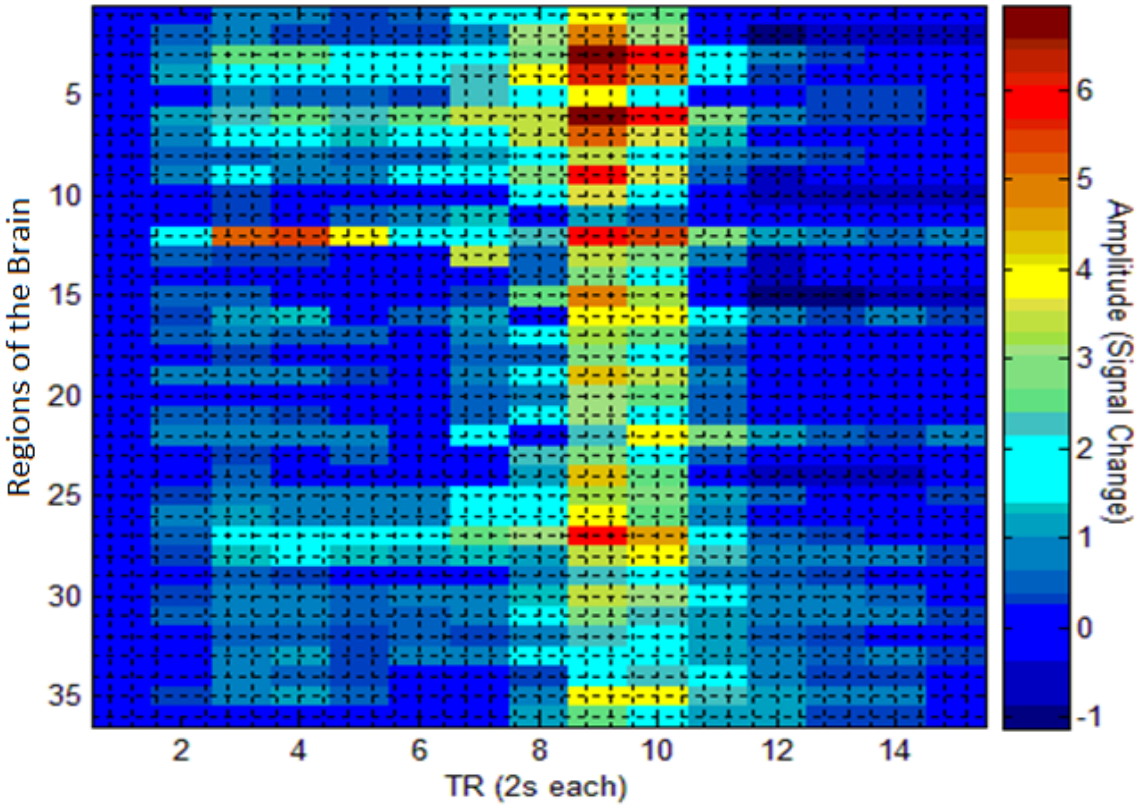

5.5.3: Model Convergence.

Figure 5.9 shows the convergence of the model. The total number of training epochs were 500, but for visualization of the convergence point, only 40 epochs have been shown on the x-axis and the percent error on the y-axis was shown from zero to 1%. Each epoch represents 14040 data points that were analyzed by the model. Convergence was achieved after 9 epochs. The final output error after convergence does not go down to zero, rather the average value for epochs past the convergence point was determined to be 0.15%. The data past the 9^{th} epoch does not stay at a constant value, rather experiences small variations around the mean.

FIGURE 5.9: Plot of Model Output Error Showing Convergence. Note that the first 40 out of 500 epochs were plotted on the x-axis and the percent error was plotted from zero to one percent error on the y-axis for visualization purposes).

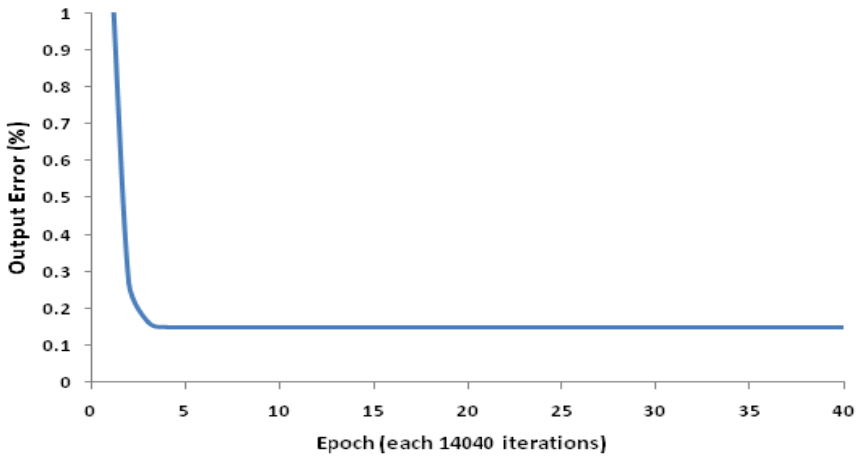

5.5.4: Weight Analysis.

The data in figures 5.10a through 5.10h show the weight distributions for the hidden layers. The patterns for each layer show that there were different weight values for each layer. Furthermore, there were no weights that had a value of zero, or that shared constant values within or between layers.

FIGURE 5.10a : Weight matrix for 1st hidden layer

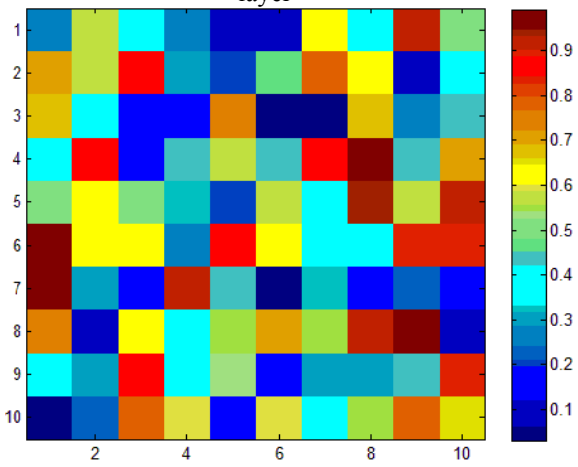

FIGURE 5.10b : Weight matrix for 2nd hidden layer

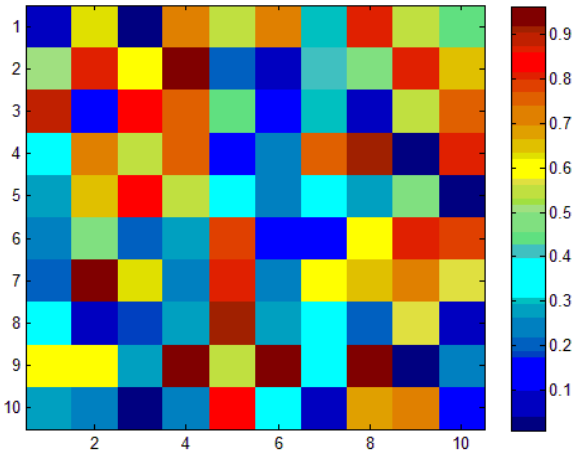

FIGURE 5.10c : Weight matrix for 3rd hidden layer

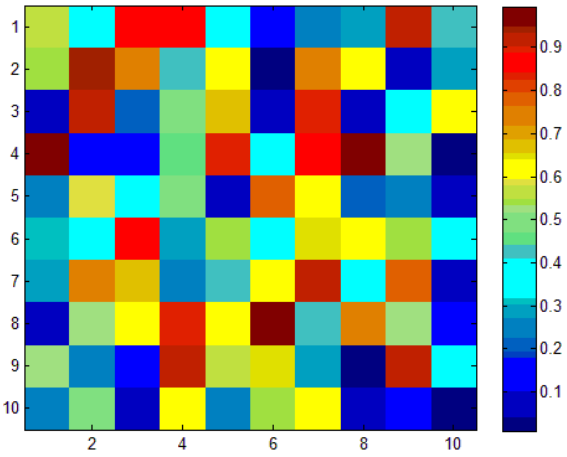

FIGURE 5.10d : Weight matrix for 4th hidden layer

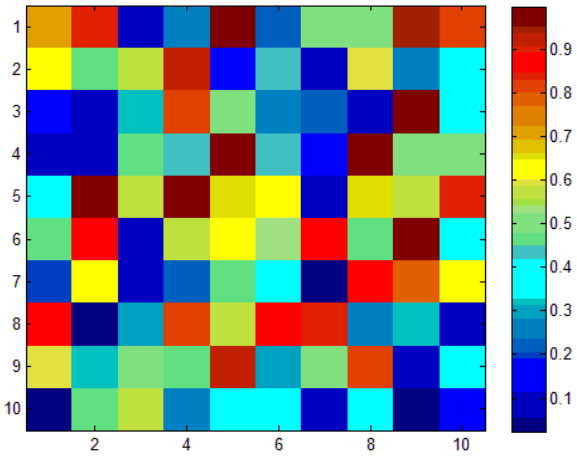

FIGURE 5.10e : Weight matrix for 5th hidden layer

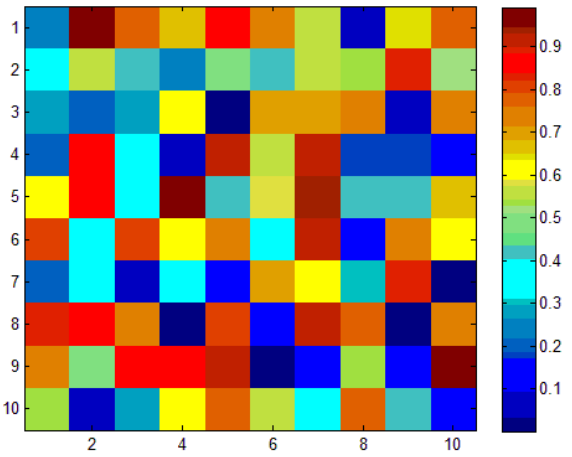

FIGURE 5.10f : Weight matrix for 6th hidden layer

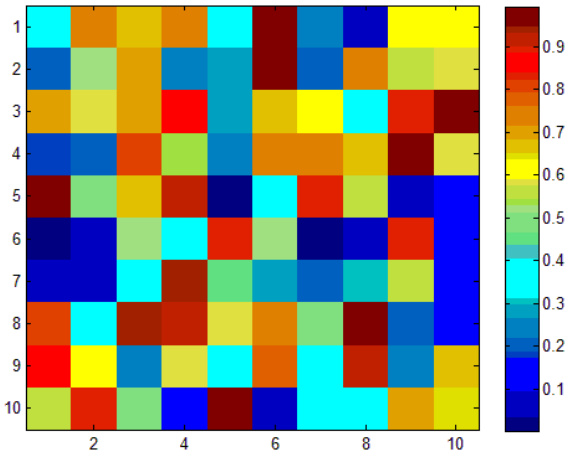

FIGURE 5.10g : Weight matrix for 7th hidden layer

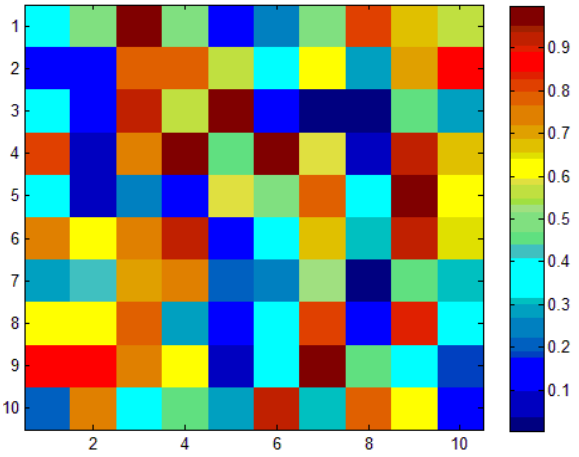

FIGURE 5.10h : Weight matrix for 8th hidden layer

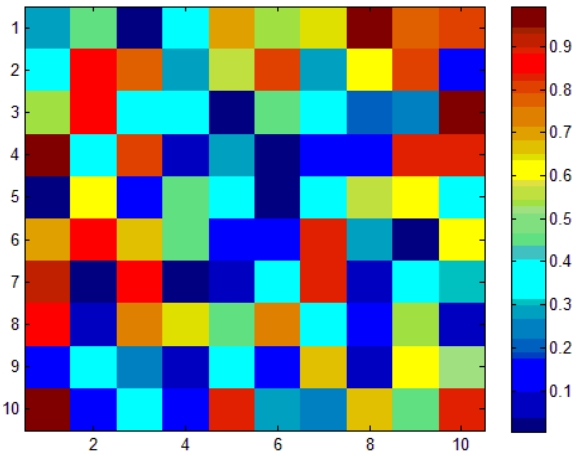

The data in table 5.5 lists the weights at all layers, the corresponding mean value of the weights at each layer, the standard deviation and total number of neurons.

TABLE 5.5 : Descriptive Statistics for the Weight Layers showing the Mean, Standard Deviation and Number of Neurons per layer.

Layer	Mean Weight	Standard Deviation	Number of Neurons
1	0.5	0.29	328
2	0.49	0.27	100
3	0.47	0.28	100
4	0.47	0.28	100
5	0.48	0.29	100
6	0.52	0.29	100
7	0.51	0.30	100
8	0.51	0.28	100
9	0.45	0.30	100
10	0.55	0.27	60

The results from Mauchly's test of sphericity (p>0.05*)* performed on weight values from layers 2 through 9 indicated there were no significant differences present in the variance. These results are summarized in table 5.6.

TABLE 5.6 : Results of the Mauchly's test for Sphericity (p significant < 0.05).

Mauchly's W	Approx. Chi-Square	df	*Calculated p-value*
0.871	13.312	27	0.987

The one factor repeated measures ANOVA was calculated using the assumed sphericity of the data set without any correction, and the results indicate that there were no significant differences between each layer, $F(7,693) = 0.744$, $p = 0.635$ (table 5.7).

TABLE 5.7 : Test of Within Subjects Effects (p significant < 0.05).

	Source	Type III Sum of Squares	df	Mean Square	F	Calculated p-value
Layers	Sphericity Assumed	0.426	7	0.061	0.744	0.635
Error	Sphericity Assumed	56.657	693	0.082		

When comparing within subjects effects for the ANOVA analysis of layers 2 through 9, a significant cubic trend (p=0.048) was observed as shown in the following table 5.8 and in the plot of the means and standard deviations presented in figure 5.11.

TABLE 5.8 : Analysis of Within Subjects Effects Showing Comparisons of Trends (p significant <0.05).

Source	Layers	Type III Sum of Squares	Df	Mean Square	F	Calculated p-value
Layers	Linear	0.004	1	0.004	0.045	0.832
	Quadratic	0.081	1	0.081	0.939	0.335
	Cubic	0.313	1	0.313	4.006	0.048
	Order 4	0.001	1	0.001	0.006	0.938
	Order 5	0.003	1	0.003	0.04	0.842
	Order 6	0.007	1	0.007	0.086	0.77
	Order 7	0.017	1	0.017	0.212	0.647
Error(Layers)	Linear	7.826	99	0.079		
	Quadratic	8.546	99	0.086		
	Cubic	7.743	99	0.078		
	Order 4	8.48	99	0.086		
	Order 5	8.424	99	0.085		
	Order 6	7.643	99	0.077		
	Order 7	7.994	99	0.081		

FIGURE 5.11 : Mean and Standard Deviations of the Input, Hidden and Output Layers for the Model. ANOVA calculations showed the presence of a cubic trend among layers 2 through 9.

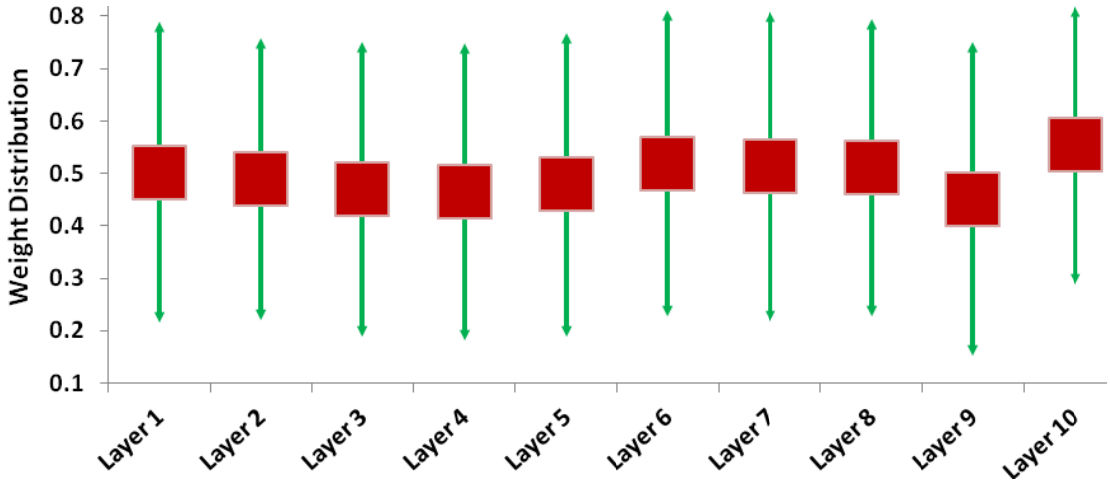

5.6: DISCUSSION.

The convergence data in figure 5.9 shows that the final output error of the model is approximately 0.15%. This output error does not settle on a constant value, and this is a characteristic that is important for two reasons. First, if the final error went down to zero, this would suggest that the model has memorized the entire data set. Second, the small deviations in the output error signify that the model is learning and still attempting to minimize the error. If the output was constant, this would suggest data set memorization or saturation of the weights. Saturation of the weights would cause the model to be unstable and lead to an amplification effect where the output would increase toward infinity. Results from a model that has saturated weights would be highly biased, inaccurate and unreliable when applied to the analysis of new stimuli or data sets. The plots of figures 5.10a through 5.10h showed that each layer had different weight values and that there were no repeated values or zero values. Further analysis of the weights

using the repeated measures ANOVA showed no significant differences; however there was a cubic trend for the mean values of each layer. This trend was seen in the 5.11. The trend would suggest the presence of structure and organization in the weights values of each layer that has a distinct feature or characteristic. This is the results of the learning process that has been learned and the combined output from these layers of the ANN would result in prediction of the desired analysis. However the specific significance of this cubic trend and its correlation with the physiological signals that are being modeled is not clear at this moment.

The performance of the model demonstrates an ability to extract, classify and learn patterns in the brain that correspond to the motor planning phase for movement pertaining to functional task initiation from fMRI data. The convergence results for the model indicate that the model was able to accurately identify hand use in right handed individuals for motor task performance, through the analysis of brain activation. These accomplishments strongly support the hypothesis for this chapter; that it is possible to accurately model the temporal patterns of brain activation corresponding to functional reaching and grasping in a population of normal subjects.

This model is unique because it is highly data driven and uses temporal activation in the brain that corresponds to functional upper extremity task performance combined with real-world objects; features currently not used in a majority of functional brain connectivity models. The analysis of the layer weights in the model show that there was no weight saturation, and that the model was stable. The model does not make any prior assumptions pertaining to statistical parameters such as the distribution, mean or variance of the data set. This is important because to realize proper estimation of these statistical

parameters, using methods other than neural networks, a large subject population would be needed. Furthermore, such a method is not practical for the implementation of the whole brain model to function as a neuroprosthetic controller since the ability to predict motor intent would require present and past values of activation in the brain to compute information that relates to the data and distributions. In addition, literature suggests that these parameters have a tendency to vary based factors such as recoding modality, data acquisition location, stimuli or task performed and noise (physiological and environmental) noise [265,293,294]. Estimation of these parameters in real-time would lead to huge computing cost and delays in information processing as the result of acquiring sufficient data samples needed to produce accurate estimates. Excluding those methods that require the foregoing assumptions, statistical parameters and mathematical operations on the data set such as smoothing, filtering and rotations, the development of this custom whole-brain model is largely data driven and is able to account for naturally occurring human neuromotor strategy represented by temporal activation patterns in the brain. This is a desired characteristic that can enable the practical application of this model as a neuroprosthetic controller.

5.7: CHAPTER CONCLUSION.

These model development results support the hypothesis of the chapter to accurately model temporal patterns of brain activity, acquired using fMRI, that pertain to upper extremity functional task performance. This model is unique as it is highly data driven and uses whole brain data from functional task performance combined with real-

world objects; features that are currently not used in a majority of contemporary brain models that represent function. Such a model has implications for upper extremity neuroprosthetic control.

CHAPTER 6

Validation of Whole-Brain Model for Upper Extremity Neuroprostheses Application

6.1: ABSTRACT.

This chapter presents the validation process of the custom developed feed forward upper extremity neuroprosthetic controller model. Right hand dominant neurologically intact subjects (N=4) were used in this study. Validation is important for two main reasons; the first was to verify that the training paradigm did not saturate or bias the learning process of the model and lead to the memorization of training data set. The second purpose of the validation was to demonstrate that the model was indeed robust and able to perform feature extraction and pattern classification of data sets in its intended proof-of-concept application: an effective upper extremity neuroprosthetic controller. Testing consisted of determining the ability of the model to accurately predict movement intention, using the left or right hand, through the analysis of the planning phase of motor task performance s represented by temporal activation in the brain. It was determined from these experiments that the model is able to predict hand use through analysis of the motor planning phase at an accuracy level of 81%. The work in this section supports the functionality of the model and confirms the hypothesis of the dissertation.

6.2: INTRODUCTION.

This chapter presents the validation process of the custom developed feed forward upper extremity neuroprosthetic controller model. There are two main reasons that this validation process is important. The first is to verify that the training paradigm did not saturate or bias the learning process of the model. During training, the quick convergence

of the training error would be a cause for concern because that implies that the model could have potentially memorized the training data set. Over-training the model can also be caused by multiple iterations through large training data sets and this can also induce memorization of the training data set, and a quick convergence of the error [262-264]. The process of over training and memorization of the specific data sets could lead to neuronal death as the results of inaccurate attempts by the ANN model to optimize its performance. This is a method of ANN models to reduce excessive and irrelevant weights and the scale of neuronal death could be from a single neuron to several neurons within a hidden weight layer. Neuronal death is also an indication that the number of hidden layers and hidden layer sizes for the ANN model were not properly designed. Over-training of the ANN and false optimization attempts are undesired as these factors could lead to inaccurate data classification which will render the model useless. Results from chapter 5 indicated that there were no neuronal deaths or weight saturation in each of the ANN layers, however the process of testing the whole-brain model on a novel data set would determine if overtraining had indeed affected the model or if the model had been sufficiently trained.

The second purpose for testing the model on a separate set of data that is independent from that used for the development of the model is to demonstrate that the model is indeed robust, and able to perform feature extraction and pattern classification on other subjects. This analysis of functional data sets using the model is important to assess the performance of the model in its intended proof-of-concept application; and that is to predict hand use through the analysis of functional motor intention. The hypothesis for this chapter is that the brain model developed will accurately predict hand use of the

new subject population during the imagined performance of functional reaching and grasping tasks through the analysis of temporal activation patterns of the brain.

6.3: METHODS.

A total of 4 neurologically intact subjects (M= 4, Mean Age 23.5 years) were used for this validation study. These subjects were part of the subjects who had been initially recruited for the second specific aim described in chapter four. The four subjects used in this study were separate from the 13 subjects used in the development of the model. All subjects were determined to be right hand dominant using the Edinburgh Handedness survey [223].The data acquisition parameters, experiment paradigm, and preliminary data processing and extraction were consistent and in agreement with the procedures outlined in the Methods section of chapter four. The right hand time series data was stacked on top of the left hand data set in a manner similar to the data preparation for training of the model as presented in chapter five. The time series data consisted of reaching and grasping with the right hand and left hand separately. Inter-task interval of 2s., 4s. and 6s. were implemented in random order. However, the random order of the delays was the same as used for the training group. Each task was 30 seconds long and was repeated 12 times to yield a total of 288 events and 4,320 time points for all 4 subjects combined.

Validation of the developed artificial intelligence model was performed using custom written MATLAB (version R2010a) code on an HP Compaq dc7900 convertible minitower [Hewlett-Packard Company, Palo Alto, CA, USA]. The computer had an Intel [Intel Corporation, Santa Clara, CA, USA] Core 2 Duo 3.16GHz processor with 4.0GB of

Random Access Memory (RAM) and running the 32-bit version of Windows 7 [Microsoft Corporation, Redmond, WA, USA] operating system. The data was fed through the model once and the resulting model predicted output and error were saved. Once the validation process was completed, the output and error were analyzed to determine accuracy using the following equation 9.

$$Model\ Accuracy = \frac{\sum Total\ number\ of\ correct\ detections}{Total\ number\ of\ events} \times 100\% \quad (9)$$

6.4: RESULTS.

The following table shows the results of the validation process for which the model analyzed the time series data from four healthy subjects. The model attempts to predict hand use by analysis of the motor planning phase. This was determined to be the first 4 time points in the data set. The following table 6.1 shows the detection of hand use for functional upper extremity tasks as performed by the four subjects' from whom data were used in the validation study. It is observed that subject 3 had the largest number of successful detections, and subject 4 had the lowest number of successful detections. The average accuracy of the model was determined to be 81.4 ±1.9%.

TABLE 6.1 : Detections of Hand Use During Functional Task Performance for Validation Study

Subject	R Motor Task Detections (%)	Left Motor Task Detections (%)
1	77	80
2	86	83
3	88	91
4	69	77
Average Detection Rate (%)	80	82.7

6.5: DISCUSSION.

The validation study results for the model showed that it is capable of extracting, classifying and identifying the appropriate patterns associated with the motor planning phase of functional task initiation. In addition, the model is able to separate handedness for motor task performance at an accuracy level of about 81%. The ability of the model to perform these processes on a separate data set, that was independent of the training data set, strongly suggests that the model was not over trained, and there was no weight saturation present. The results obtained from the performance of the custom developed brain model in this validation study strongly support the hypothesis of the final specific aim of this dissertation - the ability of the brain model to accurately predict hand use during a reach-to-grasp functional task using data that is specific to the planning phase of upper extremity motor task performance.

The results indicate some variability in the accuracy of detection for the model developed. Subject 3 had the most number of successful detections and subject 4 had the lowest number of successful detections. The underlying principle of the model is to predict movement by analysis of the planning phase for motor task performance. The lower number of successful detections for subject 4 could be the result of mental fatigue

or distractions in the fMRI scanner area during task performance that hindered proper concentration. This could have led to an increase in variability in some of the regions, which were beyond the present processing capabilities of the model. Additionally, the ability of each subject to plan the task was not measured in this work. The level of mental effort required to imagine doing a task is likely to vary enormously across any population. The example of two golfers, one professional and one 'weekend duffer' should suffice to illustrate the difference. The professional can drop a ball on the turf and strike it with virtually no mental effort. The weekend duffer drops the same ball and then stands over it for a long period, imagining various aspects of his planned motor performance. The subjects used to build the model and validate it, were not evaluated for personal histories which may have had an impact on the level of effort required to imagine reaching and grasping. The effect of past experience in skilled physical activities such as sports or dance, where reaching and grasping are an essential part of the game has been determined to have an effect on motor imagery activation [271,283].

At first glance, 81.4% accuracy result for the model's predictive ability seems rather low. This decrease in performance was attributed to the results from subject 4. However the performance of the model is impressive because it is able to accomplish classification of motor task strategy represented in the brain using minimal post processing of the data. Furthermore, implementation of the model did not need any calibration nor did it require the subjects to be trained. All subjects who were used in the validation study performed the tasks at their own pace in a natural manner, without being coached or trained. The results show that the model is able to incorporate naturally occurring neuromotor strategies represented by the key anatomical locations in the brain

that are involved with functional upper extremity tasks. The ability of the brain model to distinguish hand use from motor intent by analysis of brain activation patterns meets the objective of the proof-of-concept for the intended application in upper extremity neuroprosthetic control.

6.6: CHAPTER CONCLUSION.

The model developed is able to predict hand use during functional task performance through the analysis of the temporal brain patterns that correspond to the motor intention phase. This completes the objectives of the dissertation project - to develop a proof-of-concept whole brain model for application toward upper extremity neuroprosthetic control.

CHAPTER 7

Dissertation Conclusions

7.1: INTRODUCTION.

The goal of this dissertation is to develop a whole brain model as a proof-of-concept for upper extremity neuroprosthetic control. The significance of this model is its ability to represent neuromotor strategy as expressed by activation in brain regions that pertain to functional upper extremity task performance. A model of whole brain temporal activity and 3-D anatomical localization of activation that corresponds to functional upper extremity task performance is a feature that is not available in contemporary brain models and upper extremity neuroprosthetic controllers. It is hoped that the implementation of this whole brain model for upper extremity neuroprosthetic applications will provide users with a robust control platform and reduce the development of compensatory behaviors and the need for extensive training.

7.2 : Review of Specific Aims.

This dissertation project consisted of 4 specific aims as follows:

Specific Aim 1: The first specific aim was to identify anatomical regions of the brain that are involved in planning, execution of functional upper extremity tasks. The experimental paradigm involved neurologically healthy individuals who performed 3 actual motor tasks and 3 motor imagery tasks. These tasks consisted of reaching, grasping and combination of reaching and grasping of a sponge ball. FMRI data was collected from the entire brain. This work is unique because many contemporary functional imaging studies

have not holistically examined brain activation with respect to functional motor tasks using real world objects. Furthermore most surface recording modalities such as EEG and MEG do not provide 3-D anatomical localization of activation in the cerebellum or in deep brain structures such as the thalamus. The analysis of the activation regions from the actual motor and motor imagery tasks revealed the presence of activation regions common to both real and imagined performance. As might be expected, numerous regions were activated common to different tasks. Whether this is simply the result of insufficient spatial resolution remains to be seen. When comparing the grasp only task with functional reaching and grasping, it was observed that there were differences in activation organization, that were very pronounced in the cerebellum. It can be speculated that the grasping task is much more akin to a rhythmic task like finger tapping which requires far less planning than does movement in preparation to contact a target. Motor imagery tasks and actual motor tasks shared some common regions of activation such as the SMA, premotor cortex, cerebellum and calcrine gyrus, suggesting the presence of an overlap for motor task planning. These findings suggest that neuromotor strategies that are used for upper extremity movements have a 'common' control that can be fine tuned to achieve specific task goals.

Specific Aim 2: The second specific aim was to identify the temporal activation patterns in the brain during goal-oriented reaching and grasping in neurologically intact healthy individuals using fMRI. In the experimental paradigm, subjects performed actual motor tasks using the left and right hands with a variable delay (2s.,4s.,6s.) between task planning and execution activities. FMRI data from the entire brain was collected. The

purpose of the delay was to maximize motor imagery by forcing the subject to hold in their mind the thought of performing the reach and grasp task. Making the delays variable reduced the stimulus anticipatory effect. It is probable, although not proven, that if the delay was to have been constant, the reach and grasp task would have become rhythmic, defeating the intended effect. The analyses of the temporal activation patterns from the entire brain yielded two distinct phases, one for task planning and the other for task execution. These patterns of activation are distinct and quantifiable and represent features that are important in the development of a whole brain model.

Specific Aim 3: The third specific aim consists of developing a whole brain model that permits extraction and classification of temporal patterns of the brain that correlate with neuromotor strategy of upper extremity control. Development of the brain model was achieved using data from neurologically healthy subjects (N=13) who performed the unilateral functional tasks of reaching and grasping with the left and right hand. This model was developed using artificial neural networks with back propagation. The artificial neural networks with back propagation was chosen because of its ability to discriminate and to extract key features from physiological signals and classify them. Furthermore neural network models are able to apply the knowledge learned for pattern recognition in new data sets. The advantage of using neural networks is that the model can be developed with minimal assumptions about the data and without having to specify characteristics such as means, variance, standard deviations or features of the data distribution *a priori*. The results from this specific aim indicate that the model is stable and free of training data set memorization, weight saturation and instability.

Specific Aim 4: The last specific aim is to validate the whole brain model developed in Specific Aim 3 for potential upper extremity feed forward neuroprosthetic control. The validation process consisted of analyzing a dataset (N=4) of neurologically intact individuals whose data were independent of the data used in the model development. These subjects performed a series of functional reaching and grasping tasks with a specified target. The model predicts the hand in which the task would be performed solely by the analysis of the planning phase from the temporal information of the whole brain data set. The results indicate that the model is accurate (81.4 ±1.9%.) and able to predict motor task performance and hand usage from the analysis of brain activation patterns and sequences that were specific to the planning phase of the task. A key feature of the developed whole brain model is the ability to perform feature extraction and pattern classification without the need for calibration or for the subjects to undergo training or modification of behavior.

7.3: Limitations and Future Directions.

The first and most important limitation in this study is the nature of the fMRI signal. The fMRI signal arises from a vascular response to increased oxygen demand during the performance of a task. The time constants involved in the response are long compared to neuronal activity or actual physical movement of the limbs. The lag of response after stimulus is on the order of 1-2 seconds which is far slower than the time scales on which motion can be initiated. Further, the lag times are variable within the brain and may be dependent on the route of the arterial blood. Much of the cortex and

anterior portions of the brain are fed from the internal carotid arteries, while the occipital lobes and cerebellum are fed from the vertebral arteries.

The ability of the model to accurately predict hand usage through the analysis of upper extremity neuromotor strategy as represent by temporal activation patterns acquired from the whole brain makes it a good proof-of-concept for application to upper extremity neuroprosthetic control. This is because natural upper extremity neuromotor strategy is a distributed process and is represented by several regions in the brain. The whole-brain model enables accurate representation of these strategies. The results from chapter six in which the model was tested in its intended proof-of-concept neuroprosthetic controller application indicate the potential for robust use without the need for training or behavior modification. These features are currently not available from contemporary upper extremity neuroprosthetic controllers. Furthermore by detecting naturally occurring strategy using the whole brain, the risk of signal decay is reduced. This is a common unwanted feature of neuroprosthetic devices that are reliant on compensatory or modified behaviors [115,117]. However there are several items that need to be addressed to be able to apply the whole brain model developed in practical applications.

The first item is a needed improvement in the extraction and classification algorithm for greater sensitivity and accuracy. The ANN model developed in this dissertation analyzes changes in the amplitude of region specific activation to determine the sequences activations that correspond to the planning of upper extremity functional tasks. Temporal activations that results from the brain's hemodynamic response are not limited to changes in amplitude but also experience changes in phase. Future work could

examine these changes in phase combined with changes in amplitude in specific regions of the brain. More specifically, the effect of task features such as planning and execution combined with varying levels of task complexity on the phase of the activation signal, can be examined and quantified through modifications in the model. This can be achieved by adding more hidden layers and increasing the number of weights in each layer. It is hoped that through the implementation of a model that can account for amplitude and phase changes, the detection and classification portions of the model will be more sensitive to stimulus specific changes in activation patterns, and enable a higher level of accuracy than the present 80%.

A second suggested area of improvement of the model is to understand the changes in temporal activation patterns of the brain during real world functional task performance in everyday life, such as the activities of daily living. Such tasks require combination of unilateral and bilateral hand use together with interaction with the lower extremities. To adequately account for these added activations, the current whole-brain model would have to be expanded from single handed upper extremity tasks to permit detection of other neuromotor strategies represented within the brain that are induced by bilateral hand movements and functional usage of the lower extremities. Such data will yield insight into how the neural correlates of active task performance are naturally represented in the cortex and how the different brain regions interact with one another. Using this information, analysis of multiple processes and their influence on upper extremity neuromotor strategies can be quantified. Bilateral hand use and lower extremity task induced activation could influence the performance of the current whole-brain model that was developed using unilateral hand use. Neuromotor strategy is distributed across

multiple brain regions and the level of activation is likely to change depending on limb use. An experiment that examines bilateral hand use and lower limb use could address questions that pertain to cross talk between regions of the brain and the influence of these tasks on the signal-to-noise ratio of unilateral tasks, from which the current brain model was developed. Results from functional imaging studies have revealed activation in regions that are common to upper extremity and lower extremity tasks such as the primary motor cortex, SMA, sensory cortex and cerebellum [266,267]. However, somatotopic organization of the extremities influences the locations of upper and lower extremity activation patterns within these common anatomical regions of the brain. If the developed whole-brain model is applied in a practical application, the extent of common and overlapping brain strategies related to other tasks, such as lower limb use, would need to be adequately accounted.

The third area of improvement lies in the performance of the studies presented in chapters 3 and 4 on a higher field strength MR scanner, such as 7 Tesla. The increase in field strength has been shown provide not only an increase in the signal-to-noise ratio of the acquired data but also better spatial resolution of the acquired functional data sets [268]. Such features could reduce the effects of subject drop out and enhance the activations of each subject. This is important and could be used to improve the sensitivity of the model prediction abilities.

The fourth area of improvement is to understand changes in the hemodynamic response based on pathology. Presently the ability of the model to predict hand use is dependent upon stimulus induced temporal activation and region specific changes in the brain in healthy neurologically intact individuals. Plasticity is a key brain feature that

provides flexibility in development and learning. Pathologies such a stroke, arthritis, dystonia, spinal cord injury and even limb loss affect the brain by inducing reorganization that could change vasculature and synaptic organization. Such changes influence the manner in which upper extremity neuromotor strategy is executed, and is likely to lead to changes in the patterns associated with all phases of the task. Therefore pathology induced changes could lead to diminished accuracy of the developed whole-brain model.

The last recommendation for future work is to examine methods in which the model can be practically applied in order to perform as an included controller of an upper extremity neuroprosthetic device. While the model was designed as a proof-of-concept using fMRI data, potential applications of the model would require the development of sensors that are able to detect changes in the entire brain that correspond to blood oxygenation levels that are task specific. Such sensors would require implantation in multiple regions of the brain, and at this moment this seems impractical due to the highly invasive nature of such a procedure. Furthermore, if these sensors were developed the detection lag time would need to be rapid to enable real-time processing of information flow in the brain. This suggests that the measurement of a different signal source that is faster than the BOLD response (such as chemical or voltage potential signaling) that can provide faster temporal responses. In addition, such a realization requires significant computing hardware, software and energy sources that are portable and long lasting. The use of deep brain stimulation suggests that long lasting electrode placement in the brain may be a viable method. For Parkinsonism and dystonia, these stimulators are placed in part by recoding direct discharge potentials while the affected side limb is physically

manipulated. These stimulators are also beginning to see use in pain control applications where the placement is on the cortical surface [269,270].

This work has shown that the intention to perform a functional task can be detected and used to predict that task with very good accuracy. The robust detection of intention using regions from the whole brain will be the backbone of a whole new era in neuroprosthesis.

BIBLIOGRAPHY

1. _____, Limb loss, a grim growing global crisis, MSNBC Mar 20, 2010.

2. Kristin McHugh, "Civil Wars How the World Suffers", *Confronting Today's Global Threats Security Check, The Stanley Foundation*, pp. 2-6, May 2005.

3. _____, Maiming the people guerilla use of antipersonnel landmines and other indiscriminate weapons in Columbia, Human Rights Watch, vol. 19, no. 1B, July 2007.

4. NE Walsh and WE Walsh, "Rehabilitation of landmine victims – the ultimate challenge", Bulletin of the World Health Organization, vol. 81, pp. 665 – 670, 2003.

5. _____, Haiti Revised Humanitarian appeal, United Nations, February 2010.

6. TR. Dillingham, LE. Pezzin and EJ. MacKenzie, "Limb amputation and limb deficiency: epidemiology and recent trends in the United States", *Southern Medical Journal,* vol. 95, no. 8. pp. 875 – 883, Aug 2002.

7. K. Ziegler-Graham, EJ. MacKenzie,PL. Ephraim, TG. Travison and R Brookmeyer, "Estimating the Prevalence of Limb Loss in the United States: 2005 to 2050", *Archives of Physical Medicine Rehabilitation*, vol. 89, pp. 422 – 429, March 2008.

8. _____, Amputation statistics by Cause Limb Loss in the United States, National Limb Loss Information center, Amputee Coalition of America 2008.

9. SLH Winkler, "Upper Limb Amputation and Prosthetics Epidemiology Evidence and Outcomes", *Care of the Combat Amputee*, P. Pasquina and RA Cooper (Eds.). Textbooks of Military Medicine, Washington DC, Borden Institute, 2010.

10. _____, The Burden of Musculoskeletal Conditions at the Start of the New Millennium, World Health Organization Technical Report Series, Geneva, 2003.

11. _____, Spinal Cord Injury Facts and Figures at a Glance, National Spinal Cord Injury Statistical Center, April 2009.

12. _____, Heart Disease and Stroke Statistics 2010 Update at-A-Glance, American Heart Association, 2010.

13. _____, Ten statistical highlights in global public health, World Health Statistics, 2007.

14. Reva C. Lawrence, *et. al.*, "Estimates of the prevalence of arthritis and other rheumatic conditions in the United States: Part II", *Arthritis & Rheumatism*, vol. 58, no. 1, pp. 26-35, Jan 2008.

15. _____, Dystonia making a difference today, Society for Neuroscience, 2005.

16. _____, Dystonia Fact Sheet, Dystonia Medical Research Foundation, 2010.

17. AEH Emery, "The muscular dystrophies", *The Lancet*, vol. 359, no. 9307, pp. 687-695, Feb 2002.

18. P Romitti, *et al.*, "Prevalence of Duchenne/Becker Muscular Dystrophy among Males Aged 5–24 Years — Four States 2007", *Morbidity and Mortality Weekly Report*, vol. 58, no. 40, pp. 1119-1122, 2009.

19.William L Fodor, "Tissue engineering and cell based therapies, from the bench to the clinic: The potential to replace, repair and regenerate", *Reproductive Biology and Endocrinology*, vol. 1, no. 102, 2003.

20. JH Kim, *et al.*, "Dopamine neurons derived from embryonic stem cells function in an animal model of Parkinson's disease", *Nature*, vol. 418, pp. 50 – 56, July 2002.

21. Lars M. Bjorklund, *et al.,* "Embryonic stem cells develop into functional dopaminergic neurons after transplantation in a Parkinson rat model", *Proceedings of the National Academy of Sciences of the United States of America*, vol. 99, no. 4, pp. 2344-2349, Feb 2001.

22. E. Arenasa, "Stem cells in the treatment of Parkinson's disease", *Brain Research Bulletin*, vol. 57, no. 6, pp. 795-808, Apr 2002.

23. Y. Ogawa, *et. al.*, "Transplantation of in vitro-expanded fetal neural progenitor cells results in neurogenesis and functional recovery after spinal cord contusion injury in adult rats", *Journal of Neuroscience Research*, vol. 69, no. 6, pp. 925 – 933, 2002.

24. J. W. McDonald, *et al.*, "Transplanted embryonic stem cells survive, differentiate and promote recovery in injured rat spinal cord", *Nature Medicine*, vol. 5, pp. 1410 – 1412, 1999.

25. BJ. Cummings, *et al.*, "Human neural stem cells differentiate and promote locomotor recovery in spinal cord-injured mice", *Proceedings of the National Academy of Sciences of the United States of America, vol.* 102, no. 39, pp. 14069-14074, Sept 2005.

26. A. Iwanami, *et al.,* "Transplantation of Human Neural Stem Cells for Spinal Cord Injury in Primates", *Journal of Neuroscience Research*, vol. 80, pp. 182–190, 2005.

27. HC Park, YS Shim, Y Ha, SH Yoon, SR Park, BH Choi, HS Park, "Treatment of complete spinal cord injury patients by autologous bone marrow cell transplantation and administration of granulocyte-macrophage colony stimulating factor", *Tissue Eng*ineering. vol. 11, no. 5-6, pp. 913-922, May 2005.

28. S. Kelly, *et. al.*, "Transplanted human fetal neural stem cells survive, migrate, and differentiate in ischemic rat cerebral cortex", *Proceedings of the National Academy of Sciences of the United States of America*, vol. 101, no. 32, pp.11839-11844, Aug 2004.

29. Yasushi Takagi, *et al.,* "Survival and differentiation of neural progenitor cells derived from embryonic stem cells and transplanted into ischemic brain", *Journal of* Neurosurgery, vol. 103, no. 2, pp. 304-310, Aug 2005,

30. J Hayashi, *et al.,* "Primate embryonic stem cell-derived neuronal progenitors transplanted into ischemic brain", *Journal of Cerebral Blood Flow and Metabolism*, vol. 26, pp. 906–914, 2006.

31. R Ikeda, *et. al.*, "Transplantation of neural cells derived from retinoic acid-treated cynomolgus monkey embryonic stem cells successfully improved motor function of hemiplegic mice with experimental brain injury", *Neurobiology of Disease*, vol. 20, no. 1, pp. 38-48, Oct 2005.

32. B. C. Choa, D. H. Leeb, J. W. Parka, J. S. Byuna and B. S. Baika, " Second toe to index finger transfer", *British Journal of Plastic Surgery*, vol. 53, no. 4, pp. 324-330, June 2000.

33. M. Cascalho and JL. Platt, "Xenotransplantation and other means of organ replacement", *Nature reviews Immunology*, vol.1, no.2, pp. 154-160, Nov 2001.

34. RS Boneva, TM Folks and LE Chapman, "Infectious Disease Issues in Xenotransplantation", *Clinical Microbiology Reviews*, vol. 14, no. 1, pp. 1-14, Jan 2001.

35. LD Schultz, *et. al,* "Human Lymphoid and Myeloid Stem Cells with Mobilized Human Hemopoietic IL2R{gamma}null Mice Engrafted with Mobilized Human Hemopoietic Stem Cells", *The Journal of Immunology, vol.* 174, pp. 6477-6489, 2005.

36. K Yamada, *et al.,* "Marked prolongation of porcine renal xenograft survival in baboons through the use of alpha1,3-galactosyltransferase gene-knockout donors and the cotransplantation of vascularized thymic tissue", *Nature Medicine*, vol. 11, no.1, pp. 32 – 34, Jan 2005.

37. T. Deacon, *et al.*, "Histological evidence of fetal pig neural cell survival after transplantation into a patient with Parkinson's disease", *Nature Medicine*, vol.3, no.3, pp. 350-353, Mar 1997.

38. A. Iwanami, *et al.*, “Transplantation of human neural stem cells for spinal cord injury in primates”, *Journal of Neuroscience Research*, vol. 80, no. 2, pp. 182 – 190, Mar 2005.

39. LL. Bailey, SL. Nehlsen-Cannarella, W Concepcion, WB. Jolley, “ Baboon-to-Human Cardiac Xenotransplantation in a Neonate”, *Journal of the American Medical Association*, vol. 254, no. 23, pp. 3321-3329, 1985.

40. T Sablinski, *et. al*, “Xenotransplantation of pig kidneys to nonhuman primates: I. Development of the model”, *Xenotransplantation*, vol. 2, no. 4, Nov 2008, pp. 264 – 270.

41. T. E. Starzl, *et. al*, “Baboon-to-human liver transplantation”, *The Lancet*, vol. 341, no. 8837, jan 1993, pp. 65-71.

42. XJ Meng, *et al.,* “Genetic and Experimental Evidence for Cross-Species Infection by Swine Hepatitis E Virus”, *Journal of Virology*, vol. 72. no. 12, pp. 9714-9721, Dec. 1998.

43. MG Michaels, *et. al.”,*Detection of Infectious Baboon Cytomegalovirus after Baboonto-Human Liver Xenotransplantation”, *Journal of* Virology, vol. 75, no. 6, pp. 2825–2828, Mar. 2001.

44. LJW Van Der Laan, “Infection by porcine endogenous retrovirus after islet xenotransplantation in SCID mice”, *Letters to Nature*, vol. 407, pp. 90 – 94, June 2000.

45. A Tucker, *et. al.,* “The production of transgenic pigs for potential use in clinical xenotransplantation : microbiological evaluation”, *Xenotransplantation*, vol. 9, pp. 191-202, 2002.

46. S. Levitt, *Treatment of cerebral palsy and motor delay*, 5th ed., Malden, MA, Wiley-Blackwell, 2010

47. CE. Schmidt, VR. Shastri, JP. Vacanti and R. Langer, “Stimulation of neurite outgrowth using an electrically conducting polymer”, *Proceedings of the National Academy of Science, vol.* 94, pp. 8948–8953, Aug. 1997.

48. PO Carlsson, F Palm and G Mattsson, “Low Revascularization of Experimentally Transplanted Human Pancreatic Islets”, The *Journal of Clinical Endocrinology & Metabolism,* vol. 87, no. 12 5418-5423, 2002.

49. SC. Robson, DKC. Cooper, AJF. D'Apice, “Disordered regulation of coagulation and platelet activation in xenotransplantation”, *Xenotransplantation*, vol. 7, no. 3, pp. 166 – 176, Aug. 2000.

50. GM. Friehs, VA. Zerris, CL. Ojakangas, MR. Fellows and JP. Donoghue, “Brain–Machine and Brain–Computer Interfaces”, *Stroke,* vol. 35, pp. 2702 – 2705, 2004.

51. M.V. Radomski and C.A. Trombly, *Occupational Therapy for Physical Dysfunction*, 5th ed., Philadelphia, PA, USA: Lippincott Williams & Wilkins, 2001.

52. R. Braddom, *Handbook of Physical Medicine and Rehabilitation*, Philadelphia, PA, USA: Saunders, 2003.

53. E. Biddiss, D. Beaton and T. Chau, "Consumer design priorities for upper limb prosthetics", *Disability & Rehabilitation: Assistive Technology, vol.* 2, no. 6, pp. 346-357, 2007.

54. CD. Murray, "The Social Meanings of Prosthesis Use", *Journal of Health Psychology*, vol. 10, no. 3, pp. 425 – 441, May 2005.

55. A. Saradjian, AR. Thompson, and D. Datta, "The experience of men using an upper limb prosthesis following amputation: Positive coping and minimizing feeling different", vol. 30, no. 11, pp. 871-883, 2008.

56. A. Roby-Brami, A. Feydy, M. Combeaud, E.V. Biryukova, B. Bussel and M.F. Levin, "Motor compensation and recovery for reaching in stroke patients", *Acta Neurologica Scandinavica,* vol.107, no. 5, pp. 369-81, May 2003.

57. S. Messier, D. Bourbonnais, J. Desrosiers and Y. Roy, "Weight-bearing on the lower limbs in a sitting position during bilateral movement of the upper limbs in post-stroke hemiparetic subjects." *Journal of Rehabilitation Medicine, vol.* 37, pp. 242-246, 2005.

58. H.I. Krebs, B.T. volpe, M. Ferraro, S. Fasoli, J. Palazzolo,B. Rohrer, L. Edelstein and N. Hogan, " Robot-aided neurorehabilitation: from evidence-based to science based rehabilitation". *Topics in Stroke Rehabilitation.* vol. 8, no. 4, pp. 54-70, 2002.

59. C.D. Takahashi, L. Der-Yeghiaian, V.H. Le and S.C. Cramer, "A Robotic Device for Hand Motor Therapy After Stroke", *Conf proc 9th IEEE-ICORR*, Chicago, Illinois, USA, pp. 17-20, 2005.

60. T.G. Sugar, *et. al*, "Design and Control of RUPERT: A Device for Robotic Upper Extremity Repetitive Therapy", *IEEE Trans Neural Systems Rehab Eng*, vol. 15, no. 3, pp. 336-346, Sept. 2007.

61. P.S. Lum, C.G. Burgar and P.C. Shor, "Evidence for improved muscle activation patterns after retraining of reaching movements with the MIME robotic system in subjects with post-stroke hemiparesis", *IEEE Transactiosn in Neural Systems and Rehabilitation Engineering, vol.* 12, no.2, 2004, pp. 186 – 194.

62. DE Nathan, MJ Johnson and JR McGuire, "Design and validation of low-cost assistive glove for hand assessment and therapy during activity of daily living-focused robotic stroke therapy.", *Journal of Rehabilitation Research and Design,* vol. 46, no.5, pp. 587 - 602, Nov 2009.

63. DE Nathan, SG Guastello, DC Jeutter, J McGuire and MJ Johnson, "Development of a FES sensorized glove and modeling of human reaching and grasping for task-oriented, robotic assisted therapy", Master's Thesis, Marquette University Press, 2008.

64. G. Kwakkel, B.J. Kollen, and R.C. Wagenaar, "Therapy impact on functional recovery in stroke rehabilitation: a critical review of the literature", *Physiotherapy*, vol. 85, pp. 337 – 391, 2000.

65. A. Sunderland, D. Fletcher, L. Bradley, D. Tinson, R.L. Hewer and D.T.J. Wade, "Enhanced physical therapy for arm function after stroke: a one year follow up study", *Neurol Neurosurg Psychiatry,* vol. 57, no. 7, pp. 856-858, Jul. 1994.

66. E. Ernst, "A review of stroke rehabilitation and physiotherapy", *Stroke,* vol. 21, pp. 1081-1085, 1990.

67. KW. Horsch and GS Dhillon, *Neuroprosthetics Theory and Practise*, Singapore, Singapore, World Scientific Publishing Co.,2004.

68. JK. Chapin an KA Moxon, *Neural Prostheses for Restoration of Sensory and Motor Function*, Boca Raton, FL, USA, CRC Press, 2001.

69. WE. Finn and PG LoPresti, *Handbook of Neuroprosthetic Methods*, Boca Raton, FL, USA, CRC Press, 2003.

70. MA. Lebedev and MAL. Nicolelis, "Brain–machine interfaces: past, present and future", *Trends in Neurosciences*, vol. 29, no. 9, pp. 536-546, Sep. 2006.

71. SH. Scott, "Converting thoughts into action", *Nature Neuroscience*, vol. 442, pp. 141 – 142, Jul. 2006.

72. W. Craelius, "The Bionic Man: Restoring Mobility", *Nature*, vol. 442, pp. 141-142, Jul. 2006.

73. Alison Abbott, "In search of the sixth sense", *Nature, vol.* 442, pp. 125-127, Jul 2006.

74. ER. Kandel, J.H. Schwartz and T.M. Jessell, *Principles of Neural Science*, 4th ed., New York, NY, USA, McGraw-Hill, Jan. 2000.

75. LR. Squire, D Berg, F Bloom, S du Lac, *et al., Fundamental Neuroscience*, 3rd ed., Burlington, MA, USA, Academic Press, 2008.

76. DR. Humphrey, EM. Schmidt, WD Thompson, "Predicting measures of motor performance from multiple cortical spike trains", *Science*, vol. 170, no. 959, pp. 758-762, Nov. 1970.

77. EM. Schmidt, "Single neuron recording from motor cortex as a possible source of signals for control of external devices", *Annals of Biomedical Engineering*, vol. 8, no. 4-6, pp. 339-349, 1980

78. RB. Muir and RN. Lemon, "Corticospinal neurons with a special role in precision grip", *Brain Research*, vol. 261, no. 2, pp. 312 – 316, Feb. 1983.

79. M. Gentilucci, *et al.*, "Functional organization of inferior area 6 in the macaque monkey", *Experimental Brain Research*, vol. 71, no. 3, pp. 475-490, 1988.

80. JK. Chapin, KA. Moxon, RS. Markowitz and MAL. Nicolelis, "Real-time control of a robot arm using simultaneously recorded neurons in the motor cortex", *Nature Neuroscience*, vol. 2, no. 7, pp. 664 – 670, 1999.

81. M. Velliste, S. Perel, MC. Spalding, AS. Whitford and AB. Schwartz, "Cortical control of a prosthetic arm for self-feeding", *Nature*, vol. 453, pp. 1098-1101, Jun. 2008.

82. G. Santhanam, *et al.*, "HermesB: A Continuous Neural Recording System for Freely Behaving Primates", *IEEE Transactions On Biomedical Engineering*, vol. 54, no. 11, pp. 2037 – 2050, Nov. 2007.

83. J Wessberg, *et. al.*, "Real-time prediction of hand trajectory by Ensembles of cortical neurons in primates", *Nature*, vol. 408, pp. 361 – 365, 16th Nov. 2000.

84. JP. Donoghue, JN. Sanes, NG. Hatsopoulos and G. Gaál, "Neural Discharge and Local Field Potential Oscillations in Primate Motor Cortex During voluntary Movements", *The Journal of Neurophysiology*, vol. 79, no. 1, pp. 159-173, Jan. 1998.

85. PR. Kennedy, RAE, Bakay, MM. Moore, K. Adams, and J. Goldwaithe, "Direct control of a computer from the human central nervous system", *IEEE Transactions on Rehabilitation Engineering*, vol. 8, no. 2, pp. 198 – 202, Jun. 2000.

86. T Keller, A Curt, Mr. Popovic, V Dietz And A Signer, "Grasping In High Lesioned Tetraplegic Subjects Using The EMG Controlled Neuroprosthesis*", Journal of NeuroRehabilitation*, vol. 10, pp. 251-255, 1998.

87. PR. Kennedy,MT Kirby, MM. Moore, BKing, and A Mallory, "Computer Control Using Human Intracortical Local Field Potentials", *IEEE Transactions On Neural Systems And Rehabilitation Engineering*, vol. 12, no. 3, pp. 339 – 345, Sep. 2004.

88. GS Dhillon and KW. Horch, "Direct Neural Sensory Feedback and Control of a Prosthetic Arm*", IEEE Transactions On Neural Systems And Rehabilitation Engineering*, vol. 13, no. 4, pp. 468 – 473, Dec. 2005.

89. KL. Kilgore, HA. Hoyen, AM. Bryden, RL. Hart, MW. Keith, and PH Peckham, "An Implanted Upper-Extremity Neuroprosthesis Using Myoelectric Control", *Conf Proc 2nd*

International IEEE EMBS Conference on Neural Engineering, Arlington, VA, USA, pp. 368 – 371, Mar. 2005.

90. LR. Hochberg, *et al.*, "Neuronal ensemble control of prosthetic devices by a human with tetraplegia", *Nature,* vol. 442, pp. 164 – 172, Jul. 2006.

91. JG. Webster, *Medical Instrumentation: Application and Design*, 3rd ed, New York, NY, USA, Wiley, 1997.

92. JD. Bronzino, *The Biomedical Engineering Handbook*, 3rd ed. New York, NY, USA, CRC Press, 2006.

93. A Kostov and M Polak, "Parallel Man–Machine Training in Development of EEG-Based Cursor Control", *IEEE Transactions On Rehabilitation Engineering*, vol. 8, no. 2, pp. 203 – 205, Jun 2000.

94. RT. Lauer, PH. Peckham and KL. Kilgore, "EEG-based control of a hand grasp neuroprosthesis", *NeuroReport*, vol. 10, pp. 1767-1771, 1999.

95. J del R. Millan, F Renkens, J Mouriño and W Gerstner, "Noninvasive Brain-Actuated Control of a Mobile Robot by Human EEG", *IEEE Transactions in Biomedical Engineering*, vol. 51, no. 6, pp. 1026 – 1033, 2004.

96. G Pfurtscheller, GR. Muller-Putz, J Pfurtscheller, and R Rupp, "EEG-Based Asynchronous BCI Controls Functional Electrical Stimulation in a Tetraplegic Patient", *EURASIP Journal on Applied Signal Processing*, vol. 19, pp. 3152–3155, 2005.

97. A. Chatterjee, V. Aggarwal, A. Ramos, S. Acharya1 and NV Thakor, "A brain-computer interface with vibrotactile biofeedback for haptic information", *Journal of NeuroEngineering and Rehabilitation*, vol. 4, no. 40, 2007.

98. DJ McFarland,WA Sarnacki and JR Wolpaw, "Electroencephalographic (EEG) control of three-dimensional movement", *Journal of Neural Engineering*, vol. 7, 2010.

99. JM. Heasman, TRD. Scott, L. Kirkup, RY. Flynn, VA. Vare, and C.R. Gschwind, "Control of a hand grasp neuroprosthesis using an electroencephalog ram-triggered switch: demonstration of improvements in performance using wavepacket analysis", *Medical and Biological Engineering and Computing*, vol. 40, pp. 588-593, 2002.

100. B Blankertz, G Dornhege, S Lemm, M Krauledat, G Curio and KR Müller, "The Berlin Brain-Computer Interface: Machine Learning Based Detection of User Specific Brain States", *Journal of Universal Computer Science*, vol. 12, no. 6, pp. 581-607, 2006.

101. MR. Popovic, TA Thrasher, V Zivanovic, J Takaki and V Hajek, "Neuroprosthesis for Retraining Reaching and Grasping Functions in Severe Hemiplegic Patients", *Neuromodulation: Technology at the Neural Interface*, vol. 8, no. 1, pp. 58–72, Jan 2005.

102. J Chae and R Hart, “Intramuscular Hand Neuroprosthesis for Chronic Stroke Survivors”, *Journal of Neurorehabilitation and Neural Repair*, vol. 17, pp. 109-117, 2003.

103. H Ring And N Rosenthal, “Controlled Study Of Neuroprosthetic Functional Electrical Stimulation In Sub-Acute Post-Stroke Rehabilitation”, *Journal of Rehabilitation Medicine*, vol. 37, pp.32–36, 2005.

104. RF *ff* Weir, PR Troyk, G DeMichele, T Kuiken, “Implantable Myoelectric Sensors (IMES) for Upper-E:xtremity Prosthesis Control - Preliminary Work”, *Conf Proc 25th Annual IEEE EMBS,* Cancun, Mexico, pp. 1562 – 1565, Sept. 2003.

105. TA. Kuiken, LA. Miller, RD. Lipschutz, KA. Stubblefield and GA. Dumanian, “Prosthetic Command Signals Following Targeted Hyper-Reinnervation Nerve Transfer Surgery”, *Conf Proc 27th Annual IEEE EMBS,* Shanghai, China, pp. 7652 – 7655, 2005.

106. LA. Miller, *et al.*, “Control of a six degree of freedom prosthetic arm after targeted muscle reinnervation surgery”, *Archives of Physical Medicine and Rehabilitation*, vol. 89, no. 11, pp. 2057-2065, Nov. 2008.

107. F. Popescu, B. Blankertz and KR. Müller, “Computational Challenges for Noninvasive Brain Computer Interfaces”, *IEEE Intelligent Systems*, vol. 23, no. 3, pp. 78-79, 2008.

108. R. Triolo, *et al.,* “Challenges to clinical deployment of upper limb neuroprostheses”, *Journal of Rehabilitation Research and Development*, vol. 33, no. 2, pp. 111-122, Apr. 1996.

109. E. Todorov, “Optimality principles in sensorimotor control”, *Nature Neuroscience*, vol.7, pp. 907 – 915, Aug. 2004.

110. CD. Takahashi, RA. Scheidt, and DJ. Reinkensmeyer, “Impedance Control and Internal Model Formation When Reaching in a Randomly Varying Dynamical Environment”, *Journal of* Neurophysiology, vol. 86, pp. 1047-1051, 2001.

111. JL Summers, *Approaches to the study of motor control and learning*, New York, NY, USA, Elsevier, 1992.

112. RA. Schmidt and TD Lee, *Motor control and learning a behavioral emphasis,* 4th ed., Champaign, IL, USA, Human Kinetics, 2005.

113. NR. Carlson, *Physiology of Behavior*, 8th Ed., Boston,MA, USA, Allyn and Bacon, 2004.

114. RA Magill, *Motor learning and control concepts and applications*, 8th ed., New York, NY, USA, McGraw-Hill, 2007.

115. W. Shain, *et al.,* "Controlling cellular reactive responses around neural prosthetic devices using peripheral and local intervention strategies", *IEEE Transactions in Neural Systems and Rehabilitation Engineering*, vol. 11, no. 11, pp. 186-188, Jun. 2003.

116. R.W. Griffith and D.R. Humphrey, "Long-term gliosis around chronically implanted platinum electrodes in the Rhesus macaque motor cortex", *Neuroscience Letters*, vol. 406, pp.81-86, Oct. 2006.

117. VS. Polikova, PA. Trescob and WM. Reicherta, "Response of brain tissue to chronically implanted neural electrodes", *Journal of Neuroscience Methods*, vol. 148, no. 1, pp. 1 – 18, Oct. 2005, pp.1-18.

118. Y. Attal, *et al.*, "Modeling and detecting deep brain activity with MEG and EEG", *Conf Proc 29th IEEE EMBS,* Lyon, France, pp. 4937 – 4941, Aug. 2007.

119. I.A. Cook, R. O'Hara, SH. J. Uijtdehaage, M Mandelkern, and AF. Leuchter, "Assessing the accuracy of topographic EEG mapping for determining local brain function", *Electroencephalography and Clinical Neurophysiology, vol.* 107, no. 6, Dec. 1998, pp. 408 – 414.

120. AM. Dale and MI. Sereno, "Improved Localization of Cortical Activity by Combining EEG and MEG with MRI Cortical Surface Reconstruction: A Linear Approach", *Journal of Cognitive Neuroscience, vol.*5 no. 2, 1993, pp. 162 – 176.

121. MT. Turvey, "Coordination", *American Psychologist*, vol. 45, pp. 938-953, Aug. 1990.

122. IT Jolliffe, *Principal Component Analysis*, 2nd Ed, New York, New York, USA, Springer-Verlag, 2002.

123. R. Viviani, G. Gron, and M. Spitzer, "Functional Principal Component Analysis of fMRI Data", *Human Brain Mapping*, vol. 24, pp. 109 –129, 2005.

124. TW. Boonstra, A. Daffertshofera, CE. Pepera and PJ. Beeka, "Amplitude and phase dynamics associated with acoustically paced finger tapping", *Brain Research*, vol. 1109, no. 1, pp. 60 – 69, Sep. 2006.

125. KJ. Friston CD. Frith, PF. Liddle and RSJ. Frackowiak, "Functional connectivity: The Principal-Component Analysis of Large (PET) Data Sets", *Journal of Cerebral Blood Flow and Metabolism*, vol. 13, pp. 5 – 14, 1993.

126. Y. Zhong, *et al.*, "Detecting Functional Connectivity in fMRI Using PCA and Regression Analysis", *Brain Topography*, vol. 22, pp. 134 – 144, 2009.

127. SH. Laia and M. Fanga, "A novel local PCA-Based method for detecting activation signals in fMRI", *Magnetic Resonance Imaging*, vol. 17, no. 6, pp. 827 – 836, Jul. 1999.

128. JJ. Baker, *et al.,* "Decoding Individuated Finger Flexions with Implantable MyoElectric Sensors", *Conf Proc. 30th IEEE EMBS Conference*, Vancouver, British Columbia, Canada, pp. 193 – 196, Aug. 2008.

129. L. Hargrove, E. Scheme, K. Englehart, and B. Hudgins, "Principal Components Analysis Preprocessing to Reduce Controller Delays in Pattern Recognition Based Myoelectric Control", *Conf Proc 29th IEEE EMBS*, Cité Internationale, Lyon, France, pp. 6511 – 6514, Aug. 2007.

130. A. Hyvärinen, J. Karhunen, E. Oja, *Independent Component Analysis*, New York, New York, USA, John Wiley and Sons, 2001.

131. CF. Beckmann and SM. Smith, "Probabilistic Independent Component Analysis for Functional Magnetic Resonance Imaging", *IEEE Transactions on Medical* Imaging, vol. 23, no.2, pp. 137-152, Feb. 2004.

132. CH. Moritz, VM. Haughton, D. Cordes, M Quigley, and ME. Meyerand, "Wholebrain functional MR imaging activation from a finger-tapping task examined with independent component analysis", *American Journal of Neuroradiology*, vol. 21, pp. 1629 – 1635, 2000.

133. MG. Wentrup, K. Gramanny, E. Wascherz and M. Bussx, "EEG Source Localization for Brain-Computer-Interfaces", *Conf Proc 2nd IEEE-EBMS conference on Neural Engineering*, Arlington, Virginia, USA, pp. 128 – 131, Mar. 2005.

134. D. Popivanova, S. Jivkovaa, V. Stomonyakova and G. Nicolovaa, " Effect of independent component analysis on multifractality of EEG during visual-motor task", *Signal Processing*, vol. 85, no. 11, pp. 2112 – 2123, Nov. 2005.

135. K. Arfanakis, D. Cordesa, VM. Haughtonb, CH. Moritzb, MA. Quigleya and ME. Meyeranda, "Combining independent component analysis and correlation analysis to probe interregional connectivity in fMRI task activation datasets", *Magnetic Resonance Imaging*, vol. 18, no. 8, pp. 921 – 930, Oct. 2000.

136. L. Ma, B. Wang, X. Chena and J. Xiong, "Detecting functional connectivity in the resting brain: a comparison between ICA and CCA", *Magnetic Resonance Imaging*, vol. 25, pp. 47-56, 2007.

137. F. Esposito, "Independent component analysis of fMRI group studies by self-organizing clustering", *NeuroImage*, vol. 25, pp. 193 – 205, 2005.

138. JF Hair, B Black, B Babin, RE Anderson, and RL Tatham, *Multivariate Data Analysis*, 6th Ed., Upper Saddle River, New Jersey, USA, 2006.

139. A. Baune, *et al.,* "Dynamical Cluster Analysis of Cortical fMRI Activation", *NeuroImage*, vol. 9, no. 5, pp. 477 – 489, May 1999.

140. L. Shi, PA. Heng, and TT. Wong, "A Spectral Clustering Approach to fMRI Activation Detection", *Conf Proc 27th Annual IEEE EMBS*, Shanghai, China, pp. 5892 – 5895, Apr. 2006.

141. M. Singh, P. Patel, D. Khosla and T. Kim, "Segmentation of Functional MRI by K-Means Clustering", *IEEE Transactions on Nuclear Science*, vol. 43, no. 3, pp. 2030 – 2036, Jun 1996.

142. C. Goutte and L. Kai, "Feature-space clustering for fMRI meta-analysis", *Human Brain Mapping*, vol. 13, no. 3, pp. 165 – 183, Jul. 2001.

143. H. Jahanian, GA. Hossein-Zadeh, H. Soltanian-Zadeh, BA. Ardekani, "Controlling the false positive rate in fuzzy clustering using randomization: application to fMRI activation detection", *Magnetic Resonance Imaging*, vol. 22, pp. 631–638, 2004.

144. SH. Yee and JH. Gao, "Improved detection of time windows of brain responses in fMRI using modified temporal clustering analysis", *Magnetic Resonance Imaging*, vol. 20, pp. 17 – 26, 2002.

145. C. Neuper, R. Scherer, M. Reiner and G. Pfurtscheller, " Imagery of motor actions: Differential effects of kinesthetic and visual–motor mode of imagery in single-trial EEG", *Cognitive Brain Research, vol.* 25, pp. 668 – 677, 2005.

146. N. Ye, A. Roontiva and J. He, "A Cluster Analysis of Neuronal Activity in the Dorsal Premotor Cortical Area for Neuroprosthetic Control", *Conf Proc 30th Annual IEEE EMBS,* Vancouver, British Columbia, Canada, pp. 2638 – 2641, Aug. 2008.

147. Eric A. Pohlmeyer*, et al.,* "Use of Intracortical Recordings to Control a Hand Neuroprosthesis", *Conf Proc 3rd International IEEE – EBMS Neural Engineering*, Kohala Coast, Hawaii, USA, pp. 418 – 420, May 2007.

148. CT. Moritz, TH. Lucas, SI. Perlmutter and EE. Fetz, "Forelimb Movements and Muscle Responses Evoked by Microstimulation of Cervical Spinal Cord in Sedated Monkeys", *Journal of Neurophysiology*, vol. 97, pp. 110–120, 2007.

149. JAS. Kelso, *Dynamic Patterns The Self-Organization of Brain and Behavior*, MIT Press, Cambridge, MA, USA, 1995.

150. D. Gallez and A. Babloyantz, "Predictability of human EEG: a dynamical approach", *Biological Cybernetics*, vol. 64, pp. 381 – 391, 1991.

151. KJ. Friston, L. Harrison and W. Penny, "Dynamics Causal Modelling", *Neuroimage*, vol. 19, pp. 1273 – 1302, 2003.

152. Dong Song, et al.",Nonlinear Dynamic Modeling of Spike Train Transformations

for Hippocampal-Cortical Prostheses", *IEEE Transactions on Biomedical Engineering, vol.* 54, no. 6, Jun. 2007.

153. O. Sporns and G. Tononi, "Classes of Network Connectivity and Dynamics", *Complexity*, vol. 7, no. 1, 2001.

154. O Sporns, DR. Chialvo, M Kaiser and CC. Hilgetag, "Organization, development and function of complex brain networks", *Trends in Cognitive Sciences*, vol. 8, no. 9, Sept. 2004, pp. 418 – 426.

155. O Sporns, R Kotter, " Motifs in Brain Networks", *Public Library of Science Biology*, vol. 2, no. 11, Nov. 2004, pp. 369-378.

156. O Sporns, G. Tononi and Gm Edelman, "Theoretical Neuroanatomy: Relating Anatomical and Functional Connectivity in Graphs and Cortical Connection Matrices", *Cerebral Cortex*, vol. 10, Feb. 2000, pp. 127 – 141.

157. JW. Scannell, GAPC. Burns, CC. Hilgetag, MA. O'Neil and MP. Young, "The Connectional Organization of the Cortico-thalamic System of the Cat", *Cerebral Cortex*, vol. 9, no. 3, pp. 277 – 299, 1999.

158. DJ. Felleman and DC van Essen, "Distributed hierarchical processing in the primate cerebral cortex", *Cerebral Cortex*, vol. 1, pp. 1–47, 1991.

159. L. Astolfi, *et al.,* "Imaging functional brain connectivity patterns from high-resolution EEG and fMRI via graph theory", *Psychophysiology*, vol. 44, no. 6, pp. 880–893, Nov. 2007.

160. E. Bullmore and O. Sporns, "Complex brain networks: graph theoretical analysis of structural and functional systems", *Nature Reviews Neuroscience*, vol.10, pp. 186-198, Mar. 2009.

161. FDV. Fallani, "Extracting Information from Cortical Connectivity Patterns Estimated from High Resolution EEG Recordings: A Theoretical Graph Approach", *Brain Topography*, vol. 19, pp. 125 – 136, 2007.

162. D. Garrett, DA. Peterson, CW. Anderson, and MH. Thaut, "Comparison of Linear, Nonlinear, and Feature Selection Methods for EEG Signal Classification", *IEEE Transactions on Neural Systems and Rehabilitation* Engineering, vol. 11, no. 2, Jun. 2003.

163. MJ. McKeown, *et al*., "Local Linear Discriminant Analysis (LLDA) for group and region of interest (ROI)-based fMRI analysis", *NeuroImage*, vol. 37, no. 3, pp. 855 – 865, Sep. 2007.

164. JW. Sensinger, BA. Lock and TA. Kuiken, “Adaptive Pattern Recognition of Myoelectric Signals:Exploration of Conceptual Framework and Practical Algorithms”, *IEEE Transactions on Neural Systems and Rehabilitation Engineering, vol.* 17, no.3, Jun. 2009.

165. G. Li, and TA Kuiken, “EMG Pattern Recognition Control of Multifunctional Prostheses by Transradial Amputees”, *Conf Proc IEEE EMBS*, Minneapolis, MN, USA, pp. 6914 – 1917, Sep. 2009.

166. H. Motulsky and A. Christopoulos, *Fitting Models to Biological Data Using Linear and Nonlinear Regression a Practical Guide to Curve Fitting*, New York, NY, USA, Oxford University Press, 2004.

167. C. Büchel, AP. Holmes, GRees and KJ. Friston, “Characterizing Stimulus–Response Functions Using Nonlinear Regressors in Parametric fMRI Experiments”, *NeuroImage*, vol. 8, no. 2, pp. 140 – 148, Aug. 1998.

168. O. Hauk, MH. Davis, M. Ford, F. Pulvermüller and WD. Marslen-Wilson, “The time course of visual word recognition as revealed by linear regression analysis of ERP data”, *NeuroImage*, vol. 30, no. 4, pp. 1383 – 1400, May 2006.

169. Eduardo M. Castillo, *et al.,* “Integrating sensory and motor mapping in a comprehensive MEG protocol: Clinical validity and replicability”, *NeuroImage*, vol. 21, no. 3, pp. 973 – 983, Mar. 2004.

170. L. Jäncke, *et. al.,* “A parametric analysis of the ‘rate effect' in the sensorimotor cortex: a functional magnetic resonance imaging analysis in human subjects”, *Neuroscience Letters*, vol. 252, no.1, pp. 37 – 40, Jul. 1998.

171. MD. Serruya, NG. Hatsopoulos, L. Paninski, MR. Fellows and JP Donoghue, “Brain-machine interface: Instant neural control of a movement signal”, *Brief Communications Nature*, vol. 416, pp. 141-142, Mar. 2002.

172. GS. Dhillon and KW. Horch, “Direct Neural Sensory Feedback and Control of a Prosthetic Arm”, *IEEE Transactions on Neural Systems and Rehabilitation* Engineering, vol. 13, no. 4, pp. 468 – 472, Dec. 2005.

173. H. Halide and P. Ridd, “Complicated ENSO models do not significantly outperform very simple ENSO models”, *International Journal of Climatology,* vol. 28, no. 2, pp. 219-233, 2007.

174. CTW Moonen and PA Bandettini, *Functional MRI,* Berlin, Germany, Springer-Verlag, 2000.

175. SA. Huettel, AW. Song and G. McCarthy, *Functional Magnetic Resonance Imaging,* Sunderland, MA, USA, Sinauer Associates, 2004.

176. SS Yoo, “Brain-computer interface using fMRI: spatial navigation by thoughts”, *Neuroreport, vol.* 15, no. 10, pp. 1591-1595, Jul. 2004.

177. N. Weiskopf, K. Mathiak, SW. Bock and F. Scharnows, “Principles of a Brain-Computer Interface (BCI) Based on Real-Time Functional Magnetic Resonance Imaging (fMRI)”, *IEEE Transactions on Biomedical* Engineering, vol. 51, no. 6, pp. 966-970, Jun. 2004.

178. S. Ogawa, TM. Lee, AR. Kay and DW. Tank, “Brain magnetic resonance imaging with contrast dependent on blood oxygenation”, *Proceedings of the National Academy of Sciences of the United States of* America, vol. 87, pp. 9868-9872, Dec. 1990.

179. PA. Bandettini, EC. Wong, RS Hinks, RS. Tikofsky, JS. Hyde, “Time course EPI of human brain function during task activation”, *Magnetic Resonance in Medicine*, vol. 25, no. 2, pp. 390 – 397, Jun. 1992.

180. KK. Kwong, *et al.*, “Dynamic magnetic resonance imaging of human brain activity during primary sensory stimulation”, *Proceedings of the National Academy of Sciences of the United States of America, vol.* 89, no. 12, pp. 5675-5679, Jun. 1992.

181. GM. Shepherd, *The Synaptic Organization of the Brain*, 5th ed., New York, NY, USA, Oxford University Press, Nov. 2003.

182. D. Purves, *et al., Neuroscience*, 3rd ed., Sunderland, MA, USA, Sinauer Associates, Jun 2004.

183. RS. Snell, *Clinical Neuroanatomy*, 7th ed. Baltimore MD,USA, Lippincott, Williams and Wilkins, 2010.

184. A Gail and RA. Andersen, “Neural Dynamics in Monkey Parietal Reach Region Reflect Context-Specific Sensorimotor Transformations”, *Journal of Neuroscience*, vol. 26, no. 37, pp. 9376 – 9384, Sep. 2006.

185. AP. Batista and RA. Andersen, “The Parietal Reach Region Codes the Next Planned Movement in a Sequential Reach Task”, *Journal of Neurophysiology, vol.* 85, pp. 539-544, 2001.

186. EA. Zillmer, MV. SPiers and WC. Culbertson, *Principles of Neuropsychology,* 2nd ed., Belmont, CA,USA, Thompson Wadsworth Publishing, 2008.

187. JD. Connolly, RA. Andersen, and MA. Goodale, “FMRI evidence for a parietal reach region in the human brain”, *Experimental Brain* Research, vol. 153, pp. 140 – 145, 2003.

188. MA. Mayka, DM. Corcos, SE. Leurgans and DE. Vaillancourt, “Three-dimensional

locations and boundaries of motor and premotor cortices as defined by functional brain imaging: A meta-analysis", *NeuroImage*, vol. 31, no. 4, pp. 1453 – 1474, Jul. 2006.

189. N. Picard and PL Strick, "Imaging the premotor areas", *Current Opinion in Neurobiology*, vol. 11, no. 6, pp. 663 – 672, Dec. 2001.

190. S. Schaal, D. Sternad, R. Osu and M. Kawato, "Rhythmic arm movement is not discrete", *Nature Neuroscience*, vol. 7, pp. 1136 – 1143, 2004.

191. C. Wu, C.A. Trombly, K. Lin and L. Tickle-Degnen L, "Effects of object affordances on reaching performance in persons with and without cerebrovascular accident", *American Journal of Occupational Therapy, vol.* 52, no. 6, pp. 447 – 456, 1998.

192. C. Wu, C.A. Trombly, K. Lin and L. Tickle-Degnen, "A kinematic study of contextual effects on reaching performance in persons with and without stroke: Influences of object availability", *Archives of Physical Medicine and REhabilitation*, vol. 81, no. 1, pp. 95-101, 2000.

193. SE Fasoli, CA Trombly, L. Tickle-Degnen and M. Verfaellie, "Context and goal-directed movement: the effect of materials-based occupation", *Occupation Participation and Health*, vol. 22, no. 3, pp. 119 – 128, 2002.

194. S.H. Jang, Y.H. Kim, S.H. Cho, J.H. Lee, J.W. Park and Y.H. Kwon, "Cortical reorganization induced by task-oriented training in chronic hemiplegic stroke patients", *Neuroreport*, vol. 14, pp. 131-141, 2003.

195. N.A. Bayona, J. Bitensky, K. Salter, and R. Teasell, "The role of taskspecific training in rehabilitation therapies." *Topics in Stroke Rehabilitation*, vol. 12, pp. 58 – 65, 2005.

196. G.T. Thielman, C.M. Dean and A.M. Gentile, "Rehabilitation of reaching after stroke: task-related training versus progressive resistive exercise", *Archives of Physical Medicine and Rehabilitation*, vol. 85, no. 10, pp. 1613-1618, Oct. 2004.

197 A. Sunderland, D.J. Tinson, E.L. Bradley, D. Fletcher, H.R. Langton and D.T. Wade, "Enhanced physical therapy improves recovery of arm function after stroke. A randomised clinical trial." *Journal of Neurology, Neurosurgery and Psychiatry*, vol. 55, no.7, pp. 530 – 535, 1992.

198. Mitsuo Kawatoa, "Internal models for motor control and trajectory planning", *Current Opinion in Neurobiology*, vol. 9, no. 6, pp. 718 – 727, Dec. 1999.

199. DM. Wolpert and M. Kawato, "Multiple paired forward and inverse models for motor control", *Neural Networks*, vol. 11, no. 7-8, pp. 1317 – 1329, Oct. 1998.

200. JR. Flanagan and AM. Wing, "The Role of Internal Models in Motion Planning and Control: Evidence from Grip Force Adjustments during Movements of Hand-Held Loads", *Journal of Neuroscience*, vol. 17, no. 4, pp. 1519 – 1528, Feb. 1997.

201. JW. Krakauer, MF. Ghilardi and C. Ghez, "Independent learning of internal models for kinematic and dynamic control of reaching", *Nature Neuroscience*, vol. 2, pp. 1026 -1031, 1999.

202. RE. Suri, "Anticipatory responses of dopamine neurons and cortical neurons reproduced by internal model", *Experimental Brain Research, vol.* 140, pp. 234 – 240, 2001.

203. RL. Sainburg, MF. Ghilardi, H. Poizner and C. Ghez, "Control of Limb Dynamics in Normal Subjects and Patients Without Proprioception", *Journal of Neurophysiology*, vol. 73, no.2, pp. 820 – 835, Feb. 1995.

204. KP. Kording and DM. Wolpert, "Bayesian decision theory in sensorimotor control", *Trends in Cognitive* Sciences, vol. 10, no.7, Jul. 2006.

205. C. Tong, DM. Wolpert and JR. Flanagan, "Kinematics and Dynamics Are Not Represented Independently in Motor Working Memory: Evidence from an Interference Study", *Journal of Neuroscience*, vol. 22, no. 3, pp. 1108 – 1113, Feb. 2002.

206. MA. Conditt, F. Gandolfo and FA. Mussa-Ivaldi, "The Motor System Does Not Learn the Dynamics of the Arm by Rote Memorization of Past Experience", *Journal of Neurophysiology*, vol. 78, no. 1, pp. 554 – 560, Jul. 1997.

207. E. Guigon, P. Baraduc and M. Desmurget, "Computational Motor Control: Redundancy and Invariance", *Journal of Neurophysiology*, vol. 97, pp. 331-347, 2007.

208. R. Grush, "The emulation theory of representation: Motor control, imagery, and perception", *Behavioral and Brain Sciences*, vol. 27, pp. 377 – 442, 2004.

209. R. Shadmehr and T. Brashers-Krug, "Functional Stages in the Formation of Human Long-Term Motor Memory", *Journal of Neuroscience*, vol. 17, no. 1, pp. 409 – 419, Jan 1997.

210. R Grush, "Internal models and the construction of time: generalizing from state estimation to trajectory estimation to address temporal features of perception, including temporal illusions", *Journal of Neural Engineering,* vol. 2, pp. 209 – 218, 2005.

211. PL. Gribble, DJ. Ostry, V. Sanguineti and R. Laboissière, "Are Complex Control Signals Required for Human Arm Movement?", *Journal of Neurophysiology*, vol. 79, no. 3, pp. 1409 – 1424, Mar. 1998.

212. DM. Wolpert, RC. Miall and M. Kawato, “Internal models in the cerebellum”, *Trends in Cognitive Sciences*, vol. 2, no. 9, pp. 338 – 347, Sep. 1998.

213. A. Sirigu, *et al.*, “Altered awareness of voluntary action after damage to the parietal cortex”, *Nature Neuroscience*, vol. 7, pp. 80 – 84, Nov. 2003.

214. M. Lotze, *et al.,* “Activation of Cortical and Cerebellar Motor Areas during Executed and Imagined Hand Movements: An fMRI Study”, *Journal* of *Cognitive Neuroscience*, vol. 11, no. 5, pp. 491 – 501, Sep. 1999.

215. M. Jeanneroda, “The representing brain: Neural correlates of motor intention and imagery”, *Behavioral and Brain Sciences*, vol. 17, pp. 187 – 202, 1994.

216. JB. Rowe, AM. Owen, IS. Johnsrude and RE. Passingham, “Imaging the mental components of a planning task”, *Neuropsychologia*, vol. 39, no. 3, pp. 315 – 327, 2001.

217. J. Annetta, “Motor imagery: Perception or action?”, *Neuropsychologia*, vol. 33, no. 11, pp. 1395 – 1417, Nov. 1995.

218. M. Jeannerod and V. Frak, “Mental imaging of motor activity in humans”, *Current Opinion in Neurobiology*, vol. 9, no. 6, pp. 735 – 739, Dec. 1999.

219. P. Dechent, KD. Merboldt and J. Frahm, “Is the human primary motor cortex involved in motor imagery?”, *Cognitive Brain Research*, vol. 19, no. 2, pp. 138 – 144, Apr. 2004.

220. M. Leonardo, et al., "A Functional Magnetic Resonance Imaging Study of Cortical Regions Associated with Motor Task Execution and Motor Ideation in Humans", *Human Brain Mapping*, vol. 3, pp. 83 - 92, 1995.

221. MG. Lacourse, EL. Orr, SC. Cramer and MJ. Cohen, “Brain activation during execution and motor imagery of novel and skilled sequential hand movements”, *Neuroimage*, vol. 27, no. 3, pp. 505 – 519, Sep. 2005.

222. DC. Van Essen, HA. Drury, S. Joshi and MI Miller, “Functional and structural mapping of human cerebral cortex: Solutions are in the surfaces”, *Proceedings of the National Academy of Science*, vol. 95, pp. 788 – 795, Feb. 1998.

223. RC. Oldfield, “The assessment and analysis of handedness: The Edinburgh inventory”, *Neuropsychologia*, vol. 9, no.1, pp. 97 – 113, Mar. 1971.

224. RW. Cox, “AFNI: software for analysis and visualization of functional magnetic resonance neuroimages”, *Computers and Biomedical Research*, vol. 29, no.3, Jun. 1996.

225. NA. Lazar, *The Statistical Analysis of Functional MRI Data*, New York, NY, USA, Springer, 2008.

226. JE. Desmond and GH. Glover, “Estimating sample size in functional MRI (fMRI) neuroimaging studies: Statistical power analyses”, *Journal of Neuroscience Methods*, vol. 118, pp. 115 – 128, 2002.

227. RL. Ott and MT. Longnecker, *An Introduction to Statistical Methods and Data Analysis*, 5th ed., Pacific Grove, CA, USA, Duxbury Press, 2000.

228. LJ. Gleser, “A Note on the Sphericity Test”, *The Annals of Mathematical Statistics*, vol. 37, no. 2, pp. 464 – 467, Apr. 1996.

229. SW. Greenhouse and S. Geisser, “On methods in the analysis of profile data”, *Psychometrika*, vol. 24, no. 2, pp. 95-112, 1959.

230. D.L. Gallahue, J.C. Ozmun, *Understanding Motor Development infants, children, adolescents, Adults*, 6th ed, Singapore, Singapore, McGraw Hill, 2006.

231. MF. Nitschke, A. Kleinschmidt, K. Wessel and J. Frahm, “Somatotopic motor representation in the human anterior cerebellum A high-resolution functional MRI study”, *Brain*, vol. 119, pp. 1023 – 1029, 1996.

232. RB. Ivry, SW. Keele and HC. Diener, “Dissociation of the lateral and medial cerebellum in movement timing and movement execution”, *Experimental Brain Research*, vol. 73, pp. 167 – 180, 1988.

233. M. Synofzik, A. Lindner and P. Their, “The Cerebellum Updates Predictions about the Visual Consequences of One’s Behavior”, *Current Biology*, vol.18, pp. 814–818, Jun. 2008.

234. ML. Latash, JP Scholz, and G Schöner, “Motor control strategies revealed in the structure of motor variability”, *Exercise and sport sciences review*, vol. 30, no. 1, pp. 26 – 31, 2002.

235. CA. Porro, “Primary Motor and Sensory Cortex Activation during Motor Performance and Motor Imagery: A Functional Magnetic Resonance Imaging Study”, vol. 16, no. 23, pp. 7688 – 7698, Dec. 1996.

236. M. Jahanshahi and M. Hallett, *The Bereitschaftspotential: movement-related cortical potentials*, New York, NY, USA, Kluwer Academic, 2003.

237. RQ. Cui, D. Huter, A. Egkher, W. Lang, G. Lindinger and L. Deecke, “High resolution DC-EEG mapping of the Bereitschaftspotential preceding simple or complex bimanual sequential finger movement”, *Experimental Brain Research*, vol. 134, no. 1, pp. 49 – 57, 2000.

238. W. Richter, PM. Andersen, AP. Georgopoulos and SG. Kim, “Sequential activity in human motor areas during a delayed cued finger movement task studied by time-resolved

fMRI", *NeuroReport, vol.*8, pp. 1257–1261, 1997.

239. F. Weilke, *et al.,* "Time-Resolved fMRI of Activation Patterns in M1 and SMA During Complex voluntary Movement", *Journal of Neurophysiology*, vol. 85, pp. 1858-1863, 2001.

240. R. Cunnington, C. Windischberger, S. Robinson and E. Moser, "The selection of intended actions and the observation of others' actions: A time-resolved fMRI study", *NeuroImage*, vol. 29, pp. 1294 – 1302, 2006.

241. PE. Dux, J. Ivanoff, CL. Asplund and R. Marois, "Isolation of a Central Bottleneck of Information Processing with Time-Resolved fMRI", *Neuron*, vol. 52, pp. 1109–1120, Dec. 2006.

242. I. Fried, *et al.*, "Functional organization of human supplementary motor cortex studied by electrical stimulation", *Journal of Neuroscience*, vol. 11, pp. 3656-3666, 1991.

243. W. Grodd, E. Hulsmann, M. Lotze, D. Wildgruber, and M. Erb, "Sensorimotor Mapping of the Human Cerebellum: fMRI Evidence of Somatotopic Organization", *Human Brain Mapping*, vol. 13, pp. 55 – 73, 2001.

244. M. Rijntjes, C. Buechel, S. Kiebel and C. Weiller, "Multiple somatotopic representations in the human cerebellum", *Neuroreport Motor Control*, vol. 10, no. 17, pp. 3653 – 3658, Nov. 1999.

245. H. Imamizu, T. Kuroda, S. Miyauchi, T. Yoshioka, and M. Kawato, "Modular organization of internal models of tools in the human cerebellum", *Proceedings of the National Academy of Science, vol.* 100, no. 9, pp. 5461 – 5466, Apr. 2003.

246. AR. Luft, M. Skalej, A. Stefanou, U. Klose and K. Voigt, "Comparing Motion- and Imagery-Related Activation in the Human Cerebellum:A Functional MRI Study", *Human Brain Mapping*, vol. 6, pp. 105–113, 1998.

247. A. Bashashati, M. Fatourechi, RK. Ward and GE. Birch, "Survey of signal processing algorithms in brain–computer interfaces based on electrical brain signals, *Journal of Neural Engineering*, vol. 4, pp. 32 – 57, 2007.

248. RT. Lauer, PH. Peckham, KL. Kilgore and WJ. Heetderks, "Applications of Cortical Signals to Neuroprosthetic Control: A Critical Review", *IEEE Transactions on Rehabilitation Engineering*, vol. 8, no.2, pp. 205 – 208, Jun. 2000.

249. M. Zecca, S. Micera, MC. Carrozza and P. Dario, "Control of Multifunctional Prosthetic Hands by Processing the Electromyographic Signal", *Critical Reviews in Biomedical Engineering*, vol. 30, no. 4–6, pp. 459–485, 2002.

250. PA. Bandettini and RW. Cox, "Event-Related fMRI Contrast When Using Constant

Interstimulus Interval: Theory and Experiment", *Magnetic Resonance in Medicine*, vol. 43, pp. 540–548, 2000.

251. M. Gentilucci, "Object familiarity affects finger shaping during grasping fruit stalks", *Exp Brain Res*, vol. 149, pp.395–400, 2003.

252. E.B. Torres and D. Zipser, "Simultaneous control of hand displacements and rotations in orientation-matching experiments." *J Appl Physiol*, vol. 96, pp. 1978-1987, 2004.

253. C. Ansuini, M. Santello, S. Massaccesi and U. Castiello, "Effects of End-Goal on Hand Shaping", *J Neurophysiol, vol.* 95, pp. 2456–2465, 2006.

254. J. Fan, J. He and S. I. Tillery, "Control of hand orientation and arm movement during reach and grasp", *Exp. Brain Res, vol.* 171, pp. 283-296, May 2006.

255. FAM. Ivaldi, P. Morasso and R. Zaccaria, "Kinematic Networks A Distributed Model for Representing and Regularizing Motor Redundancy", Biological Cybernetics, vol. 60, pp. 1 – 16, 1988.

256. JM. Kilner, KJ. Friston and CD. Frith, "The mirror-neuron system: a Bayesian Perspective", *Neuroreport:Review*, vol. 18, no. 6, pp. 619 – 623, Apr. 2007.

257. D. Michel, "Learning from human's strategies of motor control: a challenge for robotic systems design", *Conf Proc IEEE Robot and Human Communication*, Tsukuba, Japan, pp. 223 – 228, Nov. 1996.

258. TJ. Ross, *Fuzzy logic with engineering applications*, 3rd ed., Chichester, U.K, John Wiley, 2010.

259. G. Chen, TT Pham, *Introduction to fuzzy sets, fuzzy logic, and fuzzy control systems* Boca Raton, FL, USA, CRC Press, 2001.

260. WM. Bolstad, *Understanding computational Bayesian statistics*, Hoboken, N.J. USA, John Wiley & Sons, 2010.

261. S. James, *Subjective and objective Bayesian statistics : principles, models, and applications*, 2nd ed., Hoboken, NJ, USA, Wiley-Interscience, 2003.

262. RO. Duda, PE. Hart, and DG Stork, *Pattern Classification*, 2nd ed., New York, NY, USA, Wiley-Interscience, 2001.

263. S. Haykin, *Neural Networks and Learning Machines*, 3rd ed., Upper Saddle River, NJ, USA, Prentice Hall, 2008.

264. BD. Ripley, *Pattern recognition and neural networks,* New York, NY, USA, Cambridge University Press, 1996.

265. MD. Fox and ME. Raichle, "Spontaneous fluctuations in brain activity observed with functional magnetic resonance imaging", *Nature Reviews Neuroscience*, vol. 8, pp. 700-711, Sep. 2007.

266. W. Grodd and E. Hülsmann, "Sensorimotor mapping of the human cerebellum: fMRI evidence of somatotopic organization", *Human Brain Mapping*, vol. 13, no. 2, pp. 55–73, Jun 2001.

267. Andreas R. Luf, *et al*., "Comparing brain activation associated with isolated upper and lower limb movement across corresponding joints", *Human Brain Mapping*, vol. 17, no. 2, pp. 131 – 140, Oct. 2002.

268. E. Yacoub, A. Shmuel, N. Logothetis and K. Uğurbila, "Robust detection of ocular dominance columns in humans using Hahn Spin Echo BOLD functional MRI at 7 Tesla", *NeuroImage, vol.* 37, pp. 1161 – 1177, 2007.

269. C. Hamani, JN. Nobrega and AM. Lozano, "Deep Brain Stimulation in Clinical Practice and in Animal Models", *Clinical Pharmacology & Therapeutics*, vol. 88, no. 4, pp. 559 – 562, Oct. 2010.

270. J. Jacobs and MJ. Kahana, "Direct brain recordings fuel advances in cognitive electrophysiology", *Trends in Cognitive Sciences*, vol. 14, no. 4, pp. 162 – 171, Apr 2010.

271. B. Calvo-Merino, DE. Glaser, J. Grezes, RE. Passingham and P. Haggard, "Action Observation and Acquired Motor Skills: An fMRI Study with Expert Dancers", *Cerebral Cortex*, vol. 15, pp. 1243—1249, Aug. 2005.

272. M. Serruya, N. Hatsopoulos, M. Fellows, L. Paninski and J. Donoghue, "Robustness of neuroprosthetic decoding algorithms", *Biological Cybernetics*, vol. 88, no. 3, pp. 219 – 228, 2003.

273. A. Solodkin, P. Hlustik, DC. Noll and SL. Small, " Lateralization of motor circuits and handedness during finger movements", *European Journal of Neurology*, vol. 8. no. 5, pp. 425–434, Sep. 2001.

274. LH. Snyder, AP. Batista and RA. Andersen, "Change in Motor Plan, Without a Change in the Spatial Locus of Attention, Modulates Activity in Posterior Parietal Cortex", *The Journal of Neurophysiology,* vol. 79, no. 5, pp. 2814-2819, May 1998.

275. LM. Ross and DL. Nelson, "Comparing materials-based occupation, imagery-based occupation, and rote movement through kinematic analysis of reach", *The Occupational Therapy Journal of Research*, vol. 20, no. 1, pp. 45 – 53, 2000.

276. E. Todorov and MI. Jordan, “Optimal feedback control as a theory of motor coordination”, *Nature Neuroscience*, vol. 5, pp. 1226 – 1235, 2002.

277. SJ. Sober and PN. Sabes, “Flexible strategies for sensory integration during motor planning”, *Nature Neuroscience*, vol. 8, pp. 490 – 497, 2005.

278. J. Decety, “The neurophysiological basis of motor imagery”, *Behavioral Brain Research*, vol. 77, no. 1 – 2, pp. 45 – 52, May 1996.

279. Gert Pfurtscheller and Christa Neuper, “Motor imagery activates primary sensorimotor area in humans”, *Neuroscience Letters*, vol. 239, no. 2 – 3, pp. 65 – 68, Dec. 1997.

280. R. Hari, *et al.”,*Activation of human primary motor cortex during action observation: A neuromagnetic study”, *Proceedings of the National Academy of Science*, vol. 95, no. 25, pp. 15061 – 15065, Dec. 1998.

281. Emmanuel Gerardin, “Partial overlapping neural networks for real and imagined hand movements”, *Cerebral Cortex*, vol. 10, pp. 1093 – 1104, Nov. 2000.

282. C. Kranczioch, S. Mathews, PJA. Dean and A. Sterr, “On the Equivalence of Executed and Imagined Movements: Evidence from Lateralized Motor and Nonmotor Potentials”, *Human Brain Mapping*, vol. 30, pp. 3275–3286, 2009.

283. CJ. Olsson and L. Nyberg, “Motor imagery: if you can’t do it, you won’t think it”, *Scandinavian Jouenal of Medicine and Science in Sports*, vol. 20, pp. 711–715, 2010.

284. F. Malouin, “Brain Activations During Motor Imagery of Locomotor-Related Tasks: A PET Study”, *Human Brain Mapping*, vol. 19, pp. 47– 62, 2003.

285. KO. Bushara, “Multiple tactile maps in the human cerebellum”, *Neuroreport: Developmental Neuroscience*, vol. 12, no. 11, pp. 2483 – 2486, Aug. 2001.

286. JD. Schmahmann and D. Caplan, “Cognition, emotion and the cerebellum”, *Brain*, vol. 129, 288–292, 2006.

287. JD. Schmahmann, “From movement to thought: Anatomic substrates of the cerebellar contribution to cognitive processing”, *Human Brain Mapping*, vol. 4, no. 3, pp. 174 – 198, 1996.

288. MP. Deiber, V. Ibañez, M. Honda, N. Sadato, R. Raman and M. Hallett, “Cerebral Processes Related to Visuomotor Imagery and Generation of Simple Finger Movements Studied with Positron Emission Tomography”, *NeuroImage*, vol. 7, no.2, pp. 73 – 85, Feb. 1998.

289. DE. Nathan and M.J. Johnson, “Should Object Function Matter during Modeling

of Functional Reach-to-Grasp Tasks in Robot-Assisted Therapy?", *Conf proc IEEEMBS,* pp. 5695 – 5698, 2006.

290. DE. Nathan and DC Jeutter, "The importance of object geometric properties for trajectory modeling of functional reach-to-grasp robotic therapy tasks", *Biomedical Science and Instrumentation*, vol. 45, pp. 226 – 231, 2009.

291. DE. Nathan and DC. Jeutter, "Exploring the Effects of Cognitive Load on Muscle Activation during Functional Upper Extremity Tasks", *Conf Proc IFMBE 25th Southern Biomedical Engineering*, Miami, FL, USA, pp. 15 – 17, May 2009.

292. SH. Tillery and DM. Taylor, "Signal acquisition and analysis for cortical control of neuroprosthetics", *Current Opinion in Neurobiology*, vol. 14, pp. 758 – 762, 2004.

293. D. Tkach, H. Huang and TA. Kuiken, "Study of stability of time-domain features for electromyographic pattern recognition", *Journal of NeuroEngineering and Rehabilitation*, vol. 7, no. 21, pp. 1 – 13, 2010.

294. P. Zhou, MM. Lowery, RF. ff Weir and TA. Kuiken, "Elimination of ECG Artifacts from Myoelectric Prosthesis Control Signals Developed by Targeted Muscle Reinnervation", *Conf Proc 27th IEEE – EBMS*, Shanghai, China, pp. 5276 – 5279, Sept. 2005.

APPENDIX

Table A.1 : TTN27 Anatomical Atlas Regions (regions 1 – 59).

	Region		Region
1	L Precentral Gyrus	31	L Anterior Cingulate Cortex
2	RPrecentral Gyrus	32	R Anterior Cingulate Cortex
3	L Superior Frontal Gyrus	33	L Middle Cingulate Cortex
4	R Superior Frontal Gyrus	34	R Middle Cingulate Cortex
5	L Superior Orbital Gyrus	35	L Posterior Cingulate Cortex
6	R Superior Orbital Gyrus	36	R Posterior Cingulate Cortex
7	L Middle Frontal Gyrus	37	L Hippocampus
8	R Middle Frontal Gyrus	38	R Hippocampus
9	L Middle Orbital Gyrus	39	L ParaHippocampal Gyrus
10	R Middle Orbital Gyrus	40	R ParaHippocampal Gyrus
11	L Inferior Frontal Gyrus (p. Opercularis)	41	L Amygdala
12	R Inferior Frontal Gyrus (p. Opercularis)	42	R Amygdala
13	L Inferior Frontal Gyrus (p. Triangularis)	43	L Calcarine Gyrus
14	R Inferior Frontal Gyrus (p. Triangularis)	44	R Calcarine Gyrus
15	L Inferior Frontal Gyrus (p. Orbitalis)	45	L Cuneus
16	R Inferior Frontal Gyrus (p. Orbitalis)	46	R Cuneus
17	L Rolandic Operculum	47	L Lingula Gyrus
18	R Rolandic Operculum	48	R Lingula Gyrus
19	L SMA	49	L Superior Occipital Gyrus
20	R SMA	50	R Superior Occipital Gyrus
21	L Olfactory cortex	51	L Middle Occipital Gyrus
22	R Olfactory cortex	52	R Middle Occipital Gyrus
23	L Superior Medial Gyrus	53	L Inferior Occipital Gyrus
24	R Superior Medial Gyrus	54	R Inferior Occipital Gyrus
25	L Mid Orbital Gyrus	55	L Fusiform Gyrus
26	R Mid Orbital Gyrus	56	R Fusiform Gyrus
27	L Rectal Gyrus	57	L Postcentral Gyrus
28	R Rectal Gyrus	58	R Postcentral Gyrus
29	L Insula Lobe	59	L Superior Parietal Lobule
30	R Insula Lobe	**R**	Right
		L	Left

Table A.2 : TTN27 Anatomical Atlas Regions (regions 60 – 116).

	Region		Region
60	R Superior Parietal Lobule	90	R Inferior Temporal Gyrus
61	L Inferior Parietal Lobule	91	L Cerebelum (Crus 1)
62	R Inferior Parietal Lobule	92	R Cerebelum (Crus 1)
63	L SupraMarginal Gyrus	93	L Cerebelum (Crus 2)
64	R SupraMarginal Gyrus	94	R Cerebelum (Crus 2)
65	L Angular Gyrus	95	L Cerebelum (III)
66	R Angular Gyrus	96	R Cerebelum (III)
67	L Precuneus	97	L Cerebelum (IV-V)
68	R Precuneus	98	R Cerebelum (IV-V)
69	L Paracentral Lobule	99	L Cerebelum (VI)
70	R Paracentral Lobule	100	R Cerebelum (VI)
71	L Caudate Nucleus	101	L Cerebelum (VII)
72	R Caudate Nucleus	102	R Cerebelum (VII)
73	L Putamen	103	L Cerebelum (VIII)
74	R Putamen	104	R Cerebelum (VIII)
75	L Pallidum	105	L Cerebelum (IX)
76	R Pallidum	106	R Cerebelum (IX)
77	L Thalamus	107	L Cerebelum (X)
78	R Thalamus	108	R Cerebelum (X)
79	L Heschls Gyrus	109	Cerebellar Vermis (1/2)
80	R Heschls Gyrus	110	Cerebellar Vermis (3)
81	L Superior Temporal Gyrus	111	Cerebellar Vermis (4/5)
82	R Superior Temporal Gyrus	112	Cerebellar Vermis (6)
83	L Temporal Pole	113	Cerebellar Vermis (7)
84	R Temporal Pole	114	Cerebellar Vermis (8)
85	L Middle Temporal Gyrus	115	Cerebellar Vermis (9)
86	R Middle Temporal Gyrus	116	Cerebellar Vermis (10)
87	L Medial Temporal Pole	**R**	Right
88	R Medial Temporal Pole	**L**	Left
89	L Inferior Temporal Gyrus		